Novel cell models for the study of Spinocerebellar Ataxia type 7 pathogenesis and therapy in a South African patient cohort

Lauren M Watson

Thesis Presented for the Degree of

DOCTOR OF PHILOSOPHY

in the Division of Human Genetics, Department of Clinical Laboratory Sciences

UNIVERSITY OF CAPE TOWN

September 2012

The financial assistance of the National Research Foundation (NRF) towards this research is hereby acknowledged. Opinions expressed and conclusions arrived at, are those of the author and are not necessarily to be attributed to the NRF.

Acknowledgements

I am indebted to so many for their assistance throughout my PhD journey. To my supervisor, Prof Jacquie Greenberg, thank you for your valuable guidance, for championing my cause and for encouraging me to keep going! To my co-supervisors – Prof Matthew Wood, thank you for hosting me, for mentoring me in research and writing, and for offering me the opportunity to fulfil a lifelong dream of studying in Oxford; and to Assoc Prof Marco Weinberg, thank you for patiently coaching me in molecular biology, and for your hospitality during my time in Johannesburg.

I have had the privilege of working in three amazing laboratories, and I would like to thank everyone who has made me feel part of the family and assisted me with my research. In particular, I would like to express my sincere gratitude to Dr Janine Scholefield, for all the advice, encouragement and hard work which have helped make this project a success. I would also like to thank Dr Sally Cowley and Ms Jane Vowles for guiding me through the process of iPSC generation, and providing continued technical support; Ms Danielle Smith, for being willing to share results and ideas with seemingly limitless patience; Helen Curtis, Dr Martina Hallegger, Dr Miguel Varela, Tom Roberts and Dr Elizabeth Hartfield, for their assistance in maintaining cell lines, sharing data and offering advice; and Prof Raj Ramesar and the Division of Human Genetics for providing me with a supportive and nurturing research environment. I would also like to acknowledge Assoc Prof Ana-Lena Ström and Dr Chris Sibley, for the donation of antibodies and siRNA, respectively; Unistel Medical Laboratories, for assistance in karyotyping; Assoc Prof Collet Dandara, for advice regarding statistical analysis; and Ms Ingrid Baumgarten, for establishing the fibroblast cell lines for this study.

My work would not have been possible without the generous financial support of the National Research Foundation (NRF), the Harry Crossley Foundation, and the Commonwealth Scholarship Commission, for which I am deeply appreciative. Research funding, provided by the NRF, UCT Research Council, Ataxia UK, the John Fell Fund, the Wellcome Trust, Parkinson's Disease UK, MRC UK and the James Martin 21st Century School, as well as conference funding provided by the SASHG and NAF, is also gratefully acknowledged.

Finally, I would like to thank the patients who participated in this study – we continue to work towards a better understanding of this disease, for you and your families.

On a personal note, I would like to thank all my friends and family, in Cape Town, Johannesburg and Oxford, who have supported me, hosted me, and kept me sane over the past few years. To Pete, Helen, Rochelle, Sarah and Tereza, thank you for giving me a home away from home, and for putting up with my crazy hours! To everyone on the Oxford Bucket List team – thank you for helping me make the most of my time overseas. To Mom, Dad, Glen, Granny and the rest of the family, thank you for your prayers, weekly calls to Oxford, and for being willing to listen – I love you all. And to Grandpa, thank you for teaching me to love learning – I hope you would have been proud of the result.

To my other half, my best friend and the love of my life, Garth – thank you, thank you, thank you, for cheering me on, loving me, and being willing to sacrifice to give me the freedom to follow my dreams. You are my Once in a Lifetime, and I couldn't have made it to the finish line without you. Here's to more adventures!

Jeremiah 29:11

Abstract

Spinocerebellar ataxia type 7 (SCA7) is a dominantly-inherited neurodegenerative disease, resulting from a CAG trinucleotide repeat expansion in the *ataxin-7* gene. The Ataxin-7 protein is known to play a role in transcriptional regulation through association with cellular histone acetylation complexes, and several studies have highlighted the role of transcriptional dysregulation, caused by the presence of mutant Ataxin-7, in the neuronal dysfunction that precedes the onset of disease symptoms.

This study aimed to establish patient-derived cell models of SCA7, for use in the investigation of pathogenesis (with particular reference to transcriptional alterations), and in the evaluation of previously-developed therapies for the disease. The high prevalence of SCA7 in the South African population, as a result of a founder effect, makes this disease particularly amenable to allele-specific RNA interference (RNAi)-based therapy. Thus, this study also evaluated the feasibility of these cell models as a vehicle to test previously-developed RNAi therapeutics, using the alteration of expression of key transcripts as a phenotypic marker. SCA7 patient and control dermal fibroblasts were reprogrammed to pluripotency by retroviral transduction. The resultant induced pluripotent stem cell (iPSC) lines were characterised with respect to endogenous markers of pluripotency, differentiation capacity and transgene silencing. These cells were then subjected to neuronal differentiation, the success of which was confirmed by the expression of early neuronal markers.

The expression levels of key transcripts, previously demonstrated to be differentially regulated in SCA7 disease models, were compared between SCA7 and control fibroblasts, iPSCs and iPSC-derived neurons by means of quantitative real-time PCR. Significant differences in expression were observed, particularly with regard to genes involved in the heat shock protein and ubiquitin-proteasome pathways, which have been previously implicated in SCA7 pathology. Using SCA7 patient fibroblasts, this study also demonstrated that allele-specific RNAi-mediated silencing of *ataxin-7* may lead to a degree of amelioration of the disease-associated transcriptional phenotype.

The development of these novel cell models for the South African SCA7 patient cohort offers the opportunity, for the first time, to study the molecular basis of SCA7 in disease-relevant cell types from human patients. The identification of a transcriptional phenotype in these cells provides further evidence of the central role of transcriptional regulation in the aetiology and pathogenesis of the disease, and may serve as a valuable marker for the evaluation of population-specific gene silencing therapies in the future.

Table of Contents

Figures

Tables

Abbreviations

°C	Degrees Celsius
µg	Micrograms
µl	Microlitres
µM	Micromolar
3’	Three prime
5’	Five prime
A	Adenosine
A_{260}	Absorbance at 260nm
A_{280}	Absorbance at 280nm
ADCA	Autosomal dominant cerebellar ataxia
AFP	α-fetoprotein
ALS	Amyotrophic lateral sclerosis
AMPA	α-amino-3-hydroxy-5-methyl-4-isoxazolepropionic acid
AON	Antisense oligonucleotide
Ascl1	Achaete-scute homolog 1
ATM	Ataxia telangiectasia mutated
ATN1	Atrophin 1
ATP	Adenosine triphosphate
ATR	Ataxia telangiectasia and Rad3-related protein
BAX	Bcl-2 associated X protein
BDNF	Brain-derived neurotrophic factor
Bex1	Brain expressed, X-linked 1.
bFGF	Basic fibroblast growth factor
bHLH	Basic helix-loop-helix
BMP	Bone morphogenetic protein
bp	Base pairs

C	Cytosine
C. elegans	*Caenorhabditis elegans*
CACNA1A	Calcium channel, voltage-dependent, P/Q type, alpha 1A subunit
cAMP	Cyclic adenosine monophosphate
Cbl	Casitas B-lineage Lymphoma
CBP	CREB-binding protein
cDNA	Complementary DNA
CHCHD2	Coiled-coil-helix-coiled-coil-helix domain containing 2
CNS	Central nervous system
CO_2	Carbon dioxide
CREB	cAMP response element-binding
CRX	Cone-rod homeobox
CSIR	Council for Scientific and Industrial Research
D.melanogaster	*Drosophila melanogaster*
DAPI	4', 6-diamidino-2-phenylindole
DMEM	Dulbecco's Modified Eagle Medium
DMSO	Dimethyl sulphoxide
DNA	Deoxyribonucleic acid
DNAJA1	DnaJ homolog subfamily A member 1
dNTPs	Deoxyribonucleotide triphosphate
DRPLA	Dentatorubral-pallidoluysian atrophy
ds	Double-stranded
EB	Embryoid body
EBV	Epstein-Barr virus
EGF	Epidermal growth factor
ER	Endoplasmic reticulum
ESC	Embryonic stem cell
FACS	Fluorescence-activated cell sorting

FCS	Foetal calf serum
FOXA2	Forkhead box protein A2
FOXP2	Forkhead box protein P2
G	Guanine
GABA	Gamma-aminobutyric acid
GAD67	Glutamic acid decarboxylase
GAPDH	Glyceraldehyde 3-phosphate dehydrogenase
GFAP	Glial fibrillary acidic protein
GluR2	Glutamate receptor, ionotropic, AMPA2 protein
GRIA2	Glutamate receptor, ionotropic, AMPA 2 gene
HAT	Histone acetyltransferase
h-	Human
HD	Huntington's disease
HDAC	Histone deacetylase
HEK	Human embryonic kidney
HIV	Human immunodeficiency virus
HLA	Human Leukocyte Antigen
hrs	Hours
HSP	Heat shock protein
HSR	Heat shock response
HTT	Huntingtin
huESC	Human embryonic stem cell
I	Isoleucine
IDT	Integrated DNA Technologies
IGFBP5	Insulin-like growth factor-binding protein 5
IgG	Immunoglobulin G
iMEF	Inactivated mouse embryonic fibroblast
iN	Induced neuron

iPSC	Induced pluripotent stem cell
K	Lysine
KAT2A	K (lysine) acetyltransferase 2A
KO	Knockout
LCL	Lymphoblastoid cell lines
M	Molar
M	Methionine
MAP2	Microtubule-associated protein 2
MEF	Mouse embryonic fibroblast
MET	Mesenchymal-epithelial transition
mg	Milligrams
min	Minute(s)
miRNA	MicroRNA
ml	Millilitres
mM	Millimolar
MMLV	Moloney Murine Leukemia Virus
MOI	Multiplicity of infection
mRNA	Messenger ribonucleic acid
mTOR	Mammalian target of rapamycin
N/D	Not determined
NaN_3	Sodium Azide
NBM-A	Neurobasal Medium A
NES	Nuclear Export Signal
ng	Nanograms
NI	Nuclear inclusions
NLS	Nuclear localisation signal
nM	Nanomolar
Nr2E3	Nuclear receptor subfamily 2, group E, member 3

NRL	Neural retina leucine zipper
NS	Non-specific
NSC	Neural stem cell
N-terminal	Amino terminal
OSK	*OCT4/SOX2/KLF4*
OSKM	*OCT4/SOX2/KLF4/c-MYC*
OSNL	*OCT4/SOX2/NANOG/LIN28*
PAX6	Paired box gene 6
PBS	Phosphate buffered saline
Pcp-2	Purkinje cell protein 2
PCR	Polymerase chain reaction
PDGF	Platelet-derived growth factor
PEI	Polyethylenimine
PGPH	Peptidyl-Glutamyl Peptide-Hydrolysing (enzyme)
PKIB	Protein kinase (cAMP-dependent, catalytic) inhibitor beta
Plat-GP	Platinum-GP
PO	Pathology Oxford outbred
Pol	Polymerase
Poly-HEMA	Poly 2-hydroxyethyl methacrylate
PolyQ	Polyglutamine
PrP	Prion protein
Q	Glutamine
qPCR	Quantitative polymerase chain reaction
rAAV	Recombinant adeno-associated virus
RBM3	RNA-binding protein 3
RISC	RNA-induced silencing complex
RNA	Ribonucleic acid
RNAi	RNA interference

RNAse	Ribonuclease
rpm	Revolutions per minute
RT-PCR	Reverse transcriptase polymerase chain reaction
SAGA	Spt/Ada/Gcn5/acetylase
SBMA	Spinal bulbar muscular atrophy
SCA	Spinocerebellar ataxia
SCAANT1	SCA7/*ataxin-7* antisense RNA 1
SDS	Sodium dodecyl sulphate
SEM	Standard error of the mean
shRNA	Short hairpin RNA
siRNA	Small interfering RNA
SLC17A6	Solute carrier family 17 (sodium-dependent inorganic phosphate cotransporter), member 6.
SMA	Spinal muscular atrophy
SMN	Survival of motor neuron protein
SNP	Single nucleotide polymorphism
SNRK	SNF-related serine/threonine-protein kinase
SOD1	Superoxide dismutase 1
Sp1	Specificity protein 1
STAGA	SPT3/TAF9/GCN5 acetyltransferase complex
SUMO	Small Ubiquitin-like Modifier
T_a	Annealing temperature
Taq	*Thermus aquaticus*
TBE	Tris-Borate-EDTA
TBP	TATA binding protein
TE	Tris-EDTA
TFTC	TATA-binding protein-free TAF-containing complex
TGFβ	Transforming growth factor beta
TGS	Transcriptional gene silencing

U	Units
UCHL1	Ubiquitin carboxy-terminal hydrolase L1
UCT	University of Cape Town
UK	United Kingdom
UPS	Ubiquitin-proteasome system
USA	United States of America
Usp22	Ubiquitin specific peptidase 22
UTR	Untranslated region
UV	Ultraviolet
V	Volts
v/v	Volume per volume
VLGUT2	Vesicular glutamate transporter 2
VPA	Valproic acid
VSV-G	Vesicular stomatitis virus glycoprotein
w/v	Weight per volume
XPO5	Exportin 5

Chapter 1 **Introduction**

Disorders of the nervous system represent a significant proportion of the global burden of non-communicable diseases, largely due to the trend towards aging populations (Bergen and Silberberg, 2002). Although traditionally believed to be the concern of developed nations, improvements in healthcare and increased life expectancy could soon see this phenomenon spreading to developing countries. Inherited neurodegenerative diseases in particular, characterised by progressive symptoms and a lengthy disease course, present a significant economic and psychological burden to affected families (de Villiers et al., 1997).

A subset of these conditions, known collectively as the polyglutamine (polyQ) diseases, have a well-defined genetic aetiology, making them attractive targets for research and therapeutic development. There are currently nine known inherited polyQ diseases, including Huntington's Disease (HD), dentatorubral-pallidoluysian atrophy (DRPLA), spinal bulbar muscular atrophy (SBMA), and six of the spinocerebellar ataxias (SCA1, 2, 3, 6, 7 and 17) (Watson and Wood, 2012). All arise from a common type of mutation – an expanded trinucleotide CAG repeat within the coding region of the disease-causing gene, which is translated into an abnormally long polyglutamine tract in the mutant protein (Durr, 2010). As a result, these disorders share many features, including late onset of disease symptoms, anticipation, and repeat instability during vertical transmission (Watson and Wood, 2012).

The number of CAG repeats required for presentation of disease symptoms varies according to gene, however, many of the polyglutamine disorders share similar CAG threshold levels, such that 37- 40 repeats in most of these conditions results in neurodegeneration (Orr and Zoghbi, 2007). Although the common pathogenic number of repeats has also been shown to differ from one polyglutamine

disorder to the next, most lie in the 40-60 range, with numbers extending into the hundreds (Rosenblatt et al., 2001; Lindblad et al., 1996).

The length of the CAG repeat tract is prone to expansion from one generation to the next (Stevanin et al., 1998), and shows a strong correlation with both the age of onset and disease severity (Globas et al., 2008; Garden and La Spada, 2008; Pulst et al., 2005; Lebre and Brice, 2003). Most polyQ diseases exhibit the phenomenon of "anticipation", whereby larger expansions in successive generations result in earlier, more severe phenotypes, and more rapid disease progression (Lebre and Brice, 2003).

Symptoms, including chorea, dystonia and dementia (HD), ataxia and dysarthria (SCAs and DRPLA), seizures (SCA17) and motor weakness (SBMA), result from the selective degeneration of well-defined subpopulations of neurons (Shirendeb et al., 2011; Bichelmeier et al., 2007; Saegusa et al., 2007; Helmlinger et al., 2006a; Goti et al., 2004; Li and Li, 2004; Huynh et al., 2003; Yoo et al., 2003; Cemal et al., 2002; Watase et al., 2002; La Spada et al., 2001; Burright et al., 1995). Although the precise mechanisms underlying this selectivity are not yet fully understood, the identification of common hallmarks of pathology suggests that many, if not all, of the polyQ diseases may be amenable to similar therapeutic approaches.

1.1 Spinocerebellar Ataxia 7

1.1.1 Phenotype

Spinocerebellar ataxia type 7 (SCA7) is a late-onset, dominantly-inherited polyQ neurodegenerative disease, the major clinical manifestations of which include cerebellar ataxia, dysarthria, dysphagia, exaggerated deep tendon reflexes, and progressive macular degeneration (Horton et al., 2012; Lebre and Brice, 2003; Aleman et al., 2002). Classified as a type II autosomal dominant cerebellar ataxia

(ADCA), it is distinct from other polyQ diseases by virtue of the presence of an ocular phenotype, which results in severe visual impairment, in addition to the gait and speech difficulties characteristic of cerebellar degeneration (Garden and La Spada, 2008; Einum et al., 2001; Mauger et al., 1999). In adult-onset SCA7, cerebellar symptoms tend to precede visual impairment, while earlier-onset cases often present with vision loss prior to the development of ataxia (Johansson et al., 1998). Adolescent cases typically progress more rapidly than adult-onset forms of the disease, with a more severe clinical presentation. Infantile SCA7 on the other hand, may be seen as a phenotypically distinct, rapidly-progressing multisystem disorder, presenting within the first two years of life with symptoms including weight loss, cardiac abnormalities, motor regression, wasting, hypotonia and failure to thrive (Whitney et al., 2007; van de Warrenburg et al., 2001; Johansson et al., 1998).

1.1.2 Genetics

The identification of linkage to the short arm of chromosome 3 in affected families (Benomar et al., 1995) suggested strongly that SCA7 was genetically distinct from other ADCAs. Fine-mapping of the region resulted in identification of the causative gene, dubbed "*ataxin-7*", at position 3p12-21.1 (Michalik et al., 1999; Del-Favero et al., 1998; David et al., 1996). Shortly thereafter, an unstable CAG repeat region was identified within exon 3 of the gene and expansion of this region was demonstrated to co-segregate with the disease in several affected families, confirming the causative nature of the CAG expansion, and allowing the molecular classification of SCA7 as a polyQ disease (David et al., 1997; Lindblad et al., 1996).

Non-pathogenic *ataxin-7* alleles contain between 4 and 35 CAG repeats, with the most common allele being $(CAG)_{10}$ (David et al., 1998; Johansson et al., 1998), although this may differ according to population group (Alluri et al., 2007). Alleles in the 28-35 CAG repeat range are classified as "mutable" or "expansion prone" and may undergo further expansion into the pathogenic range during vertical transmission (particularly in the case of paternal transmission), resulting in the

appearance of disease in the offspring of asymptomatic carriers (Lebre and Brice, 2003; Stevanin et al., 1998). Pathological alleles range in length from 36 to over 400 repeats (Lebre and Brice, 2003; Einum et al., 2001), although the lower threshold is not precisely defined (Nardacchione et al., 1999).

The CAG repeat tract in *ataxin-7* shows the greatest propensity for expansion upon vertical transmission of any of the polyQ disorders, particularly through the paternal line, indicating a predisposition towards instability during spermatogenesis (Monckton et al., 1999). This bias towards expansion via paternal transmission is not unique to SCA7 (Mandel, 1994; Trottier et al., 1994), and may reflect the high mitotic turnover of spermatocytes in comparison to oocytes (Yoon et al., 2003). However, the extreme cases of instability of the *ataxin-7* CAG repeat greatly surpass those of the other polyQ disease genes, with a report of a $(CAG)_{49}$ allele expanding to $(CAG)_{460}$ in a single generation (van de Warrenburg et al., 2001). This may be due, at least in part, to the genomic context within which the *ataxin-7* expansion is situated – a theory supported by findings in SCA7 mice, in which removal of *ataxin-7* flanking sequences reduces the instability in transmission to offspring (Libby et al., 2003); while mutations in binding sites for the regulatory factor CTCF, situated in close proximity to many genomic repeat sequences, significantly enhance the instability of the *ataxin-7* CAG repeat (Libby et al., 2008).

1.1.3 Pathology

The neuropathology of SCA7 (namely, the marked degeneration of cerebellum and retina in affected individuals) shows a strong correlation with the disease phenotype. Cerebellar atrophy is often preceded by significant atrophy of the pons, a feature characteristic of SCA7 (Fig. 1a-c) (Garden and La Spada, 2008; Bang et al., 2004; Michalik et al., 2003). Within the cerebellum, SCA7 patients typically exhibit extensive loss of Purkinje cells, with only minimal alterations to the cerebellar

granule layer (Fig. 1g-h) (Garden and La Spada, 2008; Einum et al., 2001). In the brainstem, atrophy of the olivocerebellar, spinocerebellar and pyramidal tracts has been observed, with the inferior olive undergoing substantial neuronal loss together with gliosis. Additional pathologies include neuronal loss in the brainstem cranial nerve motor nuclei, demyelination of pyramidal tracts and posterior columns of the spinal cord, and, in some patients, degeneration of the substantia nigra, globus pallidus and subthalamic nucleus (Garden and La Spada, 2008).

A pathogenic hallmark of SCA7 shared by many of the polyQ diseases is the formation of nuclear inclusions (NIs), aggregates of mutant *ataxin-7* which sequester numerous key proteins, including ubiquitin-proteasome components and transcription factors (Zander et al., 2001; Chai et al., 1999a; Chai et al., 1999b; García-Mata et al., 1999; Cummings et al., 1998a). The role of these NIs in the molecular pathogenesis of the disease remains controversial, however, particularly since their presence is not limited to vulnerable neuronal populations, but extends to unaffected areas of the brain (for example, the cerebral cortex) (Lindenberg et al., 2000; Holmberg et al., 1998).

The retinal phenotype in SCA7 results primarily from the dysfunction of the cone, and later, rod photoreceptors, hence its classification as a cone-rod dystrophy (Hugosson et al., 2009). The initial impairment of central vision, caused by dysfunction of cone cells in the foveal region, is followed by the progressive dysfunction of rods and cones throughout the retina, leading ultimately to total blindness (Fig. 1d-f, i-j) (Gouw et al., 1994; To et al., 1993).

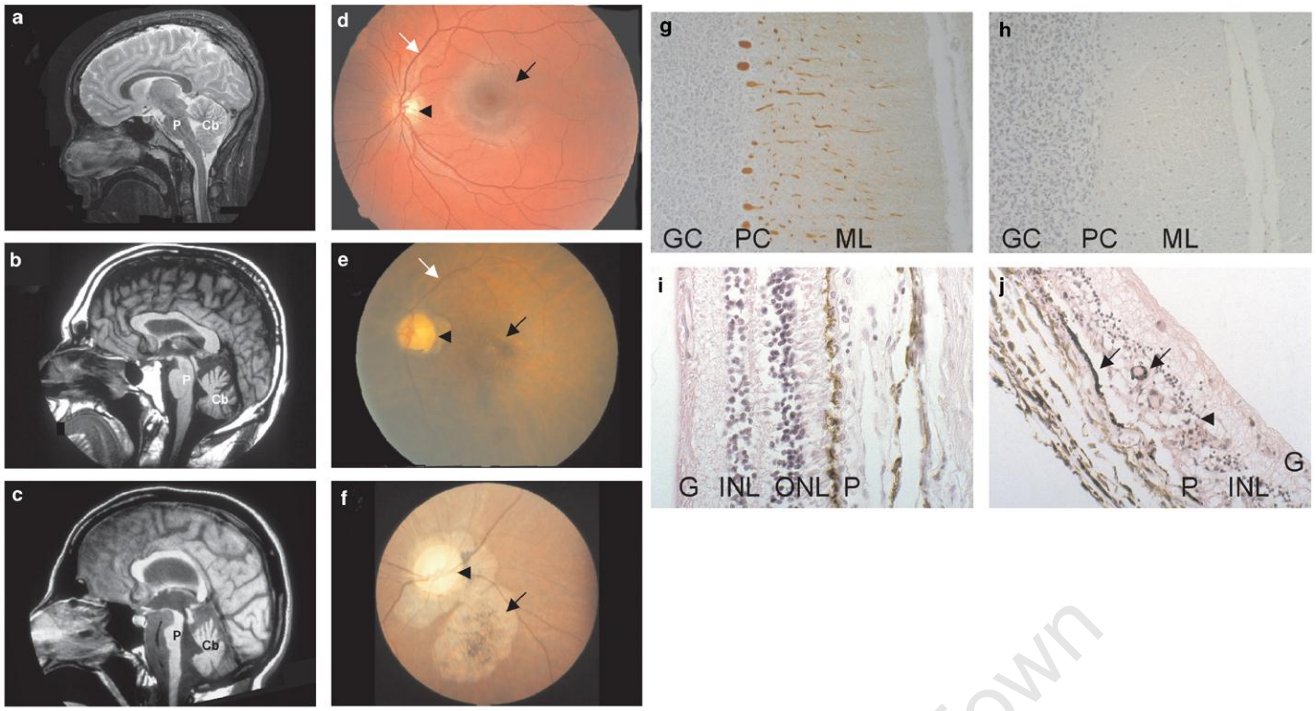

Figure 1 Cerebellar and retinal pathology in SCA7. (a-c) Magnetic resonance imaging of a control individual (a) and two SCA7 patients (b), (c). The patient depicted in (b) has severe cerebellar atrophy (Cb), while the pons (P) is almost completely spared. The patient in (c) shows severe atrophy of the cerebellum, as well as marked atrophy of the pons (P). (d-f) Fundoscopy images of a control individual (d) and two SCA7 patients (e, f). In the control individual, the macula (black arrow) and optic disk (arrowhead) appear normal, and vasculature (white arrow) is well-developed (d). By contrast, the retina of patient (e) displays macular atrophy (black arrow), very pale optic disk (arrowhead), and poor vasculature (white arrow). The retina of patient (f) shows an extremely pale optic disc (arrowhead), and degeneration of the pigmentary epithelium and choroid (arrow). (g, h) Calbindin staining of the cerebellar cortex of a control individual (g) and a SCA7 patient (h), to visualise Purkinje neurons. The control displays strongly labelled bodies of Purkinje cells (PC), and dendritic extensions within the molecular layer (ML) (g). The cerebellum of a SCA7 patient (h) on the other hand, shows a dramatic loss of Purkinje neurons. (i, j) Histology of the retina of a control individual (i) and a SCA7 patient (j). The control individual (i) shows proper organization of the retinal layers: the pigment epithelium (P), nuclei of photoreceptors within the outer nuclear layer (ONL), nuclei of bipolar neurons within the inner nuclear layer (INL), and the ganglion cell layer (G). By contrast, the SCA7 patient (j) displays severe retinal degeneration, with complete demise of photoreceptor segments and nuclei, disorganization of the INL (arrowhead), and migration of melanin into the atrophic retina (arrows). Adapted by permission from Macmillan Publishers Ltd: European Journal of Human Genetics (Michalik et al., 2003), copyright 2003.

1.1.4 Wildtype *ataxin-7* function

The *ataxin-7* gene encodes an 892 amino-acid protein, Ataxin-7 (David et al., 1997), comprising several known functional domains, including the disease-associated polyQ repeat, a phosphate binding site (Mushegian et al., 2000), a nuclear localization signal (NLS) (Kaytor et al., 1999), and a nuclear export signal (NES) (Taylor et al., 2006). Studies of cell models transfected with truncated and full-length *ataxin-7* constructs have demonstrated the ability of the NLS to shuttle both wildtype and mutant Ataxin-7 into the nucleus (Kaytor et al., 1999). Nuclear export, mediated by the leucine-rich NES, occurs via the CRM-1/exportin pathway in a polyQ length-dependent manner, with longer repeats inhibiting the cytoplasmic trafficking of the protein (Taylor et al., 2006).

Wildtype Ataxin-7 is widely expressed in the brain and retina, and peripheral tissues including testis, thyroid, striated muscle, lymphoblasts, kidney and pancreas (Jonasson et al., 2002; Einum et al., 2001; Cancel et al., 2000). Within the CNS, Ataxin-7 is preferentially expressed in neurons, although low levels have also been detected in astrocytes (Cancel et al., 2000). The distribution of Ataxin-7 does not, however, correlate with the selective neuronal loss observed in SCA7 pathology – highly vulnerable Purkinje cells, for example, have been shown in some cases to express relatively low levels of the protein (Cancel et al., 2000).

In normal human brains, Ataxin-7 is found in the cell bodies and processes of neurons, as well as the nucleus, with subcellular localization varying according to cell type (Einum et al., 2001; Cancel et al., 2000). An age-dependent shift in subcellular compartmentalisation has also been postulated, based on observations in the brains of control individuals, which showed predominantly nuclear Ataxin-7 immunostaining at a young age, followed by cytoplasmic staining later in life (Jonasson et al., 2002). This model should be viewed with caution, however, as the results represent a collation of several independent studies, the results of which remain to be verified. Within the cytoplasm,

Ataxin-7 co-localises with the endoplasmic reticulum (ER), but not with mitochondria or the Golgi network (Cancel et al., 2000).

Early studies of Ataxin-7 protein function identified two interacting proteins – R85, a splice variant of Cbl-associated protein (Lebre et al., 2001), and the ATPase subunit S4 of the proteasomal 19S regulatory complex (Matilla et al., 2001). The former provided a potential mechanism for the ubiquitination of Ataxin-7; while the latter interaction, inversely correlated with the length of the polyQ tract, suggested a role for the proteasome in SCA7 pathogenesis (see Section 1.2.1) (Lebre et al., 2001; Matilla et al., 2001).

The high degree of homology between human and mouse Ataxin-7 (88.7%) (Ström et al., 2002), and between human and vertebrate Ataxin-7 (Taylor et al., 2006), point to an evolutionarily conserved function for the wildtype protein. Indeed, the identification of a yeast orthologue predicted to be a component of the histone acetyltransferase Spt/Ada/Gcn5/acetylase (SAGA) complex – a key modulator of yeast transcription – has provided valuable insight into the role of Ataxin-7 as a transcriptional regulator (Scheel et al., 2003). Subsequent studies of mammalian Ataxin-7 have confirmed its role in the SAGA-like complexes, the TATA-binding protein-free TAF-containing complex (TFTC) and the SPT3/TAF9/GCN5 acetyltransferase complex (STAGA), where it interacts directly with the Gcn5 histone acetyltransferase subunit to activate gene transcription via the acetylation of histone H3 (Palhan et al., 2005; Helmlinger et al., 2004a). The incorporation of mutant expanded Ataxin-7 inhibits the histone acetylation function of Gcn5 in a dominant-negative fashion, possibly accounting for the transcriptional dysregulation frequently observed in SCA7 (Palhan et al., 2005).

Further evidence for the role of Ataxin-7 in transcriptional regulation has come from the observation that Ataxin-7 interacts directly with the photoreceptor transcription factor, cone-rod homeobox

(CRX) protein (La Spada et al., 2001), mutations in which are known to result in retinal degenerative disorders and dysregulated expression of photoreceptor genes (Sohocki et al., 1998). The interaction, mediated by the glutamine regions of both proteins, is required for the transactivation of CRX-dependent genes *in vivo*, and may be disrupted by the expansion of the Ataxin-7 polyQ tract (Chen et al., 2004).

The aforementioned hypotheses account, at least in part, for the function of Ataxin-7 in the nucleus. However, the ability of the protein to shuttle between the nucleus and the cytoplasm via its NLS and NES suggests that Ataxin-7 may also perform certain cytoplasmic functions. In a recent study by Nakamura and colleagues, the expression levels, nuclear:cytoplasmic ratio and intracytoplasmic distribution of fluorescent-tagged Ataxin-7 in transfected HeLa cells were found to change dramatically during the cell cycle (Nakamura et al., 2012). Data from immunofluorescence and immunoprecipitation experiments were used to confirm that the filamentous structures formed by Ataxin-7 during mitosis overlapped with the spindle, the result of a physical interaction between Ataxin-7 and α-tubulin which occurred independently of repeat length (Nakamura et al., 2012). Reduced sensitivity of Ataxin-7 transfected cells to nocodazole, an inhibitor of microtubule polymerisation, served as further confirmation of the role of Ataxin-7 in the stabilisation of the microtubule network; although it is possible that the interaction of Ataxin-7 and α-tubulin may be a reflection of the transport of excess protein to aggresomes – a significant limitation of overexpression models of disease (Nakamura et al., 2012).

1.2 Pathogenic mechanisms of PolyQ disease

1.2.1 Protein aggregation and impairment of the ubiquitin-proteasome pathway

Nuclear inclusions (NIs), containing aggregates of proteolytically-cleaved mutant protein, have long been recognised as a common pathogenic marker of polyQ diseases. In SCA7, studies of cell models

and human brain tissue have confirmed the presence of intra- and perinuclear fibrillar aggregates of Ataxin-7, particularly in models in which truncated, polyQ-containing fragments of the protein are expressed (Zander et al., 2001). These aggregates have been shown to contain key cellular components including transcription factors, ubiquitin-proteasome components, heat shock proteins (such as HSP40 and HSP70), and activated caspase-3, in addition to other polyQ proteins, suggesting that their formation may disrupt important biological processes (Fig. 2) (Zander et al., 2001; Chai et al., 1999a; Chai et al., 1999b; García-Mata et al., 1999; Cummings et al., 1998a). However, these findings have not been robustly reproduced in animal models, with several studies failing to demonstrate any deleterious effects of NIs on transcription factor function (Sadri-Vakili et al., 2006; Yu et al., 2002). Wildtype Ataxin-7 has also been shown to be recruited to NIs, suggesting that a loss-of-function may contribute to disease manifestation (Jonasson et al., 2002; Zander et al., 2001).

Proteolytic cleavage by caspase-7, which generates an amino-terminal fragment containing the polyQ tract but not the NES (Garden and La Spada, 2008; Young et al., 2007), has been found to be an important modulator of SCA7 aggregation and toxicity (Young et al., 2007; Garden et al., 2002). The resultant truncated fragments demonstrate enhanced nuclear localisation (Taylor et al., 2006), and may be more prone to aggregation, increasing the likelihood of NI formation (Young et al., 2007).

The sequestration of molecular chaperones and proteasome components into NIs, together with the presence of elevated levels of ubiquitin conjugates associated with deposits of aggregated mutant Ataxin-7, are indicative of a link between dysfunction of the ubiquitin proteasome system (UPS) and SCA7 pathogenesis (Bence et al., 2001; Chai et al., 1999b), particularly given the essential role of the UPS in the turnover of both mutant and wildtype Ataxin-7 (Yu et al., 2012). Indeed, overexpression of two aggregation-prone proteins has been shown to directly impair the UPS in vitro (Bence et al., 2001), while in vivo evidence for UPS dysfunction has been investigated in several

human patients (De Pril et al., 2004; Chan et al., 2002; Fernandez-Funez et al., 2000; Cummings et al., 1998b).

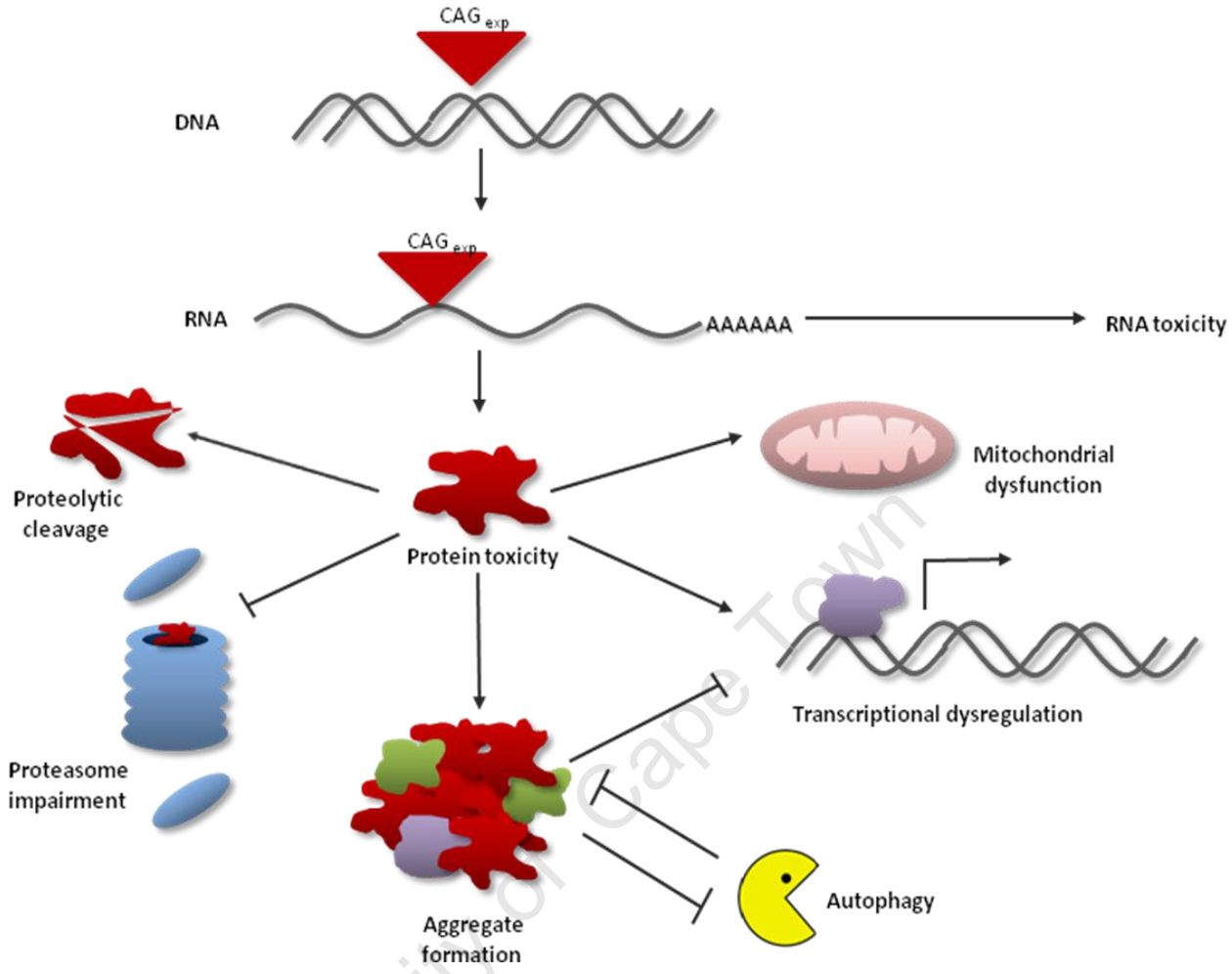

Figure 2 Mechanisms of polyQ toxicity. The expansion of CAG trinucleotide repeats within the coding region of several genes results in the expression of proteins containing pathologically expanded polyglutamine (polyQ) tracts. Pathogenesis has largely been attributed to the effects of the mutant protein, although a role for RNA toxicity in the development of disease has also been proposed. The mechanism by which polyQ proteins exert their toxic effects varies according to protein context, and may include proteolytic cleavage (leading to the production of toxic fragments), impairment of the ubiquitin–proteasome pathway, formation of aggregates of mutant protein (involving the sequestration of wild-type polyQ protein and other important cellular components such as transcription factors), dysregulation of transcription, either directly or as a result of aggregate formation, and mitochondrial dysfunction, all of which result in deleterious downstream consequences. Adapted by permission from Expert Reviews in Molecular Medicine (Watson and Wood, 2012), copyright 2012.

Early theories for the inhibition of the UPS in polyQ disease included the saturation of molecular chaperones required for UPS function, and direct interaction of "indigestible" polyQ tracts with the proteasome (Bence et al., 2001). In the latter case, proteasomes could theoretically become blocked by degradation-resistant, ubiquitinated aggregates, thereby limiting their availability for degrading other cellular substrates (Bence et al., 2001). This hypothesis was supported by the observation that eukaryotic proteasomes appeared unable to process polyQ sequences, resulting in direct blockage of the 20S core proteasome in a length-dependent manner (Venkatraman et al., 2004). Protein aggregates, such as the NIs observed in SCA7, were thus assumed to function as both inhibitors of the UPS pathway and the products resulting from its inhibition – a decrease in UPS activity resulting in the further accumulation of misfolded proteins, leading in turn to a further decrease in UPS function – a positive feedback mechanism thought to account for the progressive loss of neuronal function that characterises neurodegenerative diseases (Bence et al., 2001). Considering the central role of the UPS in regulating cellular events such as cell division and apoptosis, this link provided a mechanism by which protein aggregation might result in cellular dysregulation and cell death (Bence et al., 2001).

More recent evidence has revealed a vastly different relationship between polyQ proteins and the UPS. The discovery of UPS impairment in the absence of protein aggregates, together with lack of discernible effects of aggregation on the 26S proteasome observed in several models, indicate that UPS impairment is unlikely to result from the choking of proteasomes by aggregated proteins (Bennett et al., 2005; Michalik and Van Broeckhoven 2004). Instead, analyses of single cells suggest that UPS dysfunction precedes inclusion body formation, and may actually be ameliorated by the formation of inclusions (Mitra et al., 2009). An investigation into the temporal and mechanistic relationship between N-terminal *HTT* aggregation and UPS function by Hipp et al. (2012) further supported these findings, leading the authors to propose a model whereby the accumulation of ubiquitin results from competition for limited proteasome capacity, rather than

direct impairment by polyQ tracts. In this model, UPS components become gradually overwhelmed by folding-impaired, aggregation prone proteins, resulting in a disruption of protein homeostasis (Hipp et al., 2012; Finkbeiner 2011).

The role of NIs in polyQ pathogenesis therefore remains controversial (Watson et al., 2012; Michalik and Van Broeckhoven, 2003). The presence of aggregates in unaffected tissues (Ansorge et al., 2004; Jonasson et al., 2002), together with the observed lack of NIs in at least one SCA7 affected individual (Einum et al., 2001), suggest that their formation does not entirely coincide with disease pathology. A protective role for the aggregation of mutant Ataxin-7 has even been suggested, based on an observed inverse correlation between neuropathology and the presence of NIs in the vulnerable neurons of a SCA7 knock-in mouse model (Bowman et al., 2005).

Autophagy, literally "self-eating", refers to the lysosomal enzymatic mechanism employed by cells to degrade long-lived cytosolic proteins (Duncan et al., 2010). The discovery of an association between mutant HTT and the accumulation of autophagic vacuoles in HD patient brain tissue, lymphoblasts and mouse models provided the first concrete link between autophagy and polyQ disease (Fig. 2) (Nagata et al., 2004; Petersén et al., 2001; Kegel et al., 2000; Sapp et al., 1997). Hallmarks of autophagy have subsequently been reported in other polyQ diseases, including SBMA, SCA1 and SCA7 (Montie et al., 2009; Vig et al., 2009; Zander et al., 2001).

The presence of accumulating autophagosomes in degenerating neurons suggested at first that autophagy could contribute to the demise of these cells, particularly in light of the established role for autophagy in programmed cell death (Duenas et al., 2006; Yue et al., 2002). This hypothesis has been refined over time to reflect the current understanding of the role of basal autophagy in normal mammalian tissues, and it is now widely believed that the increase in autophagic vacuoles observed

in polyQ diseases may reflect a defect in autophagic flux, rather than the induction of the pathway (Atwal et al., 2007).

The rate of basal autophagy differs between different tissues, with a particularly high demand for protein turnover in the liver, and in post-mitotic cells such as neurons (Komatsu et al., 2007; Hara et al., 2006; Komatsu et al., 2006). Neurons in particular are highly vulnerable to perturbations in the autophagy-lysosomal system, due to their highly metabolically active state, and their unique cellular architecture, which requires that autophagosomes produced in dendrites, axons or synaptic terminals travel substantial distances in order to fuse with lysosomes, located adjacent to the nucleus (La Spada and Taylor, 2010). The importance of basal autophagy in the CNS is further highlighted by the observation that conditional knockout of certain key autophagy genes results in neurodegeneration and accumulation of ubiquitinated inclusions, similar to those seen in human neurodegenerative diseases (Hara et al., 2006).

Although autophagic impairment in polyQ diseases has yet to be convincingly demonstrated, it is hypothesised to arise in one of two ways: either through the over-burdening of the autophagy-lysosomal pathway with aggregated, misfolded proteins which are resistant to degradation, or through direct impairment, in cases where the disease protein plays an important role in the process of autophagy (as is the case in HD) (Atwal et al., 2007; Shibata et al., 2006).

The potential neuroprotective function of autophagy should, however, also be noted. Indeed, the upregulation of autophagy genes, and sequestration of the autophagic inhibitor mammalian target of rapamycin (mTOR) observed in polyQ diseases results in activation of autophagy and enhanced clearance of mutant polyQ proteins (Ravikumar et al., 2004). This effect has been mimicked with some success in animal models of polyQ disease, in which pharmacological or genetic augmentation of autophagy have both been shown to enhance turnover of expanded polyQ protein and decrease

neurodegeneration, offering a potential avenue for therapy for these diseases (Sarkar et al., 2008; Pandey et al., 2007; Sarkar et al., 2007; Davies et al., 2006; Ravikumar et al., 2004; Tanaka et al., 2004). Most recently, results from a stable, inducible SCA7 cell model have provided strong evidence for the importance of autophagy in the clearance of proteolytically cleaved Ataxin-7 fragments, providing further confirmation that enhancement of this key pathway could serve as a valuable therapeutic strategy (Yu et al., 2012).

1.2.2 Altered protein-protein interactions and post-translational mechanisms

The expanded polyQ tract imparts a conformational change to the mutant protein, thereby directly affecting native protein-protein interactions (Matilla et al., 2001). In addition, post-translational modifications such as phosphorylation, SUMOylation and acetylation of specific residues in several polyQ proteins may be altered in the presence of the mutation, affecting interactions with their natural binding proteins (reviewed by La Spada and Taylor, 2010). Post-translational mechanisms may also influence the stability and rate of turnover of the mutant protein, as is the case in SCA7, in which acetylation of lysine 257 (K257) has been shown to regulate caspase-7-mediated cleavage of Ataxin-7 in a repeat length-dependent manner (Mookerjee et al., 2009). SUMOylation of Ataxin-7 at K257 has also been observed, and is believed to decrease the aggregation propensity and cellular toxicity of the mutant protein (Janer et al., 2009).

1.2.3 Transcriptional alterations

Transcriptional dysregulation is a common feature of polyQ diseases (Fig. 2) (Helmlinger et al., 2006b). Many polyQ proteins play a role in transcriptional regulation, and several reports have identified transcriptional changes in molecular chaperones and genes involved in neuronal differentiation, prior to cellular dysfunction, suggesting that transcriptional alteration may be one of the first cellular manifestations of disease (Lin et al., 2000; Luthi-Carter et al., 2000). The

differences in transcriptional phenotypes of different polyQ diseases are likely to reflect the specific function(s) of the disease-causing proteins (Helmlinger et al., 2006b).

Transcriptional dysregulation in polyQ disease is hypothesised to result either from the recruitment and sequestration of transcription factors in NIs (thereby interfering with their normal function), or via direct interactions between the mutant protein and transcription factors (that is, an alteration of wildtype function, or a gain of function resulting from the expansion of the polyQ tract). These proposed mechanisms are supported by the detection of numerous transcription factors capable of interaction with polyQ-containing proteins, including the cAMP response element binding protein (CREB), the TATA-binding protein associated factor 4 (TAF4) and specificity protein 1 (Sp1) (Dunah et al., 2002; McCampbell et al., 2000; Shimohata et al., 2000; Steffan et al., 2000; Kazantsev et al., 1999). Although many of these proteins have been shown to localise in NIs, evidence from mouse models suggests that direct interactions between mutant protein monomers or oligomers and transcription factors may have a more profound effect on gene expression than their sequestration into protein aggregates (Sadri-Vakili et al., 2006; Schaffar et al., 2004).

In most cases, the precise causes of transcriptional changes, and their relationship to the polyQ disease phenotype have proved difficult to elucidate (Helmlinger et al., 2006b). However, the discovery of a role for wildtype Ataxin-7 in the mammalian STAGA/TFTC complexes (Helmlinger et al., 2006c; Palhan et al., 2005; Helmlinger et al., 2004a) has provided valuable insights into the role of transcriptional dysregulation in the development of SCA7.

The TFTC and STAGA complexes are members of an important class of transcriptional co-activators – multi-protein complexes recruited to gene promoters by specific co-activators, where they facilitate the assembly of the general transcriptional machinery and the acetylation of histones, via the catalytic subunit Gcn5 (Taatjes et al., 2004; Narlikar et al., 2002). Reporter assays and

immunoprecipitation studies have confirmed that Ataxin-7 is required for transcriptional activation by TFTC/STAGA, and that this activation is mediated by CRX, a photoreceptor-specific transcriptional co-activator. These results have led to extensive investigations of the effects of mutant Ataxin-7 on transcriptional regulation in SCA7 mouse models (Helmlinger et al., 2006a).

As retinal degeneration is a unique feature of SCA7, most studies have focused on retinal photoreceptors in order to gain insight into the function of mutant Ataxin-7, with several groups reporting severe transcriptional dysregulation in the retinas of SCA7 transgenic and knock-in mouse models (Carlson et al., 2009). In all cases, the expression of mutant Ataxin-7 induced dramatic, early downregulation of most photoreceptor-specific genes, including many of those encoding components of the phototransduction cascade (Abou-Sleymane et al., 2006; Helmlinger et al., 2006a; Yoo et al., 2003; La Spada et al., 2001). Downregulation of Rhodopsin expression, the earliest molecular abnormality detected, correlated with a decrease in rod electrophysiological responses and thinning of rod photoreceptor segments, observed well before the onset of cell death in the mouse retina (Helmlinger et al., 2004b; Yoo et al., 2003). Transcriptomic analysis provided further confirmation of the preferential downregulation of genes whose expression is both restricted to the retina, and required for normal photoreceptor function (Abou-Sleymane et al., 2006). These findings indicated strongly that the retinopathy observed in SCA7 mice and patients may result from the decreased expression of photoreceptor genes (Helmlinger et al., 2006b). This was further corroborated by significant reduction in expression in SCA7 mouse retina of three photoreceptor-specific activators – CRX, NRL (a basic motif leucine zipper transcriptional activator) and Nr2E3 (an orphan nuclear receptor) – suggesting that photoreceptors in SCA7 mice may lose their ability to maintain a differentiated state over time, resulting ultimately in dysfunction (Helmlinger et al., 2006a).

The effect of mutant Ataxin-7 on TFTC/STAGA function remains controversial. Evidence from transfected cell models, yeast and SCA7 transgenic mice has confirmed that polyQ-expanded Ataxin-7 incorporates into TFTC/STAGA as efficiently as the wildtype protein (Helmlinger et al., 2006c; McMahon et al., 2005; Palhan et al., 2005; Helmlinger et al., 2004a). However, *in vitro* studies suggest that the polyQ-expanded protein may affect the assembly of the transcriptional complexes, by interfering with recruitment of SPT3, ADA2b and TAF12 (Balasubramanian et al., 2002; Grant et al., 1999; Grant et al., 1998; Grant et al., 1997). Mutant Ataxin-7 has also been shown to interfere with Gcn5 histone H3 activity and CRX-mediated recruitment of TFTC/STAGA to promoters, in a dominant-negative manner in transfected HEK293T cells (Palhan et al., 2005).

In contrast to these *in vitro* findings, studies of SCA7 mice have failed to demonstrate a direct interaction between CRX and Ataxin-7 or TFTC/STAGA (Helmlinger et al., 2006a; La Spada et al., 2001). In addition, the presence of polyQ-expanded Ataxin-7 *in vivo* was found to induce a global downregulation of all rod-specific genes, rather than just those regulated by CRX, leading researchers to question the role of CRX in the recruitment of TFTC/STAGA (Yoo et al., 2003).

Analysis of the composition of purified TFTC/STAGA from the retinas of R7E transgenic mice revealed normal levels of all components, including mutant Ataxin-7, as well as normal levels of histone acetylation activity (Helmlinger et al., 2006a). However, incorporation of the polyQ-expanded mutant protein into TFTC/STAGA *in vivo* resulted in a gain of function of these complexes, inducing histone H3 hyperacetylation, leading to severe chromatin decondensation in the rod photoreceptors of SCA7 transgenic and knock-in mice (Helmlinger et al., 2006a). Surprisingly, the hyperacetylated genes were transcriptionally downregulated, a counterintuitive finding proposed to result from an increase in photoreceptor nuclear volume, leading to the "dilution" of retina-specific transcription factors and hence to the downregulation of strongly-expressed retina-specific genes (Helmlinger et al., 2006a). This is consistent with the known role of higher order chromatin

packaging in the control of gene expression and cell type determination (Francastel et al., 2000). Indeed, photoreceptor dysfunction, measured electrophysiologically, histologically and by a decrease in Rhodopsin expression, was directly correlated with the degree of chromatin decondensation in R7E and knock-in mouse models (Helmlinger et al., 2006a).

The discrepancies in TFTC/STAGA HAT activity observed between *in vitro* and *in vivo* models of SCA7 may be partly explained by the different model systems used in each study. For instance, the effect of incorporation of mutant human Ataxin-7 into the yeast SAGA complex may not accurately reflect its effects on the mammalian version of the complexes, while the absence of transcriptional alterations in transfected HEK293T cells makes it difficult to correlate the observed HAT impairment with SCA7 pathology. Results from transgenic SCA7 mice on the other hand, are affected by the tissue-specific expression patterns of the transgene, and by its massive overexpression, which limit extrapolations of these findings to other affected tissues. The advantages, limitations and future prospects for SCA7 disease models are discussed in more detail in Section 1.5.

With the role of transcriptional dysregulation as an early marker of SCA7 retinopathy firmly established, recent studies have been expanded to include investigations of transcriptional patterns in the CNS. Chou et al. investigated the involvement of transcriptional dysregulation in cerebellar dysfunction using a transgenic mouse model of adult-onset SCA7, expressing polyQ-expanded Ataxin-7-Q52 in brain regions implicated in SCA7 neurodegeneration, including the cerebellum and inferior olivary nucleus (Chou et al., 2010). Microarray analysis of cerebellar gene expression in 10-11 month old mice revealed downregulation of genes encoding proteins responsible for glutamatergic transmission, myelin formation, signal transduction, deubiquitination, axon transport, neuronal differentiation or glial functions, and heat shock proteins (Chou et al., 2010). Upregulation of certain genes, including those encoding RNA binding proteins, was also observed.

The role of transcriptional changes in initiating SCA7 pathology was confirmed by the observation that 6-month-old transgenic mice, which did not exhibit a measurable ataxic phenotype, exhibited a similar pattern of transcriptional dysregulation. The most notable difference between the two age groups was found in the expression levels of heat shock proteins, which were upregulated in 6-month-old mice. This biphasic expression pattern is likely to reflect the induction of the HSP response during the early stages of disease as part of a misfolded protein response, followed by the impairment of HSP gene transcription by accumulation of toxic mutant Ataxin-7 as the disease progresses (Chou et al., 2010). Downregulation of HSP expression is a common hallmark of advanced polyQ pathogenesis, having been identified in affected neurons in HD, SBMA, SCA3 and SCA17 transgenic mice (Chou et al., 2010; Chou et al., 2008; Katsuno et al., 2005; Hay et al., 2004).

Based on these findings, it is evident that transcriptional dysregulation plays a significant role in the development of SCA7 pathology, making it both an important early marker of disease and a promising therapeutic target.

1.2.4 Loss-of-function and additional pathogenic mechanisms

Although polyQ diseases are generally accepted to result from a toxic gain-of-function of the mutant protein, it is possible that a loss of function may contribute to pathogenesis, particularly since knockout models of some polyQ diseases show neurodegeneration, and NIs have been shown to recruit the native protein, possibly leading to impairment of its normal function (Watson and Wood, 2012). Lessons learnt from the role of Ataxin-7 in the TFTC/STAGA complex further emphasise the importance of understanding normal protein function in the elucidation of disease pathogenesis.

A number of additional polyQ disease mechanisms have been reported, including mitochondrial dysfunction, enhanced apoptosis and excitotoxicity caused by glutamate receptor overactivation (reviewed in Bauer and Nukina, 2009). Mutant Ataxin-7 has also been shown to be capable of

activating the mitochondrial apoptotic pathway in SCA7 transgenic mice, via p53-mediated upregulation of pro-apoptotic *BAX* mRNA (Wang et al., 2010). Most recently, a role for polyQ-expanded Ataxin-7 in the development of oxidative stress has also been proposed, based on its effects on NADPH oxidase complex activity and Catalase levels (both of which are key regulators of the levels of reactive oxygen species) in a SCA7 inducible cell model (Ajayi et al., 2012).

Given the multitude of cellular insults triggered by expanded polyQ tracts, developing an effective therapy appears a daunting prospect. However, based on current theories of pathogenesis, several proof-of-principle treatments have already been demonstrated. These are discussed in more detail in Section 1.4.

1.3 SCA7 in South Africa

SCA7 is one of the rarer polyQ disorders, with a prevalence of less than 1 per 100 000 worldwide (Durr, 2010; Storey et al., 2000). In South Africa, however, the situation is vastly different, with a recent report identifying SCA7 as the second most prevalent dominantly-inherited ataxia, after SCA1 (Smith et al., 2012). This unusual pattern was first described by Bryer et al., who reported an increased prevalence of SCA7 in the South African population, as compared to the rest of the world (22.2% of total dominant ataxia cases, compared with a frequency of less than 5% in countries such as China, India, the United States of America, Korea, Australia, and Spain) (Bryer et al., 2003).

Similar to their counterparts in other regions of the world, South African SCA7 patients present with either ataxia, visual impairment, or both symptoms simultaneously, with a mean age at onset of 20.3 years. Families display significant anticipation, and affected individuals die within 5 to 30 years of disease onset (Bryer et al., 2003).

The disease occurs almost exclusively in individuals of Black African origin, hypothesised to have resulted from a founder event (Greenberg et al., 2006) similar to those reported in Mixed Ancestry and Caucasian SCA1 patients in South Africa (Ramesar et al., 1997). South African SCA7 patients are thus presumed to have descended from a common ancestor, and should, as a result, share a common haplotype surrounding the *ataxin-7* gene, including alleles of common SNPs within the region. Indeed, the observation that over 50% of South African SCA7 patients are heterozygous for a common SNP (rs3774729) in the 3' region of *ataxin-7*, such that the A and G alleles of the SNP are associated with the mutant and wildtype transcripts, respectively, has provided much of the impetus for the development of RNA interference (RNAi)-based therapy for this patient population (Scholefield et al., 2009; Greenberg et al., 2006).

1.4 Therapeutic approaches for polyQ diseases

(Adapted from Watson and Wood, 2012; and Watson et al. 2012)

Historically, treatment for polyQ diseases has focused on symptomatic management. However, with greater understanding of the molecular basis of these diseases has come the opportunity to prevent or delay onset of disease symptoms, through the identification of targets within the disease pathway which may be amenable to therapy. Current experimental therapies may be classified into two categories - those aimed at alleviating the burden of accumulated mutant protein, and those targeting its downstream effects.

1.4.1 Therapies targeting polyglutamine proteins

1.4.1.1 *Oligonucleotide-based therapies*

Given the complexities of polyQ pathogenesis, one logical approach to therapy is to suppress production of the mutant protein upstream of its deleterious effects. Several lines of evidence support the therapeutic benefit of silencing poly-Q-encoding genes (Xia et al., 2002). Studies of inducible

models of disease in particular have shown that neuropathological features, which develop over time in response to the presence of mutant polyQ protein, are rapidly improved upon attenuation of mutant gene expression. These findings provide proof-of-principle that inhibition of disease-causing genes represents an effective avenue for therapy in patients already exhibiting a disease phenotype (Zu et al., 2004; Yamamoto et al., 2000). Attention has therefore turned in recent years to the development of effective transcriptional and post-transcriptional gene silencing therapies, mediated for the most part by small non-coding RNA molecules (Fig. 3).

The most straightforward method of RNA-based gene silencing involves indiscriminate suppression of both the normal and pathological alleles of the gene – termed "non allele-specific silencing" (Fig. 3b). Although technically less challenging, this approach is based on the assumption that the wildtype gene function is either non-essential or functionally redundant, since silencing of genes essential for CNS development and maintenance could have deleterious consequences.

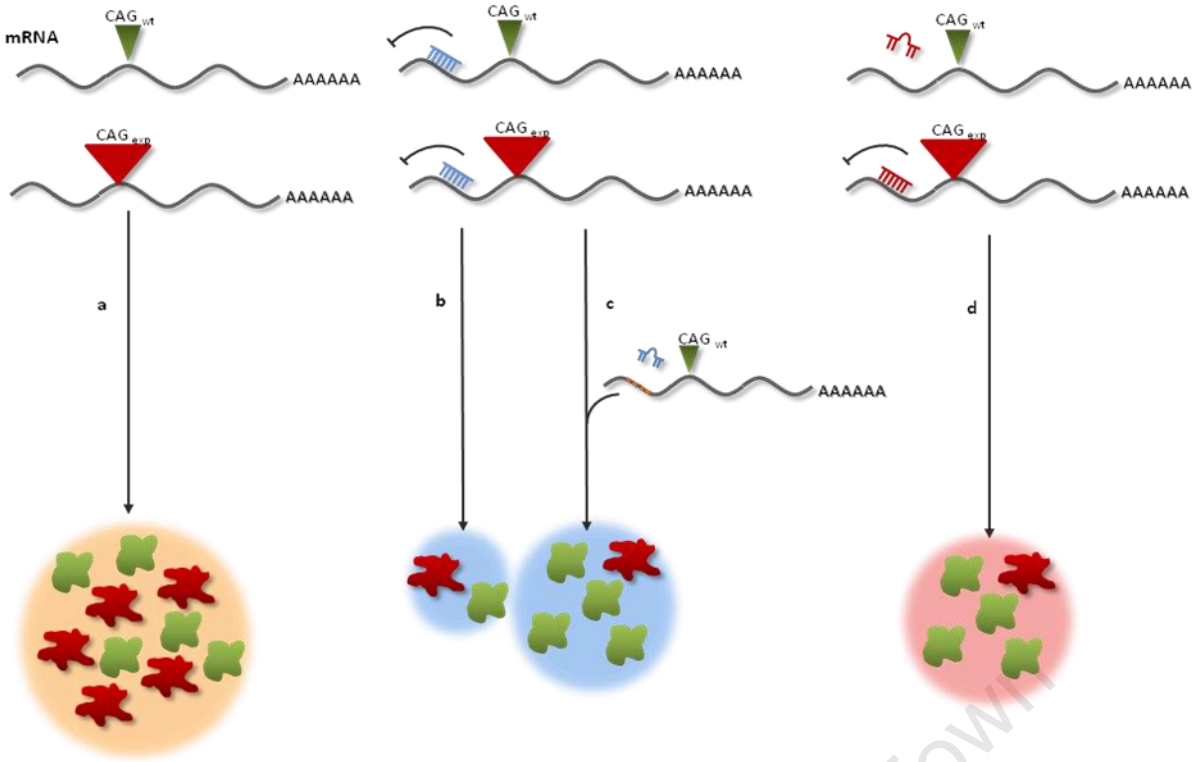

Figure 3 Principles of allele-specific, non-allele-specific, and gene knockdown and replacement therapies. (a) Translation of wild-type and pathologically expanded alleles of a CAG repeat results in the production of both mutant (red) and wild-type (green) protein. (b) Non-allele-specific post-transcriptional gene silencing (PTGS) therapy (shown in blue) prevents translation of both transcripts, leading to a reduction in wild-type and mutant polyglutamine protein levels. (c) In the case of gene knockdown and replacement, the introduction of an exogenous wild-type transcript, which is resistant to silencing as a result of modifications to the nucleotide sequence, results in restoration of wild-type protein expression despite the suppression of both endogenous transcripts in a non-allele-specific manner. (d) Allele-specific gene silencing (shown in red), based on discrimination between single-nucleotide polymorphism genotypes or differences in CAG repeat lengths, results in selective suppression of mutant protein production, while wildtype protein levels remain relatively unchanged. Effectors may be either RNA interference-based or antisense oligonucleotides Adapted by permission from Expert Reviews in Molecular Medicine (Watson and Wood, 2012), copyright 2012.

In cases where wildtype protein function is indispensable, an allele-specific approach may be required. Allele-specific silencing relies on the availability of targetable sequence differences that enable discrimination between the normal and mutant transcripts of a gene; for example, single nucleotide polymorphisms (SNPs) in linkage disequilibrium with the expansion mutation, or

differences in the CAG repeat length itself (Fig. 3d) (Rodriguez-Lebron and Paulson, 2005). In theory, an allele-specific strategy represents the preferred therapeutic mechanism for the majority of polyQ diseases, as it enables selective silencing of the mutant copy of the gene, while maintaining wildtype expression. However, in practice it is not always feasible – polymorphisms linked to the disease allele in a small number of affected individuals may not justify the development of a therapy, and may not be amenable to targeting due to their location within the gene (Scholefield and Wood, 2010). In such cases, alternative approaches such as gene knockdown and replacement may be employed. This method combines non allele-specific silencing with gene replacement therapy, in which an RNAi or antisense oligonucleotide (AON)-resistant transgene is delivered to the targeted tissues together with the therapeutic effector (Fig. 3c) (Kubodera et al., 2010; Kubodera et al., 2005).

The decision regarding which silencing method to apply to a given polyQ disease depends both on the degree to which loss of wildtype protein expression is tolerated, and the feasibility of allele-specific silencing. To date, answers to these questions have largely been based on the phenotypes observed in knockout and transgenic animal models of disease. In the case of HD, for instance, *HTT* knockout results in embryonic lethality (Nasir et al., 1995), while conditional knockout mice display a neurodegenerative phenotype and significantly shorter lifespan (Dragatsis et al., 2000). Ablation of wildtype function in transgenic HD mice results in an exacerbation of disease symptoms (Van Raamsdonk et al., 2005). Since *HTT* is known to play a role in several key pathways in brain development, retention of wildtype expression appears necessary, although the absence of a phenotype in heterozygous conditional knockout mice and in an individual expressing *HTT* at only 50% of normal levels suggests that a single functional copy may be sufficient (Persichetti et al., 1996; Ambrose et al., 1994) – a strong argument in favour of the allele-specific silencing approach.

The absence of a knockout model for SCA7 makes it difficult to determine the effect of a loss of wildtype function. However, the fact that *ataxin-7* plays an important role in the regulation of retinal

gene expression (Helmlinger et al., 2006a; Palhan et al., 2005; La Spada et al., 2001) has prompted the suggestion that an allele-specific approach be adopted until further information becomes available.

1.4.1.1.1 Principles and mechanisms of gene silencing

Therapeutic strategies based on the principle of RNAi make use of the endogenous mammalian gene silencing pathway, in which primary microRNA (miRNA) hairpins, transcribed from non-coding regions of the genome, are processed sequentially by a series of enzyme complexes to yield short double-stranded RNAs (Fig. 4a) (Weinberg and Wood, 2009). In the final step, the antisense or "guide" strand of the duplex is loaded into the RNA-induced silencing complex (RISC) which, in the case of post-transcriptional silencing, directs either cleavage or translational suppression of the complementary target mRNA, depending on the accuracy of base-pairing (Castanotto and Rossi, 2009; Zamore et al., 2000).

The pathway may be harnessed for therapeutic gene silencing through cytoplasmic delivery of synthetic short interfering RNAs (siRNAs), double-stranded molecules 21-22 nucleotides in length, which are designed to be perfectly complementary to the mRNA targeted for silencing (Fig. 4c) (Rodriguez-Lebron and Paulson, 2005). Short hairpin RNAs (shRNAs) represent a modification of this strategy in which the basic siRNA sequence is incorporated into a stem-loop construct, expressed at high levels from a PolIII promoter (Fig. 4b) (Boudreau et al., 2008a). However, since both siRNAs and shRNAs bind obligatorily to components of the RNAi pathway, large doses may result in saturation of the cellular RNAi processing machinery, disrupting endogenous miRNA biogenesis and function (Grimm et al., 2006). Additionally, the risk of off-target effects as a result of partial complementarity to unintended transcripts represents an important caveat to the clinical utility of RNAi (Boudreau et al., 2008a; Denovan-Wright et al., 2008).

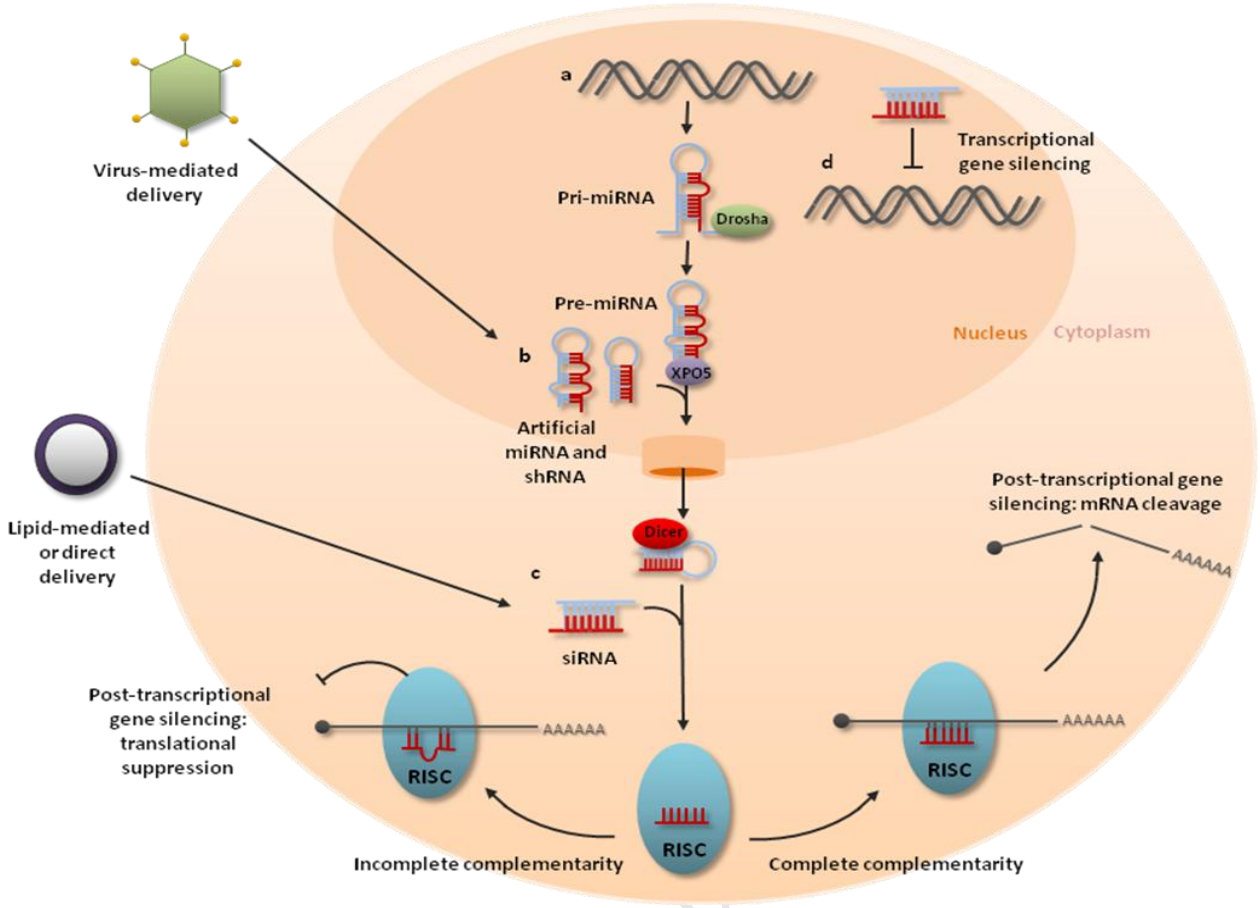

Figure 4 RNA interference-based therapies make use of the endogenous mammalian gene silencing pathway. (a) Endogenous primary microRNAs (pri-miRNAs), transcribed from genomic DNA, are processed in the nucleus by Drosha (an RNase III enzyme) and its interaction partners to yield pre-miRNAs. These are exported to the cytoplasm by means of exportin-5 (XPO5), where they are recognised and cleaved by the Dicer enzyme complex, resulting in the production of ~22 bp staggered duplexes. The guide strand (depicted in red) is loaded into the RNA-induced silencing complex (RISC), which, in the case of posttranscriptional silencing, directs cleavage or translational suppression of the cognate mRNA, depending on the accuracy of base pairing between the guide strand and the target mRNA (Castanotto and Rossi, 2009). (b) The pathway may be manipulated for therapeutic gene silencing through the introduction of artificial miRNA or short hairpin RNA (shRNA) constructs complementary to the gene or allele targeted for repression. These effectors are expressed under the control of PolII and PolIII promoters, respectively, and enter the pathway upstream of Dicer processing. (c) Alternatively, short interfering RNAs (siRNAs) that target the gene of interest can be incorporated directly into RISC. (d) Long-term suppression of gene expression may be accomplished through TGS, in which siRNAs complementary to the promoter region of the target gene induce epigenetic changes. Delivery is usually mediated by integrating lenti- or episomally-expressing (rAAV) viruses (in the case of shRNAs and miRNAs) or by direct injection or lipid-mediated transfection (in the case of siRNAs) (Adapted by permission from Expert Reviews in Molecular Medicine (Watson and Wood, 2012), copyright 2012.

One method to avoid saturation involves the incorporation of synthetic siRNA sequences into artificial miRNAs under the control of a PolII promoter, allowing for regulated, cell-specific expression of the gene silencing molecules (Fig. 4b) (Boudreau et al., 2008b). The result is a decrease in accumulation of unprocessed precursors leading to a reduction in cellular immune response, and hence to an improvement in non-specific, toxic effects (Bauer et al., 2008; Boudreau et al., 2008b; McBride et al., 2008).

Another method that has been proposed involves circumvention of the RNAi pathway altogether, through the use of antisense oligonucleotides complementary to the mRNA targeted for silencing. AONs are short synthetic molecules, 15-25 nucleotides in length, which hybridise to their target mRNA by means of Watson and Crick base pairing (Smith et al., 2006). Posttranscriptional gene silencing is achieved through RNAse H-mediated intranuclear degradation of the target transcript (Crooke, 2004), or steric blocking of translation (Gagnon et al., 2010).

1.4.1.1.2 Allele-specific gene silencing

Allele-specific silencing is accomplished through the exploitation of differences in nucleotide sequence between wildtype and mutant alleles, making it particularly applicable to dominantly inherited disorders such as the polyQ diseases, in which only one copy of the mutant gene is required for the disease to manifest. The aim is thus to achieve maximum selectivity for the mutant transcript, while ensuring that the wildtype allele is spared the effects of gene silencing (Rodriguez-Lebron and Paulson, 2005). Since the sequence of the effector must match the target exactly to elicit RISC- or RNase H-mediated degradation, it is vital that the mutant and wildtype transcripts of the gene to be targeted differ by at least one nucleotide, in order to facilitate discrimination. In many diseases caused by point mutations, insertions or deletions, the targetable sequence difference is offered by the mutation itself (Xia et al., 2006; Abdelgany et al., 2003; Gonzalez−Alegre et al., 2003). However, in the case of polyQ neurodegenerative diseases, targeting of the CAG expansion presents

a challenge, as the polymorphic nature and ubiquitous presence of the repeat tract throughout the genome make it difficult to target specifically, particularly since effectors <25 nucleotides in length are unlikely to be able to distinguish between wildtype and pathologically expanded CAG tracts (Scholefield and Wood, 2010).

Most efforts have therefore focused on targeting sequence differences created by the presence of SNPs linked to the CAG repeat expansion in a specific patient group (Rodriguez-Lebron and Paulson, 2005), using RNAi-based technologies. Once a suitable SNP has been identified, several additional mechanistic issues must be taken into account when designing siRNAs capable of optimal discrimination between transcripts that differ at a single nucleotide (reviewed in greater detail in Watson and Wood, 2012). Of critical importance, the allele of the SNP linked to the mutant copy of the gene should be identified, in order to determine the correct siRNA sequence required. This may be accomplished through studies of conserved haplotypes within patient cohorts, or through more direct methods such as allele-specific reverse trancriptase PCR (Van Bilsen et al., 2008). In addition to design, the concentration of effector administered is also important, as allele-specificity has been shown to be concentration dependent (Zhang et al., 2009). The most successful allele-specific treatment is therefore likely to be that for which adequate discrimination is achieved at a concentration sufficient to effect a clinically significant level of mutant protein inhibition (Lombardi et al., 2009; Schwarz et al., 2006).

SNP-based allele-specific approaches have been successfully demonstrated at the preclinical level in SCA3 and HD models, including patient fibroblasts (Alves et al., 2008; Van Bilsen et al., 2008; Li et al., 2004; Miller et al., 2003; Cattaneo et al., 2001; Gaspar et al., 1996). This approach has also been used to achieve allele-specific silencing of mutant *ataxin-7* in HEK293 cells, targeting the A-allele of a SNP in linkage disequilibrium with the pathogenic expansion (Scholefield et al., 2009). These results represent an important improvement on previous studies, since they demonstrate the potential

of RNAi to successfully discriminate between endogenous single nucleotide mismatches present in patient DNA, rather than relying on sequence differences between species to selectively silence mutant genes, as is often the case in transgenic animal models of disease. However, it should be noted that the cost and effort required to develop large numbers of effectors for low-frequency disease-linked SNPs are likely to hinder the progress of allele-specific therapy towards clinical trials (Zhang et al., 2009; Van Bilsen et al., 2008).

In order to address this issue, large-scale studies of polymorphic sites within the *HTT* gene have been conducted in the European and North American HD patient populations (Lombardi et al., 2009; Pfister et al., 2009). The finding that as few as five allele-specific siRNAs, targeting three SNP sites could be used to treat 75% of these patients should greatly simplify the development of therapy (Pfister et al., 2009). Including a further four SNPs increases the proportion of eligible patients to 85.6%, although targeting these additional sites would require the design of a significantly greater number of siRNAs (Lombardi et al., 2009; Pfister et al., 2009). It is difficult to extrapolate these results from the European Caucasian patient sample to other patient populations around the world. However, a similar investigation into targetable polymorphisms in Venezuelan HD patients has revealed six SNPs, which would provide options for allele-specific silencing for up to 63.5% of the patient population (Lombardi et al., 2009). Thus, it may be theoretically possible to develop a relatively small number of effectors to deliver effective allele-specific RNAi therapy to the majority of polyQ disease patients.

1.4.1.1.3 CAG repeat targeting, antisense oligonucleotides and additional therapeutic approaches

Innovations in the field of antisense oligonucleotide technology offer the opportunity to develop therapies applicable to all patients across the polyQ disease spectrum, through the discovery of molecules capable of allele-specific silencing based solely on differences in CAG repeat length

(Gagnon et al., 2010; Hu et al., 2009a). Discrimination is thought to be based either on differences in secondary structure or number of binding sites, depending on the size of the CAG repeat tract, with larger repeats demonstrating increased susceptibility to AON binding (Gagnon et al., 2010; Hu et al., 2009a). The result is steric blocking of translation, rather than RNase H-mediated cleavage of the target mRNA (Gagnon et al., 2010).

Allele-specific targeting of the CAG repeats is not limited to AONs, however. Artificial miRNAs – mismatch-containing duplexes complementary to the CAG expansion – have also been proposed to offer a potent and versatile silencing mechanism, capable of >31-fold selectivity *in vitro* despite the introduction of up to four mismatched bases into the guide strand (Hu et al., 2010a).

There are still some concerns regarding the use of CAG-targeting AONs, which may limit their efficacy *in vivo*. In particular, the presence of CAG tracts throughout the genome suggests the potential for deleterious off-target effects, although no silencing of repeat-containing genes (including *TBP*, *ATN1* and *FOXP2*) has yet been observed *in vitro* (Gagnon et al., 2010; Hu et al., 2010a). The fact that more common smaller CAG expansions appear to be less amenable to silencing using this approach, compared to rarer large expansions also presents a challenge to the clinical utility of this method, which must be addressed before such approaches can progress to clinical trials (Gagnon et al., 2010).

One alternative to sequence-based allele-specific silencing, which still results in retention of wildtype protein function, is the gene knockdown and replacement method. Silencing of both mutant and wildtype alleles of the disease gene is accomplished through the use of non-allele-specific RNAi. This is accompanied by the introduction of a full-length, codon-optimised "replacement" copy of the wildtype gene, whose nucleotide sequence is altered in such a way as to retain the amino acid sequence while abolishing the siRNA recognition site (Kim and Rossi, 2003).

In SCA6, the CAG repeat length of mutant alleles falls within the normal range of other polyQ diseases, making allele-specific approaches based on repeat-length targeting inappropriate. In a cell model of SCA6, transfection of an siRNA capable of silencing both the mutant and wildtype *CACNA1A*, together with an exogenous copy of the gene which is resistant to the gene silencing effector, resulted in restoration of wildtype protein function (Kubodera et al., 2005). A similar approach has subsequently been tested *in vivo*, to restore wildtype SOD1 function in a mouse model of amyotrophic lateral sclerosis (ALS) (Kubodera et al., 2010).

This method has the distinct advantage of being able to circumvent the laborious process of identification and validation of allele-specific siRNAs targeting disease-linked polymorphisms, particularly in diseases where no single sequence change can be targeted in a large number of patients (Kubodera et al., 2010). However, the expression of the restored wildtype protein would need to be tightly regulated, to prevent the development of side effects. In addition, delivery methods would need to be optimised to ensure that every cell treated receives both the RNAi effector and the modified replacement gene, suggesting that this method may not be as straightforward as originally believed (Kubodera et al., 2005).

1.4.1.2 ***Clearance of misfolded mutant protein and inhibition of aggregate formation***

In addition to post-translational suppression, a decrease in mutant protein levels may be achieved by enhancing the rate of polyQ protein clearance, through upregulation of the two main cellular pathways responsible for degradation of misfolded proteins – the ubiquitin-proteasome system (UPS) and autophagy. Impairment of the UPS has been observed in several of the polyQ diseases. However, therapeutic upregulation of this pathway is technically challenging, particularly since aggregation prone-proteins may be poor substrates for degradation by the UPS.

Thus, attention has shifted to the enhancement of autophagy. In the case of HD, activation of autophagy using the mTOR inhibitor rapamycin has been shown to reduce mutant HTT toxicity in both *Drosophila* and mouse models, suggesting that small molecules capable of inducing the autophagic cascade may be of therapeutic benefit (Renna et al., 2010). Similar results have since been achieved in transgenic mice expressing full-length *ataxin-3*, suggesting that induction of autophagy may also be effective in the treatment of SCA3 (Menzies and Rubinsztein, 2010). Phase I clinical trials of this therapeutic approach are due to commence in 2012.

Another approach to the clearance of mutant polyQ proteins is to upregulate the activity of molecular chaperones capable of promoting the refolding of misfolded proteins. Overexpression of heat shock proteins HSP27 and HSP104 have both been shown to suppress neurotoxicity in HD mouse and rat models (Perrin et al., 2007), while global induction of the heat shock response (HSR) has been found to rescue a subset of HD phenotypes in mice. The effects of HSR induction are transient, however, suggesting that impairment of the HSR may occur during polyQ disease progression (Labbadia et al., 2011). These findings emphasise the complexities of targeting the HSR pathway, and provide strong motivation for the development of combinatorial therapies to circumvent impairment of the HSR, such as the use of histone deacetylase (HDAC) inhibitors capable of enhancing HSR gene transcription.

Direct methods of preventing polyQ protein aggregation have also been attempted, using molecules such as Congo red, trehalose, polyQ-binding peptide 1 and cystamine, which act to stabilise the native non-toxic conformation of the protein, prevent crosslinking of the mutant isoform, or promote clearance from the cell via the mechanisms described above. All have demonstrated some therapeutic benefit *in vivo*, although questions regarding efficacy and delivery across the blood-brain barrier remain to be addressed (Bauer and Nukina, 2009).

1.4.2 Therapies targeting downstream effects of polyQ proteins

1.4.2.1 *Transcriptional dysregulation*

A key feature of many of the polyQ diseases is the alteration of gene transcription, either through direct interaction of the mutant protein with DNA, or via the action of molecular mediators such as CREB binding protein (CBP). The inhibition of HDACs, repressors of transcription, has been proposed as a method for mitigating transcriptional dysregulation. A variety of small molecule inhibitors of HDACs have previously been tested as anti-cancer drugs, several of which – including phenyl butyrate, and pimelic diphenylamide – have been shown to rescue disease phenotypes in HD mouse models (Ross and Tabrizi, 2011). In particular, the discovery that R6/2 mice engineered to be deficient in HDAC4 show an improvement in survival, motor phenotype and transcriptional dysregulation suggests that HDAC suppression may be a promising therapeutic route for future exploration.

Upregulation of specific genes known to play a role in neuroprotection (such as *Brain Derived Neurotrophic Factor* in the case of HD), either indirectly, through HDAC inhibitors, or directly, by overexpression of the gene itself, have also shown beneficial effects in animal models of disease. However, this approach requires a thorough understanding of the functions of downstream targets of transcriptional regulation by polyQ proteins, in order to identify the most promising therapeutic targets.

1.4.2.2 *Additional therapeutic approaches*

A number of additional therapeutic approaches have been proposed, which aim to reverse the downstream cellular effects of mutant polyQ proteins. These include compounds capable of alleviating energy metabolism defects or mitigating oxidative stress, such as creatine, antioxidants (including coenzyme Q), and drugs preventing ATP depletion or increasing the activity of

mitochondrial complexes II and III, all of which have demonstrated a level of efficacy in alleviating the mitochondrial dysfunction observed in some models of polyQ disease.

Compounds such as riluzole and remacemide, which mitigate excitotoxicity by intercepting excessive glutamate release, have achieved some success in preclinical studies in R6/2 HD transgenic mice, although these results have not been successfully reproduced in clinical trials (Landwehrmeyer et al., 2007). Anti-apoptotic drugs, such as minocycline and caspase inhibitors have also shown promise, resulting in significant improvements in survival in polyQ animal models, although data from long-term studies will be required in order to rule out possible side effects associated with suppression of these key cellular pathways.

1.5 Models of polyQ disease

The use of model systems is a vital step in understanding the molecular and cellular consequences of human disease mutations. This is particularly true of inherited neurodegenerative conditions with a well-defined genetic aetiology, for which (CNS-derived) biological material is not readily available (Marsh et al., 2009). A considerable number of animal models mimicking the phenotypes of polyQ diseases have become available in recent years (Ingram et al., 2011; Manto and Marmolino, 2009), enabling the identification of pathways affecting disease onset and progression, as well as the genetic and pharmacological validation of therapeutic agents proposed to affect pathogenic processes (Marsh et al., 2009). Among these are *C. elegans* and *D. melanogaster* models of HD, SCA3 and pure polyQ tracts (reviewed in Brignull et al., 2006; Marsh and Thompson, 2006), which have greatly contributed to the growing understanding of the molecular basis of disease (Bilen and Bonini, 2005). Mouse models have been generated for each of the polyQ diseases (Ingram et al., 2011), which recapitulate disease pathology, and display characteristic behavioural phenotypes amenable to quantitative assessment (Marsh et al., 2009). A non-human primate model of HD has also been

reported (Yang et al., 2008). *In vitro*, transfected commercially-available cell lines such as HEK293 and the neuroblastoma line SH-SY5Y (Zander et al., 2001), and patient-derived non-neuronal cells, including fibroblasts (Garden et al., 2002) and lymphoblasts (Tsai et al., 2005) have also provided valuable insights.

These models have been used to identify and validate therapeutic targets, to screen for disease modifiers (Bilen and Bonini, 2007; Marsh and Thompson, 2006), and to investigate the effects of post-translational modifications of disease proteins (Orr and Zoghbi, 2007). Studies in worms, flies and mice have also enabled the dissection of cellular pathways, in order to test their relevance to pathology. For example, the roles of chaperones (Orr and Zoghbi, 2007; Marsh and Thompson, 2006; Landles and Bates, 2004), modifiers of polyQ protein aggregation (Brignull et al., 2006; Marsh and Thompson, 2006), global disruption of the UPS and lysosomal pathways, and miRNA pathways (Bilen et al., 2006), in polyQ pathogenesis have all been identified through the use of model systems.

The choice of disease model depends primarily on the accuracy with which the model reflects the human phenotype and disease processes; and to a lesser extent, on the cost- and time-effectiveness of the model as a therapeutic screening tool (Marsh et al., 2009). Most investigations into the pathogenesis of SCA7 have focused on mouse models of disease, although patient-derived cells models have shown increasing promise as an *in vitro* alternative.

1.5.1 SCA7 mouse models

A number of SCA7 transgenic mouse models have been generated in recent years, many of which have focused primarily on the retina (Ingram et al., 2011). These models have enabled the elucidation of SCA7 retinopathy, leading to the current understanding of Ataxin-7-mediated

downregulation of rod-specific gene expression via histone H3 hyperacetylation (Abou-Sleymane et al., 2006; Helmlinger et al., 2006a).

Transgenic models of SCA7 affecting the mouse CNS may be divided according to whether transgene expression is restricted to Purkinje cells, or more widely distributed (summarised in Table 1). A single knock-in mouse model of the disease has been created to date, carrying a 266Q-repeat (Yoo et al., 2003). These animals developed a severe neurological phenotype as early as 5 weeks of age, despite relatively mild cerebellar pathology. NIs were detected, following the onset of motor symptoms. Downregulation of retinal photoreceptor genes was also observed, together with UPS impairment, with the latter found to be inversely correlated with the presence of NIs (Yoo et al., 2003; Bowman et al., 2005).

There are a number of challenges inherent in modelling human neurodegenerative diseases in mice. Human cases of SCA7, for instance, may have an adult onset, and progress over years or even decades (Ingram et al., 2011). In order to reproduce the disease within the short lifespan of a mouse therefore, additional genetic manipulations may be required, such as the use of abnormally long polyQ repeat tracts (associated with a very distinct phenotype in human patients (Ansorge et al., 2004)), often coupled with overexpression of multiple copies of the disease-causing transgene (Ingram et al., 2011). The result is a severe phenotype, which may not accurately reflect the slow progression of the disease. Thus, animals that overexpress non-mutant alleles should be viewed as essential controls for this approach (Ingram et al., 2011).

Table 1 SCA7 Transgenic Mouse Models

Transgenic Line	Promoter	Repeat Length	Expression Pattern	Cellular Phenotype	Behavioural Phenotype	Reference
P7E	Pcp-2	90Q	Purkinje cells	NI in Purkinje cells, dendritic simplification of Purkinje cells at 16 months	Rotarod deficit at 11 months	(Yvert et al., 2000)
R7E	Rhodopsin	90Q	Rod photoreceptors	Retinal changes, NIs, morphological changes in post-synaptic interneurons	Electroretinographic changes	(Yvert et al., 2000)
B7E2	PDGF chain B	128Q	Cortex, hippocampus, cerebellum, brainstem, inner retina	Ataxin-7 accumulation in nuclei, not restricted to degenerating neurons; transcription factors sequestered in NIs	Ataxia at 5 months	(Yvert et al., 2001)
PrP-SCA7-c92Q	Prion promoter	92Q	No Purkinje cell expression	Retinal degeneration with NIs; somatic atrophy of Purkinje cells; NI in cerebellar granular neurons	Early onset ataxia	(Garden et al., 2002; La Spada et al., 2001)
Gfa2-SCA7	Gfa 2	92Q	Bergmann glia	Decreased glutamate transporter activity; ultrastructural changes in Purkinje cells	Rotarod deficit at 12 months	(Custer et al., 2006)
Ataxin-7-Q52	PDGF chain B	52Q	Neuronal and glial	Mild somatic and dendritic atrophy of Purkinje cells by 11 months; altered gene expression; increased apoptosis	Motor problems at 7 months; rotarod deficit at 9 months	(Chou et al., 2010; Wang et al., 2010)

Q: glutamine residues

Cellular targeting of transgene expression is also an important consideration. Knock-in models, in which the mutant gene remains under the control of the endogenous promoter, are more likely to show involvement of all neuronal populations affected in the human disease. However, in many cases such models have failed to robustly mimic the human phenotype. Nonetheless, they remain vital for biochemical studies, due to the widespread expression of the mutant gene (Ingram et al., 2011).

Transgenic models offer the opportunity to target mutant gene expression to particular tissues of interest, such as the Purkinje cells. Targeting expression to a particular cell type is advantageous, as it allows all observable phenotypes to be correlated with the dysfunction of a distinct cellular population. However, such lines are often unsuitable for biochemical studies, due to the relatively small proportion of cells expressing the transgene, which may result in diluted effects within a tissue sample (Ingram et al., 2011). Since Purkinje cell-specific targeting fails to fully recapitulate human ataxia pathology, such models are less beneficial in evaluating therapeutic strategies, and may only be useful in proof-of-principle and screening experiments (Ingram et al., 2011). More generalised targeting has therefore been used in a number of transgenic models in recent years, often employing the prion protein (PrP) promoter. However, care should be taken when designing and choosing the transgenic construct, as many have been shown not to be expressed in Purkinje cells (Boy et al., 2009; Borchelt et al., 1996; Fischer et al., 1996).

A final consideration in the generation of transgenic models is the use of full-length versus truncated versions of the protein. Although a role for the full-length protein in pathogenesis has been shown for several of the polyQ diseases, studies have also demonstrated the enhanced pathogenicity of shorter fragments, consisting mainly of the polyQ tract (Helmlinger et al., 2006a), again emphasising the importance of the choice of construct in understanding the disease process.

Perhaps the most valuable application of mouse models to date has been to assess therapeutic strategies, including RNAi-based gene silencing (Xia et al., 2004). Such investigations have also enabled the development of sophisticated and effective delivery systems. One such example is the use of recombinant adeno-associated viral vectors capable of sustained suppression of mutant HTT expression both in vitro and in vivo, which have been shown to partially ameliorate both cellular and behavioural manifestations of HD in R6/1 and HD-N171- 82Q transgenic mice (Harper et al., 2005; Rodriguez-Lebron et al., 2005).

The use of transgenic mice in evaluating RNAi therapies is, however, limited by the nature of the models, in which an exogenous mutant gene or gene fragment has been introduced into a model system in which two normal endogenous copies of the gene of interest are already present (Boudreau et al., 2009). In these cases, gene silencing efficacy is evaluated based on the ability of the effector to selectively target the transgene sequence, rather than its ability to distinguish between endogenous pathogenic and normal alleles (Harper et al., 2005). As suppression of a transgene against the background of sustained endogenous gene expression provides little information about the effect of non-allele-specific silencing on the wildtype copy of the gene and hence, of the potential need for allele-specific approaches, the use of transgenic models as a screening tool is currently limited to the evaluation of non-allele-specific gene silencing therapies.

1.5.2 *In vitro* models of SCA7

While lacking the cellular context and measurable behavioural phenotype offered by animal models, *in vitro* disease models offer the unique opportunity to test and develop allele-specific therapeutic modalities. In addition, patient-derived cell models provide the advantage of examining the pathogenic mutation against the patient's own genetic background, in order to identify additional modifiers of disease.

The most rudimentary of *in vitro* models are those derived from commercially-available cell lines, into which constructs containing the disease-causing gene have been transiently transfected. Zander et al. developed two such models for SCA7, using HEK293 and SH-SY5Y cells, respectively (Zander et al., 2001). Both formed Ataxin-7-positive, fibrillar inclusions, and displayed ultrastructural signs of autophagy and nuclear indentation, indicative of a major stress response, in the presence of mutant Ataxin-7. When compared to autopsy samples of SCA7 human brain tissue, the cells displayed similar patterns of nuclear localization and aggregation of Ataxin-7, although the

profile of transcription factors recruited to the NIs differed. The composition of the aggregates also differed in composition with regards to Ataxin-7, with the full-length protein detectable in cell model, but not patient, aggregates. Although the truncated forms of the protein appeared more prone to aggregation in transfected cells, this could be partially explained by differences in expression levels of the truncated versus full-length constructs - an important caveat of this study, and of the use of transfected cell models in general (Zander et al., 2001).

The recent development of stable, inducible cell PC12 cell lines expressing N-terminal FLAG- and C-terminal GFP-tagged Ataxin-7 containing either ten (FLQ10) or 65 (FLQ65) glutamines, under the control of the Tet-off system, represents a distinct improvement over transiently transfected models (Yu et al., 2012). These cell lines, which express wildtype or mutant Ataxin-7 at similar levels following the removal of doxycycline from the culture medium, can be readily manipulated to explore the effects of mutant protein levels on cellular toxicity. Indeed, these models have already provided valuable insights into the aggregation and turnover of polyQ-expanded Ataxin-7, as well as its role in the induction of oxidative stress (Ajayi et al., 2012; Yu et al., 2012). They have also been used to evaluate the efficacy of existing therapies for polyQ disease, such as antioxidants and pharmacological activators of autophagy (Ajayi et al., 2012; Yu et al., 2012).

Transfected cell models have also proven extremely useful in the development of allele-specific RNAi-based therapy for SCA7. A study by Scholefield et al. in 2009 demonstrated the ability of an allele-specific shRNA to selectively suppress expression of mutant *ataxin-7* in transfected HEK293 cells, based on the presence of a disease-linked SNP, resulting from a founder effect in the South African SCA7 patient population (Scholefield et al., 2009; Greenberg et al., 2006). Expression of the wildtype construct, by contrast, was not affected.

Such studies provide a valuable proof-of-concept regarding the efficacy of allele-specific RNAi therapy for SCA7. However, they offer little information about the restoration of wildtype function, or the alleviation of other cellular markers of disease, emphasising the need for further studies in more physiologically relevant models (Scholefield et al., 2009).

Patient-derived primary cells are well-established as models of disease pathogenesis and as screening tools for potential therapies. Neurodegenerative diseases, however, face a choice between readily-available cells from "unaffected" tissues (such as dermal fibroblasts and peripheral blood lymphoblasts), and the disease-relevance afforded by CNS tissues, infrequently harvested at autopsy from consented individuals.

A key breakthrough has been the identification of a cellular phenotype in cells previously believed to be unaffected in neurodegenerative disease. In HD in particular, the discovery of proteasome impairment (Seo et al., 2004) and RNA toxicity (de Mezer et al., 2011) in patient fibroblasts has strengthened the argument in favour of their use for RNAi screening (Gagnon et al., 2010; Van Bilsen et al., 2008; Zhang et al., 2009).

In SCA7, patient fibroblasts have been shown to express an N-terminal truncated fragment of mutant Ataxin-7, similar to that found in patient brain tissue, and in PrP-SCA7-c92Q transgenic mice (Garden et al., 2002). Most recently, SCA7 fibroblasts have been used to confirm the presence of a regulatory antisense transcript associated with CTCF-mediated regulation of *ataxin-7* gene expression (Sopher et al., 2011). To date, however, there have been no investigations into the presence of transcriptional dysregulation in these patient cells. (The role of fibroblasts in understanding SCA7 pathogenesis and therapy is discussed in more detail in Chapter 3, Section 3.1.)

1.5.2.1 ***Induced pluripotent stem cell-derived models***

Since the first derivation of human embryonic stem cells (ESCs), the inherent properties of pluripotent cells, namely their ability to propagate indefinitely without commitment *in vitro*, and their capacity to differentiate into cell lineages belonging to the three germ layers, have made them an attractive source of cells for basic research, as well as regenerative medicine (Drews et al., 2012; Thomson et al., 1998). However, ethical and immune rejection concerns arising from the use of stem cells derived from human blastocysts have prompted research into alternative sources of pluripotent cells.

Although once believed to arise through the progression of distinct developmental stages in strict temporal order, mammalian development is now widely regarded as being epigenetically regulated and thus, reversible (Yu et al., 2007). The results of seminal somatic cell nuclear transfer experiments demonstrated that nuclei from differentiated amphibian and mammalian cells could be reprogrammed to an undifferentiated state by trans-acting factors present in the cytoplasm of the recipient oocyte (Wilmut et al., 1997; Gurdon 1962). This led to a search for factors which might mediate similar reprogramming without the need for nuclear transfer.

The generation of embryonic stem cell (ESC)-like cells, termed "induced pluripotent stem cells" (iPSCs), from mouse and human fibroblasts using the defined factors *OCT3/4, SOX2, c-MYC* and *KLF4*, or *OCT4, SOX2, NANOG* and *LIN28*, was first described in 2006 and 2007 (Takahashi et al., 2007; Yu et al., 2007; Takahashi and Yamanaka, 2006). These findings have subsequently been replicated in several studies, confirming the ability of both four-factor combinations of transcription factors to reprogram differentiated human cells to a pluripotent state, and opening up exciting new opportunities in the field (Maherali et al., 2007; Okita et al., 2007; Park et al., 2007; Wernig et al., 2007). The potential of iPSCs to differentiate into almost any cell type has also been widely

exploited; notably in the derivation of neurons from patients with a variety of neurodegenerative conditions (Koch et al., 2011; Zhang et al., 2010; Dimos et al., 2008; Ebert et al., 2008).

Dimos et al. (2008) provided the first evidence that iPSCs could be generated directly from elderly patients with chronic disease – in their case, an 82-year old female patient with familial ALS. Patient fibroblasts were retrovirally transduced with the reprogramming factor combination *OCT4/SOX2/KLF4/c-MYC*, and gave rise to colonies with a distinctive ESC-like morphology after approximately three weeks in culture. Colonies displayed typical ESC markers, and could spontaneously differentiate into representative phenotypes of the three embryonic germ layers, a hallmark of pluripotency. Furthermore, using an established protocol which recapitulates aspects of spinal motor neuron differentiation, iPSCs could be differentiated to a spinal motor neuron phenotype, expressing key motor neuron markers such as HB9. However, the cells failed to display any disease-associated phenotypic changes (Dimos et al., 2008).

A similar approach was followed by Ebert et al. (2008), who sought to address the major spinal motor neuron disease of childhood, spinal muscular atrophy (SMA), caused by a genetic mutation in the survival motor neuron-1 gene (*SMN1*). In this case, fibroblasts from a single patient and his unaffected mother were transduced with lentiviral constructs containing the reprogramming factors *OCT4/SOX2/NANOG/LIN28*, resulting in the generation of iPSCs which could be differentiated into a variety of different cell types, including cells with a spinal motor neuron phenotype. Over time, these iPSC-derived motor neurons were shown to reduce in size and number in patient cultures versus controls. In addition, patient iPSCs showed a deficiency in nuclear SMN protein aggregates similar to that observed in the disease, which could be ameliorated by treatment with VPA or tobramycin – known chemical inducers of SMN protein expression (Ebert et al., 2008).

At the time of initiation of this study, no iPSC-derived models were available for SCA7. The generation of iPSC-derived neurons from a single adult SCA7 patient in China, carrying 45 CAG repeats, has subsequently been reported (Luo et al., 2012). However, there is currently no data available concerning the presence of a cellular phenotype in these neurons. Furthermore, no iPSC-derived models have yet been generated from patients in South Africa, a country with a uniquely high number of SCA7 affected individuals, and a disease-linked SNP ideally suited to therapeutic targeting. Indeed, the importance of iPSC-based research in African populations cannot be overstated, as the high degree of structural and population genetic diversity provide a unique opportunity to dissect genetic risk for both infectious and complex diseases through the generation of iPSC lines which represent a vast spectrum of human genetic variation (Fakunle 2012).

(The importance of iPSC-derived models for neurodegenerative disease is addressed in more detail in Chapters 4 and 5).

1.6 Aims and objectives

This project aimed to establish and evaluate patient-derived cell models of SCA7, to be used in the investigation of the molecular pathogenesis of SCA7 (with particular reference to transcriptional dysregulation), and in the evaluation of previously-developed therapies for the disease.

1.6.1 Objectives

The objectives of the investigation were as follows:

1. To investigate the presence of disease-associated transcriptional changes in SCA7 patient fibroblasts, using a candidate gene approach.
2. To evaluate the efficacy of a previously-designed siRNA therapy for SCA7 in patient fibroblasts, with particular reference to the restoration of observable transcriptional changes.
3. To establish and characterise induced pluripotent stem cell (iPSC) lines derived from SCA7 patient fibroblasts.
4. To differentiate these iPSCs into neurons using established protocols.
5. To investigate the presence of transcriptional changes in SCA7 iPSCs and iPSC-derived neurons.

Chapter 2 **Materials and Methods**

2.1 Ethics approval and patient recruitment

Ethics approval for the study was granted by the University of Cape Town (UCT) Faculty of Health Sciences Human Research Ethics Committee (REC REF. 380/2009 and 460/2010), and was renewed annually, incorporating amendments to the project protocol where necessary. Confirmation of ethics approval, together with an example of a patient information sheet and consent form, can be found in Appendix 1.

Suitable patients were identified from the UCT Division of Human Genetics DNA database, based on a positive diagnosis for SCA7, and the availability of contact details. Two patients were enrolled in the study once they had given written informed consent to participate.

Patient 1518 is a 44-year old affected female of Black African origin, with a recorded CAG repeat expansion length of 42 at diagnosis, and a reported age of onset of approximately 29 years. Patient 1519 is the son of patient 1518, a 25 year old male of Black African origin, with a recorded CAG repeat expansion of approximately 51 repeats, and an age of onset of approximately 14 years.

2.2 Establishment of primary fibroblast cultures

Primary fibroblast cultures were established from punch skin biopsies taken from the two patients who had consented to participate in the study, as previously described (Freshney, 2010). Control fibroblast lines were obtained from Lonza (Basel, Switzerland). The control designations are as follows: “SC Con”: Lonza CC-2511, lot 0000086510, a 44 yr old female of Caucasian origin; “JS Con”: Lonza CC-2611, lot 0000160309, a 51 year old female of Caucasian origin; “BA Con”: Lonza CC-2511, lot 0000237203, a 33 year old female of Black African origin. An additional SCA7

fibroblast line was obtained from the cell repositories of the Coriell Institute for Medical Research (Camden, New Jersey, USA), and was designated "SCA7 Coriell" (GM03561, a 22 year old female of Black African origin). A summary of the fibroblast cell lines used in this study can be found in Table 2.

Table 2 Summary of patient and control fibroblast cell lines used in this study

Fibroblast line	$(CAG)_{exp}$	Age	Sex	Ethnicity	Age at Disease Onset	Clinical data
1518	42	44yrs	F	Black African	29yrs	Impaired mobility from 22yrs
1519	51	25yrs	M	Black African	14yrs	Ocular symptoms from 14yrs
SCA7 Coriell	55	22yrs	F	Black African	Unknown	Positive family history
JS Con	N/A	44yrs	F	Caucasian	N/A	N/A
SC Con	N/A	51yrs	F	Caucasian	N/A	N/A
BA Con	N/A	22yrs	F	Black African	N/A	N/A

$(CAG)_{exp}$: Number of CAG repeats on expanded (mutant) allele; N/A: not applicable

Cells were cultured in GIBCO Dulbecco's Modified Eagle Medium (DMEM) (Life Technologies, Carlsbad, California, USA), supplemented with 10% (v/v) Foetal Calf Serum (Life Technologies), and 1X Antibiotic/Antimycotic containing Penicillin, Streptomycin and Amphotericin B (Life Technologies) (hereafter referred to as DMEM+10% FCS+1X antibiotic/antimycotic). Cells were maintained at 37°C in a humidified atmosphere with 5% CO_2. Media was replaced every 3-5 days. General protocols and reagents for cell culture can be found in Appendix 2.

2.3 DNA isolation

DNA used for the confirmation of disease status was extracted from whole fresh blood samples using the PUREGENE Genomic DNA Isolation Kit (Gentra Systems, Minneapolis, Minnesota, USA). DNA extraction from cultured cells was performed using the DNeasy Blood and Tissue Kit (QIAGEN, Hilden, Germany), following the manufacturer's instructions. After extraction the quality and quantity of DNA was assessed using a NanoDrop spectrophotometer (Thermo Scientific, Wilmington, Massachusetts, USA). Samples with an A_{260}/A_{280} absorbance ratio of 1.8 to 2.0 were stored at -20°C for further experiments.

2.4 RNA isolation and cDNA synthesis

RNA was isolated from cultured cells using the HighPure RNA Isolation Kit (Roche Diagnostics, Basel, Switzerland), as per the manufacturer's instructions. The quality and quantity of RNA was assessed using a NanoDrop spectrophotometer (Thermo Scientific). Samples with an A_{260}/A_{280} absorbance ratio of 1.8 to 2.0 were stored at -80°C for further experiments.

Synthesis of cDNA was performed using the Applied Biosystems High Capacity cDNA Reverse Transcription Kit (Life Technologies) as per the manufacturer's instructions, using 500ng-1µg template RNA, together with 1X reverse transcriptase (RT) Buffer, 4mM dNTPs, 1X random RT primers and 1µl MultiScribe reverse transcriptase, in a final reaction volume of 20µl. The reaction conditions were as follows: 10min at 25°C, 2hrs at 37°C, and 5min at 85°C.

2.5 CAG repeat length determination

The length of the disease-causing CAG repeat in *ataxin-7* was determined from DNA by means of polymerase chain reaction (PCR) and automated fluorescent genotyping. The PCR reaction mix consisted of 0.4µM each, forward and reverse primer (Appendix 3, A3.1), 0.6units of GoTaq DNA polymerase (Promega, Madison, WI, USA), 100ng of DNA, and Failsafe buffer J (Epicentre Biotechnologies, Madison, WI, USA) at a final concentration of 1X, made up to a final reaction volume of 10µl. Cycling conditions were as follows: 95°C for 5min; followed by 30 cycles of 95°C for 30 seconds, 53°C for 6 seconds and 72°C for 40 seconds; and a final elongation step at 72°C for 7min. To confirm the presence of a product, an aliquot (usually 5µl) of each PCR reaction was resolved on a 2% (w/v) agarose gel, containing 500ng/ml Ethidium Bromide (Sigma-Aldrich, St Louis, MO, USA), for approximately 40min, at 160V, before visualisation under UV light, using the UVIPro Gel Documentation System (UVITec, Cambridge, UK). Images were acquired using UVIPro software v12.3 for Windows (Copyright 1999-2005 UVITec). To determine the relative

molecular mass of the bands observed, 500ng of the Gene Ruler 100bp DNA Ladder Plus Molecular Weight Marker *Improved* (Fermentas International Inc., Burlington, Canada) (Appendix 3, A3.2) was included as a size standard.

Automated fluorescent genotyping was performed using the ABI PRISM 3100*xl* Genetic Analyzer (Applied Biosystems by Life Technologies). Samples were prepared by mixing 1µl of PCR product with 8µl HiDi formamide (Applied Biosystems) and 0.4µl of the size standard GeneScan 500 ROX (Applied Biosystems), and denatured for 5min at 95°C, before snap-cooling on ice. Genotyping results were collected using ABI PRISM 3100 Data Collection software (Applied Biosystems) and analysed using the ABI PRISM GeneMapper software v3.0 (Applied Biosystems).

The length of the CAG repeat [$(CAG)_n$] was approximated using the following equation, adapted from Dorschner et al. (2002):

$$n = \frac{(0.3063 \times \text{Length of major PCR product in base pairs}) - 76.475\text{bp}}{3}$$

where the major PCR product was defined as the product generating the highest fluorescent peak, as detected using the ABI PRISM 3100*xl* Genetic Analyzer. A repeat in the pathogenic range was defined as any allele with a repeat length >36 (Lebre and Brice, 2003; Einum et al., 2001).

2.6 SNP genotyping

To determine the alleles of the disease-linked SNP (rs3774729) present in each patient, PCR was performed using the standard reaction mix and conditions outlined in Appendix 3 (A3.3 and 3.4), with an annealing temperature (T_a) of 61°C. The primers for this reaction are also listed in Appendix

3 (A3.1). An aliquot of the resultant PCR product was electrophoresed on a 1% (w/v) agarose gel as described in Section 2.5.

Depending on the efficiency of PCR, between 3 and 8µl of PCR product was then subjected to cycle sequencing using the ABI PRISM BigDye Terminator v3.1 Cycle Sequencing Kit (Applied Biosystems), following the manufacturer's instructions outlined in the Automated DNA Sequencing Chemistry Guide (Applied Biosystems, Copyright 1998). The reaction mix consisted of 0.5µM of the reverse primer, 2µl BigDye Terminator Mix (Applied Biosystems), and 4µl BigDye Sequencing Dilution Buffer, made up to a final volume of 20µl. Reaction conditions were as follows: 96°C for 5min; followed by 30 cycles of 96°C for 30 seconds, 50°C for 15 seconds and 60°C for 4min.

Following cycle sequencing, the amplified DNA was purified from contaminating reagents (such as dNTPs, excess primer or DNA polymerase) by subjecting the reaction mixture to ethanol precipitation. Two microlitres of 1.5M Sodium Acetate (pH>8, 250mM EDTA) (Atria Genetics, San Francisco, California, USA) and 2.5 volumes of 100% ethanol were added to the reaction mixture, which was then incubated at -20°C for at least 2 hours. This mixture was centrifuged for 10min at 10 000rpm using a standard benchtop microcentrifuge. The supernatant was discarded, and the pellet resuspended in 20µl 70% ethanol, followed by a second centrifugation step for 10min at 10 000rpm. The supernatant was again discarded, and the pellet left to air dry for at least 1 hour at room temperature. Finally, the pellet, containing purified, amplified DNA for sequencing, was resuspended in 10µl Hi-Di formamide.

Automated sequencing was performed on the ABI PRISM® 3100 Genetic Analyzer (Applied Biosystems) at 60°C, using the POP-7 separation polymer (Applied Biosystems). Sequencing results were collected using ABI PRISM 3100 Data Collection software (Applied Biosystems), and

analysed initially using Sequencing Analysis v3.7 software (Copyright 1989-2001, Applied Biosystems). The sequences generated for each sample were edited, reverse complemented, and aligned with the reference sequence (obtained from NCBI) using the ClustalW Multiple Alignment accessory application available in BioEdit Sequence Alignment Editor v7.0.0 (Hall, 1999).

2.7 Neon transfection (RNAi)

Transfection of control and patient (1519) fibroblasts with siRNA was performed using the Neon Transfection System (Life Technologies), following manufacturer's instructions. Briefly, aliquots of three siRNAs – siR-atxn7 (targeting both alleles of the *ataxin-7* transcript), siR-p16 (targeting the mutant allele) and siR-NS (a non-specific siRNA kindly provided by Dr Christopher Sibley, University of Cambridge) – were prepared, at concentrations of 20nM, 5nM and 1nM, in sterile distilled water. The siRNA sequences can be found in Appendix 3 (A3.5). Fibroblasts, cultured as described in Section 2.2, were dissociated in TrypLE (Life Technologies), centrifuged at 1500rpm for 5min in a standard benchtop centrifuge, and resuspended in phosphate buffered saline (PBS) (Life Technologies) at a concentration of $6x10^5$ cells/ml. One millilitre aliquots of the cell suspension were decanted into microcentrifuge tubes and centrifuged for a further 3min at 1000rpm, in a standard benchtop microcentrifuge. The supernatant was aspirated, and cells were resuspended in Buffer R before being mixed with aliquotted siRNA immediately prior to electroporation. Electroporation was performed in triplicate at the following settings: Volts: 1700, Width: 20; Pulse Number: 1. Transfected fibroblasts were seeded onto poly-L-lysine (Life Technologies) coated 6-well plates in antibiotic-free DMEM + 10% FCS and incubated at 37°C, 5% CO_2 for 24 hours, before being changed to DMEM+10% FCS+1X antibiotic/antimycotic. RNA was harvested seven days after transfection, as described in Section 2.4.

2.8 Real-time quantitative PCR

Real-time quantitative PCR (qPCR) was performed on the Applied Biosystems StepOne Plus Real-time PCR System (Life Technologies), using the Power SYBR Green PCR Master Mix (Applied Biosystems). Primers (listed in Appendix 3, A3.6) were obtained from PrimerDesign Ltd (Southampton, UK), IDT (Leuven, Belgium), or Sigma-Aldrich.

The reaction mix for all qPCRs was as follows: 10µl of Power SYBR Green PCR Master Mix (Applied Biosystems), 1µl of PrimerDesign Primer Mix (if PrimerDesign primers were used), or 125nM each of forward and reverse primer (if IDT primers were used), and 10ng of sample cDNA, made up to a final volume of 20µl with sterile distilled water.

Relative quantities of target mRNA were determined using the relative standard curve method. Standard curves were prepared for each primer pair, from serial dilutions of pooled sample cDNA. Universal cycling conditions were used (95°C for 10min, followed by 40 cycles of 95°C for 15 seconds and 60°C for 1min). PCRs were performed in technical duplicate or triplicate, on at least three biological replicates, and results analysed using the StepOne Software v2.1 (Applied Biosystems). Gene of interest expression was normalised to β-Actin expression in each case.

The design and reporting of qPCR experiments aimed to comply with the Minimum Information for publication of Quantitative real-time PCR Experiments guidelines (Taylor et al., 2010; Bustin et al., 2009) as far as possible.

2.9 Generation and characterisation of patient-derived iPSCs

The iPSC lines used in this study were generated in collaboration with Dr Sally Cowley and Ms Jane Vowles (James Martin Stem Cell Facility, Sir William Dunn School of Pathology, University of

Oxford), and Dr Janine Scholefield (Gene Expression and Biophysics Laboratory, CSIR, Pretoria/ Department of Physiology, Anatomy and Genetics, University of Oxford). Their kind provision of protocols for this section is hereby acknowledged.

2.9.1 Bulk preparation of plasmids containing reprogramming and viral packaging genes

The pMXs-hKlf4 (plasmid # 17219), pMXs-hSox2 (# 17218), pMXs-hOct3/4 (# 17217) and pCMV-VSV-G (# 8454) plasmids, as well as pMXs-hc-Myc (# 17220) and pMXs-Nanog (# 13354) (in the case of iPS SC NHDF), were obtained from Addgene (Cambridge, MA, USA) (Takahashi et al., 2007; Takahashi and Yamanaka, 2006; Stewart et al., 2003). Bulk stocks of each plasmid were obtained by transformation into competent DH5α *Escherichia coli* cells grown on ampicillin selective agar plates, followed by preparation using the EndoFree Plasmid Maxi Kit (QIAGEN), following manufacturer's instructions.

2.9.2 Preparation of retroviral vectors

The Platinum-GP (Plat-GP) retroviral packaging cell line (Cell Biolabs, San Diego, California, USA) was used in the production of retroviral vectors for reprogramming. For routine cell culture, Plat-GP cells were maintained in DMEM+10% FCS+1X antibiotic/antimycotic (all Life Technologies), containing 10µg/ml blasticidin (Sigma-Aldrich), at 37°C, 5% CO_2.

At Day 0, Plat GP cells were seeded at a density of approximately 14 million per T175 flask, in DMEM+10% FCS+1X antibiotic/antimycotic (all Life Technologies), and incubated overnight at 37°C, 5% CO_2. No blasticidin was added to the culture medium from this point onwards.

On Day 1, the following transfection mix was prepared for each of the pMXs plasmids:

Tube A:

42µg pMXs plasmid (i.e. pMXs-hKlf4, -hSox2 -hOct3/4, -hc-Myc or -Nanog)

28µg pCMV-VSV-G (envelope plasmid)

Made up to 8.1ml with DMEM (containing no serum or antibiotic/antimycotic)

Tube B:

191ul 10µM polyethylenimine (PEI) (Sigma-Aldrich)

7.98ml DMEM

The contents of tube B were added to tube A in a dropwise fashion with constant mixing, and incubated for 20min at room temperature. The media on the Plat-GP cells, which were by then 70-80% confluent, was replaced with the transfection mix, and the cells were incubated for four hours at 37°C, 5% CO_2. The transfection mix was then aspirated and replaced with blasticidin-free culture media, and the cells incubated for 48hrs at 37°C, 5% CO_2.

Supernatant from the cultured Plat-GP cells was harvested at 48 and 72 hrs post-transfection, pooled, and centrifuged at 1500rpm for 5min in a standard benchtop centrifuge, to remove cellular debris. The supernatant was then filtered through a 0.45µm low-protein binding filter (Millipore, Billerica, MA, USA).

To concentrate the virus, pooled supernatants were decanted into sterile 25mm x 99mm Ultraclear ultracentrifuge tubes (Beckman Coulter, Fullerton, California, USA), and centrifuged for 90min at 25 000rpm, at 4°C, in a Beckman L8-80M ultracentrifuge (Beckman Coulter, SW28 rotor). The pellet was resuspended in a small volume of ice-cold sterile PBS (Life Technologies) to give a

concentration of greater than 100X, and incubated for 1 hour on ice before aliquotting for storage at -80°C.

2.9.3 Determination of viral titre

To determine viral titre, HEK293 cells (seeded at 30 000 cells/well in a 24-well format, and incubated overnight at 37°C, 5% CO_2) were infected with a virus cocktail consisting of 10µl concentrated virus stock and 5µg/ml polybrene (Sigma-Aldrich) in a total volume of 1ml DMEM+10% FCS+1X antibiotic/antimycotic (all Life Technologies). Plates containing infected cells were centrifuged at 1200xg for 45min at 15°C, and incubated for 72hrs at 37°C, 5% CO_2. In parallel, HEK293 cells transfected with 430ng of each plasmid (pMXs-hKlf4, -hSox2, -hOct3/4or -hc-Myc), mixed with 6µl PEI (Sigma-Aldrich) were included as positive controls. Medium was changed 4hrs after transfection.

After 72hrs, the infected and transfected cells were washed with PBS, and fixed in 4% (w/v) paraformaldehyde in FACS buffer (Appendix 3, A3.7) at room temperature for 10min. The cells were then permeabilised in FACS buffer + 0.1% (v/v) saponin (Sigma-Aldrich) + 10% serum (specific to the species in which the secondary antibody was raised), at room temperature for 40min. Cells were incubated with primary antibody (10µg/ml in FACS buffer+0.1% (v/v) saponin) at room temperature for 1-2hrs, washed, and incubated with secondary antibody (10µg/ml in FACS buffer+0.1% (v/v) saponin) for 1hr at room temperature, protected from light. Following counterstaining with DAPI, cells were washed and fixed in 4% formaldehyde in FACS buffer (Fig. 5). Antibodies used are listed in Appendix 3 (A3.8).

Viral titre was calculated using the following equation:

Number of infectious particles per ml = (% of infected cells x total number of HEK293 cells seeded into well) x100

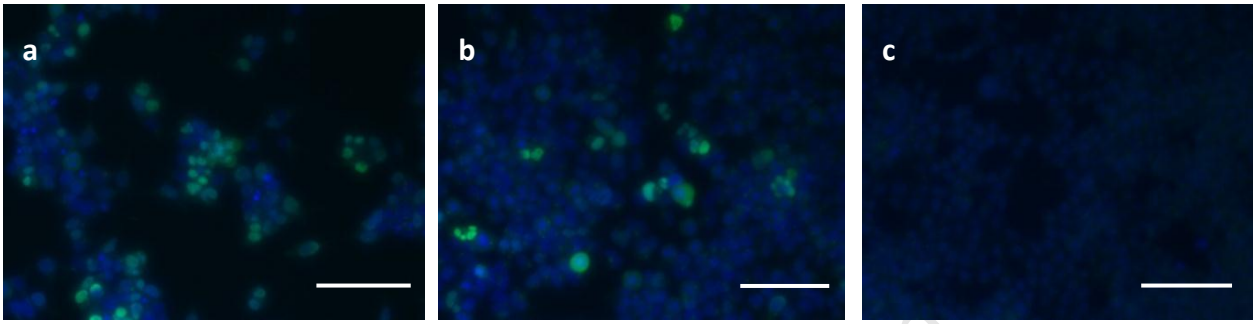

Figure 5 Immunostaining to calculate retroviral titre. (a) HEK293 cells infected with 10µl of concentrated pMXs-hKlf4-retrovirus stock were subjected to immunostaining for Klf4 (green) 72hrs post-infection to determine the viral titre for subsequent reprogramming experiments. (b) Cells transfected with the reprogramming gene plasmid were used as a positive control. (c) Untransfected cells served as a negative control. Nuclei are stained with DAPI (blue). Scale bar: 100µm.

2.9.4 Reprogramming fibroblasts to iPSCs

Reprogramming of patient and control fibroblasts to iPSCs was based on the protocol outlined by Takahashi et al., 2007. The SCA7 and iPS George (control) iPSC lines used in this study were generated using the method described below. The control line iPS SC NHDF was generated by collaborators Dr Sally Cowley and Ms Jane Vowles following a similar protocol, using a combination of five reprogramming factors – *OCT4*, *SOX2*, *KLF4*, *c-MYC* and *NANOG*.

Primary fibroblasts from either patient or control individuals were plated at a concentration of 50 000 cells/well in a 6-well format (Day 0). After 24hrs (i.e. on Day 1), fibroblasts were infected with the concentrated virus stock (Section 2.9.3), at a multiplicity of infection (MOI) of approximately 1,

diluted in DMEM+10% FCS+1% antibiotic/antimycotic (all Life Technologies), containing 5µg/ml polybrene (Sigma-Aldrich). A second infection was performed 24hrs later (Day 2).

On Day 3 (48hrs after the first infection), virus-containing medium was replaced with DMEM+10% FCS+1X antibiotic/antimycotic (all Life Technologies), and cells were incubated for a further 48hrs. On Day 5, infected fibroblasts were trypsinised, and re-seeded onto a previously-prepared inactivated mouse embryonic fibroblast (iMEF) feeder layer (Appendix 4, A4.2 and 4.3) at a concentration of approximately 8 000 cells/well, in DMEM+10% FCS+1X antibiotic/antimycotic (all Life Technologies). An aliquot of fibroblasts from each line was seeded in iMEF-free conditions to determine the efficiency of infection, using the immunostaining protocol outlined in Section 2.9.3.

On Day 6, media on the fibroblast/iMEF plates was removed and replaced with human embryonic stem cell medium (huESC medium – see Appendix 4, A4.1). From Day 7 to Day 13, a half-medium change (i.e. removal of half the volume of culture medium and replacement with half the volume of fresh medium) was performed every second day. Valproic acid (VPA), at a final concentration of 2mM, was included in the medium for the first 10 days post-infection. Thereafter, medium was replaced every day with fresh, sterile-filtered iMEF-conditioned huESC medium (Appendix 4, A4.4), supplemented with 10ng/ml basic fibroblast growth factor (bFGF, R&D Systems, Minneapolis, Minnesota, USA). In most cases, iPSC colonies were observed approximately 20 to 40 days post-infection, whereupon they were manually dissected using a pulled-glass pipette, and subcultured as described in Section 2.9.5.

2.9.5 iPSC maintenance culture

In the case of iPSC colonies grown on an iMEF feeder layer, manual dissection was performed approximately once every 7 days. Colonies were split in an approximate ratio of 1:4, and cultured in

huESC medium (Appendix 4, A4.1) at 37°C, 5% CO_2. A detailed protocol for the preparation of iMEF feeders can be found in Appendix 4 (A4.2 and 4.3).

In preparation for DNA or RNA isolation or the formation of embryoid bodies (see Section 2.9.6.4), iPSCs were transitioned from growth on an iMEF feeder layer to growth in feeder-free conditions, on the commercially-available growth matrix, Matrigel (BD Biosciences, Franklin Lakes, New Jersey, USA). Matrigel-coated plates were prepared according to the manufacturer's instructions. Details of the conversion of iPSCs from growth on iMEF feeders to feeder-free culture can be found in Appendix 4 (A4.5).

Where iPSCs had been grown on Matrigel (BD Biosciences), cells were dissociated every 5-7 days using TrypLE (Life Technologies) and re-plated at a concentration of approximately $5x10^5$ cells/well in supplemented mTeSR medium (Stem Cell Technologies, Vancouver, Canada), containing 10µM Rho-Kinase inhibitor Y-27632 (Sigma Aldrich), as described in Appendix 4 (A4.6).

Half (in the case of iPSCs on iMEF feeders) or full (in the case of iPSCs grown in feeder-free conditions) medium changes were performed every day.

2.9.6 iPSC characterisation

2.9.6.1 *Expression of exogenous and endogenous pluripotency genes*

The expression levels of exogenous and endogenous pluripotency genes were measured by endpoint RT-PCR, using the primers listed in Appendix 4 (A4.7 and 4.8). The reaction mix in each case was as follows: 200nM each of forward and reverse primer, 200µM PCR Nucleotide Mix (Roche), 1 unit of *Taq* DNA Polymerase (New England Biolabs, Ipswich, MA, USA), 1x ThermoPol Buffer (New

England Biolabs) and 50ng template cDNA, made up to a final volume of 25µl with sterile distilled water. No RT controls were included where necessary.

The standard PCR cycling conditions (Appendix 3, A3.4) were used, and expression was determined by electrophoresis of the PCR product on a 1% (w/v) agarose gel incorporating 500ng/ml Ethidium Bromide, as described in Section 2.5.

2.9.6.2 ***Expression of pluripotency markers***

The expression of pluripotency markers was determined by subjecting iPSC colonies grown on iMEF feeder layers to immunofluorescence staining as follows:

Cells were fixed in 4% paraformaldehyde for 15min at room temperature. Blocking was performed in a solution of 10% (v/v) serum (specific to the species in which the secondary antibody was raised) in PBS + 0.1% (v/v) Triton X-100 for 1-3hrs at room temperature. Cells were then incubated with primary antibody (see Appendix 3, A3.8), at a dilution of between 1:100 and 1:500 in 1% (v/v) serum + PBS+ 0.1% (v/v) Triton X-100, overnight at 4°C. After washing three times for 10min each in PBS+ 0.1% (v/v) Triton X-100, cells were incubated with secondary antibody (Appendix 3, A3.8), diluted 1:500 in 1% (v/v) serum + PBS+ 0.1% (v/v) Triton X-100, for 1hr at room temperature, protected from light. This was followed by a further three washes for 10min each in PBS. Where used, a nuclear stain (either DAPI or Hoechst, at 500ng/ml) was added to the PBS during the second wash. In the case of cells fixed to coverslips, coverslips were mounted onto microscope slides using FluoroMount G (Southern Biotech, Birmingham, Alabama, USA), and sealed with clear nail varnish, prior to visualisation. Mounted slides were stored at 4°C, protected from light, to prevent loss of immunofluorescence.

2.9.6.3 ***Genomic integrity***

The genomic integrity of iPSC lines generated in Section 2.9.4 was assessed using the Infinium HD assay, on HumanCytoSNP-12v2.1 bead-chips (Illumina, San Diego, California, USA), at the Wellcome Trust Centre for Human Genetics, University of Oxford, Oxford, UK. DNA extracted from iPSCs, and the fibroblast lines from which they had been derived, was quantified using the Quant-iT PicoGreen dsDNA Assay Kit (Life Technologies), following the manufacturer's instructions. The final concentration of DNA was adjusted to 50ng/µl in TE (10mM Tris, 1mM EDTA) solution, and 200 to 500 ng of high quality genomic DNA with an $A_{260/280}$ ratio of 1.65-2.1 was subjected to array analysis.

Genomestudio software (Illumina) was used to carry out quality control checks of the procedure, and Karyostudio software (Illumina) was used to provide final reports.

Standard G-banding chromosome analysis was performed for a single control iPSC line (iPS George), and its parental fibroblast line (JS Con), at Unistel Medical Laboratories (Cape Town, South Africa).

2.9.6.4 ***In vitro differentiation from embryoid bodies***

Embryoid bodies (EBs) were generated from using $5x10^6$ iPSCs cultured on Matrigel (BD Biosciences) in mTeSR medium (Stem Cell Technologies) using Aggrewell 800 plates (Stem Cell Technologies), following the manufacturer's instructions,. EBs were cultured in mTeSR medium + 10mM Rho-Kinase Inhibitor (Sigma-Aldrich), and a 75% medium change was performed daily for three days. For undirected differentiation, EBs were harvested on day 4 using a 40µm cell strainer, and transferred to ultra low attachment plates in mTeSR medium (Stem Cell Technologies). Media was changed every second day. After eight days of suspension culture, EBs were transferred to

gelatin-coated plates and cultured for a further 8 days. RNA was isolated from each cell line in triplicate (as described in Section 2.4), and expression of germ-layer specific markers (endoderm: *FOXA2* and *AFP*, mesoderm: *MSX1*, ectoderm: *PAX6* and *MAP2*) was assessed by endpoint RT-PCR, as described in Section 2.9.6.2. Primers are listed in Appendix 4 (A4.9).

Directed differentiation was performed as follows (protocol adapted from the Barcelona Stem Cell Bank): For endoderm, mTeSR medium was replaced with EB medium (Appendix 4, A4.1) after 24hrs of EB formation, and EBs were cultured for a further 2-3 days in suspension. EBs were then seeded into gelatin-coated slide flasks in EB medium, and cultured for a further 15-20 days, with medium changed every 2-3 days.

For mesoderm, mTeSR medium was replaced with EB medium supplemented with 0.5mM ascorbic acid, after 24hrs of EB formation, and EBs were cultured for a further 2-3 days in suspension. EBs were then seeded into gelatin-coated slide flasks in EB medium supplemented with 0.5mM ascorbic acid, and cultured for a further 15-20 days, with medium changed every 2-3 days.

Differentiation into ectoderm was assessed by the ability of the iPSC lines to differentiate into neuronal cells, as described in Section 2.10.

To confirm the expression of germ-layer specific markers, EBs were subjected to immunofluorescence staining for germ layer-specific markers as described in Section 2.9.6.3. Markers and antibodies are listed in Appendix 3 (A3.8).

2.10 Neuronal differentiation from iPSCs

The differentiation of iPSCs into neurons has been previously described (Dottori and Pera, 2008). Briefly, iPSCs were cultured on an iMEF feeder layer as described in Section 2.9.5. At the time of manual dissection and transfer onto a fresh feeder layer, 500ng/ml human recombinant Noggin (R&D Systems) was added to the huESC culture medium. The iPSC colonies were cultured for 14 days without passage, with replacement of Noggin-containing media every second day.

After 14 days of Noggin treatment, colonies were manually dissected in PBS, and single patches transferred to individual wells of a non-adherent 96-well plate, to allow neurosphere formation (the preparation of non-adherent plates is described in Appendix 5, A5.2). Neurospheres were cultured in suspension in Neurobasal Medium A (NBM-A) (Life Technologies) supplemented with 10ng/ml human recombinant epidermal growth factor (EGF) (Millipore) and 10ng/ml bFGF (R&D Systems) (Appendix 5, A5.1) for approximately seven days. For long-term culture, neurospheres were subcultured by manual dissection.

To promote differentiation into neurons, whole neurospheres were seeded onto plates coated with 10µg/ml poly-D-lysine (Sigma Aldrich) and 5µg/ml natural mouse laminin (Sigma-Aldrich) in NBM-A without bFGF and EGF supplements, and maintained at 37°C, 5% CO_2 (Appendix 5, A5.3). Medium was changed every second day.

2.10.1 Expression of neuron-specific markers

The expression of neuron- and glial-specific markers, including βIII-tubulin, gamma-aminobutyric acid (GABA), and glial fibrillary acidic protein (GFAP) was assessed by immunofluorescence as described in Section 2.9.6. Antibodies are listed in Appendix 3 (A3.8).

2.11 Statistical analysis

In cases where data from two groups were compared, statistical analysis was performed using the Mann-Whitney test for unpaired samples. A two-tailed distribution, assuming unequal variances, was used to analyse the data. In cases where comparisons were made between three or more groups, the Kruskal-Wallis test was used, followed by the Dunn's post-test for multiple comparisons. Analysis was performed in GraphPad Prism v.5.0 (GraphPad Software, San Diego, CA, USA).

Significance was defined using a type I error, or p-value of 0.05.

Chapter 3 **Fibroblasts as a Model for Testing RNA interference-based Therapy for SCA7**

3.1 Introduction

The selection of appropriate models of disease which are easy to access and manipulate, and which recapitulate the human phenotype, remains one of the major challenges in the development of effective therapies for neurodegenerative conditions. The plethora of SCA7 transgenic mouse models developed over the past decade has yielded many valuable insights into the mechanisms underlying cellular pathology (see Section 1.5.1). However, as the focus of neurodegenerative disease research shifts from understanding disease mechanisms towards the development of allele-specific gene silencing therapies, the development of models in which both the mutant and wildtype alleles of a particular disease gene are present, is becoming increasingly necessary.

Mounting evidence from polyQ disease patients suggests that peripheral tissues display a cellular phenotype in the presence of the mutant protein, including the formation of intranuclear inclusions (de Mezer et al., 2011; Squitieri et al., 2010; Seo et al., 2004; Giuliano et al., 2003; Sathasivam et al., 1999). Although not generally associated with clinical pathology, such phenotypes may nonetheless prove useful as measures of therapeutic efficacy *in vitro*.

3.1.1 A polyQ disease phenotype in non-neuronal cells

Of the peripheral cell types, cultured skin fibroblasts and Epstein Barr Virus (EBV)-transformed lymphoblastoid cell lines (LCLs) have been the subjects of extensive study, and have yielded many valuable insights into the molecular pathogenesis of polyQ diseases, including the discovery of somatic mosaicism as a modifier of age of disease onset (Cannella et al., 2009; Veitch et al., 2007),

an observation which may prove valuable in predicting the age of onset in presymptomatic individuals (Swami et al., 2009).

Similar to observations in autopsied brain tissue, polyQ patient fibroblasts show nuclear localization (De Rooij et al., 1996) and proteolytic cleavage of the mutant protein to yield toxic N-terminal truncated fragments (Garden et al., 2002). At the ultrastructural level, fibroblasts from HD homozygotes display numerous morphological abnormalities when compared to age-matched controls, including vacuolization, structural derangements of the mitochondria and endoplasmic reticulum, and multiple autophagic vacuoles similar to those occurring in neurons within affected brain regions (Squitieri et al., 2010). Indeed, despite cell-type specific variations in pathology, arising as a result of differential patterns of gene expression dysregulation, the influence of specific microenvironments, and differences in kinetics of polyQ aggregation (and hence, in the timing of protein aggregation), fibroblasts appear, at least at the ultrastructural level, to most closely mimic the neuronal pathological phenotype (Squitieri et al., 2010).

In HD and SCA2 fibroblasts, the identification of markers of DNA damage and repair pathways suggests that expanded polyQ proteins may activate the ataxia telangiectasia mutated kinase/ATM and Rad3-related kinase (ATM/ATR)-dependent DNA damage response through the accumulation of reactive oxygen species (Giuliano et al., 2003); while a reduction in glyceraldehyde-3-phosphate dehydrogenase (GAPDH) activity in HD and Alzheimer's disease fibroblasts provides a potential mechanism for the hypometabolism and programmed cell death which are key features of these diseases (Mazzola and Sirover, 2003; Mazzola and Sirover, 2002; Mazzola and Sirover, 2001). Studies of fibroblasts have also provided evidence for the role of HTT in the trafficking of secretory and endocytic vesicles, revealing co-localisation of mutant HTT with clathrin in the Golgi network and in cytoplasmic and membrane-associated vesicles (Velier et al., 1998).

Non-neuronal cells have also offered insights into the most prominent manifestations of polyQ pathogenesis, including autophagy (Nagata et al., 2004), RNA toxicity (de Mezer et al., 2011), and the effects of polyQ protein on the UPS and heat shock protein pathways.

UPS dysfunction in HD fibroblasts has been used as a model to understand why certain cells and tissues are able to cope with the effects of abnormal gene products, while others dysfunction and die (Davies et al., 2007; Seo et al., 2004). HD patient fibroblasts display a similar degree of UPS inhibition to affected brain regions. However, since other factors known to contribute to HD pathology are not affected in HD fibroblasts, it is possible that an impaired UPS alone is not sufficient to induce cell degeneration in HD. Instead, it may be viewed as one of several markers of polyQ disease progression, resulting in severe pathology only when coupled with other catastrophic cellular events, such as the decreases in ubiquitin, *BDNF* and mitochondrial complexes observed in the caudate putamen of HD patients (Seo et al., 2004).

Indeed, UPS inhibition appears to be compensated for in most cell types by protein quality control mechanisms capable of regulating the turnover of the misfolded protein, or by rapid dilution of the mutant protein by cell division (Zijlstra et al., 2010; Seo et al., 2004). This is further supported by the observation that SCA3 patient fibroblasts, which express mutant Ataxin-3, show no sign of protein aggregation. One mechanism proposed to account for this phenomenon is the significant upregulation of heat shock proteins HSPB1 (HSP27) and DNAJB (HSP40) family members in the fibroblasts of these SCA3 patients, with levels of the latter showing a correlation with age of onset, and hence a possible modifying role in disease progression (Zijlstra et al., 2010). However, a study of similar markers of the HSR in SCA7 patient LCLs suggests that the role of these molecular chaperones in polyQ disease may be more complex.

Tsai et al. used LCLs from two SCA7 patients, with 100 and 41 CAG repeats, respectively, to examine the effects of polyglutamine expression on the HSR (Tsai et al., 2005). Under basal conditions, levels of HSP27 and HSP70 proteins were significantly reduced in cells containing expanded Ataxin-7, when compared to normal LCLs. Results from semiquantitative PCR analysis confirmed that the reduction in HSP70, but not HSP27, was a result of a transcriptional defect. Despite these defects in expression, however, mutant LCLs were still capable of heat shock protein induction in response to heat stress, suggesting that the HSR may remain intact (Tsai et al., 2005). Taken together with the observations of HSR function in SCA3 fibroblasts, these results suggest that HSP levels may vary according to disease, patient age and stage of progression, as well as cell type. Nevertheless, it appears that alterations of HSP expression in peripheral cells may also serve as useful markers of polyQ disease pathogenesis.

These data together provide strong motivation for the use of peripheral cells in investigating the molecular mechanisms of polyQ disease. In addition to subcellular pathology comparable to that of affected neurons, non-neuronal cells offer the advantages of easy accessibility, as well as the potential to harvest and culture sufficient cells for statistical analysis of pathogenic effects (Squitieri et al., 2010; Zijlstra et al., 2010). Unlike patient brain tissue, obtained at autopsy, peripheral cells allow for the monitoring of early-stage modifiers of disease, without the confounding effects of post-mortem artefacts (Zijlstra et al., 2010).

Most recently, the discovery in fibroblasts of a novel antisense non-coding RNA, SCAANT1, which represses *ataxin-7* transcription in a *cis*-dependent fashion, has underscored the importance of non-neuronal cells in understanding polyQ pathogenesis (Sopher et al., 2011). Based on observations in SCA7 patient fibroblasts carrying 55 and 150 CAG repeats respectively, it appears that SCAANT1 expression is dependent on *ataxin-7* CAG repeat length, with an expansion resulting in decreased SCAANT1 promoter activity, and hence, in de-repression of the *ataxin-7* transcript. This leads, in

turn, to significantly elevated Ataxin-7 protein levels, creating a feed-forward effect which accelerates the SCA7 disease pathway by promoting increased production of the mutant protein (Sopher et al., 2011).

3.1.2 A cellular phenotype for SCA7 in non-neuronal cells

A strong case has been made for the role of transcriptional dysregulation as an early marker of SCA7 pathogenesis (see Section 1.2.3). However, to date, limited data is available regarding transcriptional dysregulation in patient peripheral cell types. Since non-neuronal cells such as skin fibroblasts have been shown to be valuable tools in understanding disease progression and evaluating therapies, this study sought to identify a pattern of disease-associated transcriptional alterations in SCA7 patient fibroblasts, using a pool of candidate genes encoding proteins implicated in the pathogenesis of SCA7, which had been previously shown to be differentially expressed in SCA7 models of disease (Chou et al., 2010; Tsai et al., 2005). All of the genes investigated had previously shown approximately 1.5-fold (or greater) up- or downregulation in SCA7 mouse cerebellum or retina, validated by qPCR and/or western blot.

.

3.1.3 Fibroblasts as a tool for evaluating therapies

In addition to their role in elucidating pathogenic mechanisms, patient-derived fibroblasts have been used increasingly in the evaluation of allele-specific gene silencing therapies for polyQ disease. In HD in particular, a series of studies have determined the efficacy of silencing molecules targeting the disease-causing CAG repeat. These silencing effectors, which include chemically modified antisense oligonucleotides, as well as siRNAs and microRNA mimics, demonstrated robust, allele-specific silencing of mutant HTT (based on cumulative binding of multiple silencers to the expanded CAG repeat), with reports of >30-fold selectivity for the mutant transcript in some cases (Hu et al., 2010a).

Allele-specificity was reportedly enhanced by oligonucleotide modifications (Hu et al., 2009a), and by shifting the mechanism of silencing from mRNA cleavage to translational suppression (Hu et al., 2010a; Fiszer et al., 2011). Although enhanced selectivity was observed in cell lines with larger disease-causing repeat lengths, allele discrimination was still possible in fibroblast lines containing minimal CAG repeats representative of most HD patients (Fiszer et al., 2011; Gagnon et al., 2010; Hu et al., 2010a; Hu et al., 2009a).

While preferable to CAG-targeted effectors due to the reduced risk of off-target effects, SNP-based gene silencing molecules are subject to a number of design constraints, some of which have been identified and refined within the context of fibroblast disease models. Critically, the disease-linked allele of the SNP must be ascertained, in order to determine the correct siRNA sequence required. Additional design constraints include the selection of purine:purine mismatches as targets where possible, as these result in the greatest disruption of the siRNA-mRNA helix, and hence confer the greatest degree of discriminatory power (Pfister et al., 2009). In cases where purine:purine mismatches are unavailable, the introduction of additional mismatches (particularly in the seed region of the siRNA, which directs binding and recognition of the target mRNA) has been suggested to enhance selectivity of SNP sites predicted to be poor candidates for the development of allele-specific siRNAs (Ohnishi et al., 2008). In general, however, mismatches in the 5' seed region offer only moderate discrimination, whereas mismatches 3' to the seed region – in particular at positions 10 and 16 of the siRNA – promote robust allele selectivity (Lombardi et al., 2009). This is likely due to the functions of the different regions, since allele-specificity is enhanced when the conformation of the siRNA-target complex blocks catalysis and RISC-mediated cleavage, rather than siRNA binding (Schwarz et al., 2006).

In addition to design considerations, allele-specificity has been shown to be concentration dependent (Zhang et al., 2009); the optimal dose of any allele-specific treatment is therefore one at which allele

discrimination is achieved at a concentration sufficient to elicit clinically significant inhibition of the mutant protein (Lombardi et al., 2009; Schwarz et al., 2006).

Fibroblasts have been instrumental in evaluating the silencing efficiency of allele-specific effectors designed to target disease-linked SNPs. In the case of HD, for example, an siRNA was successfully designed to specifically target the mutant *HTT* transcript in a patient heterozygous for the rs363125 SNP, in which the C-allele was found to be linked to the expansion (Van Bilsen et al., 2008). Transfection of cultured patient fibroblasts with the siRNA resulted in an approximate 80% reduction in mutant mRNA and protein expression, while wildtype levels were not significantly altered (Van Bilsen et al., 2008). A similar study (Zhang et al., 2009) evaluated the efficacy of allele-specific siRNAs in patient fibroblasts carrying the three base-pair Δ2642 deletion, present in 38% of mutant HD, but only 7% of wildtype HD alleles (Ambrose et al., 1994). SiRNAs designed to target the deletion reduced expression of mutant *HTT* by up to 50% in patient fibroblasts, and showed similar potent, dose-dependent effects in HeLa- and SH-SY5Y-based luciferase reporter systems, suggesting that RNAi-based therapy is likely to be effective in a range of different cell types. Allele-specific knockdown of the mutant allele also resulted in partial correction of HD-associated nuclear abnormalities in patient fibroblasts, while avoiding the activation of caspase-3 associated with silencing of both copies of the gene (Zhang et al., 2009).

Such approaches are likely to be effective in other polyQ disorders in which disease-linked SNPs have been identified, including SCA3 (Miller et al., 2003) and SCA7 (Scholefield et al., 2009).

3.1.4 RNAi-based therapy for SCA7 in South Africa

The concept of allele-specific RNAi-based therapy for the South African SCA7 patient cohort was first explored by Scholefield and colleagues, in HEK293 cells transiently transfected with

fluorescently-conjugated *ataxin-7* constructs containing 10 (wildtype) or 100 (mutant) CAG repeats, using an shRNA designed to target a disease-linked SNP within the *ataxin-7* transcript (rs3774729) (Scholefield et al., 2009). The A allele of the SNP had been previously shown to co-segregate with the ataxin-7 CAG expansion, as a result of a founder effect in the South African population (Greenberg et al., 2006). Almost complete ablation of mutant expression (to less than 10% of control levels) was observed when the allele-specific single nucleotide mismatch was located at position 16 of the shRNA guide strand ($p<0.044$), with a minimal effect on the wildtype target. Silencing resulted in a decrease in the number of Ataxin-7 aggregates, as well as a release of wildtype protein from sequestration (Scholefield et al., 2009).

Although the abovementioned study served as proof-of-principle of the feasibility of allele-specific silencing as a therapeutic avenue for SCA7, the model employed provided very little information regarding the restoration of wildtype function, or the reversal of other cellular markers of disease, such as transcriptional dysregulation or loss of wildtype protein function. In order for such a therapy to progress to clinical trials, it will therefore be necessary to further evaluate its efficacy in a model which more closely resembles the patient genetic background. Since the applicability of transgenic models to the study of allele-specific silencing to date has been limited, this study has focused on the development of patient-derived models of the disease.

3.1.5 Aims

The aims of the experiments described in this chapter were thus:

1. to ascertain the presence of a cellular phenotype (transcriptional dysregulation) in SCA7 patient fibroblasts
2. to validate the allele-specificity of a previously-designed siRNA targeting the mutant allele of *ataxin-7* (Scholefield et al., 2009) and
3. to determine whether siRNA-mediated silencing of *ataxin-7* was sufficient to ameliorate any observed cellular phenotype,

with the ultimate goal of evaluating SCA7 patient fibroblasts as a model for testing RNAi-based therapies.

This work was completed in collaboration with Dr Janine Scholefield (Department of Physiology, Anatomy and Genetics, University of Oxford), and Ms Danielle Smith (Division of Human Genetics, University of Cape Town) and is currently being prepared as a manuscript for submission to a peer-reviewed journal.

3.2 Results

3.2.1 Altered expression of transcripts in SCA7 patient fibroblasts

In order to evaluate differences in gene expression between SCA7 patient and control dermal fibroblasts, six candidate transcripts were chosen, based on their relevance to known polyQ disease pathways. These included genes encoding proteins involved in cellular stress such as *HSP27, -70, -105* and DNAJ/HSP40 homologue, Subfamily A, member 1 (*DNAJA1*) as well an RNA chaperone, RNA Binding Motif protein 3 (*RBM3*); and the ubiquitin carboxy-terminal hydrolase L1 (*UCHL1*), involved in deubiquitination. All of these genes had previously been shown to be differentially expressed in SCA7 disease models (Chou et al., 2010; Tsai et al., 2005).

Comparison of transcript levels of these six genes between control and SCA7 patient fibroblasts was performed by means of qPCR (Fig. 6). Consistent with the SCA7 models previously described, a two-fold increase in *DNAJA1* expression (p=0.03), as well as a two-fold decrease in *UCHL1* expression (p=0.04), was observed in SCA7 patient fibroblasts relative to control lines. No significant changes in the levels of *HSP27, -70, -105* or *RBM3* were observed.

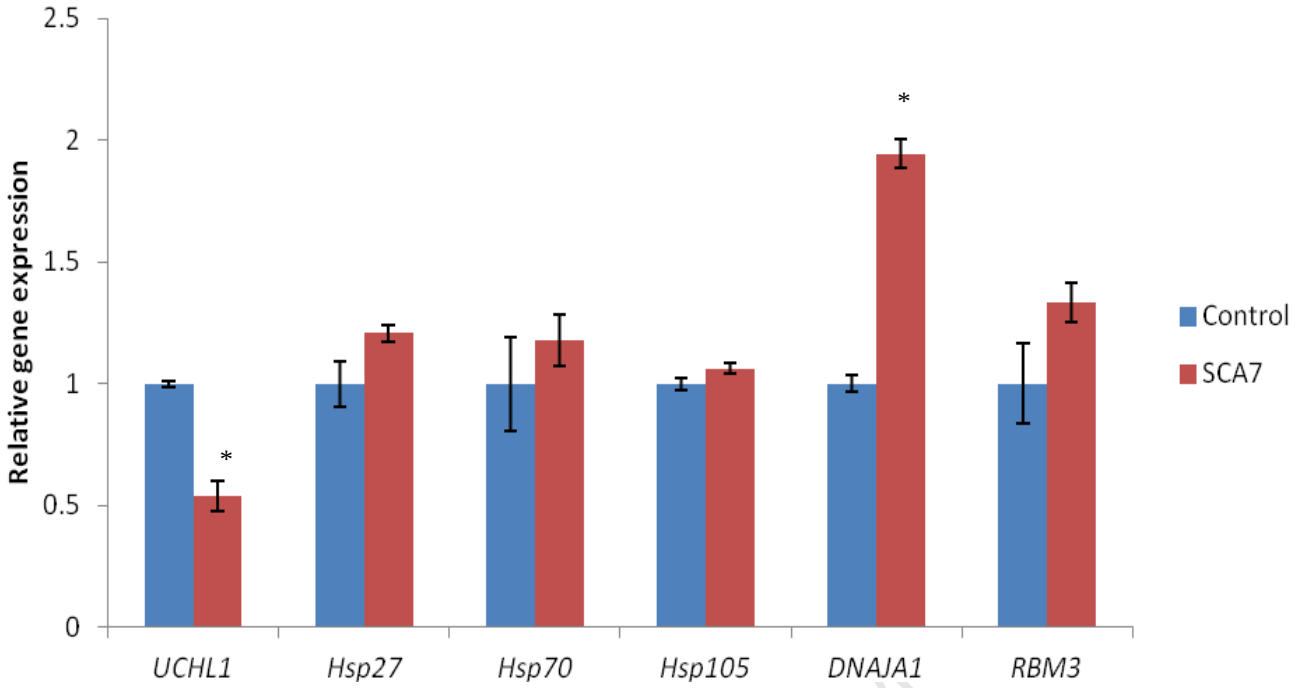

Figure 6 Transcriptional changes in SCA7 patient fibroblasts. Expression of endogenous transcripts in SCA7 fibroblasts relative to controls is shown, normalised to β-Actin. Values are mean ± SEM. Control fibroblasts, n = 2, SCA7 fibroblasts, n = 3. *UCHL1*, Ubiquitin carboxy-terminal hydrolase LI; *HSP-*, heat shock protein *-27*; *-70*; *-105*; *DNAJA1* (HSP40), DNAJ homolog, subfamily A, member 1; *RBM3*, RNA-binding motif protein 3. * indicates a p value < 0.05.

3.2.2 Validation of a previously-designed allele-specific siRNA targeting *ataxin-7*

One of the key challenges to be addressed when designing RNAi-based therapies is the question of whether or not an allele-specific approach is required (see Section 1.4.1.1.2). The feasibility of allele-specific silencing for SCA7 has been previously demonstrated in an artificial cell model, using an siRNA targeting a common SNP linked to the mutation in the South African patient population (Scholefield et al., 2009; Greenberg et al., 2006).

In order to evaluate the efficacy of this allele-specific therapy in patient-derived cells, the expression of the wildtype and mutant alleles of *ataxin*-7 were evaluated in fibroblasts from a SCA7 patient heterozygous for the SNP (patient 1519) (Fig. 7a), following treatment with either siR-atxn7, or siR-

P16. siR-atxn7 is a non-allele-specific siRNA which targets the 3' untranslated region (3' UTR) of both wildtype and mutant *ataxin-7*, while siR-P16 was designed to specifically silence the A allele linked to the mutant transcript, with reduced activity against the G allele linked to the wild-type transcript (Scholefield et al., 2009; Greenberg et al., 2006) (Fig. 7b).

To determine the relative abundance of each transcript following siRNA treatment, allele-specific qPCR was performed, using a method developed by Ms Danielle Smith. A common reverse primer, located 3' of the SNP was used in combination with one of two forward primers, complementary to either the A or G allele of the SNP, to amplify the mutant or wild-type cDNA, respectively. The specificity of the qPCR reaction had been previously validated for each allele, using cDNA samples of known genotype, to confirm the absence of a detectable product when using G allele primers on homozygous AA samples, or when using A allele primers on homozygous GG samples (Smith, 2011).

Results indicated that siR-atxn7 was capable of effecting silencing of both the mutant and wild-type transcripts with similar efficacy across all three doses (Fig. 7c). In contrast, siR-P16 mediated silencing of the mutant transcript by as much as 34% ($p<0.05$) at a 1nM dose, with no effect on the wildtype transcript (Fig. 7d). This allele-specificity was maintained at 5nM; resulting in silencing of the mutant transcript by 49%, with only modest silencing of the wild-type allele (by 25%). Only at the highest dose of siRNA (20nM) is this discriminating effect lost, possibly the result of a saturating effect, which has been previously described (Zhang et al., 2009).

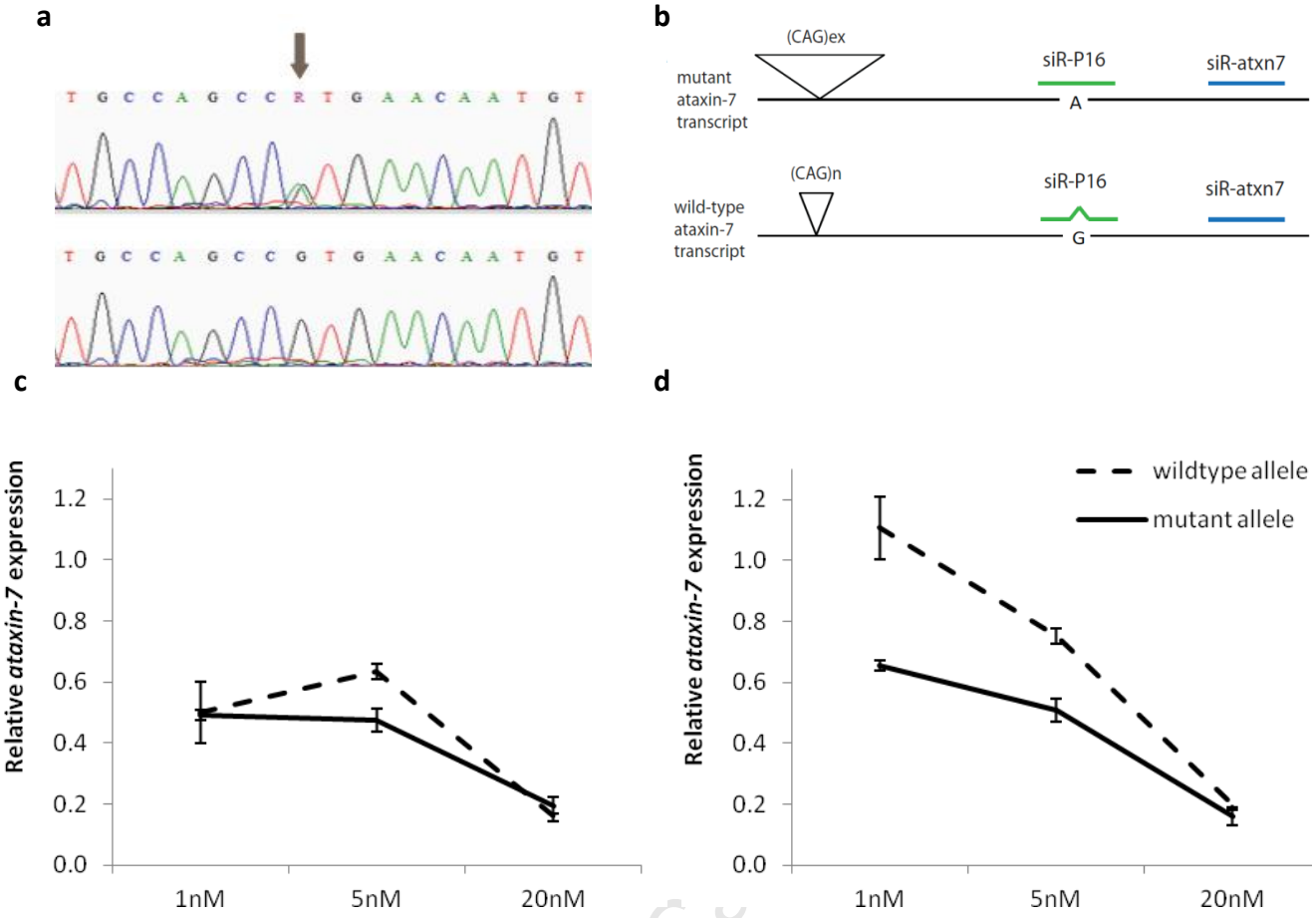

Figure 7 Allele-specific silencing of *ataxin-7* in SCA7 patient fibroblasts. (a) Chromatogram showing the sequence of the region surrounding the SNP rs3774729 (indicated by the arrow), confirming the heterozygous A/G genotype in 1519 fibroblasts (above) compared to a homozygous G/G control (below). (b) Schematic diagram showing the allele-specific design of siR-P16 (green) targeting the A allele of the SNP, and a non-allele-specific siRNA, siR-atxn7 (blue), complementary to the 3' UTR of both alleles of the transcript. The CAG repeat expansion, (CAG)ex, and the normal sized repeat, (CAG)n, are linked to the A and G allele of the SNP respectively. (c) Levels of the wild-type allele do not differ significantly from levels of mutant allele transcript following treatment with siR-atxn7. (d) Treatment with siR-P16 reduces the levels of mutant allele expression at a similar rate to that of siR-atxn7. However, wild-type allele levels are significantly unaffected by siR-P16 over low doses. Transfection efficiency was calculated to be approximately 80%. Silencing was determined relative to a non-targeting siRNA, and gene expression was normalised to β-Actin. * indicates a p value < 0.05.

3.2.3 Effect of RNAi-mediated silencing of *ataxin-7* on transcriptional changes

To determine the effect of *ataxin-7* repression on the transcriptional alterations observed in SCA7 fibroblasts, patient fibroblasts were transfected with either siR-atxn7 or siR-P16. Total RNA was harvested seven days after the initial siRNA administration. Both siRNAs silenced total *ataxin-7* in a dose-dependent manner, ranging from 21% (at 1nM) to 77% knockdown (at 20nM) for siR-P16, and 29% to 68% for siR-atxn7, as measured by qPCR (Fig. 8a).

Following *ataxin-7* silencing, levels of *DNAJA1* and *UCHL1* transcripts were also determined by qPCR. At low levels of silencing (less than 50%) no significant change in *DNAJA1* levels was observed (Fig. 8b). However, repression of *ataxin-7* expression to below 50% of normal transcript levels resulted in a significant reduction in *DNAJA1* expression ($p < 0.05$) by up to 30% (siR-P16) or 41% (siR-atxn7) – approaching the levels observed in control fibroblasts (Fig. 6). Of interest was the observation that robust silencing by both siRNAs did not have the same effect on levels of *DNAJA1* if assessed at a shorter time point of 96 hours (data not shown). This may indicate a requirement for sustained inhibition of *ataxin-7* expression, in order to sufficiently reduce mutant polyQ protein to allow for alleviation of the cell stress response, as measured by heat shock protein induction.

At low levels of *ataxin-7* knockdown (21- 48%), *UCHL1* levels were elevated towards those observed in control samples, with an observed increase in *UCHL1* expression of between 30 and 59% (Fig. 8c). However, when total *ataxin-7* expression was reduced by 68% (following treatment with 20nM siR-atxn7), *UCHL1* expression reverted to levels similar to those observed in the absence of *ataxin-7* silencing. In contrast, silencing of *ataxin*-7 by up to 77%, following treatment with the allele-specific siR-P16, resulted in a sustained increase (of approximately 25%) in *UCHL1* expression.

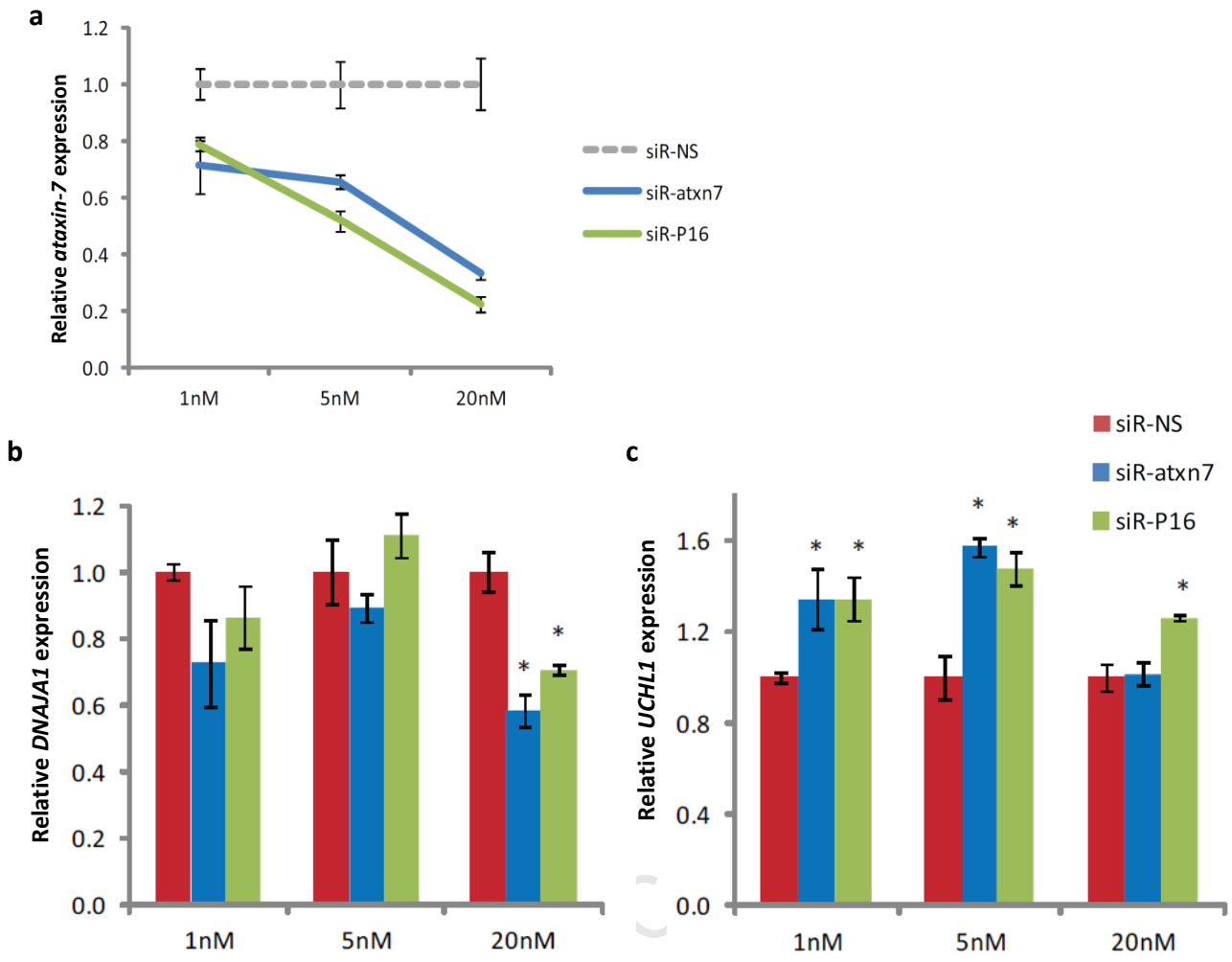

Figure 8 siRNA-mediated silencing of *ataxin-7* alters the levels of differentially expressed transcripts in SCA7 patient fibroblasts towards those observed in controls. (a) Two siRNAs (siR-atxn7 and siR-P16) silence total *ataxin-7* transcript levels in a dose-dependent manner relative to a non-targeting siRNA (siR-NS). (b) Corresponding levels of *DNAJA1* expression after treatment with increasing doses of siR-P16 and siR-atxn7. Silencing of *ataxin-7* reduces levels of *DNAJA1* at high doses of both siRNAs. (c) Corresponding levels of *UCHL1* expression after treatment with increasing doses of siR-P16 and siR-atxn7. Levels of *UCHL1* increase across a wide range of *ataxin-7* silencing, except at the 20nM dose of siR-atxn7. Concentrations of siRNAs are shown on the x-axis. Gene expression was calculated relative to a non-targeting control siRNA (siR-NS), and normalised to β-Actin. Values are mean ± SEM. * indicates a p value of < 0.05.

In order to confirm that the effects of siRNA administration on expression of these transcripts were associated with removal of mutant *ataxin-7*, and to exclude the possibility of off-target effects, parallel silencing experiments were performed in control fibroblasts (JS Con line). Dose-dependent silencing of *ataxin-7* by both siRNAs was highly similar to results obtained in patient fibroblasts,

ranging from 30% to 64% knockdown (Fig. 9a). However, in contrast to the results obtained in SCA7 fibroblasts, no significant correlative decrease in *DNAJA1* was observed (Fig. 9b). Furthermore, at low doses of siRNA, no concomitant elevation of *UCHL1* expression was observed (Fig. 9c). However, a 30% decrease in *UCHL1* expression ($p<0.05$) was observed at 20nM siR-atxn7, consistent with the reduced expression in SCA7 patient cells at the same levels of silencing.

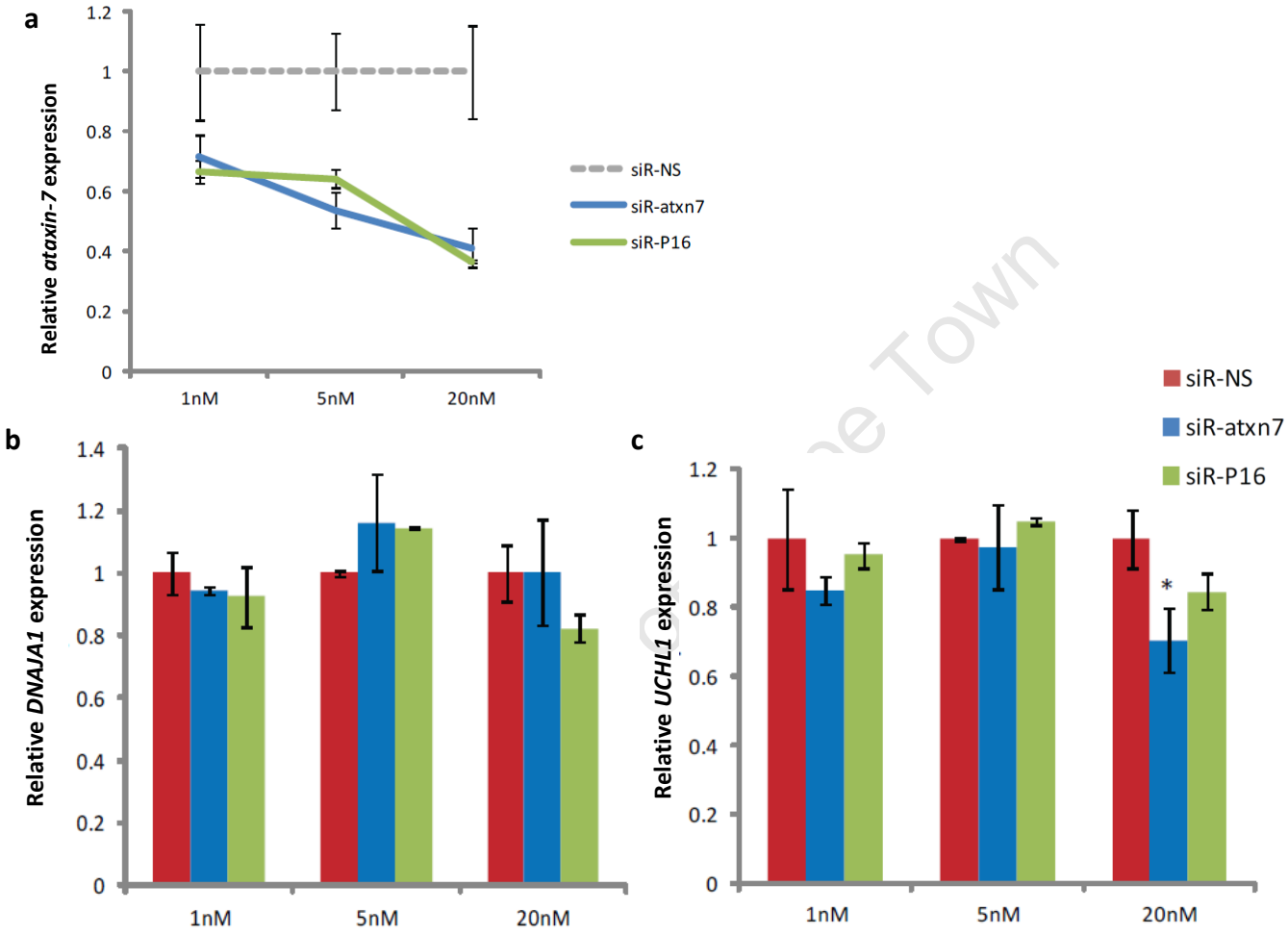

Figure 9 Effects of siRNA-mediated silencing of *ataxin-7* in control (JS Con) fibroblasts. (a) Two siRNAs (siR-atxn7 and siR-P16) silence *ataxin-7* transcript levels in a dose dependent manner relative to a non-targeting siRNA (siR-NS). (b) Corresponding levels of *DNAJA1* expression after treatment with increasing doses of siR-P16 and siR-atxn7. Silencing of *ataxin-7* has no effect on levels of *DNAJA1*. (c) Corresponding levels of *UCHL1* expression after treatment with increasing doses of siR-P16 and siR-atxn7. Levels of *UCHL1* are reduced only at high doses of siR-atxn7. Concentrations of siRNAs are shown on the x-axis. Gene expression was calculated relative to a non-targeting control siRNA (siR-NS), and normalised to β-Actin. Values are mean ± SEM. * indicates a p value of < 0.05.

3.3 Discussion

The results of this study provided the first evidence of the presence of a disease-relevant transcriptional phenotype in SCA7 patient fibroblasts, which could be ameliorated by RNAi-mediated silencing of *ataxin-7*, using both allele-specific and non-allele-specific siRNAs targeting the SCA7 disease-causing gene. Furthermore, the use of a heterozygous SCA7 patient cell line provided the first confirmation of allele-specificity of the therapeutic effector, siR-P16, whose capacity for allele discrimination had previously only been demonstrated in an artificial cell model (Scholefield et al., 2009).

3.3.1 A disease-relevant phenotype in SCA7 patient fibroblasts

The role of transcriptional dysregulation in the early stages of polyQ pathogenesis has been widely documented (Helmlinger et al., 2006b). In SCA7 in particular, the role of wildtype Ataxin-7 in the TFTC/STAGA transcriptional regulatory complexes has further emphasised the importance of transcriptional alterations in the development of the disease (Helmlinger et al., 2006a) with evidence from SCA7 mouse models revealing a spectrum of disease-associated transcriptional changes (Chou et al., 2010; Abou-Sleymane et al., 2006; Yoo et al., 2003; La Spada et al., 2001). Although expression of many of the dysregulated transcripts is restricted to affected cells in the retina and CNS, studies of patient-derived lymphoblasts (Tsai et al., 2005) and fibroblasts (Zijlstra et al., 2010) suggest that patterns of transcriptional dysregulation in polyQ disease may extend to non-neuronal tissues.

In order to investigate the presence of a transcriptional phenotype in SCA7 fibroblasts, six candidate transcripts were selected, in which robust changes had been previously demonstrated (Chou et al., 2010; Tsai et al., 2005). Transcripts which could be linked to a more general cell response that might present in fibroblasts, which are not considered to be a disease-susceptible cell type, were

prioritised. These included genes encoding heat shock proteins, an RNA binding protein and a deubiquitinating enzyme. Of these six, the expression of four genes was not significantly affected by mutant *ataxin-7,* likely reflecting the tissue-specific nature of the cellular stress response. However, genes encoding one of the heat shock proteins, *DNAJA1,* and the deubiquitinating enzyme, *UCHL1,* were found to be differentially expressed in patient cell lines compared to control lines, corresponding to changes observed in a SCA7 mouse model (Chou et al., 2010).

DNAJA1 encodes the heat shock protein DnaJA1 (also known as Hdj2/HDJ-2), a member of the family of proteins known as "J proteins", which stimulate the catalytic activity of the HSP70 proteins via a conserved 70 amino acid signature region known as the J domain (Zhao et al., 2008a). Although the presence of DnaJA1 has been detected in NIs in HD, SCA1 and SCA7 (Michalik and Van Broeckhoven, 2003; Watase et al., 2002; Wyttenbach et al., 2000), the role of the protein in polyQ pathogenesis remains controversial. Numerous studies have highlighted the potential of overexpression of DnaJA1 to reduce aggregation of the mutant protein in cell models of SCA1 (Cummings et al., 1998), SBMA (Kobayashi et al., 2000; Stenoien et al., 1999), SCA3 (Chai et al., 1999b) and SCA7 (Helmlinger et al., 2004b). However, these findings have not been robustly replicated in animal models (Helmlinger et al., 2004c; Chan et al., 2000). Moreover, results from three different HD cell models directly contradict these findings, suggesting instead that overexpression of DnaJA1 may even promote the formation of aggregates of mutant protein in COS-7 cells (Wyttenbach et al., 2000). It therefore appears that the net effect of DnaJA1 depends on the overall balance of HSR components, which varies between cell types.

Chou et al. observed an approximately two-fold increase in *DNAJA1* in the cerebellum of Ataxin-7-Q52 transgenic mice at 6 months of age ($p<0.01$), which decreased as the mice approached 11 months of age, in agreement with previous reports regarding the biphasic nature of the heat shock response in polyQ disease (Chou et al., 2010; Chou et al., 2008; Katsuno et al., 2005; Hay et al.,

2004). This phenomenon, in which an initially robust heat shock response becomes progressively impaired in polyQ diseased animals of advanced age, is thought to arise from hypoacetylation of histone H4, resulting in reduced chromatin accessibility across heat shock genes, and leading to a decrease in their transcription over time (Labbadia et al., 2011).

The initial increase in *DNAJA1* in SCA7 mouse cerebellum, and the observed increase in the patient derived fibroblasts reported here, is likely to represent a general response to cellular stress. Cellular stress caused by the accumulation of mutant polyQ protein is well established (reviewed in Huen et al., 2007), and is not restricted to affected neurons, having been demonstrated in several non-neuronal cell types (Zijlstra et al., 2010; Tsai et al., 2005). The results of the current study therefore support a model in which *DNAJA1* is upregulated by non-neuronal cells expressing mutant *ataxin-7*, in an attempt to promote survival by facilitating protein folding and preventing aggregation (Chou et al., 2010).

It may be argued that one of the patients studied here (patient 1518), with a disease course of approximately 22 years to date, represents an advanced stage of disease, and should thus exhibit a similar depression in HSR to that observed in aged polyQ mice. However, it should be noted that mitotically active cells such as fibroblasts are capable of rapid dilution of polyQ-expanded Ataxin-7, resulting in greatly reduced levels of the mutant protein in comparison to affected neurons (Zijlstra et al., 2010; Seo et al., 2004). This, together with the presence of additional compensatory mechanisms for the clearance of misfolded proteins, may explain why fibroblasts do not undergo a similar epigenetic silencing of the HSR to that observed in neurons at advanced stages of polyQ disease (Labbadia et al., 2011).

The observed decrease in *UCHL1* expression in SCA7 patient fibroblasts corresponds to changes previously reported in SCA7 transgenic mice (Chou et al., 2010). *UCHL1* encodes a 223 amino acid

protein, Ubiquitin C-terminal Hydrolase 1 (UCH-L1), a component of the UPS, which functions as a deubiquitinating enzyme (Wilkinson et al., 1989), a ubiquitin ligase (Liu et al., 2002) and stabiliser of mono-ubiquitin (Osaka et al., 2003). UCH-L1 is predominantly expressed in the brain, where it is localised exclusively in neurons (Wilson et al., 1988).

UCHL1 has been linked to several neurodegenerative disorders through the impairment of the ubiquitin proteasome pathway, including Parkinson's disease, Alzheimer's disease and HD (Gong et al., 2006; Metzger et al., 2006; Ardley et al., 2004). Downregulation of *UCHL1* mRNA and protein expression has been observed in the brains of Alzheimer's and Parkinson's disease patients, as well as in patients with dementia with Lewy bodies (Barrachina et al., 2006; Choi et al., 2004). Furthermore, amino acid changes in UCH-L1, which reduce the catalytic activity of the UPS *in vitro,* have been associated with parkinsonism, cognitive deficits and cortical Lewy pathology in autosomal dominantly-inherited cases of familial Parkinson's disease (Barrachina et al., 2006; Nishikawa et al., 2003). These observations correlate strongly with early findings in mouse models lacking functional *UCHL1*, which develop ataxia and neurodegeneration (Saigoh et al., 1999). When both *UCHL1* and *UCHL3* expression is suppressed, mice develop even more pronounced degeneration of the spinal cord, together with dysphagia, a clinical hallmark of human SCA patients (Kurihara et al., 2001).

A role for UCH-L1 in the pathology of neurodegenerative diseases appears to be strongly substantiated. Levels of *UCHL1* expression have been postulated to influence neuronal life expectancy (Lombardino et al., 2005), and it appears that the precise regulation of *UCHL1* is essential for the survival and correct functioning of neurons (Setsuie and Wada, 2007). Since UCH-L1 participates in the degradation of proteins via the UPS, abnormal UCH-L1 levels may interfere with protein processing, reducing the availability of monoubiquitin, and thereby contributing to the formation of protein aggregates (Barrachina et al., 2006), a hallmark of neurodegeneration. Sequestration of UCH-L1 into abnormal protein aggregates is not, however, a prerequisite for

pathology, despite detection of the protein in Lewy bodies in some cases (Barrachina et al., 2006; Lowe et al., 1990).

Although most research on *UCHL1* function to date has focused on its role in neuronal degeneration, at least one study suggests that disease-associated changes in *UCHL1* levels may also be detected in peripheral cells. Hsu et al. used a proteomics approach in spinal muscular atrophy (SMA) patient fibroblasts to identify candidate proteins which distinguish them from normal fibroblasts. Out of six differentially-expressed proteins, UCH-L1 was identified as a key regulator of the levels of SMN (survival of motor neuron) proteins, a decrease in which underlies the pathogenesis of SMA (Hsu et al., 2010). It is not unsurprising, therefore, that downregulation of this key modulator of protein turnover should be observed in fibroblasts from patients with SCA7, a polyQ disease characterised by impairment of the UPS (See Section 1.2.1).

It should, however, be noted, that additional mechanisms, including oxidative modifications of the UCH-L1 protein, have been shown to contribute to the development of neurodegenerative disease (Choi et al., 2004; Castegna et al., 2002). Thus, the full extent of UPS disruption in SCA7 is unlikely to be captured by studies which focus exclusively on the levels of UPS-associated transcripts, without taking into account differences in protein levels or localisation. Nonetheless, this finding, together with the observed increase in the heat shock protein gene, *DNAJA1*, provide evidence for a transcriptional phenotype in SCA7 fibroblasts, involving key pathways in the pathogenesis of polyQ disease.

Despite these promising findings, it must be emphasised that a candidate gene study such as this is by definition limited, by the sample size, as well as by the pool of genes selected for study. It is therefore possible that a larger cohort may yield more informative results regarding subtle changes in gene expression. Alternatively, expression profiling of genes involved in additional polyQ disease

pathways, such as those mentioned in Section 1.2, or the use of non-hypothesis-driven methods such as whole genome expression analysis, may provide a more comprehensive picture of the disease-associated transcriptional changes in SCA7.

3.3.2 Fibroblasts as a model for therapeutic screening

3.3.2.1 *Validation of allele-specific silencing effectors*

The utility of RNAi-based therapies for neurodegenerative diseases caused by a toxic gain-of-function of the mutant protein, such as the polyQ diseases, has been extensively demonstrated (Wang et al., 2008; Harper et al., 2005; Xia et al., 2004). To date, however, relatively few studies have assessed silencing in patient-derived cells (Hu et al., 2011; Hu et al., 2010a; Hu et al., 2009b; Van Bilsen et al., 2008). This study sought to address the utility of SCA7 patient-derived fibroblasts as a model for assessing therapeutic strategies. In particular, the identification of a patient heterozygous for a common disease-linked SNP (rs3774729) in the South African SCA7 patient population offered the opportunity to compare the efficacy of allele-specific and non-allele-specific silencing approaches in genetically accurate cells. This represents a significant improvement over transfected cell models or transgenic animals, in which the background of endogenous *ataxin-7* transcripts may confound results.

Of the polyQ patient-derived cell line studies to date (Fiszer et al., 2011; Hu et al., 2011; Hu et al., 2010a; Hu et al., 2009b; Lombardi et al., 2009; Van Bilsen et al., 2008) most have focused on the development of allele-specific silencing approaches targeting SNPs linked to the mutation and/ or the CAG repeat expansion itself, with increasingly promising results. In this investigation, an siRNA was used, which had been previously designed to target the A allele of SNP rs3774729 (Scholefield et al., 2009). The clinical relevance of allele-specific approaches which target disease-linked SNPs is often limited by their low frequency in the patient population, requiring several allele-specific

effectors to be designed (Pfister et al., 2009). However, recent studies employing haplogroup analyses suggest that target SNPs may be more prevalent than was originally believed. Moreover, the high degree of linkage to the CAG expansion (100%) and heterozygosity (approximately 50%) of SNP rs3774729 in this case suggest that it is a promising candidate for therapy in the South African patient cohort (Scholefield et al., 2009).

This investigation compared the efficacy of two siRNAs, one allele-specific (siR-P16), and one non-allele-specific (siR-atxn7), by measuring the expression of endogenous mutant and wild-type transcripts in patient cells following administration of each siRNA. Results indicated that siR-P16 silences the mutant transcript more efficiently than the wild-type transcript, in comparison to the consistent silencing of both alleles by siR-atxn7, particularly at low doses of siRNA. The decrease in allele-specificity at high siRNA doses represents an important caveat of this approach, emphasising the importance of dose titration in the establishment of an allele-specific treatment regimen. Nonetheless, it may be reasonably concluded that siRNA-mediated targeting of rs3774729 represents an effective strategy for the allele-specific silencing of mutant *ataxin-7*. This is of particular clinical significance, given the important role of wildtype *ataxin-7* in the regulation of gene expression (Helmlinger et al., 2006a; Palhan et al., 2005; La Spada et al., 2001), and the absence of knockout model data regarding the effect of a loss of wildtype function, both of which motivate strongly for therapies which selectively silence mutant *ataxin-7*, while retaining wildtype gene expression.

3.3.2.2 ***Amelioration of disease phenotype***

Given previous reports regarding the role of mutant *ataxin*-7 in transcriptional dysregulation (see Section 1.2.4), it was not surprising to observe alteration of *DNAJA1* and *UCHL1* transcript levels towards wildtype levels, following silencing of the disease-causing gene. The fact that these changes only occurred after sustained (seven days) mutant *ataxin-7* silencing may be indicative of the

reported stability of mutant polyQ protein (Yvert et al., 2001); suggesting that improvements were noted only after a period of time sufficient to allow for degradation of residual protein. The high concentration of siRNA required to effect a decrease in *DNAJA1* expression indicates the presence of a threshold level of *ataxin-7* expression, below which cellular stress is alleviated. Although restoration of *DNAJA1* levels towards normal occurs only at a concentration at which the allele-specific effect of siR-P16 is no longer observed, the observation that silencing of *ataxin-7* has no effect on *DNAJA1* expression in control fibroblasts provides strong evidence that siRNA-mediated reduction of *DNAJA1* expression in patient cells results from the removal of mutant *ataxin-7*, rather than a loss of normal *ataxin-7* function, or off-target effects of the siRNAs.

Ataxin-7 silencing in patient cells resulted in an initial restoration of *UCHL1* levels towards that observed in control lines. This is encouraging given that boosting *UCHL1* levels has been suggested as a therapeutic strategy for Alzheimer's disease (Gong et al., 2006). However, this initial increase was mitigated at higher levels of *ataxin-7* knockdown, after treatment with the non-allele-specific siR-atxn7. In contrast, treatment with the allele-specific siR-P16 resulted in sustained elevated levels of *UCHL1*. This suggested that loss of *UCHL1* expression observed at high doses of non-allele-specific silencing could have resulted in some way from the loss of wildtype *ataxin*-7 expression and hence, loss of normal function of the wild-type Ataxin-7 protein. A similar loss of *UCHL1* expression was observed in control fibroblasts, following high doses of siR-atxn7, lending further weight to this assertion. These findings suggest that, in the context of SCA7 pathogenesis, loss of *UCHL1* expression may be caused by both the toxic gain-of-function of the mutant polyQ protein and by loss of wild-type *ataxin-7* function. Ataxin-7 functions as a critical component of the transcriptional co-activator complexes, STAGA/TFTC (Helmlinger et al., 2004a) and polyQ expanded Ataxin-7 has been shown to inhibit this function (Palhan et al., 2005). It is therefore possible that reduced *UCHL1* expression may result from disruption of the STAGA complex, either directly or indirectly. This is in accordance with the current understanding of polyQ pathogenesis,

which is thought to result from both gain-of-function (of the mutant protein), and loss of wildtype function. These results also underscore the need for an allele-specific silencing approach for SCA7, as a loss of wildtype Ataxin-7 function appears to exacerbate the disease phenotype (as measured here) and may have broader implications for the functioning of key cellular pathways, such as the UPS. However, given the gradual loss of allele-specificity of siR-P16 at increased doses, these conclusions are largely speculative, and do not preclude the involvement of additional mechanisms, as well as the possibility of off-target effects.

3.3.3 Concluding remarks

This study has shown that SCA7 patient derived cell lines, which are generated and manipulated with relative ease, display a disease-associated cellular phenotype, namely, alterations in expression of UPS and HSR genes. As such, these cells are highly suitable for studies of therapeutic efficacy, including the evaluation of allele-specific versus non-allele-specific siRNAs demonstrated here. Results from a heterozygous SCA7 patient indicate that the allele-specific approach first proposed by Scholefield et al. is not only feasible for South African SCA7 patients, but may represent the preferred therapeutic strategy, in order to minimise the effects of loss of wildtype Ataxin-7 function (Scholefield et al., 2009). In addition, siRNA-mediated rescue of the transcriptional phenotype provides insight into the pathogenic mechanisms of disease. Taken together, these findings suggest that although fibroblasts are not susceptible to the neuronal-specific degeneration exhibited in polyQ disorders, they may be a valuable tool for screening therapeutic molecules as well as providing insight into the pathogenesis of polyQ diseases, such as SCA7.

Chapter 4 **Generation and Characterisation of SCA7 Patient-Derived Induced Pluripotent Stem Cells**

4.1 Introduction

Rapid developments in the field of stem cell technology offer the first opportunity to combine the genetic accuracy of patient-derived cell models with the disease-relevance of CNS cell types. Groundbreaking studies by Takahashi et al. and Yu et al. in 2006 and 2007 demonstrated the ability of virus-mediated overexpression of distinct sets of reprogramming factors to generate iPSCs from mouse and human dermal fibroblasts (Takahashi et al., 2007; Yu et al., 2007; Takahashi and Yamanaka, 2006). Human iPSCs have since been generated from a wide variety of source tissues, including melanocytes (Utikal et al., 2009), cord blood-derived cells (Haase et al., 2009), adult peripheral blood cells (Loh et al., 2009), amniotic fluid (Li et al., 2009) and keratinocytes (Trond Aasen et al., 2008), to name a few.

4.1.1 Techniques for generating iPSCs

The choice of technique for generating iPSCs depends largely on the aims of the research to be conducted, and the downstream applications of the lines generated (Table 3). Depending on priorities of the application for which the cells will be used, the appropriate protocol must take into account not only the efficiency, but also the quality and reproducibility of the reprogrammed cells (González et al., 2011).

The generation of iPSCs from human cells using lenti- or retroviral-mediated overexpression of reprogramming factors has proven to be a robust method for inducing pluripotency, albeit with fairly low efficiency (0.01-0.1%). Four-factor combinations of pluripotency genes are typically employed,

although the use of increasing numbers of virally-encoded transcription factors has been advocated to enhance efficiency (Liao et al., 2008).

Delivery of the *OCT4/SOX2/KLF4/c-MYC* combination of transcription factors was originally demonstrated using Moloney murine leukaemia virus (MMLV)-derived retroviruses, such as pMXs (Takahashi et al., 2007), pLib (Wernig et al., 2007) or pMSCV (Trond Aasen et al., 2008). These vectors have cloning capacities of approximately 8kb, facilitate the insertion of genes into the genome of dividing cells, and are usually silenced in immature cells such as ESCs (Jähner et al., 1982; Stewart et al., 1982). The vector, into which the reprogramming cDNA has been cloned, also encodes a viral packaging signal, as well as transcription and processing components. When transfected into a packaging cell line expressing a specific viral envelope protein, high-titre, replication-deficient viruses are produced, capable of infecting donor cells with efficiencies of up to 90%.

Lentiviral delivery vectors have also been used to express reprogramming factors in somatic cells (Yu et al., 2007). These are generally derived from human immunodeficiency virus (HIV), have slightly higher cloning capacities (8-10kb), and are capable of higher infection efficiencies than MMLV-based retroviruses, although reprogramming efficiencies between the two types of virus are comparable. Lentiviruses offer the advantage of infecting both dividing and non-dividing cells. However, compared with MMLV-derived vectors, lentiviruses are less effectively repressed in pluripotent cells (Yao et al., 2004).

Although efficient and reproducible, virus-mediated reprogramming involves the generation of potentially harmful viral particles expressing potent oncogenes, such as *c-MYC*. iPSCs generated using these vectors also carry randomly distributed transgene insertions (Varas et al., 2009), leading to possible mutagenic effects, heterogeneity between cell lines, and the potential for tumorigenicity

(Okita et al., 2007), all of which must be taken into account when establishing and characterising such lines. As a result, attempts have been made to minimise or avoid integration of foreign DNA into reprogrammed cells using alternative methods of reprogramming. To this end, a number of small molecule-based modifiers of signalling pathways involved in the process of reprogramming have been identified, which greatly enhance reprogramming efficiency while minimising the number of transcription factors required (Zhu et al., 2010; Lin et al., 2009). Examples include vitamin C (Esteban et al., 2010), and the HDAC inhibitor valproic acid (VPA) (used in this study), which have been shown to enhance the efficiency of two- and three-factor mediated reprogramming (Huangfu et al., 2008).

The use of different somatic cell types at distinct developmental stages has also been explored as a means of reducing the number of exogenous factors required for reprogramming. Although fibroblasts remain the most popular donor cell type (accounting for 80% of all reprogramming experiments published), several studies have analysed the reprogramming capacity of alternative cell types, of particular interest due to their availability, ease of reprogramming or therapeutic relevance (González et al., 2011). The increase in reprogramming efficiency and/or decrease in factor requirement of certain cell types may be attributed to high endogenous levels of particular reprogramming factors, eliminating the need for their *trans* expression, and/or an intrinsic epigenetic state which is more amenable to reprogramming. One such example of the former is the high baseline level of *SOX2* expression in neural precursor cells, allowing them to be reprogrammed in the absence of *SOX2*, or with *OCT4* alone (Eminli et al., 2008). In addition to efficiency, differences in reprogramming among cell types have also been shown to affect the quality of reprogrammed cells (Miura et al., 2009); thus, the choice of cell type is an important consideration, reflecting a balance between cell availability and ease of reprogramming.

Table 3 The choice of reprogramming method depends upon the downstream application

Application	Species of choice	Donor cell type	Reprogramming factors used	Mode of delivery	Recommendations
Studies of mechanisms of reprogramming	Mouse	Cells from chimeric mice from iPSCs obtained using an inducible system	OSK/OSKM* as reference, any additional factor possible	Inducible lentivirus	Compare as many factors and cell types as possible
Studies of pluripotency/ differentiation	Mouse/ Human	MEFs/fibroblasts	OSK/OSKM; OSNL	Retrovirus; RNA	Reliable and reproducible methods best, non-integrative methods may reduce genetic heterogeneity
Disease modelling and drug screening	Human/pig	Reprogrammable cells easily available from patients or cell repository	OSK/OSKM; OSNL	Retrovirus; RNA	Starting cell population may be limited, so efficient models required. Safety is not crucial but avoiding integration may minimise genetic heterogeneity
Cell therapy/ transplantation	Human	Reprogrammable cells easily available from patients, cell repository or HLA-matched iPSCs obtained from cord blood	Need to avoid potent oncogenes or inhibitors of tumour suppressors	Non-integrative	Safety is the major issue. Non-integrative methods must be compared in terms of efficiency, iPSC quality and differentiation

HLA: human leukocyte antigen; MEFs: mouse embryonic fibroblasts. OSK: *OCT4*, *SOX2*, *KLF4*; OSKM: *OCT4*, *SOX2*, *KLF4*, *c-MYC* (Takahashi et al., 2007). OSNL: *OCT4*, *SOX2*, *NANOG*, *LIN28* (Yu et al., 2007). Adapted by permission from Macmillan Publishers Ltd: Nature Reviews Genetics (González et al., 2011), copyright 2011.

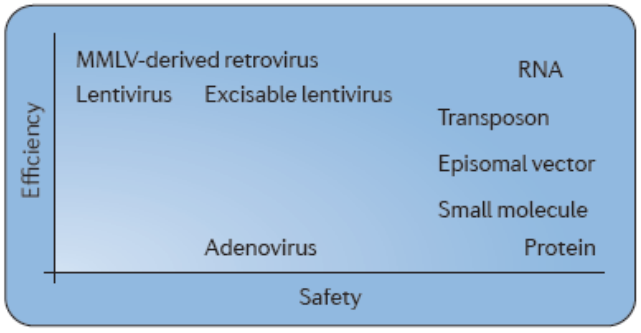

Figure 10 Comparative efficiency and safety of currently available iPSC reprogramming methods. Integrating viruses currently represent the most efficient method of reprogramming, while non-integrative methods are preferred when safety is a primary concern. Adapted by permission from Macmillan Publishers Ltd: Nature Reviews Genetics (González et al., 2011), copyright 2011.

Alternative approaches to decrease the number of genomic integrations include the development of single vectors encoding all the necessary reprogramming factors, which may be excised from iPSC genomes following successful reprogramming, as well as the use of non-integrating viruses, expression plasmids, DNA mini-circles, transposons, recombinant proteins, synthetically modified mRNAs and miRNAs (Fig. 10) (reviewed in González et al., 2011). Although effective in minimising or eliminating integration, these techniques present a number of additional technical obstacles, including the need for repeated transfection due to dilution of the reprogramming factors during cell division, leading to comparatively low reprogramming efficiencies (0.0001-0.001%); and the induction of aneuploidy, caused by the use of adenoviral vectors (Stadtfeld et al., 2008). As several of the methods remain to be replicated (Drews et al., 2012), many proof-of-concept studies of iPSC generation, particularly for disease modelling, still rely on the well-established lenti- or retroviral methods (González et al., 2011) (see Section 4.1.4).

4.1.2 Cell culture conditions

Once an appropriate reprogramming technique has been selected, the culture conditions for reprogramming must be defined. Cell culture conditions, medium composition and supportive (or feeder) cells have all been shown to modulate the efficiency of reprogramming. For example, hypoxic conditions, particularly in combination with the addition of VPA, have been found to dramatically increase the reprogramming efficiency of both mouse and human cells (Yoshida et al., 2010). Supportive feeder cells, such as inactivated mouse embryonic fibroblasts, secrete growth factors that are required for stem cell survival, proliferation and inhibition of spontaneous differentiation, while serum-free medium allows iPSCs to be obtained at an earlier time point (Okada et al., 2010; Dravid et al., 2005).

4.1.3 Molecular mechanisms of cellular reprogramming

Studies of ESCs have led to a basic understanding of the role of the *OCT4/SOX2/NANOG*-regulated transcriptional network (Boyer et al., 2005). Based on genome-wide analyses of binding sites and target genes, it has been suggested that *OCT4*, *SOX2*, and *NANOG* promote pluripotency and self-renewal via positive regulation of their own genes, as well as genes encoding additional transcription factors, miRNAs and components of key pluripotency signalling cascades, such as the TGFβ and Wnt pathways (Boyer et al., 2005). Analyses of the early events triggered by the introduction of exogenous pluripotency factors have revealed additional key steps in the reprogramming process, including promotion of the mesenchymal-to-epithelial transition (MET) (Mah et al., 2011; Eastham et al., 2007; Wong et al., 2004); elongation and epigenetic modification of telomeres (Marion et al., 2009); and a reconfiguration of mitochondria and energy metabolism similar to that observed in cancer cells (Prigione et al., 2011a; Prigione et al., 2010; Warburg, 1956). The latter, which results in a decrease in both mitochondrial number (Kelly et al., 2011; Armstrong et al., 2010; Prigione et al., 2010) and oxidative phosphorylation, leads to an increase in glycolysis (Varum et al., 2011; Zhang et al., 2011) and a decrease in levels of reactive oxygen species (Armstrong et al., 2010; Prigione et al., 2010). These metabolic changes occur before the re-establishment of ESC-like properties (Mah et al., 2011), and are thus likely to play an instrumental role in reprogramming – a fact borne out by the observation that small-molecule-based alterations of energy metabolism enhance the efficiency of reprogramming (Yoshida et al., 2010; Zhu et al., 2010).

Despite these insights, the distinct pathways and mechanisms underlying the conversion of somatic cells to a pluripotent phenotype remain incompletely understood (Drews et al., 2012). To this end, a recent study analysed the early events triggered by retroviral transduction of *OCT4*, *SOX2*, *KLF4* and *c-MYC* (Mah et al., 2011). One of the key findings of this investigation was a significant increase in levels of reactive oxygen species upon viral transduction, resulting in DNA damage and ultimately, the activation of p53, responsible for cell cycle arrest, apoptotic induction and senescence. These

results support previous observations that downregulation of p53 enhances cellular reprogramming in both human and mouse somatic cells, suggesting that this may be a crucial hurdle to overcome in reprogramming experiments (Wang and Adjaye, 2011; Hong et al., 2009).

Epigenetic remodelling, via alteration of histone modification and CpG methylation patterns, was highlighted in one of the first reports of human iPSCs (Takahashi et al., 2007), as a mechanism enabling access of the transcriptional machinery to pluripotency-associated genes, thereby facilitating major transcriptional changes during the process of reprogramming. Global studies of mouse embryonic fibroblasts (MEFs) and MEF-derived iPSCs have revealed greater details regarding the kinetics of distinct histone modifications occurring throughout de-differentiation (Mattout et al., 2011). These results support the finding that small molecules which influence chromatin remodelling, such as VPA or vitamin C, may enhance the efficiency of reprogramming, in conjunction with the overexpression of pluripotency transcription factors (Esteban et al., 2010; Zhu et al., 2010; Huangfu et al., 2008).

4.1.4 Clinical applications

Induced pluripotent stem cells may be useful for a range of applications, including the modelling of mono- and multigenic diseases, the investigation of complex genetic traits and allelic variation, autologous cell therapy, and as substrates for toxicity, drug, differentiation and therapeutic screens (González et al., 2011).

4.1.4.1 *Autologous cell replacement therapies*

The *in vitro* developmental potential and the success of iPSCs in animal models (Wernig et al., 2008; Hanna et al., 2007) suggest that iPSC-derived cells may be a viable regenerative source for transplantation therapies in human patients. Such applications will be guided by the outcomes of the

first clinical trials using human ESC-derived cells, such as the recent cell replacement therapy trial by Advanced Cell Technology, which sought to assess the safety of treating macular dystrophy with transplanted human ESC-derived retinal pigment cells (Schwartz et al., 2012). Despite initial successes, the emergence of long-term effects in patients remains to be determined, and several general and experimental obstacles must be overcome before differentiated cell types derived from iPSCs can be applied to humans. These include the prohibitive cost of generating patient-specific iPSC-derived therapeutics, the poor survival of pluripotent cells following cryopreservation (Rizzino, 2010), the necessity of using defined, xeno-free iPSC culture conditions (Takahashi et al., 2009), the development of alternatives to viral-mediated reprogramming, and the elimination of risks associated with teratoma formation, toxicity and immunological rejection, via efficient and reproducible derivation of a pure, lineage-defined cell population from iPSCs (Kriks et al., 2011). The development of alternatives to overcome these hurdles, such as the establishment of HLA-haplotyped iPSC banks (Nakatsuji et al., 2008), remains an ongoing challenge.

4.1.4.2 ***"Disease in a dish"***

The successful conversion of human fibroblasts to iPSCs has generated new opportunities for the modelling of human disease, providing the unique possibility of investigating the molecular mechanisms underlying the aetiology of many monogenic and complex diseases (Drews et al., 2012). Despite the promise of this new technology, one particularly demanding task facing researchers in the field is the need to prove that iPSC-derived models accurately convey the main features of the disease under study. This requires the recruitment of a suitable number of patients, the generation of multiple iPSC lines from each patient, and the establishment of efficient protocols for the differentiation of iPSCs into the disease-affected cell type. Nonetheless, within the past few years, several disease models have been generated, for conditions ranging from retinitis pigmentosa (Jin et

al., 2011) to Friedreich's ataxia (Liu et al., 2011), affirming the ability of iPSCs to reconstruct disease phenotypes *in vitro*.

These iPSC-derived disease models, which have given rise to the term "disease in a dish", provide the means to investigate novel diagnostic markers, to identify drug targets and to screen therapeutic agents, such as small molecule drugs or RNAi. Indeed, evidence from several disease models, including SMA (Ebert et al., 2008) and Rett's syndrome (Marchetto et al., 2010) suggests that *in vitro* drug treatment successfully restores normal distribution of the affected protein.

Perhaps most significantly, iPSCs offer the ability to study mechanisms of degeneration and recovery in conditions for which patient material is not readily available, through their directed differentiation into disease-relevant cell types, such as neurons. In this way, iPSC technology has provided a breakthrough in the study of neurodegenerative disease (discussed in more detail in Chapter 5).

4.1.5 Characterisation of iPSCs

The inherent qualities of iPSCs have made them an attractive source of cells for the development of patient-derived models of disease. However, the low rate of reprogramming, together with the high mutagenic risk associated with virus-mediated reprogramming have necessitated the establishment of criteria for the selection, propagation and cross-lab comparison of reproducible, pluripotent cell lines (Maherali and Hochedlinger, 2008). These include the presence of characteristic features of ESCs, such as the presence of ESC-like morphology, the expression of cell surface markers that characterise undifferentiated human cells (for example, TRA-1-60 or TRA-1-81), and the ability to differentiate into representative cell types of each of the three embryonic germ layers (Thomson et al., 1998). Teratoma formation in immune-deficient mice, once considered the gold standard for the latter criterion, has in recent years been replaced by methods of *in vitro* differentiation, particularly

when the iPSCs in question are to be used solely for *in vitro* purposes such as disease modelling or drug screening (Ellis et al., 2009). In addition, iPSCs derived by integrating virus transduction should demonstrate reprogramming factor independence, characterised by the shutdown of viral transgene expression, and a concomitant upregulation of endogenous pluripotency gene expression (Ellis et al., 2009; Maherali and Hochedlinger, 2008). Finally, the genomic integrity of the iPSC lines should be assessed, particularly when iPSCs are likely to be used in transplantation therapies, as chromosomal aberrations may enhance tumorigenicity and affect differentiation capacity (Mayshar et al., 2010).

4.1.6 Aims

The aims of the experiments described in this chapter were thus to generate iPSC lines through retrovirus-mediated reprogramming of SCA7 patient and control dermal fibroblasts, using a three-factor combination (*OCT4*, *SOX2* and *KLF4*), together with the HDAC inhibitor valproic acid, and to characterise the lines generated with respect to:

1. repression of retroviral transgene expression,
2. expression of endogenous pluripotency genes and cell-surface markers,
3. genomic integrity, and
4. the ability to differentiate into cells of each of the three embryonic germ layers (endoderm, mesoderm and ectoderm).

This work was completed in collaboration with Dr Janine Scholefield (Department of Physiology, Anatomy and Genetics, University of Oxford), together with Dr Sally Cowley and Ms Jane Vowles (James Martin Stem Cell Facility, Sir William Dunn School of Pathology, University of Oxford). The control iPSC line iPS-NHDF-2, designated in this thesis as iPS SC NHDF, together with its accompanying characterisation data, were kindly provided by Dr Cowley and Ms Vowles.

4.2 Results

4.2.1 Reprogramming fibroblasts to iPSCs

Patient and control fibroblasts were transduced with retroviral vectors containing the three reprogramming factors, *OCT4*, *SOX2*, and *KLF4*. In order to determine the success of infection, transduced fibroblasts were subjected to immunostaining for Klf4 protein approximately 10 days post-infection. Infected fibroblasts showed intense nuclear staining for Klf4 (Fig. 11a), compared to the markedly lower levels of endogenous Klf4 expressed in uninfected controls (Fig. 11b), indicating efficient retroviral transduction.

After approximately 20 to 40 days in culture, colonies exhibiting ESC-like morphology were observed (Fig. 11c), comprised of cells exhibiting a cobblestone appearance with high nuclear:cytoplasm ratio and pronounced individual cell borders, as has been previously described (Maherali and Hochedlinger, 2008) (Fig. 11d). After successive passages, the colonies displayed a more uniform morphology, with well-defined borders (Fig. 11e), and appeared capable of unlimited self-renewal. As is the case with ESCs, spontaneous differentiation was occasionally observed at the centre of iPSC colonies (Fig. 11f).

A complete list of the iPSC lines generated from patient and control fibroblasts can be found in Table 4. Six iPSC lines were generated from each of the SCA7 patient fibroblast lines, resulting in an estimated reprogramming efficiency of 0.012%.

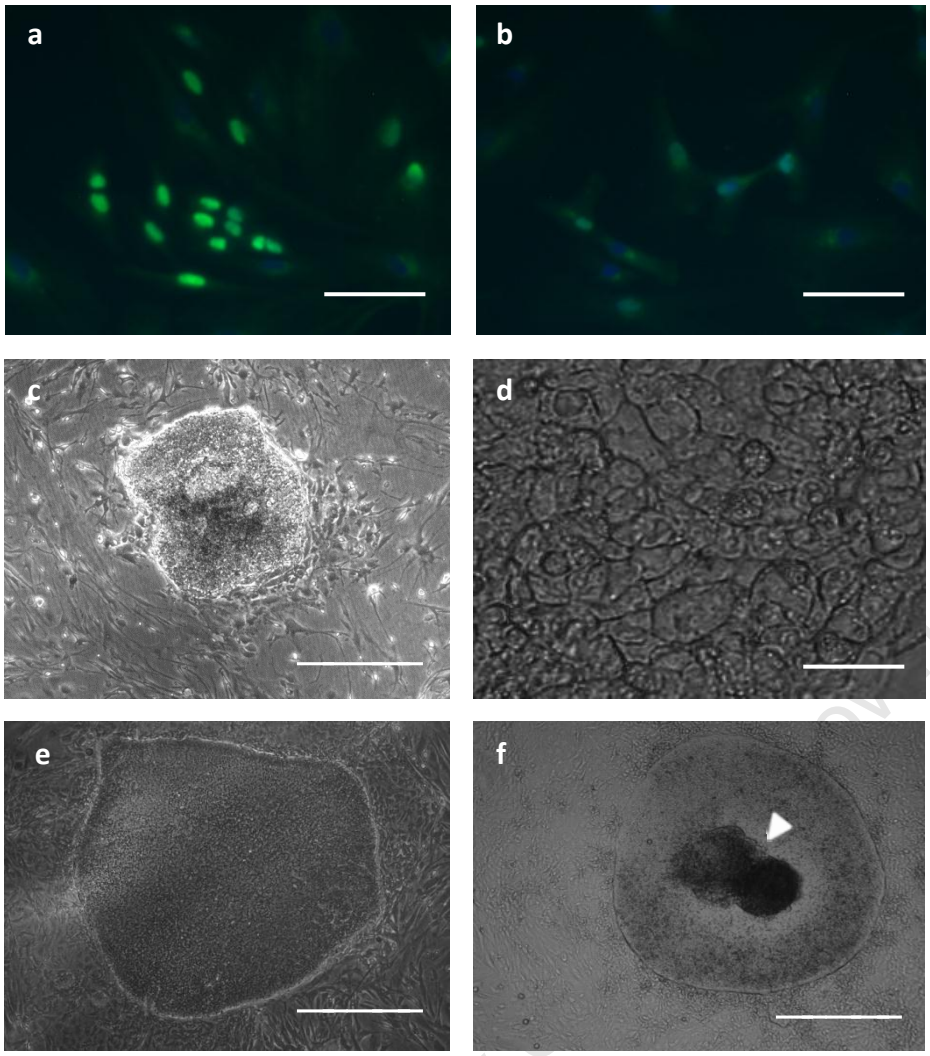

Figure 11 Reprogramming of fibroblasts to iPSCs. (a) Fibroblasts transduced with retroviral vectors showed significantly elevated expression of Klf4 (green), compared to untransduced fibroblasts (b), 10 days post-reprogramming, indicating that they had been successfully infected. Nuclei are stained with DAPI (blue). (c) Colonies exhibiting ESC-like morphology appeared after 20-40 days in culture. (d) iPS George at high magnification, showing a typical cobblestone appearance with pronounced individual cell borders. (e) Flat, uniform morphology of an established iPSC line at passage 6 (iPS George). (f) Spontaneously differentiated cells in the centre of an iPSC colony (indicated by white arrowhead). Scale bars: (a), (b), (d), 100µm; (c), (e), (f), 500µm.

Table 4 iPSC lines generated from SCA7 patients and controls.

Fibroblast line of origin		Derived iPSC lines	Reprogramming factors
Name	**Disease status***		
JS Con	Control	George	OSK
SC Con†	Control	SC NHDF†	OSKMN
1518	SCA7 patient	A‡	OSK
		B	
		C	
		D	
		F	
		G	
1519	SCA7 patient	A	
		B	
		C	
		D	
		E	
		G	

*For further information, see Sections 2.1 and 2.2. †Kindly provided by Dr Sally Cowley. ‡Each letter represents an individual colony identified on the original reprogramming plate, which was isolated and clonally expanded to generate an iPSC line.

Key to reprogramming factors: O: *OCT3/4* S: *SOX2* K: *KLF4* M: *c-MYC* N: *NANOG*

4.2.2 iPSC characterisation

Characterisation was performed on a subset of iPSC lines, which showed the most robust growth and proliferation on both iMEF feeder layers and in feeder-free conditions.

4.2.2.1 *Repression of transgene expression*

Human iPSCs have been found to silence expression of the retroviral transgenes used in reprogramming in some (Takahashi et al., 2007) but not all (Dimos et al., 2008; Takahashi et al., 2007; Yu et al., 2007) cases. Reverse transcriptase PCR, using primers specific to the retroviral transcripts (Appendix 4, A4.8), demonstrated nearly complete silencing of pMXs-hSox2 and pMXs-hKlf4 at approximately passage 10 post-reprogramming (Fig. 12). Persistent expression of pMXs-hOct3/4 was detected in four of the patient lines, as has been previously reported (Dimos et al., 2008).

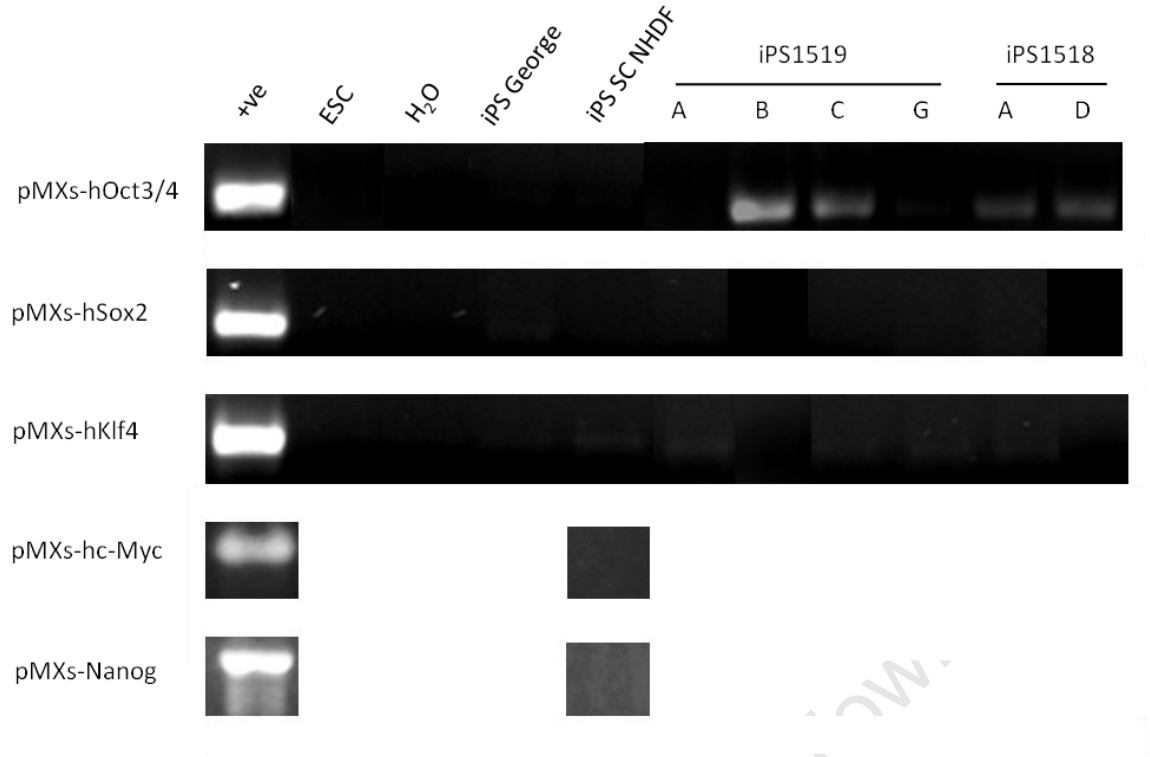

Figure 12 RT-PCR analysis of transgene expression in iPSC lines. Primers specific to the retroviral transcripts were used to detect persistent transgene in the iPSC lines generated. Both iPSC control lines (iPS George and iPS SC NHDF) appeared to have silenced expression of all transgenes, while persistent expression of pMXs-hOct3/4 was detected in four of the patient-derived iPSC lines (iPS 1519B and –C, and iPS 1518 A and –D). HEK293 cells transfected with the relevant plasmid were used as a positive control in each case, while human ESCs served as a negative control. Data for pMXs-hc-Myc and pMXs-Nanog expression in iPS SC NHDF courtesy of Dr Sally Cowley.

4.2.2.2 ***Expression of endogenous pluripotency genes***

The loss of transgene dependence, indicated by the induction of endogenous pluripotency genes, is a critical marker of complete reprogramming (Maherali and Hochedlinger, 2008). RT-PCR indicated that genes expressed in pluripotent cells (*OCT4*, *SOX2*, *NODAL*, and *c-MYC*) were expressed in human ESCs as well as in the six iPSC lines and two control lines assessed here (Fig. 13; primers listed in Appendix 4, A4.7). Moreover, these pluripotency marker genes were not expressed in the fibroblasts from which the iPSCs had been derived, with the exception of *c-MYC*, which was

expressed in one of the parental fibroblast lines, 1518, similar to previous reports (Takahashi et al., 2007).

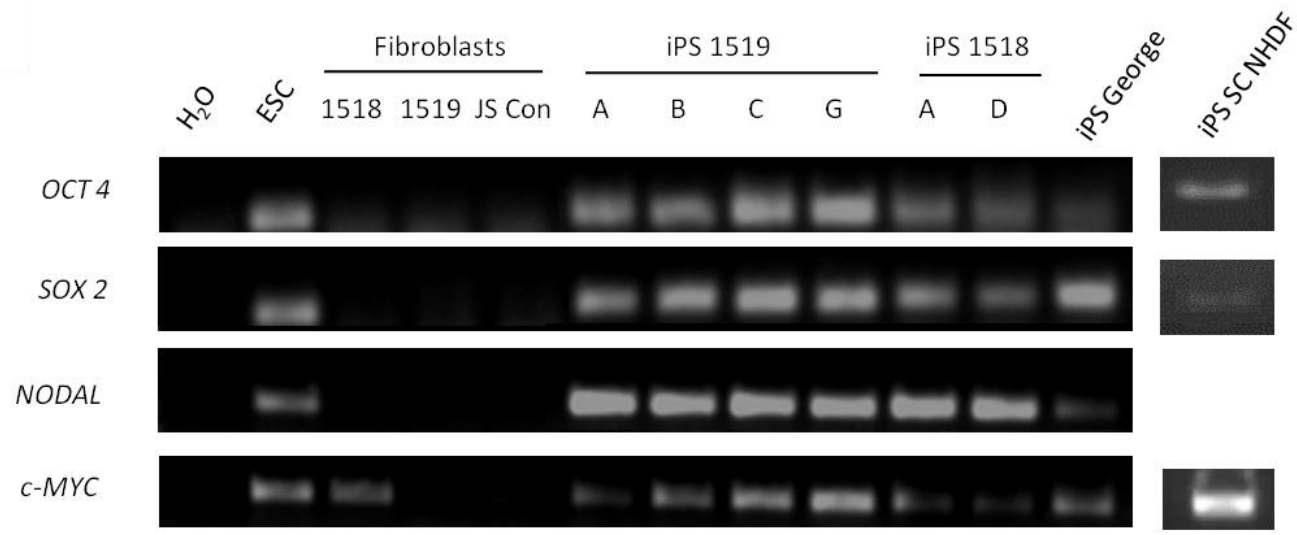

Figure 13 Expression of endogenous pluripotency genes. Primers specific for the endogenous transcripts were used to confirm that the iPSC lines generated expressed pluripotency-associated genes. Human ESCs served as a positive control. Expression of the pluripotency genes was not detected in the parental fibroblast lines, with the exception of *c-MYC*, which was expressed in the 1518 line. Data for iPS SC NHDF courtesy of Dr Sally Cowley.

4.2.2.3 *Expression of cell surface markers of pluripotency*

The expression of ESC-specific cell surface antigens is another key marker of pluripotency. The levels of two such antigens, Tra-1-160 and Tra-1-81, were assessed in several of the iPSC lines. All lines tested showed robust expression of the pluripotency markers, in contrast to the surrounding iMEF feeder cells, which served as a negative control (Fig. 14).

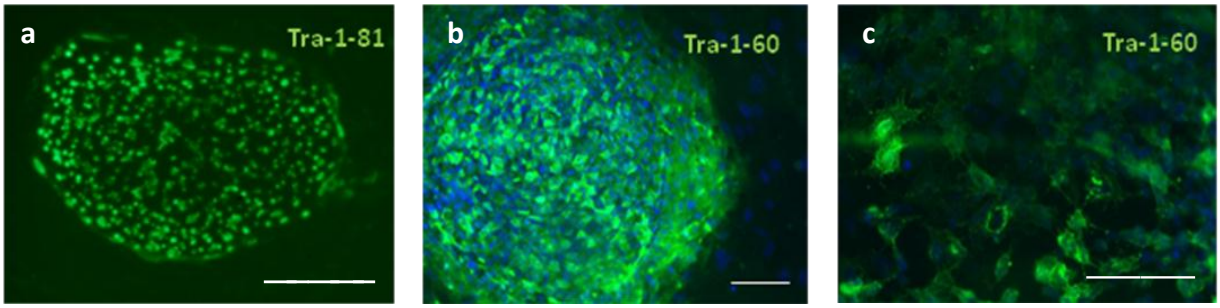

Figure 14 Expression of cell surface markers of pluripotency. All iPSC lines tested stained positive for cell surface markers of pluripotency including Tra-1-81 and Tra-1-60. (a) iPS SC NHDF (b) iPS George (c) iPS 1519A. Nuclei are stained with DAPI (blue). Images courtesy of Dr Sally Cowley and Ms Danielle Smith. Scale Bars: (a), 500µm; (b) and (c), 100µm.

4.2.2.4 ***Genomic integrity***

The genomic integrity of five of the iPSC lines (iPS SC NHDF, 1518A, 1518D, 1519A and 1519C) was determined using the Infinium HD assay, on HumanCytoSNP-12v2.1 bead-chips (Illumina). The HumanCytoSNP-12 BeadChip contains approximately 300,000 genetic markers per sample, targeting all known cytogenetic abnormalities found in genes and pathways linked to mental retardation, autism, as well as additional common chromosomal anomalies. It is therefore capable of detecting numerous types and sizes of structural variation in the human genome affecting phenotypes, including duplications, deletions, amplification, copy-neutral loss of heterozygosity and mosaicism. An additional control line, iPS George, was karyotyped using traditional G-banding.

The integrity of each iPSC line was assessed by comparison with its parental fibroblast line. Small amplifications, deletions and regions of loss of heterozygosity occasionally appear in the parental fibroblasts. Thus, iPSC lines which did not differ significantly from the parental fibroblasts were deemed acceptable for use, provided no gross structural abnormalities, such as large-scale duplications, deletions, rearrangements, or structural alterations affecting the gene-of-interest (in this case, *ataxin-7*) could be detected. On this basis, the genomic integrity of the iPSC lines 1518D, 1519A and –C, iPS SC NHDF and iPS George were all deemed sufficient for further experiments

(Fig. 15 and Appendix 6). The quality of DNA obtained for 1518A made assessment of the genomic integrity of the sample difficult, resulting in the exclusion of this sample from further analysis.

In addition, SNP patterns for chromosome 1 could be used to match parental fibroblasts to their derived iPSC lines, confirming the origin of the reprogrammed cells, and eliminating the possibility of cross-contamination of the lines.

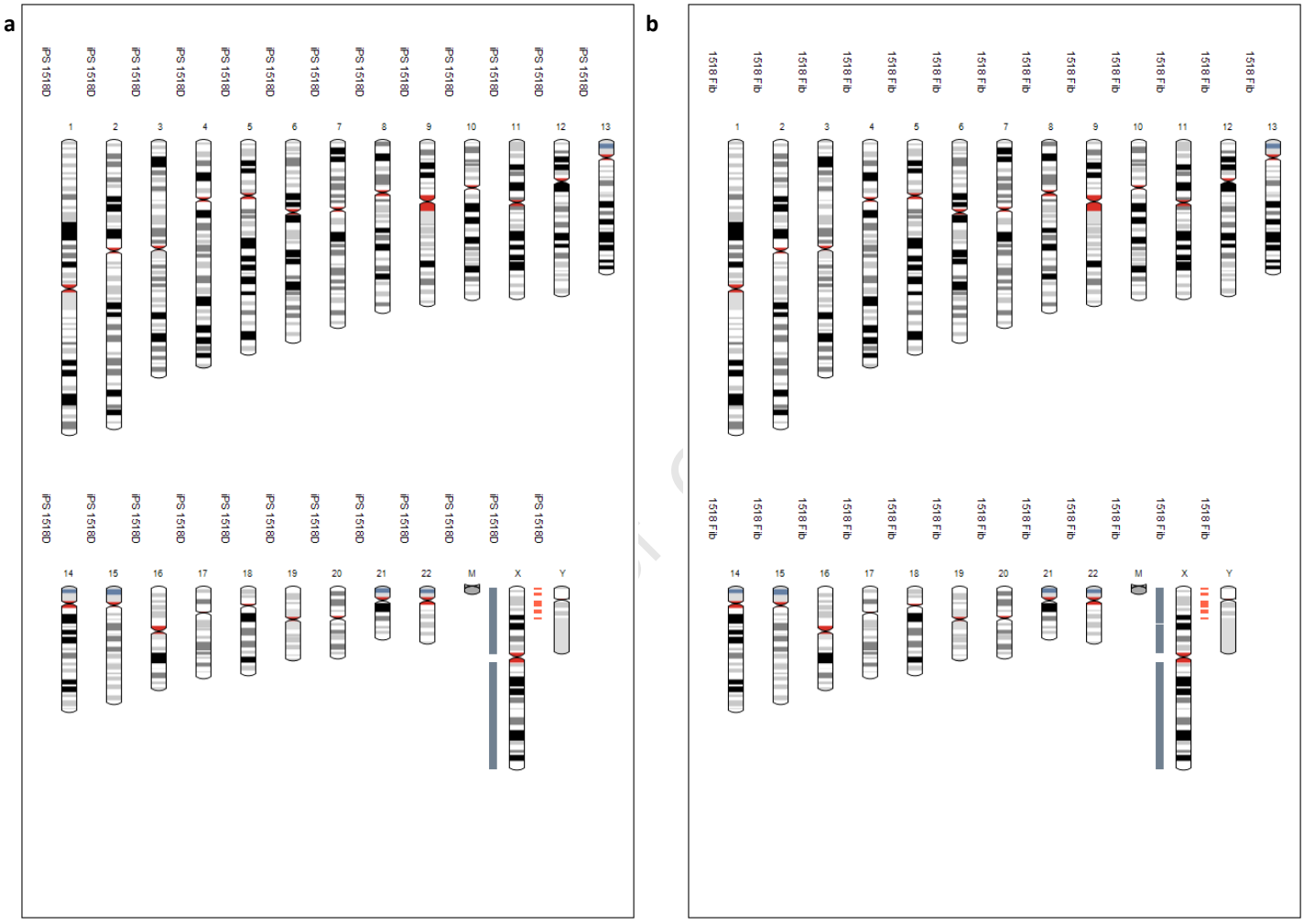

Figure 15 Chromosomal analyses of SCA7 and control iPSC lines. Representative result of the HumanCytoSNP-12 BeadChip (results for the remaining iPSC lines can be found in Appendix 6), showing no gross structural abnormalities when comparing the SCA7 iPSC line 1518D (a) to its parental fibroblast line, 1518 (b). A green horizontal line adjacent to a chromosome region indicates a copy number of more than 2; while a red horizontal line indicates a copy number of less than 2. Vertical grey bars indicate loss of heterozygosity, except in the case of the X-chromosome, where grey indicates 2 copies and red indicates 1 copy. Chromosome "M" represents mitochondrial DNA.

4.2.2.5 *In vitro differentiation from embryoid bodies*

To determine the differentiation capabilities of the iPSC lines generated *in vitro*, dissociated iPSCs were cultured in suspension to form embryoid bodies (EBs). After 8 days in suspension culture, iPSCs formed ball-like structures (Fig. 16a). Two of the iPSC lines (iPS George and 1519C) were then subjected to undirected differentiation, in which EBs were transferred to gelatin-coated plates and allowed to spontaneously differentiate for a further 8 days before RNA extraction. Reverse transcriptase PCR confirmed that these differentiated cells expressed paired box 6 (*PAX6*, a marker of ectoderm), microtubule-associated protein 2 (*MAP2*, ectoderm), Msh homeobox 1 (*MSX1*, mesoderm), forkhead box A2 (*FOXA2*, endoderm), and α-fetoprotein (*AFP*, endoderm), to varying degrees (Fig. 16b). By contrast, the undifferentiated iPSC lines did not express these germ-layer markers (with the exception of *MAP2*, which was expressed at low levels in iPSCs, compared to EBs).

EBs from a further two iPSC lines, iPS SC NHDF and 1519A, were subjected to directed differentiation into the three germ layers, as described in Section 2.9.6.4. Immunocytochemistry was used to detect cells which stained positive for markers of the three embryonic germ layers: FOXA2 and/or AFP (endoderm), α-sarcomeric actin and/or α-smooth muscle actin (mesoderm), and βIII-tubulin (ectoderm). EBs from both lines differentiated into a variety of cell types, representatives of which stained positive for all the aforementioned markers (Fig. 16c-h), indicating the ability of these iPSC lines to generate all three embryonic germ layers – further confirmation of their pluripotency.

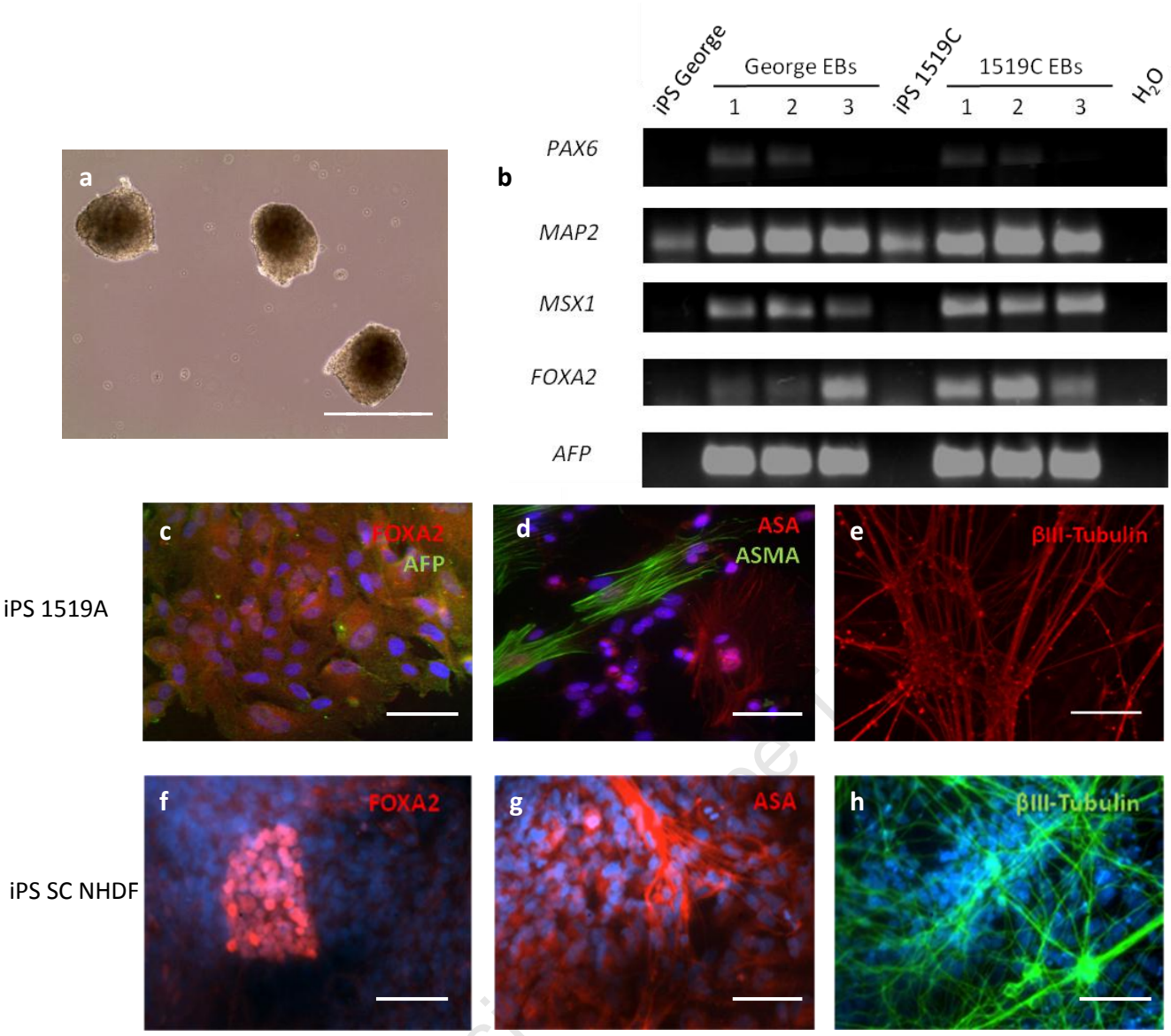

Figure 16 Embryoid body-mediated differentiation of SCA7 and control iPSCs. (a) Floating cultures of iPSCs at day 8. (b) Reverse-transcriptase PCR analysis of germ layer markers in EBs from iPSC lines iPS George and 1519C indicate their ability to differentiate into all three germ layers. Immunostaining confirmed the ability of the iPSC line 1519A to differentiate into endoderm (c) and mesoderm (d). Ectodermal differentiation was confirmed by the ability of the line to generate βIII-tubulin positive neurons (e) (see Chapter 5). Similarly, the ability of iPS SC NHDF to differentiate into endoderm (f), mesoderm (g) and ectoderm (h) was assessed by immunostaining. FOXA2, Forkhead box protein A2; AFP: α-fetoprotein; ASA, α-sarcomeric actin; ASMA, α-smooth muscle actin. Nuclei are stained with DAPI (blue). Scale bars: (a), 500µm; (c)-(h), 100µm. Immunostaining images courtesy of Dr Janine Scholefield (c), (d) and Dr Sally Cowley/Ms Jane Vowles (f), (g), (h).

4.3 Discussion

This study has demonstrated the generation of iPSCs from dermal fibroblasts of adult SCA7 patients by retroviral transduction with three reprogramming factors, namely pMXs-hOct3/4,-hSox2 and -hKlf4, in combination with the HDAC inhibitor, valproic acid. The established iPSCs resemble human ESCs in several aspects, including morphology, proliferation, expression of cell surface markers and pluripotency genes, and capacity for *in vitro* differentiation. This is only the second report of iPSC generation from SCA7 patients, and the first to demonstrate successful reprogramming using patient fibroblasts from the South African SCA7 cohort (Luo et al., 2012).

4.3.1 Retrovirus-mediated reprogramming of fibroblasts to iPSCs

The observed efficiency of reprogramming of SCA7 patient fibroblasts to iPSCs (~0.01%) is comparable to previous reports of retrovirus-mediated reprogramming of adult dermal fibroblasts (Takahashi et al., 2007). This is, in part, a reflection of the probability of simultaneous transduction with all three retroviral vectors, a prerequisite for reprogramming to pluripotency (Takahashi et al., 2007).

The use of retroviral vectors for iPSC reprogramming represents a balance between efficiency, and safety concerns regarding genomic integration. Numerous strategies to avoid viral integration have been tested (see Section 4.1.1), with some achieving enhanced reprogramming rates, while others demonstrate impractically low efficiencies. The labour intensive nature of direct delivery of proteins or RNA, requiring repeated delivery of reprogramming factors, together with the technical demands associated with the preparation of modified Sendai virus vectors or synthesised RNA initially hindered the development of these methods (Okita and Yamanaka, 2011). However, ongoing improvements in technology, together with recent evidence suggesting that integration events may affect the expression profile of iPSCs have led to increased efforts to develop reprogramming

methods which avoid genomic alterations (Liu et al., 2012). Thus, future experiments are likely to employ a combination of methods to enhance efficiency while minimising the effects of integration, including p53 suppression, and the addition of small molecule enhancers of reprogramming, in addition to the HDAC inhibitor valproic acid used here (Okita and Yamanaka, 2011; Huangfu et al., 2008). Different factor combinations may also be employed to compensate for decreases in delivery efficiency, such as the substitution of oncogenic *c-MYC* with the more potent and specific *L-MYC* (Nakagawa et al., 2010). Additional strategies, including anti-inflammatory modulation of the innate immune response (upregulated in response to viral transduction), preselection of cells expressing pluripotency-associated cell-surface antigens, and the activation of specific interaction pathways which amplify pluripotency signalling have also been suggested (Mah et al., 2011).

Nonetheless, the primary factor influencing the choice of reprogramming method remains the downstream applications of the iPSCs generated. As outlined in Table 3, the reproducibility and relative efficiency of retroviral reprogramming, in comparison to non-integrative methods, have made it the preferred method for generating iPSCs for *in vitro* disease modelling, in which integration-associated tumorigenesis is not a primary concern.

4.3.2 Repression of transgene expression

The multiple challenges associated with virus-mediated reprogramming have led to the establishment of criteria for the selection of reproducible, full reprogrammed pluripotent cell lines (Maherali and Hochedlinger, 2008). Of these, the silencing of retroviral transgenes post-reprogramming is of particular importance, as even low levels of persistent transgene expression may affect the molecular signatures, differentiation behaviour and developmental potential of iPSCs (Stadtfeld et al., 2008). As such, only iPSCs which have upregulated endogenous markers of pluripotency in conjunction with the downregulation of transgene expression can be considered to be fully reprogrammed (Hotta

and Ellis, 2008; Okita et al., 2007). Indeed, transgene silencing has been associated with an increase in germ-line competency (Okita 2007), while persistent transgene expression may be a risk factor for tumorigenicity (Okita et al., 2007) and genomic instability (Ramos-Mejia et al., 2010).

In this study, four of the iPSC lines analysed demonstrated nearly complete silencing of all retroviral transgenes, approximately 10 passages post-reprogramming. The remaining four lines tested (1519B and –C, and 1518A and –D) showed persistent expression of pMXs-hOct3/4, similar to previously-described iPSC lines (Dimos et al., 2008; Yu et al., 2007). This may have resulted from the specific integration of *OCT4* transgenes into active loci in these clones, where the transgene expression level could be influenced by the flanking promoter regions, allowing for sustained expression. Of greater importance is the confirmed silencing of the transgenes pMXs-hKlf4 and -hc-Myc (known oncogenes) in the iPSC lines into which they had been introduced, since their continuous ectopic expression may make cells more vulnerable to further oncogenic events, eventually leading to gross chromosomal abnormalities (Ramos-Mejia et al., 2010).

Variation in transgene repression between iPSC clones is a well-documented phenomenon, with possible implications for the complete conversion of iPSCs to an ESC-like state (Lowry et al., 2008). However, results from continual culture of iPSCs suggest that reprogramming continues even after the establishment of iPSC colonies, resulting over time in a gene expression pattern more similar to ESCs than that of earlier passages (Okita and Yamanaka, 2011; Chin et al., 2009). Thus, it seems likely that prolonged culture of these iPSC lines may result in silencing of even the *OCT4* transgene. Nevertheless, the observation that persistent transgene expression does not appear to affect downstream differentiation events (Dimos et al., 2008), suggests that these lines, while unsuitable for *in vivo* applications, may still be useful for modelling disease mechanisms *in vitro*.

The elimination of transgene expression remains a concern, however. Future studies are therefore likely to involve either the generation of larger numbers of iPSC lines by retroviral transduction (in order to increase the statistical likelihood of generating transgene-free clones), or a switch to non-integrating methods of reprogramming, such as those described in Section 4.1.1.

4.3.3 Expression of pluripotency markers, and capacity for *in vitro* differentiation

Similar to human ESCs, the iPSC lines generated here all showed robust expression of pluripotency-associated genes and cell surface markers – the result of global epigenetic remodelling brought about by alterations in histone modification and CpG methylation patterns (Drews et al., 2012). Consequently, expression patterns of iPSCs more closely resembled that of the ESC positive control than those of their parental fibroblasts (Mah et al., 2011). One exception was the expression of *c-MYC* observed in the 1518 fibroblast line. However, endogenous expression of *c-MYC* in fibroblasts has been previously reported (Dimos et al., 2008; Takahashi et al., 2007).

In addition to the ESC-like patterns of gene expression, all the iPSC lines tested here were capable of embryoid body formation and differentiation into the three embryonic germ layers, a hallmark of pluripotency. Results for two of the lines (iPS George and 1519C), obtained using reverse-transcriptase PCR, suggested that the expression of germ layer markers was not uniform across all EBs – a fact which has been previously reported (Okita and Yamanaka, 2011; Yu et al., 2007). While expression of germ layer markers was generally not detected in undifferentiated iPSCs, both iPS George and 1519C showed some *MAP2* expression. This is of particular interest, since previous reports have shown a correlation between another ectodermal marker (*PAX6*) and a failure to downregulate the *OCT4* transgene (Yu et al., 2007).

Due to limited cell availability, not all cell lines were subjected to EB-mediated differentiation. However, as all of the SCA7 patient iPSC clones were generated in the same manner, those which passed all other tests of integrity and pluripotency, and could be successfully differentiated into neurons using the methods described in Section 2.10, were deemed fit for use for *in vitro* modelling of the disease.

4.3.4 Genomic integrity of iPSCs

The reprogramming process has been associated with a high mutation rate (Gore et al., 2011; Hussein et al., 2011), and recent findings indicate that the derivation of iPSCs may alter the integrity of the genome of the parental cells. Indeed, the occurrence of chromosomal aberrations within human ESCs and iPSCs has been demonstrated by several groups, and it appears that certain types of aneuploidies (such as trisomy 12) may confer a proliferative advantage, by increasing the expression of pluripotency-associated genes located on the affected chromosomes, such as *NANOG*, or *LIN28* (Laurent et al., 2011; Mayshar et al., 2010).

As the genomic integrity of iPSCs is a matter of critical importance for clinical applications, it is essential to address the biological and clinical relevance of such mutations (Drews et al., 2012). To date, none of the chromosomal abnormalities detected has been found to severely compromise cellular functionality, suggesting that such aberrations may be transient (Pasi et al., 2011), particularly since several iPSC lines harbouring karyotypic variations have been shown to pass stringent tests of differentiation capacity (Boulting et al., 2011). iPSCs derived from aged donors appear most prone to abnormalities. However, these cells do not exhibit abnormally high levels of oxidative stress, DNA damage or apoptosis resistance, all hallmarks of cancer transformation (Prigione et al., 2011b). In addition, the presence of mitochondrial mutational events does not appear to affect reprogramming-associated modulation of energy metabolism (Prigione et al., 2011a).

Thus, despite the potential risks for clinical applications, the loss of nuclear and mitochondrial genome integrity detected in some iPSC lines does not appear to be associated with any particular cellular deficiency, indicating that reprogramming-related genomic alterations may not necessarily result in the acquisition of malignant features (Drews et al., 2012), although further detailed investigations will be required to distinguish harmless variations from those capable of impairing functionality and enhancing clinical risks.

Although retrovirus-mediated reprogramming poses a significantly lower risk for aneuploidy compared to adenoviral transduction (Stadtfeld et al., 2008), the persistent expression of integrated transgenes post-reprogramming has been suggested to increase the likelihood of genomic instability (Ramos-Mejia et al., 2010). To rule out this possibility, the genomic integrity of five of the iPSC lines generated here was assessed using the Infinium HD assay, on HumanCytoSNP-12v2.1 bead-chips, with a further one line (iPS George) assessed using traditional G-banding karyotypic analysis. All of the lines assessed were deemed euploid and, while several small-scale changes were observed across all iPSCs, these did not differ significantly from the parental fibroblast karyotypes in each case, confirming the absence of gross chromosomal abnormalities. No abnormalities were observed in mitochondrial DNA, which have been previously reported to occur in iPSCs (Prigione et al., 2011a).

Such a study is not without limitations, however. Although SNP arrays such as the HumanCytoSNP-12v2.1 used here offer enhanced resolution over traditional karyotyping methods, both approaches are limited to measuring changes in DNA content and chromosome morphology. They therefore provide little data regarding the effects of such changes on global gene expression. In addition, SNP arrays may fail to detect certain abnormalities, such as balanced translocations. Thus, an alternative method for assessing chromosomal integrity of iPSCs using transcriptional profiling has been

proposed, in order to identify clusters of genes with significantly elevated or reduced expression, which may be of clinical significance (Mayshar et al., 2010).

Finally, it has been shown that long-term culture of iPSCs may lead to the stochastic acquisition of adaptive copy number aberrations, which confer a growth advantage (Mayshar et al., 2010). It is therefore recommended that karyotypic analysis be periodically performed for all iPSCs intended for long term use, in order to ensure their continued genomic integrity.

4.3.5 Fibroblasts as a source of primary cells

Dermal fibroblasts remain the most common source of primary cells for reprogramming to pluripotency, accounting for 80% of the iPSC studies to date (González et al., 2011). However, the requirement for skin biopsies and the need to expand fibroblasts for several passages *in vitro* to generate sufficient numbers of cells for reprogramming experiments present distinct disadvantages. Alternative sources of primary cells have therefore been proposed, including peripheral blood (Loh et al., 2009) and keratinocytes (Trond Aasen et al., 2008), each of which have advantages and limitations.

Keratinocytes, which can be cultured and reprogrammed form a single plucked hair, offer a simple and accessible route to iPSC generation, avoiding the need for medical personnel and invasive procedures during their harvest (Trond Aasen et al., 2008). In addition, the reprogramming of ectodermal keratinocytes has been found to be two-fold faster and up to 100-fold more efficient, when compared with dermal fibroblasts. However, considerable more care is required when isolating, culturing and transducing cells, particularly since the growth and quality of hair follicles, and hence, of the keratinocytes themselves, are dependent on the age and medical condition of the donor (Krause and Foitzik, 2006; Botchkarev, 2003). This is in contrast to fibroblasts, whose age

and medical condition appear to have little bearing on the efficiency of reprogramming (Dimos et al., 2008).

The generation of iPSCs from human blood cells represents a novel method using easily accessible cells, which require little manipulation time in culture (Loh et al., 2009). However, a study based on global gene expression, microRNA expression and histone modification data has highlighted the existence of residual gene expression patterns in iPSCs – a form of "epigenetic memory" – which may result from incomplete silencing of genes specific to the parental tissue of origin (Chin et al., 2009). As a result, iPSCs may preferentially differentiate back into the lineage from which they were originally derived, suggesting that ectodermal cells (such as fibroblasts) may be more suited to generating iPSCs for neurological diseases than mesoderm-derived blood cells (Ohi et al., 2011; Marchetto et al., 2009).

4.3.6 Concluding remarks

The generation of iPSCs from patient somatic cells has revolutionised the field of pluripotent cell technology, offering the opportunity to generate an unlimited source of patient-derived cells for disease modelling, drug screening and autologous transplantation therapies, while bypassing the ethical and host-rejection issues associated with classical ESC technology (Inoue, 2010; Abeliovich and Doege, 2009).

This study has demonstrated the feasibility of generating iPSCs from the South African SCA7 patient cohort, through the transduction of patient dermal fibroblasts with retroviral vectors (Takahashi et al., 2007). The resulting iPSCs recapitulate many features of ESCs, and satisfy the criteria for the successful reprogramming of somatic cells to pluripotency (Ellis et al., 2009; Maherali and Hochedlinger, 2008), including the silencing of (the majority of) retroviral transgenes, upregulation

of endogenous pluripotency genes, ability to differentiate into the three embryonic germ layers, and karyotypic normality.

Numerous challenges to iPSC technology remain to be addressed. The process of reprogramming is relatively slow and inefficient, and the extent to which iPSCs can replace ESCs in every aspect is still a topic for debate. Persistent expression of oncogenic transgenes may limit the transplantation potential of retrovirally reprogrammed iPSCs, while the presence of tumorigenic partially-reprogrammed cells within an iPSC population may pose additional risks for cell-based therapies – an observation which has led to the exploration of alternative methods of reprogramming, which bypass iPSC intermediates altogether (Pang et al., 2011; Vierbuchen et al., 2010; Abeliovich and Doege, 2009).

Nevertheless, the SCA7 iPSCs generated here serve as a starting point for differentiation into a variety of disease-associated cell types, including neurons, providing an ideal model in which to study neurodegenerative disease.

Chapter 5 **Identification of a Transcriptional Phenotype in an iPSC-derived Model of SCA7**

5.1 Introduction

The unique characteristics of iPSCs suggest they are likely to become a powerful tool for biomedical research, as well as a source for cell-replacement therapies (Inoue, 2010; Soldner et al., 2009). Although the realization of iPSC-based therapies is still in its very early stages, the possibility of *in vitro* modelling of human disease may make patient-specific iPSCs immediately valuable, particularly for diseases affecting the CNS (Soldner et al., 2009).

5.1.1 iPSC-derived models of neurodegenerative disease

In addition to the studies of ALS and SMA described in Section 1.5.2.1 (Dimos et al., 2008; Ebert et al., 2008), neurons derived from iPSCs have been used to model a variety of other neurodegenerative disorders (Table 5), including Parkinson's disease (Soldner et al., 2009) and several of the polyQ diseases. The generation of SCA3 patient neurons from iPSCs was first reported in 2011 by Koch et al. In response to L-glutamate-induced excitation, these neurons undergo calcium-dependent proteolysis of Ataxin-3, triggering aggregation of the disease-causing protein. This aggregation, which was also found to depend on functional sodium and potassium channels, as well as ionotropic and voltage-gated calcium channels, could be abolished by calpain inhibition, confirming the key role of this protease in Ataxin-3 cleavage. Furthermore, aggregation was not observed in iPSCs, fibroblasts or glia generated by similar protocols, providing a possible explanation for the neuron-specific phenotype observed in SCA3 patients. The proteolytic liberation of highly aggregation-prone polyQ fragments had been previously proposed as a critical step in the formation of early aggregation intermediates, although the precise pathogenic mechanism of disease initiation had remained elusive (Gatchel and Zoghbi, 2005). The results of this study thus illustrate the merits of

using patient iPSC-derived neurons for the study of aberrant protein processing associated with late-onset neurodegenerative diseases (Koch et al., 2011).

It is interesting to note, however, that the aggregation phenotype observed in these neurons was not associated with the formation of NIs or macroaggregates, or with manifestations of acute cellular toxicity, but rather with the formation of SDS-insoluble microaggregates, which could only be detected by western blot. These observations are not entirely unexpected, as inclusion formation and neuronal death are generally viewed as phenomena of late-stage disease, being exacerbated by an age-related decline in protein homeostasis (Hartl et al., 2011). The findings of this study therefore support the view that early aggregation of polyQ fragments is not necessarily associated with acute toxicity, since neurons appear capable of coping, at least temporarily, with the burden of accumulated polyQ material (Koch et al., 2011).

A number of recent studies using iPSCs derived from HD patients have demonstrated phenotypes including elevated lysosomal activity, mitochondrial deficits, decreased *BDNF* expression, and altered TGFβ and cadherin signalling (An et al., 2012; Camnasio et al., 2012). A study of NSCs derived from 14 HD iPSC lines by the HD iPSC Consortium (2012), revealed a further 1601 genes which were significantly differentially expressed when compared to controls, including those involved in signalling, cell cycle, axonal guidance, and neuronal development. In addition, differentiated HD neural cells demonstrated disease-associated changes in electrophysiology, cell adhesion, metabolism and cell death, many of which were CAG repeat-length dependent (The HD iPSC Consortium, 2012). Of interest, neither the HD nor SCA3 patient derived iPSCs showed significant increases in the disease-causing CAG repeat length after reprogramming, prolonged culture, or differentiation into neurons (Camnasio et al., 2012; Koch et al., 2011).

The recent generation of βIII-tubulin-positive neurons from iPSCs of a single Chinese SCA7 patient has paved the way for similar investigations in other population groups (Luo et al., 2012). To date, however, a disease phenotype in SCA7 iPSC-derived neurons remains to be identified.

Table 5 Examples of successful iPSC-based modelling of neurodegenerative disorders

Disease	Molecular defect	Cells derived from iPSCs	Phenotype in iPSC-derived cells	Reference
Spinal muscular atrophy (SMA)	Mutations in *SMN1*	Astrocytes, neurons, mature motor neurons	Yes (lack of *SMN1* expression, selective death of motor neurons)	(Ebert et al., 2008)
ALS	Mutation in *SOD1*	Motor neurons	Yes (elevated TDP-43 protein levels, decreased survival, increased vulnerability to PI3K inhibition)*	(Bilican et al., 2012; Dimos et al., 2008)
Parkinson's disease	Mutation in *LRRK2* and/or *SNCA*	Dopaminergic neurons	No	(Soldner et al., 2009; Park et al., 2008)
Parkinson's disease (idiopathic and familial)	Mutation in *LRRK2*	Ventral midbrain dopaminergic neurons	Yes (impaired autophagy)	(Sánchez−Danés et al., 2012)
Alzheimer's disease (familial and sporadic)	APP duplication	Neurons	Yes (elevated amyloid-β levels, increased numbers of endosomes)	(Israel et al., 2012)
Huntington's disease	CAG expansion in *HTT*	Neurons	Yes (increased lysosomal activity, mitochondrial and signalling deficits, alterations in transcription, electrophysiology, cell adhesion, metabolism and cell death)	(An et al., 2012; Camnasio et al., 2012; The HD iPSC Consortium, 2012)
Friedreich's ataxia	GAA expansion in *FXN*	Cardiomyocytes, peripheral neurons	Partial (low levels of *FXN* mRNA)	(Liu et al., 2011)
SCA3	CAG expansion in *ataxin-3*	Neurons	Yes (excitation-induced aggregation of Ataxin-3)	(Koch et al., 2011)
SCA7	CAG expansion in *ataxin-7*	Neurons	Not investigated	(Luo et al., 2012)

*Dimos et al. (2008) did not demonstrate a disease-associated phenotype. Adapted by permission from Journal of Molecular Medicine (Drews et al., 2012), copyright 2012.

5.1.2 Advantages and limitations of iPSC-based models

The study by Ebert and colleagues in 2008 was the first to demonstrate the potential of human iPSCs to model the specific pathology observed in genetically inherited disease (SMA), suggesting that iPSC-derived models may be a promising resource for the study of disease mechanisms, screening novel drugs and developing new therapies (Ebert et al., 2008). Importantly, this study confirmed that the generation of iPSCs had no significant effect on critical gene expression profiles or alternative splicing events of disease-relevant genes.

Previous efforts to understand mechanisms of neurodegenerative disease in human tissues have often relied on fibroblasts, or other readily-available cultured cell lines. While these models certainly have value (see Chapter 3), one of the most intriguing aspects of many neurodegenerative diseases is that mutations in ubiquitously- (or at least, widely-) expressed genes can lead to the specific degradation of subpopulations of neurons. This suggests that the unique anatomy and physiology of these neurons may underlie their vulnerability to the disease process (Ebert et al., 2008). Thus, the use of human neurons carrying the disease-causing mutation, generated from a virtually limitless source of iPSCs, should help to clarify the role of these genes in disease initiation and progression.

The limitations of existing animal models in the study of neurodegeneration and therapeutic development have been extensively discussed (Section 1.5.1). Among these, the absence of midbrain substantia nigra dopamine neuron degeneration in mouse models of familial Parkinson's disease (Abeliovich and Doege, 2009), and the absence of SMN2 expression in models of SMA (Ebert et al., 2008) are just two examples of the failure of such models to recapitulate key phenotypes – a possible consequence of species-specific aspects of these diseases.

Neurons differentiated from patient iPSCs offer a unique compromise, providing a relatively homogenous population of disease-affected cells derived from easily accessible primary cultures

(fibroblasts, in most cases), which carry the disease-causing mutation, as well as the patient's full genetic background, and can be manipulated with relative ease for both cellular and biochemical applications *in vitro*. Although the derivation of disease-specific iPSC-based systems for neurodegenerative diseases is becoming more commonplace, there is a definite need to establish and evaluate such models in diverse population groups, particularly those in which polyQ diseases occur at an unusually high frequency, to provide insights which only patient biological material can offer. These include investigations of potential modifiers of disease onset and progression, and methods of evaluating the efficacy of population-specific therapies, such as the allele-specific RNAi (Scholefield et al., 2009).

Whether or not typical neurodegenerative disease traits can be observed in the context of iPSC-based culture models of these disorders remains to be determined. At the molecular level – for instance, in the case of disease-associated gene- or protein expression analyses – it is possible that iPSC-derived neuronal cultures may recapitulate patient phenotypes. However, for late-onset neurodegenerative diseases, the likelihood of iPSC-derived models showing typical patient brain pathology (for example, Parkinson's disease-associated Lewy bodies) has been met with scepticism (Abeliovich and Doege, 2009), despite the promising results obtained in models of (childhood onset) SMA (Ebert et al., 2008). It is possible that the phenotypes of adult-onset conditions, such as Parkinson's disease and ALS, may never be fully recapitulated under basal cell culture conditions, but may require the addition of neural stressors such as reactive oxygen species, pro-inflammatory factors or even toxins in order to manifest (Soldner et al., 2009).

In addition to their role as disease models, iPSC-derived neurons have been proposed as a source for autologous transplantation, mitigating concerns regarding immune rejection, while circumventing the ethical, political and logistical roadblocks previously associated with human ESCs. Promising results obtained using iPSC-derived neurons and neuroepithelial-like stem cells to improve

symptoms of rats with Parkinson's disease or stroke have provided strong impetus for the continuing investigation of the feasibility of cell-based iPSC therapies (Oki et al., 2012; Wernig et al., 2008). However, numerous barriers to the use of iPSC-derived cells for transplantation remain to be addressed, including the risk of cancer posed by the persistent expression of oncogenes such as c-*MYC* (Dimos et al., 2008; Okita et al., 2007), or by retroviral integration into host genome; the formation of correct synaptic connections *in vivo*; and the potential of iPSC-derived therapeutics to recapitulate patient's disease process, due to their inherent genetic propensity. It is therefore likely that iPSC-derived models will be confined to *in vitro* applications until more robust and controlled methods of reprogramming have been developed (Dimos et al., 2008; Stadtfeld et al., 2008).

5.1.3 Neuronal differentiation from iPSCs

The process of *in vitro* differentiation from human iPSCs has been shown to follow developmental principles, albeit with variable potency. Indeed, the order and timing of neurogenesis and gliogenesis in human iPSC differentiation strongly resemble those same processes in human ESCs and normal brain development (Hu et al., 2010b).

Most protocols employed to date follow the same basic steps (Table 6). These include the separation of iPSC colonies from their feeder fibroblast layer, culture in suspension to form spherical aggregates (EBs or neurospheres), and selection for neural precursors, by the addition of growth factors (such as FGF, and other lineage-specific combinations) to the culture medium. In some cases, an intermediate neuroepithelial differentiation step is employed, in which cells are cultured for up to 8 days, until the formation of neural tube-like "rosettes". Terminal differentiation is induced by culture on a laminin or polyornithine substrate, following the withdrawal of growth factors (Hu et al., 2010b; Koch et al., 2009; Soldner et al., 2009). Neurons, which stain positive for the early neuronal marker βIII-tubulin, extend processes by 5-22 days, and attain the capacity to fire action potentials

after seven to eight weeks (Hu et al., 2010b). Glial cells, which stain positive for glial fibrillary acidic protein (GFAP), are also frequently observed (Hu et al., 2010b).

To realise the full potential of iPSCs for the production of neural cells, however, the development of improved differentiation protocols will be required, to eliminate the use of undefined factors (produced by stromal feeder cells), the heterogeneous nature of EB-mediated differentiation, and the low yield associated with protocols based on the selective survival of neural progenitors (Chambers et al., 2009). Several strategies have therefore been suggested to improve the timing and efficiency of differentiation. Among these, the inhibition of SMAD signalling by the bone morphogenetic protein (BMP) inhibitor, Noggin, has been shown to induce rapid and uniform neural conversion of pluripotent cells, without the need for EB formation or stromal co-culture. Noggin, which shows neural-inducing properties in both frog (Smith and Harland, 1992) and mammalian (Valenzuela et al., 1995) models, represses the endogenous BMP signals which drive trophoblast fates, as well as repressing endodermal differentiation. Treatment with Noggin has been shown to greatly shorten the differentiation period required for the generation of neuronal subtypes (to approximately 19 days, as compared to up to 46 days for stromal feeder-mediated differentiation), while enhancing differentiation efficiency by up to 70% when used in combination with a second SMAD inhibitor, SB431542 (Chambers et al., 2009).

Although human iPSCs utilise the same transcriptional network to generate neuronal cells over the same developmental time course as ESCs, the efficiency of differentiation from iPSCs is significantly reduced, and there is a marked increase in the variability between lines compared to ESC-mediated differentiation. These observations are consistent across iPSC lines, and appear to be independent of the set of reprogramming factors used, as well as the presence or absence of reprogramming transgenes, suggesting the need for improving differentiation potency (Hu et al., 2010b).

Table 6 Overview of commonly-used protocols for general neuronal differentiation from ESCs and iPSCs.

Selected References	Methods	Factors	Duration*	Purification method	Validation method
Pomp et al., 2008; Perrier et al., 2004; Kawasaki et al., 2000	Co-culture on stromal cells (PA6, MS5 or S2) to form rosettes, suspension culture as neurospheres**, differentiation on polyornithine/ laminin	FGF, lineage-specific factors	42-46 days	Mechanical passage	Immunostaining for βIII-tubulin, TH and other lineage-specific markers; electrophysiological recordings
Hu et al., 2010b; Koch 2009; Zhang et al., 2001	Suspension culture as EBs, adherent culture to form rosettes, enzymatic digestion, suspension culture as neurospheres, differentiation on polyornithine/ laminin	FGF, EGF	>31 days	Enrichment for neuroepithelial cells at rosette stage by enzymatic treatment and adhesion	Immunostaining for βIII-tubulin, MAP2, neurotransmitters; grafting of precursors into lateral ventricles of newborn mice
Dottori and Pera, 2008; Ebert et al., 2008	Pre-treatment with Noggin, suspension culture as neurospheres, differentiation on lysine/laminin	Noggin, EGF, FGF	24 days	None	Immunostaining for βIII-tubulin
Chambers et al., 2009; Gerrard et al., 2005	Monolayer culture on Matrigel	Noggin, FGF, TGF-β inhibitor	13 days	None	Immunostaining for PAX6, differentiation into neural crest and neuronal subtypes
Pang et al., 2011; Vierbuchen et al., 2010	Transduction of fibroblasts with lentiviruses containing differentiation factors	*Ascl1*, *Brn2*, *Myt1l*	12 days	FACS	Immunostaining for NeuN, MAP2 and synapsin; electrophysiological recordings

* Approximate time from ESCs/iPSC culture to first identifiable neurons. ** Optional step omitted from some protocols.

To this end, recent studies have examined the possibility of direct differentiation from terminally differentiated cells, bypassing the pluripotent intermediate stage altogether (Yang et al., 2011). Vierbuchen et al. (2010) were the first to demonstrate the ability of three transcription factors (*Brn2,*

Ascl1 and *Myt1l*) to directly induce the formation of neuronal cells from mouse fibroblasts, yielding cells which exhibit both molecular and functional properties of neurons (Vierbuchen et al., 2010). The conversion rate from mouse embryonic fibroblasts (approximately 20% over two weeks) is substantially faster and more efficient that the rate of iPSC formation, suggesting that direct differentiation may represent an improvement over traditional differentiation methods (Yang et al., 2011). These results have subsequently been replicated in human fibroblasts, with the addition of *NeuroD1* (Pang et al., 2011); although the longer maturation times (five to six weeks) and reduced efficiency (2-4%) indicate the need for additional improvements to this protocol (Yang et al., 2011). Additional questions remaining to be addressed include the requirement for an intermediate neural progenitor state, the versatility of the induced neurons (iNs) to differentiate into a variety of different subtypes, the degree to which the epigenetic landscape is remodelled towards a neuronal pattern and, crucially, whether iN cells can integrate functionally into the brain (Yang et al., 2011). Although the elimination of pluripotent intermediates from the neuronal differentiation process offers a number of advantages, bypassing the line-to-line variation associated with iPSCs, and reducing the risk of tumour formation upon transplantation, the potential for expansion offered by iPSCs remains a major advantage of traditional methods of differentiation, suggesting that iN-based methods are unlikely to completely replace the use of iPSCs, at least in the near future (Yang et al., 2011).

The protocol employed in this study was based on the method originally described by Dottori and Pera in 2008, for neuronal differentiation from ESCs (Dottori and Pera, 2008). This method was selected based on its relative simplicity, efficiency, and short duration, allowing for the rapid generation of neurons from several different iPSC lines in parallel. Treatment of ESC colonies with Noggin for 14 days resulted in the induction of neural stem cells (NSCs), which express neuroectodermal markers, including Sox2, Pax6, and Nestin (Pera et al., 2004). Following Noggin treatment, NSCs could be mechanically dissected from colonies, and cultured in suspension in the presence of bFGF and EGF, to form spherical cell clusters, or "neurospheres". These could then be

further differentiated *in vitro* to yield either neurons or glia. The efficiency of differentiation was assessed by immunocytochemical staining for early neuronal (βIII-tubulin) and glial (GFAP) markers, following guidelines previously described by Yang et al. (2011). The transplantation of neurospheres derived from Noggin-treated human ESCs into the brains of Parkinsonian rodents has been previously shown to result in their integration and differentiation into neural and glial cells (Ben-Hur et al., 2004). This neural induction protocol is thus both highly efficient and extremely useful for downstream applications.

5.1.4 A cellular phenotype in SCA7 iPSCs and iPSC-derived neurons

The role of transcriptional dysregulation in the early stages of polyQ pathogenesis has been extensively discussed (see Section 1.2.3). Several studies have examined transcriptional phenotypes in peripheral cell and animal models of SCA7 in particular. To date, however, no disease-associated phenotype has been identified in SCA7 iPSCs or iPSC-derived neurons. This is a crucial step in the evaluation of these cell lines as models for evaluating disease pathogenesis and therapies, particularly due to the concerns associated with the ability of iPSC-derived models to recapitulate phenotypes of adult-onset conditions (Section 5.1.2). As transcriptional dysregulation represents one of the earliest manifestations of polyQ disease, preceding the onset of clinical symptoms, it seems likely that such a phenotype may be detectable in the early developmental stages represented by iPSCs and iPSC-derived neurons.

To this end, the expression of a set of candidate transcripts, previously shown to be dysregulated in the context of SCA7 disease models, was evaluated in these cells. These included the genes encoding heat shock proteins, an RNA chaperone, and the ubiquitin carboxy-terminal hydrolase L1 (*UCHL1*), assessed in SCA7 fibroblasts (Chapter 3). An additional eight genes were evaluated, including several encoding proteins involved in the STAGA complex, neuronal differentiation and

signalling, all of which had previously been shown to be differentially expressed in SCA7 disease models (Chou et al., 2010; Wang et al., 2010; Tsai et al., 2005; Palhan et al., 2005), with some showing dysregulated expression across several polyQ models (Luthi-Carter et al., 2002).

5.1.5 Aims

The aims of the experiments described in this chapter were as follows:

1. To establish and characterise SCA7 patient and control iPSC-derived neuronal lines from iPSC lines (which had been generated as described in Chapter 4),
2. To investigate the presence of a phenotype (transcriptional dysregulation) in SCA7 iPSCs and iPSC-derived neurons.

5.2 Results

5.2.1 Neuronal differentiation of iPSCs

Neuronal differentiation was performed as previously described (Dottori and Pera, 2008), using two control (iPS SC NHDF and iPS George) and three SCA7 iPSC lines (1518D, 1519A and 1519C), all of which had been extensively characterised (see Chapter 4). Multiple neuronal lines were generated from each iPSC line, to account for variability between differentiation experiments. iPSC colonies were treated with the BMP antagonist Noggin for 14 days (Fig. 17a), followed by dissociation and culture in suspension in the presence of bFGF and EGF, to produce neurospheres (Fig. 17b). Single neurospheres were transferred onto a poly-D-lysine/laminin substrate in the absence of growth factors, and allowed to differentiate for one to three weeks prior to RNA isolation and imaging. After approximately 5 days in culture, neuron-like outgrowths were observed (Fig. 17c), which stained positive for the neuronal marker, βIII-tubulin (Fig. 17d-o).

Despite following a protocol intended to favour neuronal growth and differentiation, both control and SCA7 iPSC-derived neuronal cultures also contained small numbers of GFAP-positive glial cells (Fig. 17d-i). The ratio of neurons:glia did not differ between control (Fig. 17d-f) and SCA7 (Fig. 17g-i) iPSC-derived neurons, and was sufficiently high to allow for the conclusion that neurons constituted the majority of the cell population at the one-, two- and three-week time points.

Purkinje cells are among the neuronal subtypes most severely affected by SCA7 (Garden and La Spada, 2008; Einum et al., 2001). To investigate the presence of GABAergic neurons, the lineage from which Purkinje cells are derived, levels of GABA expression were ascertained in iPSC-derived neuronal populations at one-, two- and three weeks post-differentation, by means of immunostaining (Fig. 17j-o). Very little GABA expression was detected after one week of differentiation (Fig. 17j, m). However, after two weeks of growth, both control (Fig. 17k) and SCA7 (Fig. 17n) neurons generated robust populations of putative GABAergic neurons. By three weeks, no obvious

difference in the number of GABA-positive processes was detected amongst the SCA7 iPSC-derived neurons, when compared to controls, although fluctuations in the total number of neuronal projections between samples made direct comparisons difficult.

Figure 17 Neuronal differentiation from iPSCs (next page). (a) iPSC colony cultured on iMEF feeders for 14 days without passage, in the presence of the BMP antagonist, Noggin. (b) Colonies were dissected and cultured in suspension in the presence of bFGF and EGF, to form neurospheres, three-dimensional balls of cells consisting of neuronal precursors. (c) Within five days of plating onto a poly-D-lysine/laminin substrate, neurospheres (NS) produced neuronal-type projections. The presence of a small proportion of glia within the iPSC-derived neuronal cultures is evident at one week, two weeks and three weeks post differentiation, in both control (d-f, respectively) and SCA7-derived cultures (g-i, respectively). Virtually no GABA-positive projections were present in control (j) or SCA7 (m) iPSC-derived neurons at one week post differentiation. However, after two weeks, the presence of putative GABAergic neurons was confirmed by the detection of long, GABA-positive projections in both the control (k) and SCA7 (n) neuronal populations (indicated by white arrowheads). After three weeks, staining for GABA (indicated by white arrowheads) was not significantly different in controls (l) relative to SCA7 patient-derived neurons (o). Red: βIII-tubulin. Green: (d-i), GFAP, (j-o), GABA. Scale bars: (a) and (b), 500µm. (c-o), 100µm.

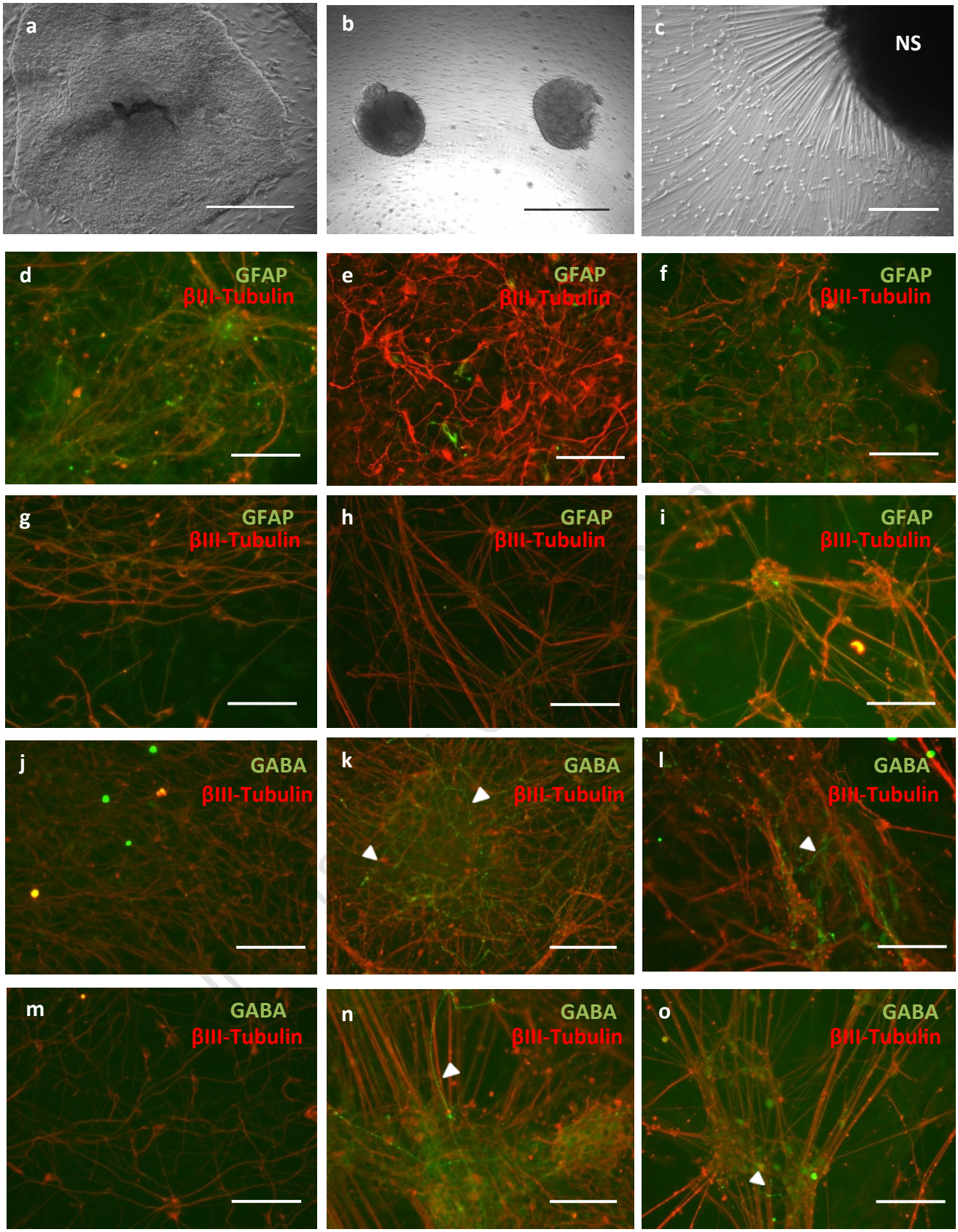
a
b
c
NS
d
GFAP
βIII-Tubulin
e
GFAP
βIII-Tubulin
f
GFAP
βIII-Tubulin
g
GFAP
βIII-Tubulin
h
GFAP
βIII-Tubulin
i
GFAP
βIII-Tubulin
j
GABA
βIII-Tubulin
k
GABA
βIII-Tubulin
l
GABA
βIII-Tubulin
m
GABA
βIII-Tubulin
n
GABA
βIII-Tubulin
o
GABA
βIII-Tubulin

5.2.2 CAG repeat length

In order to confirm the presence of a pathologically-expanded *ataxin-7* CAG repeat in the iPSCs and iPSC-derived neurons generated from SCA7 patient fibroblasts, the genomic region surrounding the CAG repeat was amplified by PCR, and subjected to agarose gel electrophoresis (Fig. 18). The approximate lengths of the CAG repeats in SCA7 fibroblasts, iPSCs and iPSC-derived neurons, determined by automated fluorescent genotyping, are listed in Table 7.

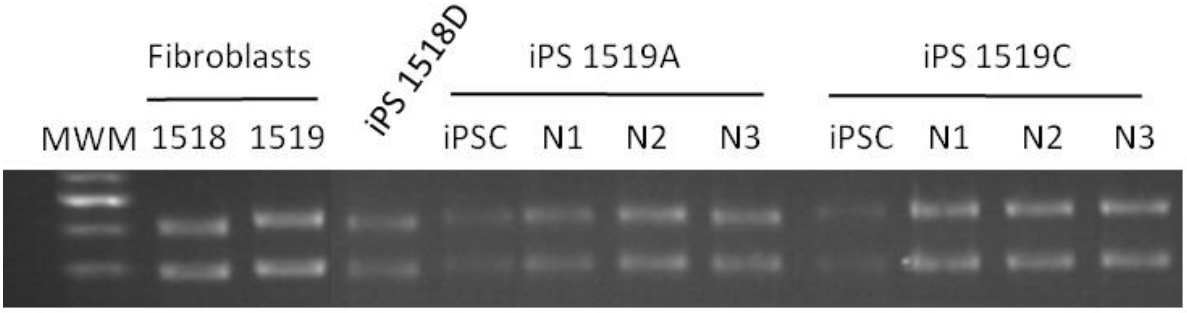

Figure 18 *ataxin-7* CAG repeat lengths in SCA7 iPSCs and iPSC-derived neurons. PCR-amplified genomic DNA containing the *ataxin-7* CAG repeat was subjected to electrophoresis on a 2% (w/v) agarose gel containing 500ng/ml ethidium bromide. Relative sizes were approximated by comparison to the Gene Ruler 100bp DNA Ladder Plus *Improved* (Fermentas) (MWM). N1, 2 and 3, neurons at 1, 2 and 3 weeks post-differentiation, respectively.

The length of the normal CAG repeat did not appear to fluctuate during reprogramming or neuronal differentiation, a finding corroborated by the results obtained from the control iPSC and neuronal lines (data not shown). However, an increase of three to four CAG repeats was observed when comparing two of the SCA7 iPSC lines (at passage 8-10) with their parental fibroblast lines. Compared to the iPSCs from which they were derived, neuronal lines showed no difference in the length of the expanded CAG repeat, when assayed at one, two and three weeks post-differentiation. The lengths of the expanded alleles in the patient fibroblasts are slightly shorter than those quoted in the diagnostic reports in Section 2.1, which were determined from DNA isolated from peripheral

blood; possibly as a result of tissue-specific differences in CAG repeat length stability (Cannella et al., 2009; Veitch et al., 2007).

Table 7 Normal and expanded *ataxin-7* CAG repeat lengths in SCA7 iPSCs and iPSC-derived neurons.

Fibroblast line	CAG repeat length	iPSC line(s)	CAG repeat length	Neurons CAG repeat length		
				1 week*	2 weeks	3 weeks
1518	9/40	1518D	9/43	N/D	N/D	N/D
1519	10/47	1519A	N/D	10/47	10/47	10/47
		1519C	10/51	10/51	10/51	10/51

Lengths are listed as normal allele/expanded allele. N/D: not determined. *Weeks post-differentiation.

5.2.3 Expression of Ataxin-7

The expression, localization and aggregation patterns of the disease-causing protein, Ataxin-7, were evaluated in control and SCA7 iPSC-derived neurons by means of immunofluorescence. Both control (Fig. 19a-c) and SCA7 (Fig. 19d-f) neurons showed predominant nuclear expression of Ataxin-7, as has been previously reported (Einum et al., 2001; Cancel et al., 2000). Of interest, Ataxin-7 nuclear staining highlighted the presence of non-neuronal cells in several of the lines – possibly a result of incomplete differentiation. However, since these cells express Ataxin-7 (albeit at lower levels when compared to βIII-tubulin-positive cells), they were considered to contribute to, rather than detract from, the results detailed in Section 5.2.5.

After three weeks of differentiation, both patient- (Fig. 19g), and control-derived neurons (Fig. 19h) showed diffuse nuclear staining of Ataxin-7. No Ataxin-7-positive NIs or macroaggregates could be detected in SCA7 patient-derived iPSCs, even at high magnification (Fig. 19g), up to six weeks post-differentiation (data not shown).

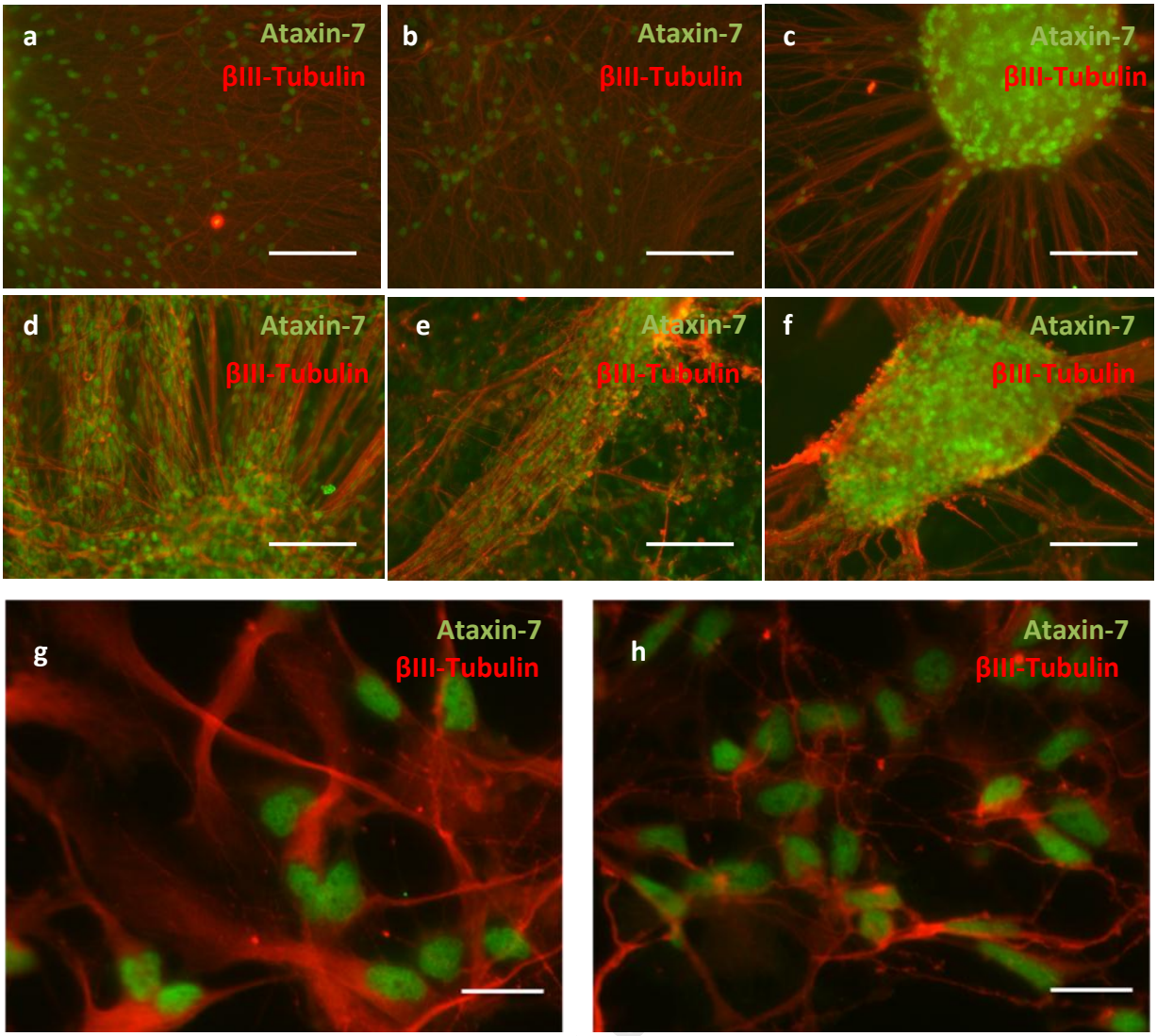

Figure 19 iPSC-derived neurons express Ataxin-7. Both control- and patient iPSC-derived neurons show predominantly nuclear localization of Ataxin-7 (green) after two to three weeks in culture. (a)-(c), control neurons (iPS George); (d)-(f), SCA7 patient neurons (1519A or C). At higher magnification, no NIs could be detected in SCA7 patient iPSC-derived neurons (g) when compared to controls (h). Red: βIII-tubulin. Scale bars: 100µm.

5.2.4 Transcriptional phenotype in iPSCs

In order to evaluate differences in gene expression between SCA7 patient and control iPSCs, 12 candidate transcripts were selected, based on their relevance to known polyQ disease pathways. These included the genes whose expression had previously been evaluated in SCA7 and control fibroblast lines – namely, *HSP27, -70, -105*, *DNAJA1, RBM3* and *UCHL1* – as well as genes encoding a component of the STAGA complex (*KAT2A*), a proapoptotic protein (*BAX*), a growth factor (*IGFBP5*), a protein involved in chromatin phosphorylation (*SNRK*), and two genes encoding proteins involved in neuronal differentiation (*Bex1* and *Olig1*). All of these genes had previously been shown to be differentially expressed in SCA7 disease models (Chou et al., 2010; Wang et al., 2010; Palhan et al., 2005; Tsai et al., 2005), with some showing dysregulated expression across several polyQ models (Luthi-Carter et al., 2002).

When expression was compared across two control iPSC lines (SC NHDF and George) and three SCA7 iPSC lines (1518D, and 1519A and -C), all of which had been extensively characterised, a significant decrease in expression of *KAT2A* ($p=0.03$), was observed in SCA7 iPSCs relative to controls (Fig. 20). Levels of *IGFBP5* were found to be approximately three-fold higher in SCA7 iPSCs compared to controls, although this result was not statistically significant. No significant changes in any of the remaining genes were observed. However, there did appear to be a trend towards increased *DNAJA1* expression in patient iPSCs, correlating with the increase in *DNAJA1* expression previously noted in SCA7 fibroblasts.

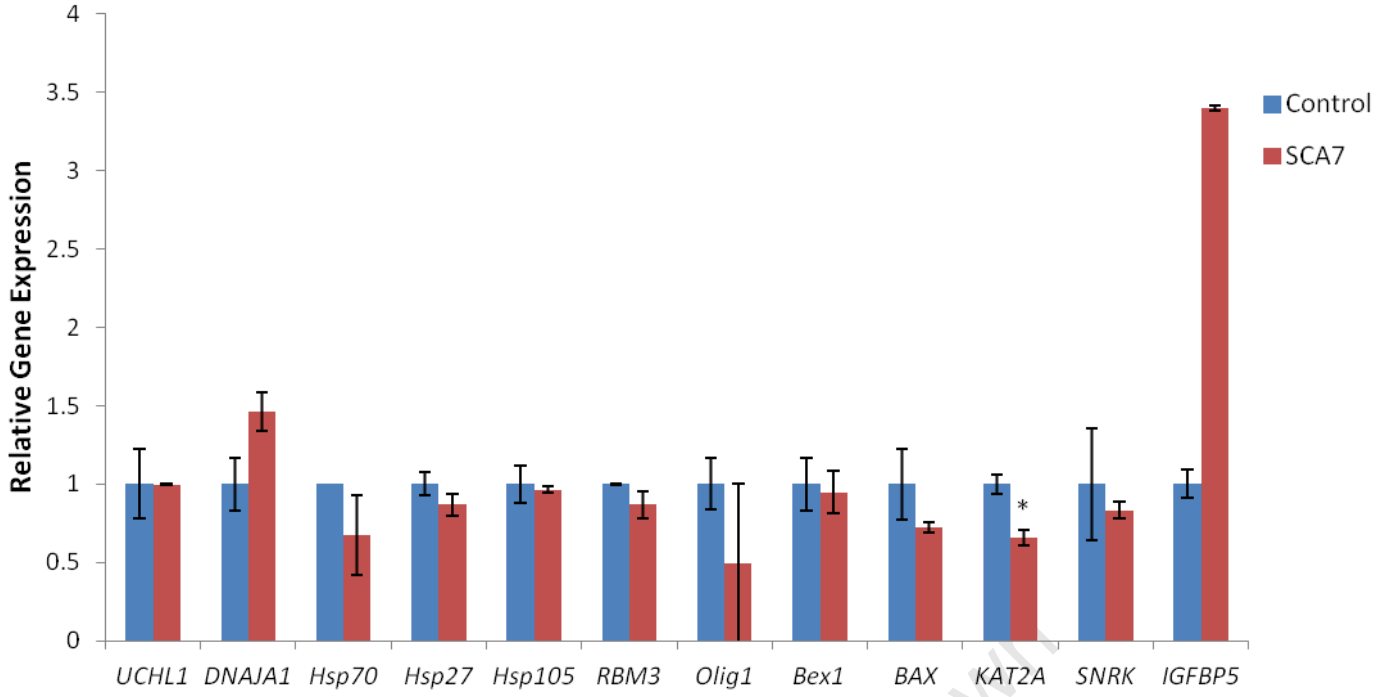

Figure 20 Transcriptional changes in SCA7 patient iPSCs. Expression of endogenous transcripts in SCA7 iPSCs relative to controls is shown, normalised to β-Actin. Values are mean ± SEM. Control iPSCs, n = 2, SCA7 iPSCs, n = 3. *UCHL1*, Ubiquitin carboxy-terminal hydrolase LI; *DNAJA1* (HSP40), DNAJ homolog, subfamily A, member 1; *HSP-*, heat shock protein *-27*; *-70*; *-105*; *RBM3*, RNA-binding motif protein 3; *Olig1*, Olig1 bHLH protein; *Bex1*, Brain-expressed X-linked 1; *BAX*, BCL2-associated X protein; *KAT2A*, K (lysine) acetyltransferase 2A; *SNRK*, SNF related kinase; *IGFBP5*, insulin-like growth factor binding protein 5. * indicates a p value < 0.05.

5.2.5 Transcriptional phenotype in iPSC-derived neurons

Differences in gene expression between SCA7 patient and control iPSC-derived neurons were also investigated. In addition to the candidate transcripts evaluated in iPSCs, expression of a further three genes was assessed. Two of these – solute carrier family 17 (sodium-dependent inorganic phosphate cotransporter), member 6 (*SLC17A6*), encoding a vesicular glutamate transporter; and glutamate receptor, ionotropic, AMPA2 (*GRIA2*) – have been previously shown to be dysregulated in the cerebellum of SCA7 mice (Chou et al., 2010). The third gene included was *ataxin-7*, encoding the disease-causing protein, whose expression has been shown to depend to some degree on the length of the CAG repeat (Sopher et al., 2011).

Multiple neuronal lines were used, which had been differentiated from five iPSC lines – two controls, iPS SC NHDF and iPS George; and three SCA7 patient lines, 1518D, 1519A and 1519C. Expression of the fifteen candidate genes was assessed in all of the lines at one and three weeks post-differentiation. No significant differences in expression were observed between any of the 1518D-derived neuronal lines and the controls at either the one or three week time points (Fig. 21 and 22).

At one week post-differentiation (Fig. 21), an approximate two-fold increase in *HSP27* expression was observed in the 1519-derived neurons, when compared to controls (p=0.01), although this trend was not sustained at three weeks post-differentiation (Fig. 22).

Also at one-week post-differentiation, a significant difference in *GRIA2* expression between 1518D-derived and 1519-derived neurons was observed, with 1518D-derived neurons showing slightly elevated *GRIA2* expression relative to controls, while 1519-derived neurons showed significantly decreased expression levels relative to both controls and 1518D-derived neurons (p=0.03). By three weeks post-differentiation, *GRIA2* expression in 1519-derived neurons had fallen to one-third of the expression levels observed in controls (p=0.03). A two-fold reduction in *GRIA2* expression was observed 1518D-derived neurons relative to controls at the same time point, although this result was not statistically significant.

A 2.3-fold increase in *ataxin-7* expression was observed at one-week post-differentiation in 1519-derived neurons, as compared to controls (p=0.004). *Ataxin-7* expression 1518D-derived neurons was 1.6-fold higher than controls at the same time point, although this change was not significant. By three weeks post-differentiation, *ataxin-7* expression in neurons from both SCA7 patients had dropped to 1.4-times control levels, and was deemed non-significant.

Several non-significant trends were observed at the one week time point in SCA7 patient-derived neurons versus controls, including decreased levels of *UCHL1* and *SLC17A6* expression, and marginally elevated levels of the heat shock protein genes *HSP70* (1519), *HSP105* (1518), and the growth factor *IGFBP5* (1519). A four-fold elevation of *Olig1* in was observed in 1518D-derived neurons, although this was also deemed non-significant.

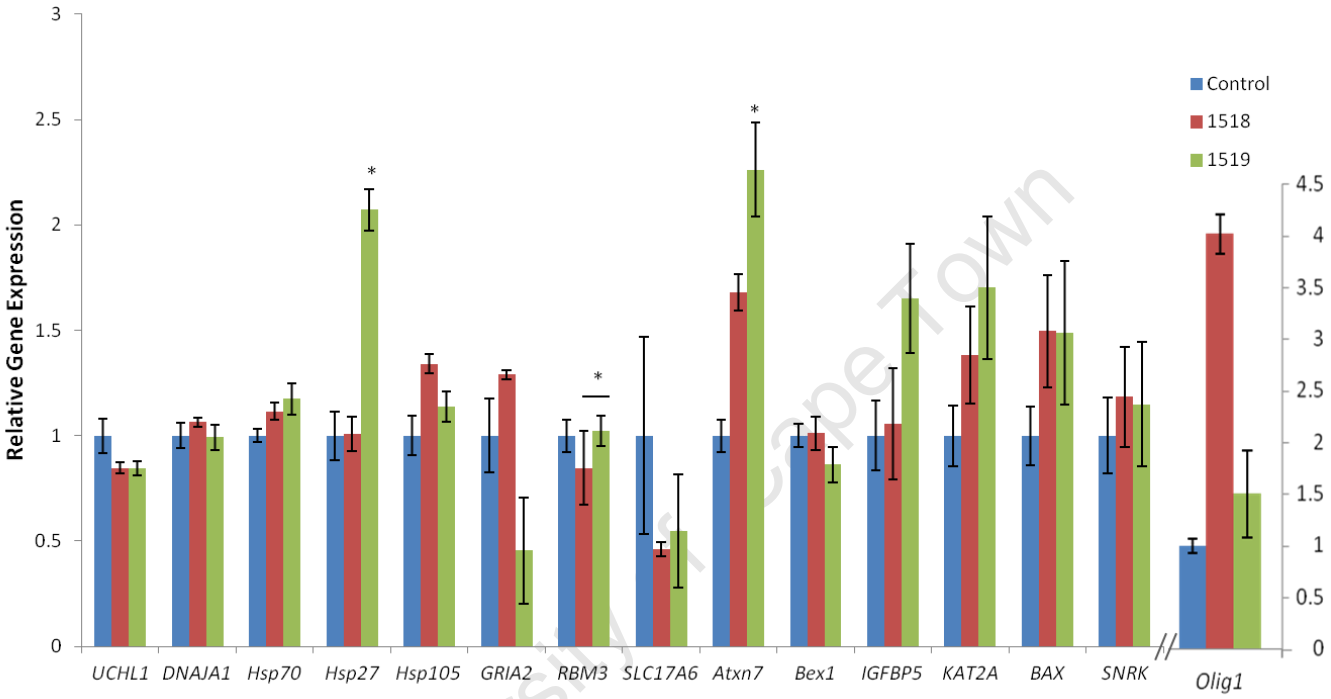

Figure 21 Transcriptional changes in SCA7 iPSC-derived neurons one week post-differentiation. Expression of endogenous transcripts in SCA7 iPSC-derived neurons relative to controls is shown, normalised to β-Actin. Values are mean ± SEM. Control iPSC-derived neuronal lines, n = 6, 1518D iPSC-derived neuronal lines, n = 3, 1519 iPSC-derived neuronal lines n = 6. *UCHL1*, Ubiquitin carboxy-terminal hydrolase LI; *DNAJA1* (HSP40), DNAJ homolog, subfamily A, member 1; *HSP-*, heat shock protein *-27*; *-70*; *-105*; *GRIA2*, glutamate receptor, ionotropic, AMPA2; *RBM3*, RNA-binding motif protein 3; *SLC17A6*, solute carrier family 17 (sodium-dependent inorganic phosphate cotransporter), member 6; *Atxn7*, ataxin-7; *Bex1*, Brain-expressed X-linked 1; *IGFBP5*, insulin-like growth factor binding protein 5; *KAT2A*, K (lysine) acetyltransferase 2A; *BAX*, BCL2-associated X protein; *SNRK*, SNF related kinase; *Olig1*, Olig1 bHLH protein. * indicates a p value < 0.05.

A 1.3-fold increase in *DNAJA1* expression was observed in 1519-derived neurons, relative to controls at three weeks post-differentiation ($p=0.01$). This corresponds with previously-published reports, as well as with the results obtained in SCA7 fibroblasts described in Chapter 3, and the non-significant trend observed in SCA7 patient-derived iPSCs.

Several additional non-significant trends were observed at three weeks post-differentiation, including decreased *UCHL1* (in both 1518D- and 1519-derived neurons), *IGFBP5* (1518D) and *Olig1* (1519) expression; and elevated *HSP27* (1519), *HSP105* (1519) and *BAX* (1518). An approximate 1.7-fold increase in *SLC17A6* expression in 1519-derived neurons relative to controls was also observed, although this was not deemed to be significant.

In order to track changes in expression of the various genes over a three-week time course, an intermediate time point (two weeks) was included. Given the lack of statistically significant results for 1518D-derived neurons at the one- and three-week time points, the detailed time-course analysis was limited to a comparison between 1519-derived neurons and control lines. These data revealed a further three significant results ($p<0.05$) – at two weeks post-differentiation, 1.2-fold increases in *DNAJA1* and *HSP105* expression, and a 2-fold decrease in *GRIA2* expression were observed in 1519-derived neurons compared to controls (Fig. 23a-c).

Trends in expression of two additional genes, *SLC17A6* and *Olig1* were of interest, although not significant. In the case of *SLC17A6*, expression increased over time in 1519-derived neurons, but decreased over the same three week period in control neurons. Thus, while 1519-derived neurons displayed deficient *SLC17A6* expression at one week post-differentiation, the same neurons showed abnormally elevated expression of the gene by the three-week time point (Fig. 23d). The opposite phenomenon was observed in the case of *Olig1*, with 1519-derived neurons showing elevated

expression at early time points, with expression falling below the levels of that of control neurons, by three weeks post-differentiation (Fig. 23e).

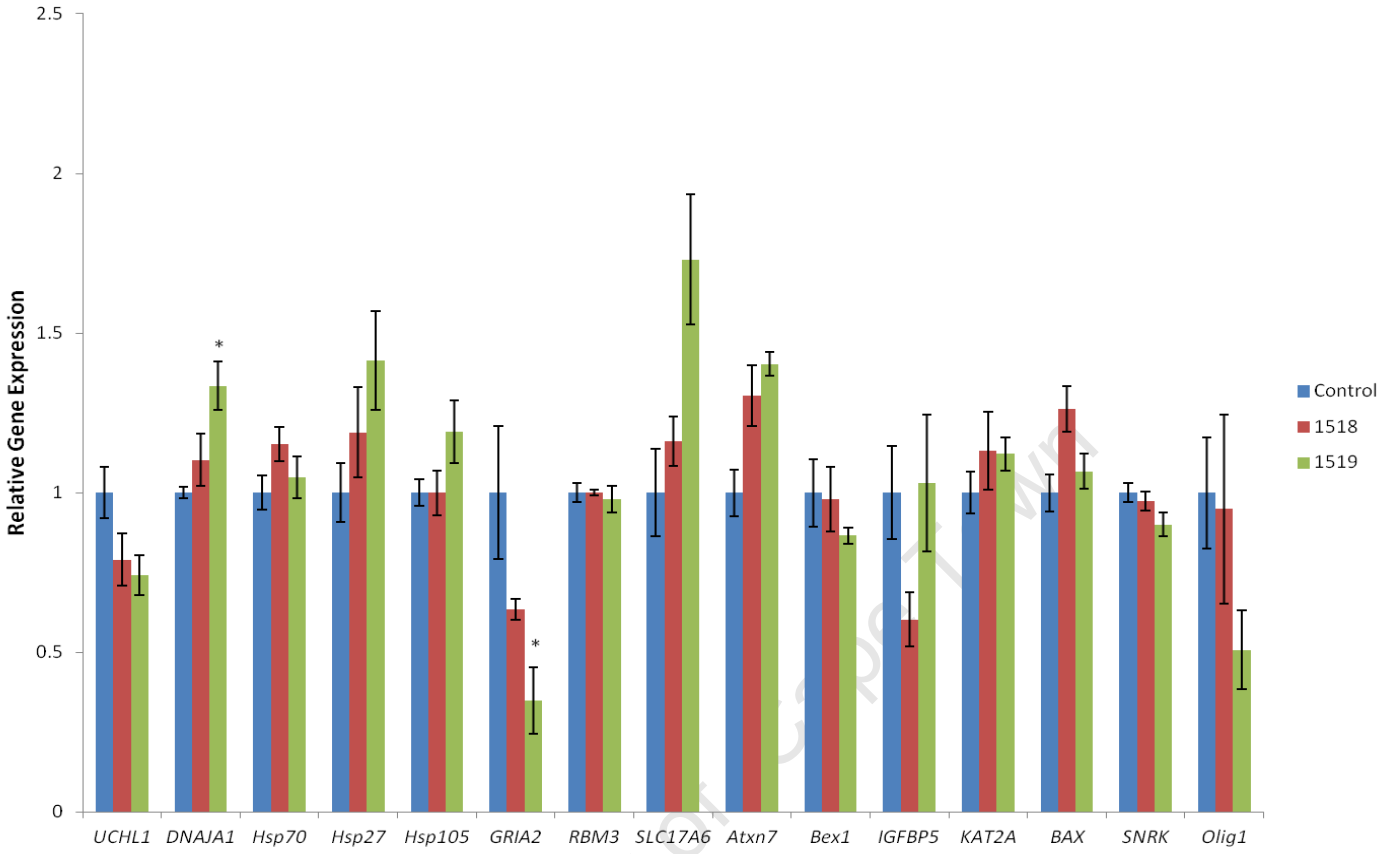

Figure 22 Transcriptional changes in SCA7 iPSC-derived neurons three weeks post-differentiation. Expression of endogenous transcripts in SCA7 iPSC-derived neurons relative to controls is shown, normalised to β-Actin. Values are mean ± SEM. Control iPSC-derived neurons, n = 6, 1518D iPSC-derived neurons, n = 3, 1519 iPSC-derived neurons n = 6. *UCHL1*, Ubiquitin carboxy-terminal hydrolase LI; *DNAJA1* (HSP40), DNAJ homolog, subfamily A, member 1; *HSP-*, heat shock protein *-27*; *-70*; *-105*; *GRIA2*, glutamate receptor, ionotropic, AMPA2; *RBM3*, RNA-binding motif protein 3; *SLC17A6*, solute carrier family 17 (sodium-dependent inorganic phosphate cotransporter), member 6; *Atxn7*, ataxin-7; *Bex1*, Brain-expressed X-linked 1; *IGFBP5*, insulin-like growth factor binding protein 5; *KAT2A*, K (lysine) acetyltransferase 2A; *BAX*, BCL2-associated X protein; *SNRK*, SNF related kinase; *Olig1*, Olig1 bHLH protein. * indicates a p value < 0.05.

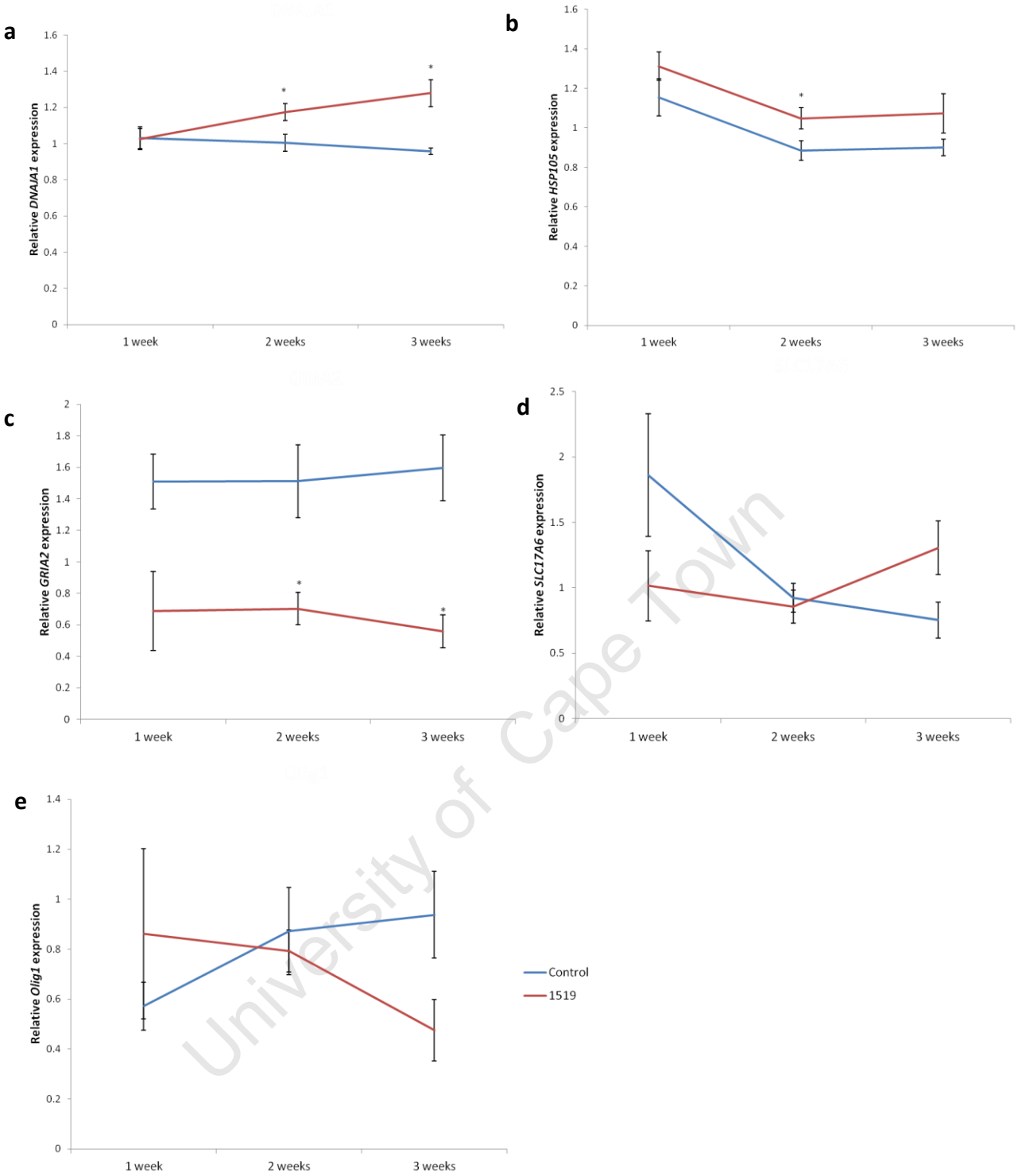

Figure 23 Transcriptional changes in SCA7 iPSC-derived neurons over time. Expression of endogenous transcripts in SCA7 iPSC-derived neurons (1519) and controls are shown for each time point, normalised to β-Actin. Values are mean ± SEM. Control iPSC-derived neurons, n = 6, SCA7 (patient 1519) iPSC-derived neurons, n = 6. Time post-differentiation (in weeks) is indicated on the x-axis. (a) *DNAJA1* (b) *HSP105* (c) *GRIA2* (d) *SLC17A6* (e) *Olig1*. * indicates a p value < 0.05.

5.3 Discussion

This study has demonstrated the feasibility of differentiating SCA7 patient iPSCs into neurons, which express neuronal markers including βIII-tubulin and GABA. Moreover, both iPSCs and iPSC-derived neurons display changes in expression of key transcripts, previously implicated in the pathogenesis of polyQ disease, suggesting that iPSC-derived cells may serve as useful models of neurodegenerative disease progression, for future studies. This is the first report of the development of iPSC-derived neurons from the South African SCA7 patient cohort. It is also the first study to identify a transcriptional phenotype in these cells.

5.3.1 Neuronal differentiation from iPSCs

Based on the criteria outlined by Yang et al. in 2011, both control and SCA7 patient iPSCs appeared capable of robust, reproducible differentiation towards neuronal fates, as demonstrated by βIII-tubulin positive staining at one, two and three weeks post differentiation. The presence of a small population of cells which did not express βIII-tubulin was occasionally detected; indicative of minor variations in differentiation efficiency between iPSC lines, as has been previously described (Hu et al., 2010b). The Yang et al. guidelines, first proposed to standardise the generation of iNs via direct differentiation from fibroblasts, list the following criteria for successful neuronal differentiation, in increasing order of stringency: development of characteristic neuronal morphology, expression of multiple neuronal markers (for example, βIII-tubulin, MAP2, NeuN, Neurofilament and Synapsin), development of membrane potential, including membrane voltage and current responses, and demonstration of synaptic competence, as determined by the presence of spontaneous and evoked pre- and postsynaptic responses (Yang et al., 2011). Given the aims of this proof-of-principle study, which sought to compare SCA7 and control iPSCs *in vitro*, in order to evaluate differences in transcriptional regulation, emphasis was placed on the first two criteria, which have been previously used to confirm neuronal identity in similar studies (Luo et al., 2012; Dimos et al., 2008).

No significant differences in morphology or propensity for βIII-tubulin expression were observed when comparing neurons derived from SCA7 patient iPSCs with those derived from controls. This contradicts a previous report of ESCs expressing expanded CAG repeats, which demonstrated aberrant neuronal differentiation, decreased survival, and the formation of dystrophic neurites, similar to pathological abnormalities observed in several polyQ diseases (Lorincz et al., 2004; DiFiglia et al., 1997; Burright et al., 1995). These results suggested that the expression of proteins harbouring CAG repeat expansions may impair the ability of pluripotent cells to generate functional neurons (Lorincz et al., 2004). However, more recent studies of polyQ and other neurodegenerative diseases have demonstrated that this is not the case. Indeed, reports of neuronal differentiation in polyQ disease (Camnasio et al., 2012; Koch et al., 2011) and Parkinson's disease (Soldner et al., 2009), among others, have found no difference in differentiation potential between patient and control iPSCs, suggesting that pathogenesis may result from the degeneration of neurons at advanced stages of disease progression, rather than from aberrant differentiation during development.

The neurons primarily affected in SCA7 are the cerebellar Purkinje cells (Garden and La Spada, 2008; Einum et al., 2001). However, at the time of experimental design, only one protocol existed for the differentiation of Purkinje cells, from mouse ESCs (Tao et al., 2010). (A more straightforward protocol for EB-mediated differentiation of cerebellar neurons from human and mouse ESCs has subsequently been published (Erceg et al. 2012).) The complexity of the method described by Tao et al., which requires co-culture with dissociated cerebellar material harvested from mice at postnatal day 6-8, precluded its use in this proof-of-principle study. Thus, the simplified general neuronal differentiation method described by Dottori and Pera (2008) was selected.

This protocol, which was adapted as per the author's recommendations to favour the production of neurons, nevertheless produced a small population of contaminating GFAP-positive glial cells. The role of non-neuronal cells in the development of polyQ diseases, particularly SCA7, has already been

established (Garden and La Spada, 2012; Inoue, 2010). Indeed, the expression of mutant polyQ protein in the glia of transgenic mice has been shown to result in non-cell-autonomous Purkinje cell degeneration (Custer et al., 2006). Thus, the presence of glial cells within the differentiated neuronal population was deemed to be an advantage in assessing the overall disease-associated phenotype.

Further characterization of the general neuronal population produced from SCA7 and control iPSCs revealed the presence of putative GABAergic neurons, the lineage from which cerebellar Purkinje cells are derived. The strong propensity for *in vitro* differentiated neurons to acquire an interneuron-like phenotype, with co-expression of GABA and the GABA-producing enzyme, glutamic acid decarboxylase (GAD67) has been previously described (Koch et al., 2009). Despite some line-to-line variation, no significant difference in the ability to generate GABA-positive processes could be detected between SCA7 and control iPSC-derived neurons, suggesting that the presence of mutant *ataxin-7* does not affect the development of Purkinje cells, at least at early stages of neuronal differentiation. It should, however, be noted that the protocol employed for neuronal differentiation relied on the generation of neurosphere intermediates – inherently heterogeneous structures whose size, number and morphology proved difficult to standardise across lines, making cross-line comparisons challenging.

5.3.2 CAG repeat length

The CAG repeat encoding the polyQ tract in disease-causing proteins such as *ataxin-7* is by nature unstable, with repeat lengths above the pathogenic threshold showing a propensity to expand during vertical transmission from parent to child (Monckton et al., 1999). A high degree of somatic instability has also been reported in transgenic mouse models and autopsied brain samples from HD and SCA7 patients (Dragileva et al., 2009; Gonitel et al., 2008; Kennedy et al., 2003), while in a human ESC line carrying the *HTT* gene, an expansion of five CAG repeats has been observed

following neural differentiation (Niclis et al., 2009), although this has not been replicated in other ESC lines (Seriola et al., 2011).

It is therefore surprising to note that iPSCs derived from the somatic cells of several polyQ disease patients, including those with SCA3 and HD, show remarkable CAG repeat stability up to 40 passages post-reprogramming (Camnasio et al., 2012; Koch et al., 2011). This stability has also been shown to be maintained over several weeks of neuronal differentiation (Koch et al., 2011). In terms of triplet repeat disorders, only Friedreich's ataxia has shown disease-associated repeat instability in patient iPSCs over time – a phenomenon believed to result from the particular structure and length of the GAA·TTC repeat (Ku et al., 2010).

In this study, the disease-causing CAG repeat in *ataxin-7* was shown to expand by between three and four repeats during the reprogramming process from fibroblasts to iPSCs. This instability was limited to the mutant allele, and was not observed in control iPSCs, suggesting that the mutant allele is more prone to expansion, as has been previously reported (Monckton et al., 1999). No changes in CAG repeat length were observed during the process of neuronal differentiation from iPSCs. The expansion of the CAG repeat in iPSC reprogramming but not differentiation may reflect the high rate of cell division during the derivation of iPSCs, in comparison to post-mitotic neurons (Yoon et al., 2003). Alternatively, the integration of retroviral transgenes has been shown to affect genomic stability, possibly resulting in mutations in already unstable regions of the genome (Ramos-Mejia et al., 2010). Despite the relative stability observed in HD and SCA3, the expansion of the CAG repeat tract in SCA7 iPSCs was not entirely unexpected, as the *ataxin-7* repeat tract has previously been identified as the most expansion-prone of all the polyQ diseases (Monckton et al., 1999).

It is important to note, however, that an error margin of three CAG repeats is considered acceptable in most diagnostic tests (Sequeiros et al., 2010). It is therefore possible that the expansions observed

in this study result simply from the limitations of the fluorescent genotyping technique employed to determine repeat length. Of critical importance to this study, no contractions or large-scale expansions were observed, which may have resulted in a different phenotype than that predicted by the diagnostic test results for the SCA7 patients.

5.3.3 Ataxin-7 expression and localization

Wildtype Ataxin-7 is widely expressed in the brain, retina, and peripheral tissues (Jonasson et al., 2002; Einum et al., 2001; Cancel et al., 2000). Within the CNS, expression is preferentially neuronal, although low levels of Ataxin-7 have also been detected in non-neuronal cells, including astrocytes (Cancel et al., 2000). In normal human brains, Ataxin-7 is localised to the cell bodies and processes of neurons, as well as the nucleus (Cancel et al., 2000). Subcellular localization varies according to cell type, patient age and polyQ repeat length (Jonasson et al., 2002; Einum et al., 2001; Cancel et al., 2000), with longer polyQ repeats showing a tendency to inhibit the cytoplasmic trafficking of the protein (Taylor et al., 2006).

The formation of nuclear inclusions (NIs), aggregates of mutant protein which sequester crucial cellular components including molecular chaperones and transcription factors, is a pathological hallmark of many polyQ diseases (see Section 1.1.3). In SCA7, the presence of intra- and perinuclear aggregates of Ataxin-7 has been confirmed in studies of cell models and human brain tissue, particularly in cases in which truncated, polyQ-containing fragments of the protein are expressed (Zander et al., 2001). Indeed, caspase-7-mediated cleavage of Ataxin-7, yielding fragments which demonstrate enhanced nuclear localisation and increasing tendency towards aggregation (Taylor et al., 2006), has been demonstrated to modulate toxicity in SCA7 (Young et al., 2007; Garden et al., 2002). Nonetheless, the role of NIs in SCA7 pathogenesis remains controversial, given the presence

of aggregates in unaffected tissues (Ansorge et al., 2004; Jonasson et al., 2002; Lindenberg et al., 2000; Holmberg et al., 1998), and the lack of NIs observed in some cases (Einum et al., 2001).

Both the SCA7 and control iPSC-derived neurons generated in this study showed predominantly nuclear localisation of Ataxin-7, as has been previously observed (Jonasson et al., 2002; Einum et al., 2001). Despite reported differences in localisation between SCA7 patients with different CAG repeat lengths, and different ages of onset, no difference in subcellular compartmentalisation of Ataxin-7 was observed between the two SCA7 patients in this study, corresponding to previously published reports (Jonasson et al., 2002; Einum et al., 2001). This suggests that iPSC-derived neurons represent an early stage of development, rather than recapitulating the age or disease stage of the patient from which the primary cells were derived.

No NIs or macroaggregates of Ataxin-7 were detected in SCA7 patient iPSC-derived neurons, up to six weeks post-differentiation. It may be argued that aggregation of Ataxin-7 obscures epitopes required for antibody recognition, resulting in selective immunostaining of unbound wildtype protein. However, this is unlikely to be the case, since the antibody used for Ataxin-7 detection in this study has been previously shown to label Ataxin-7-containing NIs in patient brains (Jonasson et al., 2002).

Previous studies employing similar models for the study of neurodegenerative disease have raised concerns regarding the relevance of modelling adolescent- and adult-onset diseases over the short lifespan of cultured neurons (Soldner et al., 2009). Indeed, pathological hallmarks of disease such as the formation of NIs may take decades to manifest, requiring the gradual accumulation of toxic proteins as a result of age-dependent deficiencies in protein homeostasis (Hartl et al., 2011). Although some studies suggest that NIs may be detected at earlier stages, the major determinants of inclusion formation remain the length of the polyQ expansion, and the levels of expression of the

polyQ-containing protein (Miller et al., 2010; Arrasate et al., 2004). Thus, a cell line derived from an individual expressing endogenous (low) levels of a moderately-expanded Ataxin-7 protein may be less likely to demonstrate an observable cellular phenotype.

The propensity for NI formation has also been shown to vary extensively between cell types (Cancel et al., 2000). Thus, it may be that the neuronal subtypes generated in this study are less prone to aggregation, although more extensive characterisation of the neuronal population generated will be necessary in order to confirm this. Alternatively, the aggregation of mutant protein may require an exogenous trigger, such as exposure to oxidative stress or neurotoxins. The recent study of SCA3 iPSC-derived neurons by Koch et al. supports this hypothesis, suggesting that excitation-induced calcium influx is required for proteolytic cleavage and aggregation of Ataxin-3 (Koch et al., 2011).

Of interest, no inclusion bodies were detected by epifluorescence staining in the SCA3 iPSC-derived neurons described by Koch et al. Instead, the SDS-insoluble Ataxin-3-containing fragments detected by western blot were deduced to be microaggregates. These minute aggregates, whose presence precedes the formation of larger NIs, have been detected in numerous models of polyQ disease, including SCA1 and SCA7 (Latouche et al., 2007; Michalik et al., 2003; Michalik and Van Broeckhoven, 2003; Yoo et al., 2003; Watase et al., 2002), where they represent an early stage of pathology. Thus, a lack of microscopically-detectable aggregates does not preclude the formation of pathological microaggregates. Further studies involving the detection of Ataxin-7 protein by western blot should help to clarify the presence of these structures in the SCA7 iPSC-derived neurons generated here.

5.3.4 Transcriptional alterations in iPSCs and iPSC-derived neurons

The role of transcriptional dysregulation the polyQ diseases has been extensively documented, particularly in cell and animal models of SCA7 (Chou et al., 2010; Zijlstra et al., 2010; Abou-Sleymane et al., 2006; Tsai et al., 2005; Yoo et al., 2003; La Spada et al., 2001). The identification of gene expression changes which precede the onset of symptoms suggests strongly that alterations in transcription may be among the earliest manifestations of disease (Helmlinger et al., 2006a). Thus, it makes sense to use gene expression changes as a tool to identify a disease-associated phenotype in cells representing early stages of development.

A recent study by Feyeux et al. succeeded in identifying early transcriptional changes linked to naturally-occurring HD mutations in human ESCs, and ESC-derived neural stem cells (NSCs) (Feyeux et al., 2012). Using multiple ESC lines derived from human blastocysts diagnosed as *HTT* mutation carriers by pre-implantation genetic diagnosis, the study aimed to investigate differences in gene expression at early stages of development, by means of differential transcriptomics. Statistical refinement of whole genome expression data revealed a total of seven up- or downregulated genes in HD cells, including genes implicated in disease-associated pathways such as mitochondrial function. Of note, no statistically significant correlation was observed between differentially expressed transcripts in patient autopsied brain samples (representing end-stage disease), and the presymptomatic state represented by ESCs and NSCs (Feyeux et al., 2012). Nonetheless, this study provided convincing evidence that a disease-associated phenotype may be identified in pluripotent cells and/or early-stage neurons. This is supported by recent findings by the HD iPSC Consortium (2012), who used HD iPSC-derived neural stem cells to identify disease-associated patterns of transcriptional dysregulation.

In order to investigate transcriptional alterations in the SCA7 iPSCs and iPSC-derived neurons generated here, 15 candidate transcripts were selected, in which robust changes had been previously

demonstrated (Sopher et al., 2011; Chou et al., 2010; Wang et al., 2010; Palhan et al., 2005; Tsai et al., 2005; Luthi-Carter et al., 2002). These included genes encoding heat shock proteins, an RNA binding protein, a growth factor and a deubiquitinating enzyme, as well as genes involved in transcriptional regulation, apoptosis, chromatin phosphorylation, neuronal differentiation and signalling. Of these 15, only three genes showed no notable changes in expression between wildtype and SCA7 iPSCs and iPSC-derived neurons over three weeks of differentiation – the RNA chaperone *RBM3* (Chou et al., 2010), *SNRK*, encoding a protein involved in chromatin phosphorylation (Luthi-Carter et al., 2002), and *Bex1*, an interactor of the p75 neurotrophin receptor, which regulates neurotrophin signalling and neuronal differentiation (Vilar et al., 2006). The remaining 12 genes demonstrated either significant alterations in expression or notable trends over time. A summary of the transcriptional changes observed in fibroblasts (Chapter 3), iPSCs and iPSC-derived neurons can be found in Table 8.

Table 8 Summary of transcriptional changes identified in SCA7 patient-derived fibroblasts, iPSCs and iPSC-derived neurons, relative to controls

Gene	Published Data*	Fibroblast	iPSC	Neurons 1wk**	Neurons 3wks**	Function
UCHL1	↓	↓	NS	(↓)	(↓)	Deubiquitinating enzyme
DNAJA1	↑, ↓	↑	(↑)	NS	↑	HSP/Chaperone
Hsp70	↓	NS	NS	(↑)	NS	HSP/Chaperone
Hsp27	↓	NS	NS	↑	(↑)	HSP/Chaperone
HSP105	↑, ↓	NS	NS	(↑)	(↑)	HSP/Chaperone
GRIA2	↑	-	-	(↓)	↓	AMPA receptor
RBM3	↑	NS	NS	NS	NS	RNA chaperone
SLC17A6	↓	-	-	(↓)	(↑)	Glutamate transport
Olig1	↓	-	NS	(↑)	(↓)	Oligodendrocyte myelination
ataxin-7	↑	-	NS	↑	(↑)	Component of STAGA
Bex1	↑	-	NS	NS	NS	Neuronal differentiation
IGFBP5	↓	-	(↑)	(↑)	(↓)	Growth factor
KAT2A	?	-	↓	NS	NS	Component of STAGA
BAX	↑	-	NS	NS	(↑)	Apoptosis
SNRK	↓	-	NS	NS	NS	Chromatin phosphorylation

*Sopher et al., 2011; Chou et al., 2010; Wang et al., 2010; Palhan et al., 2005; Tsai et al., 2005; Luthi-Carter et al., 2002

**Results for neurons derived from iPSCs of one or both SCA7 patients

Key: ↑, significantly upregulated ($p<0.05$); ↓, significantly downregulated ($p<0.05$); (↑) or (↓), trends towards up- or downregulation respectively ($p>0.05$); NS, not significant; -, not assessed.

KAT2A encodes the protein Gcn5, the histone acetyltransferase (HAT) component of the STAGA transcription coactivator complex (Strom et al., 2005; Martinez et al., 2001). The evolutionarily conserved role of STAGA in transcriptional regulation has been shown to be mediated by two histone-modifying activities – histone acetyltransferase (HAT) via Gcn5 (Martinez et al., 2001), and deubiquitination via Usp22 (Zhao et al., 2008b). Ataxin-7 is a component of the deubiquitination module of STAGA, where it appears to anchor this module to the main complex (Köhler et al., 2008). Since Gcn5 interacts directly with the zinc-binding motif of Ataxin-7 (Helmlinger et al., 2004a), a loss of Gcn5 function may result in the displacement of the deubiquitination submodule from STAGA, compromising its enzymatic functions (Atanassov et al., 2009).

The interaction of Gcn5 with Ataxin-7 is required for STAGA-mediated histone H3 acetylation, and for the activation of CRX-dependent retinal genes (Helmlinger et al., 2006a; Helmlinger et al., 2006c; Helmlinger et al., 2004a), both of which have been shown to be inhibited in a dominant negative fashion by the incorporation of mutant Ataxin-7 into the STAGA complex (Helmlinger et al., 2006a; Helmlinger et al., 2006c; McMahon et al., 2005; Palhan et al., 2005). Indeed, evidence from a SCA7 knock-in mouse model, in which transcriptional downregulation was shown to be an early event leading to photoreceptor dysfunction, retinal degeneration and visual impairment (Yoo et al., 2003), appears consistent with a decrease in STAGA transcriptional coactivation in the presence of mutant Ataxin-7 (Chen et al., 2012). In direct contrast to these results, however, Helmlinger et al. reported the isolation of STAGA complexes from SCA7 mouse models which exhibited normal levels of HAT activity (Helmlinger et al., 2006a). Moreover, they observed increased recruitment of STAGA to target promoters in the presence of mutant Ataxin-7, resulting in histone H3 hyperacetylation. In this model, the wildtype functions of Ataxin-7 and STAGA (including Gcn5) appear necessary for SCA7 disease progression.

Previous studies of Gcn5 function have demonstrated the importance of its importance in mouse embryo survival and development, including neural tube closure and anterior-posterior patterning (Lin et al., 2008; Bu et al., 2007; Xu et al., 2000). A recent study by Chen et al. sought to further investigate the importance of Gcn5 and STAGA function in the development of SCA7 by examining the effects of Gcn5 mutations in SCA7 transgenic mice (Chen et al., 2012). Their results indicated that partial loss of Gcn5 function led to accelerated neuronal dysfunction and pathology, although deletion of Gcn5 in Purkinje cells was not sufficient to induce severe ataxia in the presence of wildtype Ataxin-7. Of interest, the accelerated pathogenesis observed in SCA7 mouse retinal cells was not accompanied by expression changes in known Ataxin-7 target genes, suggesting the involvement of non-transcriptional functions of STAGA.

Thus, it would appear that a loss of Gcn5 function may contribute to SCA7 pathogenesis (Chen et al., 2012). In line with these observations, results from this study indicate significant downregulation of *KAT2A* expression in SCA7 iPSCs, relative to controls. Altered *KAT2A* expression could result in a derangement in the composition and/or function of STAGA in patient iPSCs, supporting the hypothesis that a loss of Gcn5 expression may contribute to the pathogenesis of SCA7, at least in the early stages of development.

A decrease in *KAT2A* in SCA7 iPSCs may also reflect global deficiencies in HAT activity, with possible implications for the effectiveness of reprogramming, given previous reports of the interaction between Gcn5 and c-Myc, a key pluripotency protein (Takahashi et al., 2007). This hypothesis is less likely, since no obvious differences in reprogramming efficiency, genomic integrity or pluripotency could be detected between SCA7 iPSCs and controls (see Chapter 4). However, genome-wide expression analysis may be necessary to further investigate the contribution of altered *KAT2A* expression levels to global gene expression patterns in SCA7 iPSCs.

Knockout of Gcn5 has been shown to inhibit neuronal differentiation *in vivo* (Martínez-Cerdeño et al., 2012). However, no significant differences in expression were detected between SCA7 and control iPSC-derived neuronal lines in this study. Indeed, *KAT2A* expression appeared marginally higher in the SCA7 neuronal lines, potentially due to compensatory upregulation in the presence of mutant Ataxin-7, a phenomenon previously described in a SCA7 mouse model (Palhan et al., 2005).

Despite extensive evidence for the role of *KAT2A*/Gcn5 deficiency in the exacerbation of SCA7 pathogenesis, a causative link between mutant Ataxin-7 expression and decreased *KAT2A* mRNA is difficult to establish. Indeed, the current understanding of STAGA complex composition implies that any effect of polyQ-expanded Ataxin-7 on Gcn5 is likely only to be observed at the protein level – the result of aberrant interactions between components of the complex. The observation that RNAi-mediated knockdown of Ataxin-7 in HEK293 cells leads to a concomitant reduction in Gcn5 levels suggests the possibility of a feedback loop, which may be perturbed in the presence of mutant Ataxin-7 (Palhan et al., 2005). However, such speculations remain to be verified.

The role of the heat shock response (HSR) in the pathogenesis and treatment of polyQ diseases is well documented. Aggregates of mutant polyQ proteins have been shown to recruit heat shock proteins (HSPs) (such as HSP40 and HSP70) (Zander et al., 2001; Chai et al., 1999a; Chai et al., 1999b; García-Mata et al., 1999; Cummings et al., 1998), while exogenous overexpression of several HSPs, including HSP27 and HSP104 has been shown to suppress neurotoxicity in HD mouse and rat models (Perrin et al., 2007).

Induction of the HSR, in order to promote mutant polyQ protein folding and prevent aggregation, has been observed in the CNS of presymptomatic animal models of disease, and in patient peripheral tissues (Chou et al., 2010; Zijlstra et al., 2010). It comes as no surprise, therefore, that the expression

of genes encoding numerous heat shock proteins, including HSP27, HSP105 and HSP40 (*DNAJA1*) should be significantly elevated in SCA7 iPSC-derived neurons compared to controls, at various time points during differentiation. These results correlate with previous reports of early-stage transcriptional changes in SCA7 mice cerebella, as well observations in SCA3 patient fibroblasts (Chou et al., 2010; Zijlstra et al., 2010), iPSC-derived neurons from patients with neurodegenerative disease (Byers et al., 2011), and SCA7 patient fibroblasts (as reported in Chapter 3 of this study).

Of interest, only *DNAJA1* (HSP40) showed an increase in expression over the three time points evaluated, with the remaining heat shock proteins showing a gradual decline in expression over time. This corresponds with previous reports of a biphasic nature of the HSR in polyQ diseases, in which an initial increase in HSR components at early stages of disease is followed by progressive impairment of HSP gene transcription – the result of an accumulation of toxic mutant Ataxin-7 (Chou et al., 2010), as well as possible epigenetic silencing of the HSP genes (Labbadia et al., 2011). Indeed, downregulation of HSP expression is a common hallmark of late-stage polyQ pathogenesis, having been identified in affected neurons in HD, SBMA, SCA3 and SCA17 transgenic mice (Chou et al., 2010; Chou et al., 2008; Katsuno et al., 2005; Hay et al., 2004). Investigation of HSP gene expression at later time points is likely to clarify whether or not this phenomenon can be observed in SCA7 iPSC-derived neurons.

In contrast to the results obtained from iPSC-derived neurons, SCA7 iPSCs showed no significant induction of HSP gene expression. Similar to LCLs, the rapid rate of cell division associated with iPSCs suggests that these cells are capable of efficient protein turnover, making them far less susceptible to mutant Ataxin-7 accumulation than post-mitotic neurons; thus reducing the need for induction of the HSR (Seo et al., 2004).

The only gene to show consistent downregulation in SCA7 iPSC-derived neurons across all three differentiation time points was *GRIA2*, encoding the glutamate receptor, ionotropic, AMPA2 (GluR2). GluR2 functions as a major subunit of glutamate AMPA receptors expressed in cerebellar Purkinje and granule neurons (Häausser and Roth, 1997), where it controls calcium permeability of AMPA receptors (Bai and Wong-Riley, 2003).

A previous study of SCA7 transgenic mice revealed elevated levels of GluR2 mRNA at advanced stages of disease (Chou et al., 2010). Since excitotoxicity, caused by glutamate receptor overactivation, has been proposed to contribute to SCA7 pathogenesis (Bauer and Nukina, 2009), it was hypothesised that GluR2 overexpression might lead to cerebellar malfunction through dysregulated glutamatergic transmission (Chou et al., 2010). By contrast, decreased GluR2 expression has been associated with disease progression in other neurodegenerative diseases, including Alzheimer's disease (Courtney et al., 2010) and ALS (Cozzolino et al., 2008).

GluR2 expression has been shown to be restricted to particular neuronal subtypes, with the highest levels observed in pyramidal neurons (Bai and Wong-Riley, 2003). In addition, GluR2 expression has been found to increase during development, in cultured murine cortical neurons (Jensen et al., 2001). Both mRNA and protein levels of GluR2 are also tightly controlled by neuronal activity, with decreased activity inducing a significant decrease in GluR2 expression (Bai and Wong-Riley, 2003). The decrease in *GRIA2* (GluR2) expression observed in the SCA7 iPSC-derived neurons generated in this study may thus result from aberrant development and maturation, leading to decreased neuronal activity in comparison to neurons generated from control iPSCs. Alternatively, a failure of SCA7 iPSCs to generate particular neuronal lineages, associated with high levels of GluR2 expression, could also account for the low levels of GluR2. Further studies may therefore be required to determine both the extent to which neuronal electrophysiology is impaired in SCA7 neurons, and the composition of the neuronal population generated from SCA7 iPSCs, in order to

determine whether mutant Ataxin-7 has any effect on the development and maturation of these neurons.

The final gene to show a statistically significant change in expression was the disease-causing gene itself, *ataxin-7*. An approximate two-fold increase in *ataxin-7* expression was observed in SCA7 iPSC-derived neurons in comparison to controls, one week post-differentiation. The role of the Ataxin-7 protein as a core component of the STAGA/TFTC transcriptional coactivator complexes has already been extensively discussed (see Section 1.1.4). In addition, the deleterious effects of mutant Ataxin-7 expression on cellular function suggest that increased expression levels may exacerbate SCA7 pathology (Yoo et al., 2003). A recent study by Sopher et al. examined the modulation of Ataxin-7 expression by the transcriptional regulator CTCF, via the promotion of a convergently transcribed, antisense noncoding RNA, termed SCAANT1, suggesting that this may represent a novel mechanism for the epigenetic regulation of *ataxin-7* gene expression. Of critical importance to this study, Sopher et al. identified a reduction in SCAANT1 promoter activity associated with expansion of the *ataxin-7* CAG repeat tract. The resultant reduction in SCAANT1 expression leads to derepression of the *ataxin-7* alternative promoter, significantly boosting the levels of *ataxin-7*, creating a feed forward effect which agonises the SCA7 disease pathway by promoting increased production of mutant Ataxin-7 protein (Sopher et al., 2011).

Thus, an increase in CAG repeat length should correlate with an increase in *ataxin-7* expression, as is the case in SCA7 iPSC-derived neurons one week post-differentiation. However, a subsequent decrease in *ataxin-7* expression was observed at the two- and three week time points, suggesting that Ataxin-7 upregulation may not be sustained. It may therefore be of interest to quantify SCAANT1 expression in these neurons, to determine the influence of this noncoding RNA on the levels of *ataxin-7* expression over time.

In addition to the statistically significant changes in gene expression described above, several interesting non-significant trends were observed. These included decreased expression of the deubiquitinating enzyme *UCHL1* in SCA7 iPSC-derived neurons at one week and three weeks post differentiation. This trend corresponds to changes previously reported in SCA7 transgenic mice (Chou et al., 2010), as well as the results obtained for SCA7 fibroblasts in this study (Chapter 3). A non-significant increase in *BAX*, which encodes a proapoptotic protein previously shown to be upregulated in the cerebellar and inferior olivary neurons of SCA7 transgenic mice (Wang et al., 2010), was also observed, in SCA7 neurons at three weeks post differentiation.

Although no significant differences in *Olig1* expression were observed between SCA7 and control iPSC-derived neurons, an interesting trend emerged over the three week time course. At one week post-differentiation, *Olig1* expression appeared marginally higher in patient neurons (particularly those derived from the older of the two patients, 1518), although this was followed by a consistent decrease in expression over the following two weeks. By contrast, control iPSC-derived neurons showed a gradual increase in *Olig1* expression over time, with the result that control neurons appeared to express marginally higher levels of *Olig1* than their patient-derived counterparts by three weeks post-differentiation.

Olig1 encodes a basic helix-loop-helix transcription factor which has been shown to play an essential role in oligodendrocyte myelinogenesis, through the regulation of transcription of several major myelin-specific genes (Xin et al., 2005). A study of Ataxin-7-Q52 transgenic mice demonstrated significantly decreased levels of Olig1 mRNA and protein at both early (six months of age) and late (10-11 months of age) stages of disease. In the 10-11 month-old mice, which displayed pronounced ataxic symptoms, this decrease was associated with the presence of loose and poorly compacted myelin sheaths in the cerebellar white matter, consistent with the hypothesis that Olig1 downregulation leads to defective myelination and consequently, cerebellar dysfunction (Chou et al.,

2010). The decrease in cerebellar mRNA levels of *Olig1* in 6 month-old mice, which preceded the onset of disease symptoms, suggested that *Olig1* downregulation may play an important role in initiating the pathological processes of SCA7 (Chou et al., 2010).

Olig1, together with Olig2, has been shown to play a role in motor neuron and oligodendrocyte progression (Zhou and Anderson, 2002). Thus, the gradual decrease in *Olig1* expression over time in SCA7 iPSC-derived neurons may reflect a gradual decrease in the potential of these cells to generate certain neuronal and glial lineages, or to attain developmental maturity. More extensive characterisation of the composition of the neuronal populations generated from SCA7 and control iPSCs may thus be required, in order to identify particular lineages whose development may be affected by the differences in *Olig1* expression over time.

A non-significant increase in the growth factor gene, *IGFBP5*, was also observed in SCA7 iPSCs and iPSC-derived neurons versus controls. Insulin-like growth factor binding proteins (IGFBPs) function in the transport and modulation of activity of insulin-like growth factors (IGFs) (Jones and Clemmons, 1995). IGFBP5 in particular, has been shown to stimulate the phosphorylation of the IGFBP5-receptor, activating its serine/threonine kinase activity (Andress, 1998). The expression of *IGFBP5* has been previously found to be decreased in mouse models of several of the polyQ diseases, including DRPLA, HD, SCA7 and SBMA (Luthi-Carter et al., 2002). Robust downregulation of *IGFBP5* has also been described in a mouse model of SCA1, with both SCA1 and SCA7 mice demonstrating a non-cell-autonomous decrease in *IGFBP5* expression in granule neurons, concomitant with the activation of the IGF pathway and the type I IGF receptor on Purkinje cells (Gatchel et al., 2008). Since *IGFBP5* downregulation is common across a number of polyQ diseases, in some cases in presymptomatic stages, it is more likely to be part of a general response to neuronal injury, rather than a direct target of polyQ protein-mediated pathogenesis (Gatchel et al., 2008).

The increased expression observed in this study was therefore unexpected. Indeed, only one previous report provides some supporting evidence for this finding – the discovery of abnormally high levels of IGFBP5 in the granule neurons of ataxic, "weaver" mice (Zhong et al., 2005). The aberrant increase in IGFBP5 expression, which precedes the demise of these neurons, is thought to result in a blockade of IGF-I activity. Since IGF-I is essential for the survival and differentiation of cerebellar neurons, reduced IGF-I availability resulting from excess IGFBP5 was deduced to accelerate the rate of apoptosis of granule neurons in this model. Elevated *IGFBP5* in SCA7 iPSCs and iPSC-derived neurons may thus reflect an early predisposition towards degeneration, although these results should be treated with caution, given their lack of statistical significance.

Finally, a gradual increase in *SLC17A6* in SCA7 iPSC-derived neurons was observed over three weeks of differentiation, in contrast to the gradual decline in expression of that gene over the same period in control iPSC-derived neurons. *SLC17A6* encodes the vesicular glutamate transporter 2 (VGLUT2), required for vesicular glutamate release from cerebellar glutamatergic neurons (Hioki et al., 2003). Downregulated mRNA expression of VGLUT2, observed in both early and late stages of disease progression in SCA7 transgenic mice, has been proposed to contribute to dysregulated glutamatergic transmission and consequently, cerebellar malfunction (Chou et al., 2010). By contrast, increased VGLUT2 expression has been described in the putamen of Parkinson's disease patient brains (Kashani et al., 2007).

The fraction of VGLUT2-positive neurons generated by neuronal differentiation from ESCs is small, but increases over time (Koch et al., 2009). Thus it may be that the differing trends in VGLUT2 expression between SCA7 and control neurons described here merely represent a bias towards the development of different neuronal lineages over time. Further analysis is complicated by a limited understanding of the level of maturation and neuronal connectivity achieved by iPSC-derived

neurons at three weeks post-differentiation, and conclusions should be drawn with caution, given the lack of statistical significance of the results.

In general, similar trends were observed across all patient-derived neurons, relative to controls, although neurons derived from the iPSC line 1518D (generated from the SCA7 patient carrying the shorter CAG repeat tract, consisting of 42 CAG repeats) tended to display a milder transcriptional phenotype. This may be attributed to the differences in CAG repeat lengths between the two individuals, since longer CAG repeat tracts have been associated with more rapid and severe phenotypes (Lebre and Brice, 2003). Of crucial importance, the age and stage of disease (patient 1518 is the older and more advanced case of the two patients in this study) did not appear to influence the transcriptional changes observed in iPSC-derived neurons, suggesting that markers of disease progression, such as the epigenetic alterations proposed to affect the HSR, may be "reset" during iPSC reprogramming (Labbadia et al., 2011; Takahashi et al., 2007).

This epigenetic remodelling may also account for the lack of statistically significant disease-associated transcriptional alterations in SCA7 patient iPSCs, although trends in expression of certain genes (such as *DNAJA1*), which correspond to those identified in patient fibroblasts, support the assertion that iPSCs may retain the epigenetic memory of the somatic cells from which they were derived (Kim et al., 2010).

5.3.5 The value of iPSC-derived models of SCA7 in the South African population

This is the first record of iPSC-derived neurons derived from South African SCA7 patients. The generation of patient-specific, disease-relevant cell types is particularly important in neurodegenerative diseases; as such cells provide a unique model in which to evaluate disease pathogenesis without the complications associated with transgene overexpression in cell or animal

models. In addition, the use of cells containing the patient's own genetic background offers the opportunity to investigate potential modifiers of disease onset and progression (Bilen and Bonini, 2007; Marsh and Thompson, 2006).

Perhaps most importantly to the South African context, iPSC-derived neurons provide the first opportunity to evaluate the efficacy of the allele-specific RNAi-based therapy developed by Scholefield et al. (2009), in disease-affected cells. Current efforts have now shifted to the identification of a mechanism for the efficient delivery of the gene silencing effector into post-mitotic neurons, which have thus far proven refractory to transfection.

5.3.6 Concluding remarks

This study has shown that iPSCs, derived from two South African SCA7 patients, are capable of differentiation into neuronal cells, exhibiting characteristic neuronal morphology and expressing the neuronal marker βIII-tubulin. No differences in differentiation efficiency, Ataxin-7 expression or localization were observed between SCA7 and control iPSC lines. Furthermore, no significant differences in the ability of SCA7 iPSCs to generate GABAergic neurons, the precursors of cerebellar Purkinje cells, could be detected.

Although the aggregation of mutant protein is generally viewed as a defining feature of polyQ disease, the lack of observable aggregates in the SCA7 neurons generated here was not entirely unexpected, given the early stage of differentiation assessed. These findings strongly suggest that certain early markers of pathogenesis, such as alterations in gene transcription, may precede the formation of detectable aggregates, although further studies of protein expression may be necessary to clarify the presence or absence of microaggregates of toxic protein within these cells.

However, the identification of additional phenotypic markers, in the form of alterations in transcription, suggests that these cells may still be useful for investigating pathogenesis and evaluating therapies. Significant differences in expression of HSPs, as well as genes involved in neuronal differentiation, transcriptional regulation and glutamatergic signalling were observed in both SCA7 iPSCs and iPSC-derived neurons relative to controls, suggesting that these key genes, previously implicated in polyQ toxicity in cell and animal models, may indeed play a role at the earliest stages of development of disease.

Despite these promising results, a number of limitations remain to be addressed. The general neuronal protocol used for this study generates a wide variety of neuronal as well as a small population of glia. This heterogeneity may result in a dilution of disease-specific effects, since the cell types present do not necessarily represent those most vulnerable to disease changes. Further analysis of gene expression and electrophysiology will therefore be required to fully elucidate the relative compositions of control and SCA7 iPSC-derived populations, in order to understand their contribution to the disease phenotype, as well as to identify possible disease-associated deficiencies in neuronal subtype specification and maturation.

The question of whether iPSC-derived neurons will ever fully recapitulate the phenotype of a late-onset, neurodegenerative disease has been plagued with controversy. A number of mechanisms have been proposed to improve these models, including the culture of neurons over longer time points, and the introduction of cell stressors (Wichterle and Przedborski, 2010), both of which would add value to the current study. Concerns as to whether the "age" of patient-derived neurons more closely reflects the age of the patient from which the fibroblasts of origin were derived, or the embryonic state of the iPSCs from which they were differentiated are also of critical importance. Based on previous studies, however, it seems most likely that a disease-associated phenotype will be detected

in iPSC-derived models from patients with an earlier age of onset, such as patient 1519 in this study (Ebert et al., 2008).

Finally, the extensive variations in gene expression and differentiation potential observed between iPSC lines, both here and in previous studies (Hu et al., 2010b), motivate strongly for the inclusion of additional patient iPSC lines, particularly from the older patient (1518) to further clarify the role of the transcriptional alterations described here in the development and progression of SCA7.

Despite these limitations, however, the results of this study provide the first evidence for the differentiation of neurons from iPSCs generated from the South African SCA7 patient cohort, paving the way for future analysis of disease pathogenesis, and the development of population-specific therapies.

Chapter 6 **Discussion**

This study sought to evaluate novel cell models for SCA7, a dominantly-inherited polyQ neurodegenerative disease characterised by cerebellar ataxia and macular degeneration, which is caused by the expansion of an unstable CAG repeat tract within the *ataxin-7* gene (Lebre and Brice, 2003). As with many inherited neurodegenerative conditions, research into SCA7 pathogenesis and therapy has been hindered by the lack of readily-available (CNS-derived) biological material. This has led to the development of numerous cellular and animal models, in an attempt to recapitulate the main features of the disease (Ingram et al., 2011; Zander et al., 2001). Despite the invaluable insights gained from these models, the inherent challenges associated with modelling human neurodegenerative diseases in animals suggest that their applications may be limited.

Attention has thus turned to the use of patient-derived cells as models of disease. Non-neuronal cells, including fibroblasts and lymphoblasts have previously been suggested as useful models for investigating pathogenesis and screening therapeutic modalities (Tsai et al., 2005; Garden et al., 2002). More recently, advances in pluripotent stem cell technology have given rise to a multitude of iPSC-derived models for the study of human disease, offering the opportunity (in theory, at least) for differentiation into any affected cell type (Rajamohan et al., 2012). This study therefore examined the feasibility of using patient-derived peripheral cells (dermal fibroblasts), as well as iPSCs and iPSC-derived neurons as models for the study of SCA7 pathogenesis and therapy. Each of these cell types has both advantages and disadvantages – fibroblasts, for example, are easily accessible, but are not derived from disease-affected tissue; while iPSC-derived neurons are difficult to culture, but more closely represent the disease state. Nonetheless, results indicate that all three cell models may provide valuable insights into the progression and treatment of SCA7.

6.1 Generation of SCA7 iPSC-based disease models

A number of iPSC-based models of neurodegenerative disease have been described (Koch et al., 2011; Zhang et al., 2010; Ebert et al., 2008; Dimos et al., 2008). However, the only published record of SCA7 iPSCs to date is based on a single Chinese patient, with adult onset of disease symptoms (Luo et al., 2012). The current study has demonstrated the successful reprogramming of dermal fibroblasts from two South African SCA7 patients (one with presumed adolescent onset, and one with adult onset of disease) to pluripotency, using retroviral vectors (Takahashi et al., 2007). Of the iPSC lines generated, two SCA7 (and two control) lines passed the stringent tests for pluripotency outlined by Maherali and Hochedlinger (2008), including the development of ESC-like morphological characteristics, suppression of retroviral transgenes, expression of endogenous pluripotency genes and cell surface markers of pluripotency, karyotypic normality, and the ability to differentiate into cells from each of the three embryonic germ layers. A further one patient line, 1518D, passed all the tests but one, having not been evaluated for EB-mediated *in vitro* germ layer differentiation (although its ability to generate ectodermal cells was confirmed by successful neuronal differentiation).

This represents a significant improvement over the previous SCA7 iPSC study by Luo et al. (2012), as it offers the first opportunity for comparison between patients, and for comparison between multiple iPSC lines generated from the same patient. In addition, the difference in CAG repeat length, age of onset and stage of disease progression between the two patients may allow for future investigations into the influence of these factors on cellular phenotype. However, given the observed variation between iPSC lines (Hu et al., 2010b), it is likely that additional iPSC lines, generated from these and other SCA7 patients, may be required to differentiate between disease-specific phenotypic effects, and those resulting from variations in the reprogramming process.

The inclusion of a control iPSC line (iPS SC NHDF) generated using five retroviral reprogramming factors (as opposed to the remaining control and patient iPSC lines, generated using a three-factor combination) represents a potential source of controversy. On the one hand, cells reprogrammed using a larger pool of viral vectors are at greater risk of insertional mutagenesis, and have an increased propensity for genomic instability and tumorigenesis, particularly where the reprogramming factors include the oncogene, *c-MYC*, as was the case in this study (Okita et al., 2007). However, it may also be argued that increasing the number of retroviral vectors used in reprogramming enhances the efficiency of the process, leading to a greater number of fully reprogrammed clones (Liao et al., 2008). Most pertinent to this study are questions regarding the differential effect of multiple retroviral insertions on the expression profile of iPSCs (Liu et al., 2012). However, the lack of observable variation between iPSCs and neurons derived from iPS SC NHDF and those derived from the three-factor control iPSC line (iPS George) suggested that variations in the reprogramming protocols between these lines did not affect the results obtained. Nevertheless, future studies would benefit from the inclusion of additional control iPSC lines generated using the three-factor combination of pMXs-hOct3/4, pMXs-hSox2 and pMXs-hKlf4, together with VPA, in order to minimise the potential for variation between lines.

To this end, the Division of Human Genetics at UCT has established fibroblast cell lines from a further four consented SCA7 patients, with varying CAG repeat lengths, during the course of 2012. Future work will focus on the reprogramming of these fibroblasts to iPSCs, and the characterisation of all iPSC lines generated, including outstanding iPSC lines from the current study, in order to establish a more comprehensive resource for the study of SCA7 in the South African population.

Although concerns have been raised regarding the safety and viability of retrovirally-reprogrammed iPSCs for downstream applications, this study observed no effects of viral integration on either the genomic stability or differentiation potential of any of the iPSC lines generated. In addition, all the

lines tested here showed silencing of the retroviral transgenes (with the exception of pMXs-hOct3/4) at 10 passages post-reprogramming. This is significant, as persistent transgene expression has been shown to affect the molecular signatures, differentiation behaviour and developmental potential of iPSCs (Stadtfeld et al., 2008) Taking into account the most likely application of these lines, as vehicles for *in vitro* disease modelling and therapeutic screening rather than autologous transplantation, the efficiency of retroviral reprogramming may be considered to outweigh the potential harms, at least in the context of the current study (González et al., 2011). Nonetheless, the incorporation of non-integrating methods into future iPSC reprogramming experiments may be of benefit, in order to minimise potentially deleterious effects.

Neurons derived from iPSCs have been used to model a variety of neurodegenerative disorders, including Parkinson's disease (Soldner et al., 2009) and several of the polyQ diseases (Camnasio et al., 2012; Koch et al., 2011). In order to generate disease-relevant cells from the SCA7 iPSC lines generated here, a general neuronal protocol was followed (Dottori and Pera, 2008). Despite previous reports suggesting that CAG expansions may hinder neuronal differentiation (Lorincz et al., 2004), no obvious differences in the number or morphology of βIII-tubulin positive neuronal cells were observed between SCA7 and control iPSC lines. The same was true of the small proportions of GFAP-positive glial cells and GABA-positive, putative GABAergic cells produced over three weeks of differentiation. These results confirm the ability of SCA7 and control iPSCs to generate neuronal cells with equal efficiency, corresponding to results of studies of other polyQ diseases (Koch et al., 2011; Camnasio et al., 2012).

Despite these promising results, there are several limitations to the current study, which future work will seek to address. The neuronal differentiation protocol described by Dottori and Pera (2008) served the purpose of this study, offering a relatively simple, rapid and robust means of generating a mixed population of neurons mimicking, to some extent, the variety of immature neurons expressed

in the developing brain. Immunostaining for GFAP and GABA provided some information as to the types of cells generated by each iPSC line. However, further comparisons of the neuronal populations generated by SCA7 and control iPSCs are recommended, to rule out the possibility of disease-associated deficiencies in composition and maturation which may affect the gene expression profile. Future studies should therefore expand the panel of antibodies used in immunostaining to include markers of different neuronal and glial subtypes, such as tyrosine hydroxylase (dopaminergic neurons), vesicular glutamate transporters (glutamatergic neurons) or GalC (oligodendrocytes).

This study focused on the generation of cells displaying neuronal morphology and expressing markers of early neuronal differentiation, but did not investigate the functionality of the neurons generated. Since defects in signalling leading to excitotoxicity have been previously implicated in SCA7 pathogenesis, future studies may involve a comparison of the development of membrane potentials and synaptic connections in patient versus control iPSC-derived neurons, using electrophysiological tools. Synaptic competence has previously been proposed as a defining feature of neuronal maturation *in vitro* (Yang et al., 2011); thus, such a study should also provide insight into the presence of any disease-associated developmental defects.

The ability of iPSC-derived neurons to fully recapitulate the phenotype of neurodegenerative diseases remains a subject of controversy, particularly since the age of neurons in culture is difficult to approximate. It may be argued that the time period used in this study was not sufficient to produce phenotypes reminiscent of end-stage disease. Future studies will therefore evaluate the differentiation and gene expression of iPSC-derived neurons following longer periods of culture, and may also include treatment with environmental stressors such as reactive oxygen species, designed to reproduce the effects of aging *in vitro*.

6.2 Identification of a disease-relevant phenotype in patient-derived cells

The mechanisms underlying polyQ pathogenesis are complex, involving a combination of protein aggregation, impairment of protein clearance pathways, aberrant protein-protein interactions, post-translational modifications and defects in mitochondrial energy metabolism (Watson and Wood, 2012). Although the formation of nuclear inclusions of mutant protein was once considered a hallmark of polyQ pathology, results from this study and others (Einum et al. 2001) suggest that Ataxin-7 aggregation is not a prerequisite for SCA7 pathogenesis, at least in immature neurons equivalent to early stages of disease progression.

Transcriptional dysregulation has been proposed as a common early feature of polyQ diseases (Helmlinger et al., 2006b). In SCA7 in particular, the role of the disease-causing protein, Ataxin-7, in the TFTC and STAGA transcriptional co-activator complexes has highlighted the role of transcriptional alterations in the development and progression of disease (Helmlinger et al., 2006a; Palhan et al., 2005). These transcriptional changes in response to mutant polyQ protein expression are not limited to disease-affected tissues, having previously been demonstrated in peripheral cells (Tsai et al., 2005).

Transcriptional alterations were thus chosen as a measure of the polyQ disease phenotype in the SCA7 patient-derived cell models investigated in this study. Using a candidate gene approach, significant differences in expression levels of genes involved in the heat shock response, UPS and glutamatergic transmission were detected between SCA7 and control fibroblasts, iPSCs and iPSC-derived neurons, further emphasising the known role of these pathways in polyQ pathogenesis. One gene in particular, *DNAJA1,* encoding the heat shock protein DnaJA1, was found to be upregulated in SCA7 fibroblasts and iPSC-derived neurons, emphasising the global role of the HSR in the response to cellular stress caused by misfolding of mutant Ataxin-7. The remaining genes showed differing patterns of up- and downregulation between the three cell models, reflecting differences in

expression profiles, mutant protein turnover and cell-type susceptibility. Despite these differences, the observed trends corresponded for the most part to results previously obtained in cell and animal models of SCA7 (Chou et al. 2010; Tsai et al., 2005), suggesting that the patient-derived models evaluated here may be similarly used to provide insights into the molecular pathogenesis of the disease.

This is the first study to report a transcriptional phenotype in SCA7 patient fibroblasts, iPSCs and iPSC-derived neurons, easily-accessible cell types which may readily be used for disease modelling and therapeutic screening. In addition, the appearance of transcriptional changes in SCA7 iPSC-derived neurons as early as one week post differentiation, prior to the observable aggregation of mutant Ataxin-7, confirms the role of transcriptional changes as an early marker of disease progression. Furthermore, the identification of differentially expressed transcripts in "unaffected" cell types such as cultured fibroblasts suggests that the deleterious effects of mutant Ataxin-7 are widespread, with significant clinical pathology developing only in those cells which are particularly susceptible to accumulation of the polyQ-expanded protein. The diverse range of differentially expressed transcripts identified in SCA7 patient-derived cells suggests strongly that alterations in transcription result from both the accumulation of mutant protein (leading to manifestations of cellular stress, such as impairment of the UPS and upregulation of the HSR); and its effects on transcriptional regulation via the TFTC/STAGA complex, resulting in more general dysregulation of gene expression (Helmlinger et al., 2006a).

The results of this investigation have thus provided a number of valuable insights into the role of gene expression changes in the development of SCA7. Nonetheless, several questions remain, which future studies should aim to address. Since the pattern of disease-associated alterations in gene expression has been shown to change with disease progression and advancing age, evaluation of transcriptional changes in iPSC-derived neurons after prolonged periods of culture may prove

advantageous. By the same token, derivation of neurons from iPSCs from patients with longer CAG repeat tracts, associated with more rapid progression and greater disease severity (Lebre and Brice, 2003), may provide additional insights.

The candidate gene approach, favoured in this proof-of-principle study, detects only a fraction of the potential gene expression changes between SCA7 and control lines, and offers no information regarding the effects of these changes on alterations in protein levels. Future studies may therefore involve whole-genome expression analyses, in order to capture the full extent of transcriptional dysregulation in SCA7 disease models. Such studies will require the derivation of many more iPSC lines, from a larger patient cohort, as well as further optimisation of the neuronal differentiation protocol, in order to minimise inter- and intra-individual sample variation, so that true disease-associated transcriptional changes can be identified. This is likely to include efforts to standardise the number, size and density of both iPSC colonies and neurospheres used in differentiation, as well as the use of alternative protocols which employ more defined intermediate steps and generate a more homogeneous neuronal population, such as those proposed by Koch et al. (2009) or Erceg et al. (2012). In addition, validation of the results obtained here, together with the results of future array-type studies, at the protein level should aid in understanding their pathological significance. Further investigations into the role of TFTC/STAGA in regulating the differentially expressed transcripts identified here would also be of value.

A final caveat of the present investigation, which deserves some scrutiny, is the use of related SCA7 patients. The study of affected family members (in this case, a mother and son) provides a degree of genetic homogeneity which may be advantageous. However, the possibility exists that some of the gene expression changes, attributed here to the presence of the mutant protein, may result instead from family-specific, or even population-group specific variations. The results obtained from RNAi-mediated silencing of mutant Ataxin-7 (discussed in Section 6.3) suggest strongly that this is not the

case. However, the incorporation of additional SCA7 patients, together with age-, ethnicity- and sex-matched controls would provide further proof of the disease-associated nature of these transcriptional changes; particularly in light of the recent discovery of X chromosome-associated epigenetic variability of female iPSC lines, which may influence stability and gene expression patterns (Anguera et al., 2012). To date, the size of the cohort has been hindered by a lack of access to consenting individuals. However, recent advances in patient recruitment at UCT (mentioned in Section 6.1) should aid in the expansion of the patient and control cohorts, setting the scene for larger, more comprehensive future studies of gene expression, electrophysiology and cellular pathology, similar to the recent report on CAG repeat-associated phenotypes in iPSCs by the HD iPSC Consortium (2012).

6.3 SCA7 patient-derived cells as a model for evaluating RNAi-based therapy

The toxic gain-of-function nature of the polyQ expansion mutation, together with the complexity of the pathogenic pathway described above, make diseases such as SCA7 ideal candidates for gene silencing therapies which target and suppress production of the mutant protein upstream of its deleterious effects. In particular, the high frequency and heterozygosity of a disease-linked SNP in the South African SCA7 patient population have led to the design of RNAi effectors for this cohort (Scholefield et al., 2009). The extensive pre-clinical validation required by such therapies is often hindered by a lack of suitable disease models; thus, the three patient-derived cell models of SCA7 described here were intended not only for the study of pathogenesis, but also as vehicles for the *in vitro* evaluation of previously-developed RNAi therapies, with a view to developing alternative therapies for SCA7 in the future.

Results obtained from RNAi experiments in SCA7 fibroblasts were promising, confirming the ability of two previously-designed siRNAs to target and suppress *ataxin-7* expression, and validating the

allele-specificity of siR-P16, which discriminates between wildtype and mutant copies of the *ataxin-7* transcript based on the genotype of the disease-linked SNP (Scholefield et al., 2009). Although similar results have been obtained for other polyQ diseases using patient fibroblasts (Fiszer et al., 2011; Hu et al., 2011; Hu et al., 2010a; Hu et al., 2009b; Lombardi et al., 2009; Van Bilsen et al., 2008), this is the first report confirming allele-specific silencing of *ataxin-7* in patient-derived cells.

This is also the first report of the amelioration of a transcriptional phenotype in patient cells, following RNAi-mediated gene silencing, with knockdown of *ataxin-7* resulting in restoration of disease-associated aberrations in *DNAJA1* and *UCHL1* expression to approximately normal levels. This is not only a significant proof-of-principle of the utility of transcriptional alterations as a marker for therapeutic efficacy, but also provides strong evidence for the disease-associated nature of the changes in gene expression, since *ataxin-7* silencing does not produce a similar effect on *DNAJA1* or *UCHL1* levels in controls.

A number of issues remain to be addressed, however, in the progression of such RNAi therapies towards pre-clinical trials. Among these are questions of dosage and off-target effects, highlighted by the dose-dependent nature of *DNAJA1* restoration, and the differing effects of allele-specific and non-allele-specific siRNAs on *UCHL1* expression at high doses. Of concern for future allele-specific therapies is the finding that restoration of *DNAJA1* levels towards normal occurs only at a concentration at which the allele-specific effect of siR-P16 is no longer observed. In addition, the relationship between wildtype *ataxin-7* expression and *UCHL1* levels, implied by the results obtained from non-allele-specific silencing of *ataxin-7* in both SCA7 patient and control fibroblasts, merits further investigation. As such, more detailed dose titrations of siR-P16 may be required prior to clinical application, to achieve a compromise between allele-specificity and phenotypic restoration. Whole genome expression analyses following siRNA treatment, as well as chromatin

immunoprecipitation or DNA footprinting studies to identify possible interactions between Ataxin-7 and/or STAGA/TFTC and the *UCHL1* promoter, are also potential avenues for future investigations.

Evaluation of siRNA efficacy at the level of mutant protein aggregation is currently hindered by the absence of detectable protein aggregates in the SCA7 patient cells investigated here. However, the recent study of SCA3 iPSC-derived neurons by Koch et al. (2011) suggests that western blotting may serve as an alternative to microscopy for the measurement of aggregation. Future studies may therefore involve the validation of *ataxin-7* silencing, restoration of *DNAJA1* and *UCHL1* expression, and reduction of mutant protein aggregation at the protein level, by means of western blot analysis.

Finally, since this report reflects only the results obtained from SCA7 patient cultured fibroblasts, current and future work will focus on evaluating the effects of *ataxin-7* gene silencing in iPSCs and iPSC-derived neurons. Postmitotic neurons are known to be sensitive to cytotoxicity and are notoriously difficult to transfect, requiring more complex procedures than the electroporation described here, such as those mediated by lentiviruses or magnetic nanobeads (Fallini et al., 2010). iPSCs, by contrast, are far more amenable to lipid-mediated transfection (Ma et al., 2012; Chatterjee et al., 2011). A more straightforward approach may therefore be to introduce the RNAi effector into patient-derived iPSC lines prior to neuronal differentiation, although this would require a more sustainable method of knockdown than short-lived siRNA molecules. The effects of *ataxin-7* suppression could then be measured in comparison to both control lines, and untransfected patient neurons. It should, however, be noted that this approach, while valuable, would may not provide sufficient insight into the efficacy of RNAi-mediated silencing of *ataxin-7* in end-stage disease, in which accumulation of the mutant protein results in neuronal dysfunction. A combinatorial approach is therefore likely to be required, balancing transfection efficiency with relevance to disease.

6.4 Concluding remarks

This project sought to establish and evaluate patient-derived cell models of SCA7, for use in the investigation of SCA7 pathogenesis and therapy. Three patient-derived cell types (fibroblasts, iPSCs and iPSC derived neurons) were found to exhibit disease-associated changes in transcripts previously implicated in SCA7 pathogenesis, providing insights into disease progression. Furthermore, the evaluation of RNAi-based therapy in SCA7 fibroblasts demonstrated the ability of an allele-specific siRNA, designed specifically for the South African patient population, to selectively silence mutant *ataxin-7*, leading to the restoration of the transcriptional phenotype described above.

Taken together, these results suggest that patient fibroblasts, iPSCs and iPSC-derived neurons may serve as novel, disease-relevant models for the study of SCA7 in the South African patient cohort; representing a significant advance in the study of this debilitating neurodegenerative disease in a country with one of the highest prevalence rates of SCA7 in the world.

References

Abdelgany A, Wood M, Beeson D. 2003. Allele-specific silencing of a pathogenic mutant acetylcholine receptor subunit by RNA interference. Hum Mol Genet 12:2637-2644.

Abeliovich A, Doege CA. 2009. Reprogramming therapeutics: iPS cell prospects for neurodegenerative disease. Neuron 61:337-339.

Abou-Sleymane G, Chalmel F, Helmlinger D, Lardenois A, Thibault C, Weber C, Merienne K, Mandel JL, Poch O, Devys D. 2006. Polyglutamine expansion causes neurodegeneration by altering the neuronal differentiation program. Hum Mol Genet 15:691-703.

Ajayi A, Yu X, Lindberg S, Langel Ü, Ström AL. 2012. Expanded ataxin-7 cause toxicity by inducing ROS production from NADPH oxidase complexes in a stable inducible spinocerebellar ataxia type 7 (SCA7) model. BMC Neuroscience 13:86.

Aleman TS, Cideciyan AV, Volpe NJ, Stevanin G, Brice A, Jacobson SG. 2002. Spinocerebellar ataxia type 7 (*SCA7*) shows a cone–rod dystrophy phenotype. Exp Eye Res 74:737-745.

Alluri RV, Komandur S, Wagheray A, Chaudhuri JR, Sitajayalakshmi, Meena AK, Jabeen A, Chawda K, Subhash K, Krishnaveni A, Hasan Q. 2007. Molecular analysis of CAG repeats at five different spinocerebellar ataxia loci: Correlation and alternative explanations for disease pathogenesis. Mol Cells 24:338-342.

Alves S, Nascimento-Ferreira I, Auregan G, Hassig R, Dufour N, Brouillet E, Pedroso de Lima MC, Hantraye P, Pereira de Almeida L, Déglon N. 2008. Allele-specific RNA silencing of mutant ataxin-3 mediates neuroprotection in a rat model of Machado-Joseph disease. PLoS One 3:e3341.

Ambrose CM, Duyao MP, Barnes G, Bates GP, Lin CS, Srinidhi J, Baxendale S, Hummerich H, Lehrach H, Altherr M. 1994. Structure and expression of the Huntington's disease gene: Evidence against simple inactivation due to an expanded CAG repeat. Somat Cell Mol Genet 20:27-38.

An MC, Zhang N, Scott G, Montoro D, Wittkop T, Mooney S, Melov S, Ellerby LM. 2012. Genetic correction of Huntington's disease phenotypes in induced pluripotent stem cells. Cell Stem Cell 11:253-263.

Andress DL. 1998. Insulin-like growth factor-binding protein-5 (IGFBP-5) stimulates phosphorylation of the IGFBP-5 receptor. Am J Physiol Endocrinol Metab 274:E744-E750.

Anguera MC, Sadreyev R, Zhang Z, Szanto A, Payer B, Sheridan SD, Kwok S, Haggarty SJ, Sur M, Alvarez J. 2012. Molecular signatures of human induced pluripotent stem cells highlight sex differences and cancer genes. Cell Stem Cell 11:75-90.

Ansorge O, Giunti P, Michalik A, Van Broeckhoven C, Harding B, Wood N, Scaravilli F. 2004. Ataxin-7 aggregation and ubiquitination in infantile SCA7 with 180 CAG repeats. Ann Neurol 56:448-452.

Ardley HC, Scott GB, Rose SA, Tan NGS, Robinson PA. 2004. UCH-L1 aggresome formation in response to proteasome impairment indicates a role in inclusion formation in Parkinson's disease. J Neurochem 90:379-391.

Armstrong L, Tilgner K, Saretzki G, Atkinson SP, Stojkovic M, Moreno R, Przyborski S, Lako M. 2010. Human induced pluripotent stem cell lines show stress defense mechanisms and mitochondrial regulation similar to those of human embryonic stem cells. Stem Cells 28:661-673.

Arrasate M, Mitra S, Schweitzer ES, Segal MR, Finkbeiner S. 2004. Inclusion body formation reduces levels of mutant huntingtin and the risk of neuronal death. Nature 431:805-810.

Atanassov BS, Evrard YA, Multani AS, Zhang Z, Tora L, Devys D, Chang S, Dent SYR. 2009. Gcn5 and SAGA regulate shelterin protein turnover and telomere maintenance. Mol Cell 35:352-364.

Atwal RS, Xia J, Pinchev D, Taylor J, Epand RM, Truant R. 2007. Huntingtin has a membrane association signal that can modulate huntingtin aggregation, nuclear entry and toxicity. Hum Mol Genet 16:2600-2615.

Bai X, Wong-Riley MTT. 2003. Neuronal activity regulates protein and gene expressions of GluR2 in postnatal rat visual cortical neurons in culture. J Neurocytol 32:71-78.

Balasubramanian R, Pray-Grant MG, Selleck W, Grant PA, Tan S. 2002. Role of the Ada2 and Ada3 transcriptional coactivators in histone acetylation. J Biol Chem 277:7989-7995.

Bang O, Lee P, Kim S, Kim H, Huh K. 2004. Pontine atrophy precedes cerebellar degeneration in spinocerebellar ataxia 7: MRI-based volumetric analysis. J Neurol Neurosurg Psychiatry 75:1452-1456.

Barrachina M, Castaño E, Dalfó E, Maes T, Buesa C, Ferrer I. 2006. Reduced ubiquitin C-terminal hydrolase-1 expression levels in dementia with Lewy bodies. Neurobiol Dis 22:265-273.

Bauer M, Kinkl N, Meixner A, Kremmer E, Riemenschneider M, Förstl H, Gasser T, Ueffing M. 2008. Prevention of interferon-stimulated gene expression using microRNA-designed hairpins. Gene Ther 16:142-147.

Bauer PO, Nukina N. 2009. The pathogenic mechanisms of polyglutamine diseases and current therapeutic strategies. J Neurochem 110:1737-1765.

Bence NF, Sampat RM, Kopito RR. 2001. Impairment of the ubiquitin-proteasome system by protein aggregation. Science 292:1552-1555.

Ben-Hur T, Idelson M, Khaner H, Pera M, Reinhartz E, Itzik A, Reubinoff BE. 2004. Transplantation of human embryonic stem cell–derived neural progenitors improves behavioral deficit in parkinsonian rats. Stem Cells 22:1246-1255.

Bennett EJ, Bence NF, Jayakumar R, Kopito RR. 2005. Global impairment of the ubiquitin-proteasome system by nuclear or cytoplasmic protein aggregates precedes inclusion body formation. Mol Cell 17:351-365.

Benomar A, Krols L, Stevanin G, Cancel G, LeGuern E, David G, Ouhabi H, Martin JJ, Dürr A, Zaim A. 1995. The gene for autosomal dominant cerebellar ataxia with pigmentary macular dystrophy maps to chromosome 3p12−p21. 1. Nat Genet 10:84-88.

Bergen DC, Silberberg D. 2002. Nervous system disorders: A global epidemic. Arch Neurol 59:1194-1196.

Bichelmeier U, Schmidt T, Hübener J, Boy J, Rüttiger L, Häbig K, Poths S, Bonin M, Knipper M, Schmidt WJ. 2007. Nuclear localization of ataxin-3 is required for the manifestation of symptoms in SCA3: In vivo evidence. J Neurosci 27:7418-7428.

Bilen J, Bonini NM. 2005. Drosophila as a model for human neurodegenerative disease. Annu Rev Genet 39:153-171.

Bilen J, Bonini NM. 2007. Genome-wide screen for modifiers of ataxin-3 neurodegeneration in Drosophila. PLoS Genet 3:e177.

Bilen J, Liu N, Bonini NM. 2006. A new role for microRNA pathways: Modulation of degeneration induced by pathogenic human disease proteins. Cell Cycle 5:2835-2838.

Bilican B, Serio A, Barmada SJ, Nishimura AL, Sullivan GJ, Carrasco M, Phatnani HP, Puddifoot CA, Story D, Fletcher J. 2012. Mutant induced pluripotent stem cell lines recapitulate aspects of TDP-43 proteinopathies and reveal cell-specific vulnerability. Proc Natl Acad Sci USA 109:5803-5808.

Borchelt DR, Davis J, Fischer M, Lee MK, Slunt HH, Ratovitsky T, Regard J, Copeland NG, Jenkins NA, Sisodia SS. 1996. A vector for expressing foreign genes in the brains and hearts of transgenic mice. Genet Anal: Biomol Eng 13:159-163.

Botchkarev VA. 2003. Molecular mechanisms of chemotherapy-induced hair loss. J Invest Derm Symp P 8:72-75.

Boudreau RL, Martins I, Davidson BL. 2008b. Artificial microRNAs as siRNA shuttles: Improved safety as compared to shRNAs in vitro and in vivo. Mol Ther 17:169-175.

Boudreau RL, McBride JL, Martins I, Shen S, Xing Y, Carter BJ, Davidson BL. 2009. Nonallele-specific silencing of mutant and wild-type huntingtin demonstrates therapeutic efficacy in Huntington's disease mice. Mol Ther 17:1053-1063.

Boudreau RL, Monteys AM, Davidson BL. 2008a. Minimizing variables among hairpin-based RNAi vectors reveals the potency of shRNAs. RNA 14:1834-1844.

Boulting GL, Kiskinis E, Croft GF, Amoroso MW, Oakley DH, Wainger BJ, Williams DJ, Kahler DJ, Yamaki M, Davidow L. 2011. A functionally characterized test set of human induced pluripotent stem cells. Nat Biotechnol 29:279-286.

Bowman AB, Yoo SY, Dantuma NP, Zoghbi HY. 2005. Neuronal dysfunction in a polyglutamine disease model occurs in the absence of ubiquitin-proteasome system impairment and inversely correlates with the degree of nuclear inclusion formation. Hum Mol Genet 14:679-691.

Boy J, Schmidt T, Wolburg H, Mack A, Nuber S, Böttcher M, Schmitt I, Holzmann C, Zimmermann F, Servadio A. 2009. Reversibility of symptoms in a conditional mouse model of spinocerebellar ataxia type 3. Hum Mol Genet 18:4282-4295.

Boyer LA, Lee TI, Cole MF, Johnstone SE, Levine SS, Zucker JP, Guenther MG, Kumar RM, Murray HL, Jenner RG. 2005. Core transcriptional regulatory circuitry in human embryonic stem cells. Cell 122:947-956.

Brignull HR, Morley JF, Garcia SM, Morimoto RI. 2006. Modeling polyglutamine pathogenesis in *C. elegans*. Meth Enzymol 412:256-282.

Bryer A, Krause A, Bill P, Davids V, Bryant D, Butler J, Heckmann J, Ramesar R, Greenberg J. 2003. The hereditary adult-onset ataxias in South Africa. J Neurol Sci 216:47-54.

Bu P, Evrard YA, Lozano G, Dent SYR. 2007. Loss of Gcn5 acetyltransferase activity leads to neural tube closure defects and exencephaly in mouse embryos. Mol Cell Biol 27:3405-3416.

Burright EN, Brent Clark H, Servadio A, Matilla T, Feddersen RM, Yunis WS, Duvick LA, Zoghbi HY, Orr HT. 1995. SCA1 transgenic mice: A model for neurodegeneration caused by an expanded CAG trinucleotide repeat. Cell 82:937-948.

Bustin SA, Benes V, Garson JA, Hellemans J, Huggett J, Kubista M, Mueller R, Nolan T, Pfaffl MW, Shipley GL. 2009. The MIQE guidelines: Minimum information for publication of quantitative real-time PCR experiments. Clin Chem 55:611-622.

Byers B, Cord B, Nguyen HN, Schüle B, Fenno L, Lee PC, Deisseroth K, Langston JW, Pera RR, Palmer TD. 2011. SNCA triplication Parkinson's patient's iPSC-derived DA neurons accumulate α-synuclein and are susceptible to oxidative stress. PloS One 6:e26159.

Camnasio S, Carri AD, Lombardo A, Grad I, Mariotti C, Castucci A, Rozell B, Riso PL, Castiglioni V, Zuccato C. 2012. The first reported generation of several induced pluripotent stem cell lines from homozygous and heterozygous Huntington's disease patients demonstrates mutation related enhanced lysosomal activity. Neurobiol Dis 46:41-51.

Cancel G, Duyckaerts C, Holmberg M, Zander C, Yvert G, Lebre AS, Ruberg M, Faucheux B, Agid Y, Hirsch E. 2000. Distribution of ataxin-7 in normal human brain and retina. Brain 123:2519-2530.

Cannella M, Maglione V, Martino T, Ragona G, Frati L, Li GM, Squitieri F. 2009. DNA instability in replicating Huntington's disease lymphoblasts. BMC Med Genet 10:11.

Carlson KM, Andresen JM, Orr HT. 2009. Emerging pathogenic pathways in the spinocerebellar ataxias. Curr Opin Genet Dev 19:247-253.

Castanotto D, Rossi JJ. 2009. The promises and pitfalls of RNA-interference-based therapeutics. Nature 457:426-433.

Castegna A, Aksenov M, Thongboonkerd V, Klein JB, Pierce WM, Booze R, Markesbery WR, Butterfield DA. 2002. Proteomic identification of oxidatively modified proteins in Alzheimer's disease brain. Part II: Dihydropyrimidinase-related protein 2, α-enolase and heat shock cognate 71. J Neurochem 82:1524-1532.

Cattaneo E, Rigamonti D, Goffredo D, Zuccato C, Squitieri F, Sipione S. 2001. Loss of normal huntingtin function: New developments in Huntington's disease research. Trends Neurosci 24:182-188.

Cemal CK, Carroll CJ, Lawrence L, Lowrie MB, Ruddle P, Al-Mahdawi S, King RHM, Pook MA, Huxley C, Chamberlain S. 2002. YAC transgenic mice carrying pathological alleles of the MJD1 locus exhibit a mild and slowly progressive cerebellar deficit. Hum Mol Genet 11:1075-1094.

Chai Y, Koppenhafer SL, Bonini NM, Paulson HL. 1999a. Analysis of the role of heat shock protein (hsp) molecular chaperones in polyglutamine disease. J Neurosci 19:10338-10347.

Chai Y, Koppenhafer SL, Shoesmith SJ, Perez MK, Paulson HL. 1999b. Evidence for proteasome involvement in polyglutamine disease: Localization to nuclear inclusions in SCA3/MJD and suppression of polyglutamine aggregation in vitro. Hum Mol Genet 8:673-682.

Chambers SM, Fasano CA, Papapetrou EP, Tomishima M, Sadelain M, Studer L. 2009. Highly efficient neural conversion of human ES and iPS cells by dual inhibition of SMAD signaling. Nat Biotechnol 27:275-280.

Chan HYE, Warrick JM, Andriola I, Merry D, Bonini NM. 2002. Genetic modulation of polyglutamine toxicity by protein conjugation pathways in Drosophila. Hum Mol Genet 11:2895-2904.

Chan HYE, Warrick JM, Gray-Board GL, Paulson HL, Bonini NM. 2000. Mechanisms of chaperone suppression of polyglutamine disease: Selectivity, synergy and modulation of protein solubility in Drosophila. Hum Mol Genet 9:2811-2820.

Chatterjee P, Cheung Y, Liew C. 2011. Transfecting and nucleofecting human induced pluripotent stem cells. JoVE 56:e3110.

Chen S, Peng GH, Wang X, Smith AC, Grote SK, Sopher BL, La Spada AR. 2004. Interference of CRX-dependent transcription by ataxin-7 involves interaction between the glutamine regions and requires the ataxin-7 carboxy-terminal region for nuclear localization. Hum Mol Genet 13:53-67.

Chen YC, Gatchel JR, Lewis RW, Mao CA, Grant PA, Zoghbi HY, Dent SYR. 2012. Gcn5 loss-of-function accelerates cerebellar and retinal degeneration in a SCA7 mouse model. Hum Mol Genet 21:394-405.

Chin MH, Mason MJ, Xie W, Volinia S, Singer M, Peterson C, Ambartsumyan G, Aimiuwu O, Richter L, Zhang J. 2009. Induced pluripotent stem cells and embryonic stem cells are distinguished by gene expression signatures. Cell Stem Cell 5:111-123.

Choi J, Levey AI, Weintraub ST, Rees HD, Gearing M, Chin LS, Li L. 2004. Oxidative modifications and down-regulation of ubiquitin carboxyl-terminal hydrolase L1 associated with idiopathic Parkinson's and Alzheimer's diseases. J Biol Chem 279:13256-13264.

Chou AH, Chen CY, Chen SY, Chen WJ, Chen YL, Weng YS, Wang HL. 2010. Polyglutamine-expanded ataxin-7 causes cerebellar dysfunction by inducing transcriptional dysregulation. Neurochem Int 56:329-339.

Chou AH, Yeh TH, Ouyang P, Chen YL, Chen SY, Wang HL. 2008. Polyglutamine-expanded ataxin-3 causes cerebellar dysfunction of SCA3 transgenic mice by inducing transcriptional dysregulation. Neurobiol Dis 31:89-101.

Courtney E, Kornfeld S, Janitz K, Janitz M. 2010. Transcriptome profiling in neurodegenerative disease. J Neurosci Methods 193:189-202.

Cozzolino M, Ferri A, Teresa Carri M. 2008. Amyotrophic lateral sclerosis: From current developments in the laboratory to clinical implications. Antioxid Redox Signal 10:405-444.

Crooke ST. 2004. Progress in antisense technology. Annu Rev Med 55:61-95.

Cummings CJ, Mancini MA, Antalffy B, DeFranco DB, Orr HT, Zoghbi HY. 1998a. Chaperone suppression of aggregation and altered subcellular proteasome localization imply protein misfolding in SCA1. Nat Genet 19:148-154.

Custer SK, Garden GA, Gill N, Rueb U, Libby RT, Schultz C, Guyenet SJ, Deller T, Westrum LE, Sopher BL. 2006. Bergmann glia expression of polyglutamine-expanded ataxin-7 produces neurodegeneration by impairing glutamate transport. Nat Neurosci 9:1302-1311.

David G, Abbas N, Stevanin G, Dürr A, Yvert G, Cancel G, Weber C, Imbert G, Saudou F, Antoniou E. 1997. Cloning of the SCA7 gene reveals a highly unstable CAG repeat expansion. Nat Genet 17:65-70.

David G, Dürr A, Stevanin G, Cancel G, Abbas N, Benomar A, Belal S, Lebre AS, Abada-Bendib M, Grid D. 1998. Molecular and clinical correlations in autosomal dominant cerebellar ataxia with progressive macular dystrophy (SCA7). Hum Mol Genet 7:165-170.

David G, Giunti P, Abbas N, Coullin P, Stevanin G, Horta W, Gemmill R, Weissenbach J, Wood N, Cunha S. 1996. The gene for autosomal dominant cerebellar ataxia type II is located in a 5-cM region in 3p12-p13: Genetic and physical mapping of the SCA7 locus. Am J Hum Genet 59:1328-1336.

Davies J, Sarkar S, Rubinsztein D. 2007. The ubiquitin proteasome system in Huntington's disease and the spinocerebellar ataxias. BMC Biochemistry 8:S2.

Davies JE, Sarkar S, Rubinsztein DC. 2006. Trehalose reduces aggregate formation and delays pathology in a transgenic mouse model of oculopharyngeal muscular dystrophy. Hum Mol Genet 15:23-31.

De Mezer M, Wojciechowska M, Napierala M, Sobczak K, Krzyzosiak WJ. 2011. Mutant CAG repeats of huntingtin transcript fold into hairpins, form nuclear foci and are targets for RNA interference. Nucleic Acids Res 39:3852-63.

De Pril R, Fischer DF, Maat-Schieman MLC, Hobo B, de Vos RAI, Brunt ER, Hol EM, Roos RAC, van Leeuwen FW. 2004. Accumulation of aberrant ubiquitin induces aggregate formation and cell death in polyglutamine diseases. Hum Mol Genet 13:1803-1813.

De Rooij KE, Dorsman JC, Smoor MA, Den Dunnen JT, Van Ommen GJB. 1996. Subcellular localization of the Huntington's disease gene product in cell lines by immunofluorescence and biochemical subcellular fractionation. Hum Mol Genet 5:1093-1099.

De Villiers C, Weskamp K, Bryer A. 1997. The sword of Damocles: The psychosocial impact of familial spinocerebellar ataxia in South Africa. Am J Med Genet 74:270-274.

Del-Favero J, Krols L, Michalik A, Theuns J, Löfgren A, Goossens D, Wehnert A, Van den Bossche D, Van Zand K, Backhovens H. 1998. Molecular genetic analysis of autosomal dominant cerebellar ataxia with retinal degeneration (ADCA type II) caused by CAG triplet repeat expansion. Hum Mol Genet 7:177-186.

Denovan-Wright EM, Rodriguez-Lebron E, Lewin AS, Mandel RJ. 2008. Unexpected off-targeting effects of anti-huntingtin ribozymes and siRNA in vivo. Neurobiol Dis 29:446-455.

DiFiglia M, Sapp E, Chase KO, Davies SW, Bates GP, Vonsattel J, Aronin N. 1997. Aggregation of huntingtin in neuronal intranuclear inclusions and dystrophic neurites in brain. Science 277:1990-1993.

Dimos JT, Rodolfa KT, Niakan KK, Weisenthal LM, Mitsumoto H, Chung W, Croft GF, Saphier G, Leibel R, Goland R. 2008. Induced pluripotent stem cells generated from patients with ALS can be differentiated into motor neurons. Science 321:1218-1221.

Dorschner MO, Barden D, Stephens K. 2002. Diagnosis of five spinocerebellar ataxia disorders by multiplex amplification and capillary electrophoresis. J Mol Diagn 4:108-113.

Dottori M, Pera MF. 2008. Neural differentiation of human embryonic stem cells. Methods Mol Biol 438:19-30.

Dragatsis I, Levine MS, Zeitlin S. 2000. Inactivation of hdh in the brain and testis results in progressive neurodegeneration and sterility in mice. Nat Genet 26:300-306.

Dragileva E, Hendricks A, Teed A, Gillis T, Lopez ET, Friedberg EC, Kucherlapati R, Edelmann W, Lunetta KL, MacDonald ME. 2009. Intergenerational and striatal CAG repeat instability in Huntington's disease knock-in mice involve different DNA repair genes. Neurobiol Dis 33:37-47.

Dravid G, Ye Z, Hammond H, Chen G, Pyle A, Donovan P, Yu X, Cheng L. 2005. Defining the role of Wnt/β-Catenin signaling in the survival, proliferation, and self-renewal of human embryonic stem cells. Stem Cells 23:1489-1501.

Drews K, Jozefczuk J, Prigione A, Adjaye J. 2012. Human induced pluripotent stem cells—from mechanisms to clinical applications. J Mol Med 90:735-745.

Duenas AM, Goold R, Giunti P. 2006. Molecular pathogenesis of spinocerebellar ataxias. Brain 129:1357-1370.

Dunah AW, Jeong H, Griffin A, Kim YM, Standaert DG, Hersch SM, Mouradian MM, Young AB, Tanese N, Krainc D. 2002. Sp1 and TAFII130 transcriptional activity disrupted in early Huntington's disease. Science 296:2238-2243.

Duncan C, Papanikolaou T, Ellerby LM. 2010. Autophagy: PolyQ toxic fragment turnover. Autophagy 6:312-314.

Durr A. 2010. Autosomal dominant cerebellar ataxias: Polyglutamine expansions and beyond. Lancet Neurol 9:885-894.

Eastham AM, Spencer H, Soncin F, Ritson S, Merry CLR, Stern PL, Ward CM. 2007. Epithelial-mesenchymal transition events during human embryonic stem cell differentiation. Cancer Res 67:11254-11262.

Ebert AD, Yu J, Rose FF, Mattis VB, Lorson CL, Thomson JA, Svendsen CN. 2008. Induced pluripotent stem cells from a spinal muscular atrophy patient. Nature 457:277-280.

Einum DD, Townsend JJ, Ptcek LJ, Fu YH. 2001. Ataxin-7 expression analysis in controls and spinocerebellar ataxia type 7 patients. Neurogenetics 3:83-90.

Ellis J, Bruneau BG, Keller G, Lemischka IR, Nagy A, Rossant J, Srivastava D, Zandstra PW, Stanford WL. 2009. Alternative iPSC characterization criteria for in vitro applications. Cell Stem Cell 4:198-199.

Eminli S, Utikal J, Arnold K, Jaenisch R, Hochedlinger K. 2008. Reprogramming of neural progenitor cells into induced pluripotent stem cells in the absence of exogenous Sox2 expression. Stem Cells 26:2467-2474.

Erceg S, Lukovic D, Moreno-Manzano V, Stojkovic M, Bhattacharya SS. 2012. Derivation of cerebellar neurons from human pluripotent stem cells. Curr Protoc Stem Cell Biol 1H.5.1-1H.5.10.

Esteban MA, Wang T, Qin B, Yang J, Qin D, Cai J, Li W, Weng Z, Chen J, Ni S. 2010. Vitamin C enhances the generation of mouse and human induced pluripotent stem cells. Cell Stem Cell 6:71-79.

Fakunle ES. 2012. iPSCs for personalized medicine: What will it take for Africa? Trends Mol Med (in press).

Fallini C, Bassell GJ, Rossoll W. 2010. High-efficiency transfection of cultured primary motor neurons to study protein localization, trafficking, and function. Mol Neurodegener 5:17.

Fernandez-Funez P, Nino-Rosales ML, de Gouyon B, She WC, Luchak JM, Martinez P, Turiegano E, Benito J, Capovilla M, Skinner PJ. 2000. Identification of genes that modify ataxin-1-induced neurodegeneration. Nature 408:101-106.

Feyeux M, Bourgois-Rocha F, Redfern A, Giles P, Lefort N, Aubert S, Bonnefond C, Bugi A, Ruiz M, Deglon N. 2012. Early transcriptional changes linked to naturally occurring Huntington's disease mutations in neural derivatives of human embryonic stem cells. Hum Mol Genet 21:3883-95.

Fischer M, Rülicke T, Raeber A, Sailer A, Moser M, Oesch B, Brandner S, Aguzzi A, Weissmann C. 1996. Prion protein (PrP) with amino-proximal deletions restoring susceptibility of PrP knockout mice to scrapie. EMBO J 15:1255-1264.

Fiszer A, Mykowska A, Krzyzosiak WJ. 2011. Inhibition of mutant huntingtin expression by RNA duplex targeting expanded CAG repeats. Nucleic Acids Res 39:5578-5585.

Francastel C, Schübeler D, Martin DIK, Groudine M. 2000. Nuclear compartmentalization and gene activity. Nat Rev Mol Cell Biol 1:137-143.

Freshney RI. 2010. Culture of animal cells: A manual of basic technique and specialized applications. Wiley-Blackwell.

Gagnon KT, Pendergraff HM, Deleavey GF, Swayze EE, Potier P, Randolph J, Roesch EB, Chattopadhyaya J, Damha MJ, Bennett CF. 2010. Allele-selective inhibition of mutant huntingtin expression with antisense oligonucleotides targeting the expanded CAG repeat. Biochemistry 49:10166-78.

García-Mata R, Bebök Z, Sorscher EJ, Sztul ES. 1999. Characterization and dynamics of aggresome formation by a cytosolic GFP-chimera. J Cell Biol 146:1239-1254.

Garden GA, La Spada AR. 2012. Intercellular (mis) communication in neurodegenerative disease. Neuron 73:886-901.

Garden GA, La Spada AR. 2008. Molecular pathogenesis and cellular pathology of spinocerebellar ataxia type 7 neurodegeneration. Cerebellum 7:138-49.

Garden GA, Libby RT, Fu YH, Kinoshita Y, Huang J, Possin DE, Smith AC, Martinez RA, Fine GC, Grote SK. 2002. Polyglutamine-expanded ataxin-7 promotes non-cell-autonomous Purkinje cell degeneration and displays proteolytic cleavage in ataxic transgenic mice. J Neurosci 22:4897-4905.

Gaspar C, Lopes-Cendes I, DeStefano AL, Maciel P, Silveira I, Coutinho P, MacLeod P, Sequeiros J, Farrer LA, Rouleau GA. 1996. Linkage disequilibrium analysis in Machado-Joseph disease patients of different ethnic origins. Hum Genet 98:620-624.

Gatchel JR, Watase K, Thaller C, Carson JP, Jafar-Nejad P, Shaw C, Zu T, Orr HT, Zoghbi HY. 2008. The insulin-like growth factor pathway is altered in spinocerebellar ataxia type 1 and type 7. Proc Natl Acad Sci USA 105:1291-1296.

Gatchel JR, Zoghbi HY. 2005. Diseases of unstable repeat expansion: Mechanisms and common principles. Nat Rev Genet 6:743-755.

Gerrard L, Rodgers L, Cui W. 2005. Differentiation of human embryonic stem cells to neural lineages in adherent culture by blocking bone morphogenetic protein signaling. Stem Cells 23:1234-1241.

Giuliano P, De Cristofaro T, Affaitati A, Pizzulo GM, Feliciello A, Criscuolo C, De Michele G, Filla A, Avvedimento EV, Varrone S. 2003. DNA damage induced by polyglutamine-expanded proteins. Hum Mol Genet 12:2301-2309.

Globas C, du Montcel ST, Baliko L, Boesch S, Depondt C, DiDonato S, Durr A, Filla A, Klockgether T, Mariotti C. 2008. Early symptoms in spinocerebellar ataxia type 1, 2, 3, and 6. Mov Disord 23:2232-2238.

Gong B, Cao Z, Zheng P, Vitolo OV, Liu S, Staniszewski A, Moolman D, Zhang H, Shelanski M, Arancio O. 2006. Ubiquitin hydrolase UCH-L1 rescues β-amyloid-induced decreases in synaptic function and contextual memory. Cell 126:775-788.

Gonitel R, Moffitt H, Sathasivam K, Woodman B, Detloff PJ, Faull RLM, Bates GP. 2008. DNA instability in postmitotic neurons. Proc Natl Acad Sci USA 105:3467-3472.

González F, Boué S, Belmonte JCI. 2011. Methods for making induced pluripotent stem cells: Reprogramming a la carte. Nat Rev Genet 12:231-242.

Gonzalez-Alegre P, Miller VM, Davidson BL, Paulson HL. 2003. Toward therapy for DYT1 dystonia: Allele-specific silencing of mutant TorsinA. Ann Neurol 53:781-787.

Gore A, Li Z, Fung HL, Young JE, Agarwal S, Antosiewicz-Bourget J, Canto I, Giorgetti A, Israel MA, Kiskinis E. 2011. Somatic coding mutations in human induced pluripotent stem cells. Nature 471:63-67.

Goti D, Katzen SM, Mez J, Kurtis N, Kiluk J, Ben-Haiem L, Jenkins NA, Copeland NG, Kakizuka A, Sharp AH. 2004. A mutant ataxin-3 putative-cleavage fragment in brains of Machado-Joseph disease patients and transgenic mice is cytotoxic above a critical concentration. J Neurosci 24:10266-10279.

Gouw L, Digre K, Harris C, Haines J, Ptacek L. 1994. Autosomal dominant cerebellar ataxia with retinal degeneration. Neurology 44:1441-1447.

Grant PA, Duggan L, Côté J, Roberts SM, Brownell JE, Candau R, Ohba R, Owen-Hughes T, Allis CD, Winston F. 1997. Yeast Gcn5 functions in two multisubunit complexes to acetylate nucleosomal histones: Characterization of an Ada complex and the SAGA (Spt/Ada) complex. Genes Dev 11:1640-1650.

Grant PA, Eberharter A, John S, Cook RG, Turner BM, Workman JL. 1999. Expanded lysine acetylation specificity of Gcn5 in native complexes. J Biol Chem 274:5895-5900.

Grant PA, Schieltz D, Pray-Grant MG, Steger DJ, Reese JC, Yates JR, Workman JL. 1998. A subset of TAFIIs are integral components of the SAGA complex required for nucleosome acetylation and transcriptional stimulation. Cell 94:45-53.

Greenberg J, Solomon G, Vorster A, Heckmann J, Bryer A. 2006. Origin of the SCA7 gene mutation in South Africa: Implications for molecular diagnostics. Clin Genet 70:415-417.

Grimm D, Streetz KL, Jopling CL, Storm TA, Pandey K, Davis CR, Marion P, Salazar F, Kay MA. 2006. Fatality in mice due to oversaturation of cellular microRNA/short hairpin RNA pathways. Nature 441:537-541.

Gurdon JB. 1962. The developmental capacity of nuclei taken from intestinal epithelium cells of feeding tadpoles. J Embryol Exp Morphol 10:622-640.

Haase A, Olmer R, Schwanke K, Wunderlich S, Merkert S, Hess C, Zweigerdt R, Gruh I, Meyer J, Wagner S. 2009. Generation of induced pluripotent stem cells from human cord blood. Cell Stem Cell 5:434-441.

Häausser M, Roth A. 1997. Dendritic and somatic glutamate receptor channels in rat cerebellar Purkinje cells. J Physiol (Lond) 501:77-95.

Hall TA. 1999. BioEdit: A user-friendly biological sequence alignment editor and analysis program for Windows 95/98/NT. Nucleic Acids Symp Ser (Oxf) 41:95-98.

Hanna J, Wernig M, Markoulaki S, Sun CW, Meissner A, Cassady JP, Beard C, Brambrink T, Wu LC, Townes TM. 2007. Treatment of sickle cell anemia mouse model with iPS cells generated from autologous skin. Science 318:1920-1923.

Hara T, Nakamura K, Matsui M, Yamamoto A, Nakahara Y, Suzuki-Migishima R, Yokoyama M, Mishima K, Saito I, Okano H. 2006. Suppression of basal autophagy in neural cells causes neurodegenerative disease in mice. Nature 441:885-889.

Harper SQ, Staber PD, He X, Eliason SL, Martins IH, Mao Q, Yang L, Kotin RM, Paulson HL, Davidson BL. 2005. RNA interference improves motor and neuropathological abnormalities in a Huntington's disease mouse model. Proc Natl Acad Sci USA 102:5820-5825.

Hartl FU, Bracher A, Hayer-Hartl M. 2011. Molecular chaperones in protein folding and proteostasis. Nature 475:324-332.

Hay DG, Sathasivam K, Tobaben S, Stahl B, Marber M, Mestril R, Mahal A, Smith DL, Woodman B, Bates GP. 2004. Progressive decrease in chaperone protein levels in a mouse model of Huntington's disease and induction of stress proteins as a therapeutic approach. Hum Mol Genet 13:1389-1405.

The HD iPSC Consortium. 2012. Induced pluripotent stem cells from patients with Huntington's disease show CAG repeat-expansion-associated phenotypes. Cell Stem Cell 11:264–278.

Helmlinger D, Abou-Sleymane G, Yvert G, Rousseau S, Weber C, Trottier Y, Mandel JL, Devys D. 2004b. Disease progression despite early loss of polyglutamine protein expression in SCA7 mouse model. J Neurosci 24:1881-1887.

Helmlinger D, Bonnet J, Mandel JL, Trottier Y, Devys D. 2004c. Hsp70 and Hsp40 chaperones do not modulate retinal phenotype in SCA7 mice. J Biol Chem 279:55969-55977.

Helmlinger D, Hardy S, Abou-Sleymane G, Eberlin A, Bowman AB, Gansmüller A, Picaud S, Zoghbi HY, Trottier Y, Tora L. 2006a. Glutamine-expanded ataxin-7 alters TFTC/STAGA recruitment and chromatin structure leading to photoreceptor dysfunction. PLoS Biol 4:e67

Helmlinger D, Hardy S, Eberlin A, Devys D, Tora L. 2006c. Both normal and polyglutamine-expanded ataxin-7 are components of TFTC-type GCN5 histone acetyltransferase-containing complexes. Biochem Soc Symp 73:155-163.

Helmlinger D, Hardy S, Sasorith S, Klein F, Robert F, Weber C, Miguet L, Potier N, Van-Dorsselaer A, Wurtz JM. 2004a. Ataxin-7 is a subunit of GCN5 histone acetyltransferase-containing complexes. Hum Mol Genet 13:1257-1265.

Helmlinger D, Tora L, Devys D. 2006b. Transcriptional alterations and chromatin remodeling in polyglutamine diseases. Trends Genet 22:562-570.

Hioki H, Fujiyama F, Taki K, Tomioka R, Furuta T, Tamamaki N, Kaneko T. 2003. Differential distribution of vesicular glutamate transporters in the rat cerebellar cortex. Neuroscience 117:1-6.

Holmberg M, Duyckaerts C, Dürr A, Cancel G, Gourfinkel-An I, Damier P, Faucheux B, Trottier Y, Hirsch EC, Agid Y. 1998. Spinocerebellar ataxia type 7 (SCA7): A neurodegenerative disorder with neuronal intranuclear inclusions. Hum Mol Genet 7:913-918.

Hong H, Takahashi K, Ichisaka T, Aoi T, Kanagawa O, Nakagawa M, Okita K, Yamanaka S. 2009. Suppression of induced pluripotent stem cell generation by the p53–p21 pathway. Nature 460:1132-1135.

Horton LC, Frosch MP, Vangel MG, Weigel-DiFranco C, Berson EL, Schmahmann JD. 2012. Spinocerebellar ataxia type 7: Clinical course, Phenotype–Genotype correlations, and neuropathology. Cerebellum (Epub ahead of print).

Hotta A, Ellis J. 2008. Retroviral vector silencing during iPS cell induction: An epigenetic beacon that signals distinct pluripotent states. J Cell Biochem 105:940-948.

Hsu SH, Lai MC, Er TK, Yang SN, Hung CH, Tsai HH, Lin YC, Chang JG, Lo YC, Jong YJ. 2010. Ubiquitin carboxyl-terminal hydrolase L1 (UCHL1) regulates the level of SMN expression through ubiquitination in primary spinal muscular atrophy fibroblasts. Clin Chim Acta 411:1920-1928.

Hu BY, Weick JP, Yu J, Ma LX, Zhang XQ, Thomson JA, Zhang SC. 2010b. Neural differentiation of human induced pluripotent stem cells follows developmental principles but with variable potency. Proc Natl Acad Sci USA 107:4335-4340.

Hu J, Gagnon KT, Liu J, Watts JK, Syeda-Nawaz J, Bennett CF, Swayze EE, Randolph J, Chattopadhyaya J, Corey DR. 2011. Allele-selective inhibition of ataxin-3 (ATX3) expression by antisense oligomers and duplex RNAs. Biol Chem 392:315-325.

Hu J, Liu J, Corey DR. 2010a. Allele-selective inhibition of huntingtin expression by switching to an miRNA-like RNAi mechanism. Chem Biol 17:1183-1188.

Hu J, Matsui M, Corey DR. 2009a. Allele-selective inhibition of mutant huntingtin by peptide nucleic acid-peptide conjugates, locked nucleic acid, and small interfering RNA. Ann N Y Acad Sci 1175:24-31.

Hu J, Matsui M, Gagnon KT, Schwartz JC, Gabillet S, Arar K, Wu J, Bezprozvanny I, Corey DR. 2009b. Allele-specific silencing of mutant huntingtin and ataxin-3 genes by targeting expanded CAG repeats in mRNAs. Nat Biotechnol 27:478-484.

Huangfu D, Osafune K, Maehr R, Guo W, Eijkelenboom A, Chen S, Muhlestein W, Melton DA. 2008. Induction of pluripotent stem cells from primary human fibroblasts with only Oct4 and Sox2. Nat Biotechnol 26:1269-1275.

Huen NYM, Wong SLA, Chan HYE. 2007. Transcriptional malfunctioning of heat shock protein gene expression in spinocerebellar ataxias. Cerebellum 6:111-117.

Hugosson T, Gränse L, Ponjavic V, Andréasson S. 2009. Macular dysfunction and morphology in spinocerebellar ataxia type 7 (SCA 7). Ophthalmic Genet 30:1-6.

Hussein SM, Batada NN, Vuoristo S, Ching RW, Autio R, Närvä E, Ng S, Sourour M, Hämäläinen R, Olsson C. 2011. Copy number variation and selection during reprogramming to pluripotency. Nature 471:58-62.

Huynh DP, Yang HT, Vakharia H, Nguyen D, Pulst SM. 2003. Expansion of the polyQ repeat in ataxin-2 alters its Golgi localization, disrupts the Golgi complex and causes cell death. Hum Mol Genet 12:1485-1496.

Ingram MAC, Orr HT, Clark HB. 2011. Genetically engineered mouse models of the trinucleotide-repeat spinocerebellar ataxias. Brain Res Bull 88:33-42.

Inoue H. 2010. Neurodegenerative disease-specific induced pluripotent stem cell research. Exp Cell Res 316:2560-2564.

Israel MA, Yuan SH, Bardy C, Reyna SM, Mu Y, Herrera C, Hefferan MP, Van Gorp S, Nazor KL, Boscolo FS. 2012. Probing sporadic and familial Alzheimer's disease using induced pluripotent stem cells. Nature 482:216-220.

Jähner D, Stuhlmann H, Stewart CL, Harbers K, Löhler J, Simon I, Jaenisch R. 1982. De novo methylation and expression of retroviral genomes during mouse embryogenesis. Nature 298:623-628.

Janer A, Werner A, Takahashi-Fujigasaki J, Daret A, Fujigasaki H, Takada K, Duyckaerts C, Brice A, Dejean A, Sittler A. 2009. SUMOylation attenuates the aggregation propensity and cellular toxicity of the polyglutamine expanded ataxin-7. Hum Mol Genet 19:181-195.

Jensen JB, Lund TM, Timmermann DB, Schousboe A, Pickering DS. 2001. Role of GluR2 expression in AMPA-induced toxicity in cultured murine cerebral cortical neurons. J Neurosci Res 65:267-277.

Jin ZB, Okamoto S, Osakada F, Homma K, Assawachananont J, Hirami Y, Iwata T, Takahashi M. 2011. Modeling retinal degeneration using patient-specific induced pluripotent stem cells. PloS One 6:e17084.

Johansson J, Forsgren L, Sandgren O, Brice A, Holmgren G, Holmberg M. 1998. Expanded CAG repeats in Swedish spinocerebellar ataxia type 7 (SCA7) patients: Effect of CAG repeat length on the clinical manifestation. Hum Mol Genet 7:171-176.

Jonasson J, Ström AL, Hart P, Brännström T, Forsgren L, Holmberg M. 2002. Expression of ataxin-7 in CNS and non-CNS tissue of normal and SCA7 individuals. Acta Neuropathol 104:29-37.

Jones JI, Clemmons DR. 1995. Insulin-like growth factors and their binding proteins: Biological actions. Endocr Rev 16:3-34.

Kashani A, Betancur C, Giros B, Hirsch E, Mestikawy SE. 2007. Altered expression of vesicular glutamate transporters VGLUT1 and VGLUT2 in Parkinson disease. Neurobiol Aging 28:568-578.

Katsuno M, Sang C, Adachi H, Minamiyama M, Waza M, Tanaka F, Doyu M, Sobue G. 2005. Pharmacological induction of heat-shock proteins alleviates polyglutamine-mediated motor neuron disease. Proc Natl Acad Sci USA 102:16801-16806.

Kawasaki H, Mizuseki K, Nishikawa S, Kaneko S, Kuwana Y, Nakanishi S, Nishikawa SI, Sasai Y. 2000. Induction of midbrain dopaminergic neurons from ES cells by stromal cell–derived inducing activity. Neuron 28:31-40.

Kaytor MD, Duvick LA, Skinner PJ, Koob MD, Ranum LPW, Orr HT. 1999. Nuclear localization of the spinocerebellar ataxia type 7 protein, ataxin-7. Hum Mol Genet 8:1657-1664.

Kazantsev A, Preisinger E, Dranovsky A, Goldgaber D, Housman D. 1999. Insoluble detergent-resistant aggregates form between pathological and nonpathological lengths of polyglutamine in mammalian cells. Proc Natl Acad Sci USA 96:11404-11409.

Kegel KB, Kim M, Sapp E, McIntyre C, Castaño JG, Aronin N, DiFiglia M. 2000. Huntingtin expression stimulates endosomal–lysosomal activity, endosome tubulation, and autophagy. J Neurosci 20:7268-7278.

Kelly RDW, Sumer H, McKenzie M, Facucho-Oliveira J, Trounce IA, Verma PJ, St. John JC. 2011. The effects of nuclear reprogramming on mitochondrial DNA replication. Stem Cell Rev (Epub ahead of print).

Kennedy L, Evans E, Chen CM, Craven L, Detloff PJ, Ennis M, Shelbourne PF. 2003. Dramatic tissue-specific mutation length increases are an early molecular event in Huntington disease pathogenesis. Hum Mol Genet 12:3359-3367.

Kim K, Doi A, Wen B, Ng K, Zhao R, Cahan P, Kim J, Aryee M, Ji H, Ehrlich L. 2010. Epigenetic memory in induced pluripotent stem cells. Nature 467:285-290.

Kim DH, Rossi JJ. 2003. Coupling of RNAi-mediated target downregulation with gene replacement. Antisense Nucleic Acid Drug Dev 13:151-155.

Kobayashi Y, Kume A, Li M, Doyu M, Hata M, Ohtsuka K, Sobue G. 2000. Chaperones Hsp70 and Hsp40 suppress aggregate formation and apoptosis in cultured neuronal cells expressing truncated androgen receptor protein with expanded polyglutamine tract. J Biol Chem 275:8772-8778.

Koch P, Breuer P, Peitz M, Jungverdorben J, Kesavan J, Poppe D, Doerr J, Ladewig J, Mertens J, Tüting T. 2011. Excitation-induced ataxin-3 aggregation in neurons from patients with Machado-Joseph disease. Nature 480:543-546.

Koch P, Opitz T, Steinbeck JA, Ladewig J, Brüstle O. 2009. A rosette-type, self-renewing human ES cell-derived neural stem cell with potential for in vitro instruction and synaptic integration. Proc Natl Acad Sci USA 106:3225-3230.

Köhler A, Schneider M, Cabal GG, Nehrbass U. 2008. Yeast ataxin-7 links histone deubiquitination with gene gating and mRNA export. Nat Cell Biol 10:707-715.

Komatsu M, Waguri S, Chiba T, Murata S, Iwata J, Tanida I, Ueno T, Koike M, Uchiyama Y, Kominami E. 2006. Loss of autophagy in the central nervous system causes neurodegeneration in mice. Nature 441:880-884.

Komatsu M, Wang QJ, Holstein GR, Friedrich VL, Iwata J, Kominami E, Chait BT, Tanaka K, Yue Z. 2007. Essential role for autophagy protein Atg7 in the maintenance of axonal homeostasis and the prevention of axonal degeneration. Proc Natl Acad Sci USA 104:14489-14494.

Krause K, Foitzik K. 2006. Biology of the hair follicle: The basics. Semin Cutan Med Surg 25:2-10.

Ku S, Soragni E, Campau E, Thomas EA, Altun G, Laurent LC, Loring JF, Napierala M, Gottesfeld JM. 2010. Friedreich's ataxia induced pluripotent stem cells model intergenerational GAA·TTC triplet repeat instability. Cell Stem Cell 7:631-637.

Kubodera T, Yamada H, Anzai M, Ohira S, Yokota S, Hirai Y, Mochizuki H, Shimada T, Mitani T, Mizusawa H. 2010. In vivo application of an RNAi strategy for the selective suppression of a mutant allele. Hum Gene Ther 22:27-34.

Kubodera T, Yokota T, Ishikawa K, Mizusawa H. 2005. New RNAi strategy for selective suppression of a mutant allele in polyglutamine disease. Oligonucleotides 15:298-302.

Kurihara LJ, Kikuchi T, Wada K, Tilghman SM. 2001. Loss of UCH-L1 and UCH-L3 leads to neurodegeneration, posterior paralysis and dysphagia. Hum Mol Genet 10:1963-1970.

La Spada AR, Fu YH, Sopher BL, Libby RT, Wang X, Li LY, Einum DD, Huang J, Possin DE, Smith AC. 2001. Polyglutamine-expanded ataxin-7 antagonizes CRX function and induces cone-rod dystrophy in a mouse model of SCA7. Neuron 31:913-927.

La Spada AR, Taylor JP. 2010. Repeat expansion disease: Progress and puzzles in disease pathogenesis. Nat Rev Genet 11:247-258.

Labbadia J, Cunliffe H, Weiss A, Katsyuba E, Sathasivam K, Seredenina T, Woodman B, Moussaoui S, Frentzel S, Luthi-Carter R. 2011. Altered chromatin architecture underlies progressive impairment of the heat shock response in mouse models of Huntington disease. J Clin Invest 121:3306-3319.

Landles C, Bates GP. 2004. Huntingtin and the molecular pathogenesis of Huntington's disease. EMBO Rep 5:958-963.

Landwehrmeyer GB, Dubois B, de Yébenes JG, Kremer B, Gaus W, Kraus PH, Przuntek H, Dib M, Doble A, Fischer W. 2007. Riluzole in Huntington's disease: A 3-year, randomized controlled study. Ann Neurol 62:262-272.

Latouche M, Lasbleiz C, Martin E, Monnier V, Debeir T, Mouatt-Prigent A, Muriel MP, Morel L, Ruberg M, Brice A. 2007. A conditional pan-neuronal Drosophila model of spinocerebellar ataxia 7 with a reversible adult phenotype suitable for identifying modifier genes. J Neurosci 27:2483-2492.

Laurent LC, Ulitsky I, Slavin I, Tran H, Schork A, Morey R, Lynch C, Harness JV, Lee S, Barrero MJ. 2011. Dynamic changes in the copy number of pluripotency and cell proliferation genes in human ESCs and iPSCs during reprogramming and time in culture. Cell Stem Cell 8:106-118.

Lebre AS, Brice A. 2003. Spinocerebellar ataxia 7 (SCA7). Cytogenet Genome Res 100:154-163.

Lebre AS, Jamot L, Takahashi J, Spassky N, Leprince C, Ravise N, Zander C, Fujigasaki H, Kussel-Andermann P, Duyckaerts C. 2001. Ataxin-7 interacts with a Cbl-associated protein that it recruits into neuronal intranuclear inclusions. Hum Mol Genet 10:1201-1213.

Li C, Zhou J, Shi G, Ma Y, Yang Y, Gu J, Yu H, Jin S, Wei Z, Chen F. 2009. Pluripotency can be rapidly and efficiently induced in human amniotic fluid-derived cells. Hum Mol Genet 18:4340-4349.

Li R, Liang J, Ni S, Zhou T, Qing X, Li H, He W, Chen J, Li F, Zhuang Q. 2010. A mesenchymal-to-epithelial transition initiates and is required for the nuclear reprogramming of mouse fibroblasts. Cell Stem Cell 7:51-63.

Li SH, Li XJ. 2004. Huntingtin-protein interactions and the pathogenesis of Huntington's disease. Trends Genet 20:146-154.

Li Y, Yokota T, Matsumura R, Taira K, Mizusawa H. 2004. Sequence-dependent and independent inhibition specific for mutant ataxin-3 by small interfering RNA. Ann Neurol 56:124-129.

Liao J, Wu Z, Wang Y, Cheng L, Cui C, Gao Y, Chen T, Rao L, Chen S, Jia N. 2008. Enhanced efficiency of generating induced pluripotent stem (iPS) cells from human somatic cells by a combination of six transcription factors. Cell Res 18:600-603.

Libby RT, Hagerman KA, Pineda VV, Lau R, Cho DH, Baccam SL, Axford MM, Cleary JD, Moore JM, Sopher BL. 2008. CTCF cis-regulates trinucleotide repeat instability in an epigenetic manner: A novel basis for mutational hot spot determination. PLoS Genetics 4:e1000257.

Libby RT, Monckton DG, Fu YH, Martinez RA, McAbney JP, Lau R, Einum DD, Nichol K, Ware CB, Ptacek LJ. 2003. Genomic context drives SCA7 CAG repeat instability, while expressed SCA7 cDNAs are intergenerationally and somatically stable in transgenic mice. Hum Mol Genet 12:41-50.

Lin T, Ambasudhan R, Yuan X, Li W, Hilcove S, Abujarour R, Lin X, Hahm HS, Hao E, Hayek A. 2009. A chemical platform for improved induction of human iPSCs. Nat Methods 6:805-808.

Lin W, Zhang Z, Srajer G, Chen YC, Huang M, Phan HM, Dent SYR. 2008. Proper expression of the Gcn5 histone acetyltransferase is required for neural tube closure in mouse embryos. Dev Dyn 237:928-940.

Lin X, Antalffy B, Kang D, Orr HT, Zoghbi HY. 2000. Polyglutamine expansion down-regulates specific neuronal genes before pathologic changes in SCA1. Nat Neurosci 3:157-163.

Lindblad K, Savontaus ML, Stevanin G, Holmberg M, Digre K, Zander C, Ehrsson H, David G, Benomar A, Nikoskelainen E. 1996. An expanded CAG repeat sequence in spinocerebellar ataxia type 7. Genome Res 6:965-971.

Lindenberg KS, Yvert G, Müller K, Landwehrmeyer GB. 2000. Expression analysis of Ataxin-7 mRNA and protein in human brain: Evidence for a widespread distribution and focal protein accumulation. Brain Pathol 10:385-394.

Liu J, Verma PJ, Evans-Galea MV, Delatycki MB, Michalska A, Leung J, Crombie D, Sarsero JP, Williamson R, Dottori M. 2011. Generation of induced pluripotent stem cell lines from Friedreich ataxia patients. Stem Cell Rev 7:703-713.

Liu Y, Cheng D, Li Z, Gao X, Wang H. 2012. The gene expression profiles of induced pluripotent stem cells (iPSCs) generated by a non-integrating method are more similar to embryonic stem cells than those of iPSCs generated by an integrating method. Genet Mol Biol 35:693-700.

Liu Y, Fallon L, Lashuel HA, Liu Z, Lansbury PT. 2002. The UCH-L1 gene encodes two opposing enzymatic activities that affect α-synuclein degradation and Parkinson's disease susceptibility. Cell 111:209-218.

Loh YH, Agarwal S, Park IH, Urbach A, Huo H, Heffner GC, Kim K, Miller JD, Ng K, Daley GQ. 2009. Generation of induced pluripotent stem cells from human blood. Blood 113:5476-5479.

Lombardi MS, Jaspers L, Spronkmans C, Gellera C, Taroni F, Di Maria E, Donato SD, Kaemmerer WF. 2009. A majority of Huntington's disease patients may be treatable by individualized allele-specific RNA interference. Exp Neurol 217:312-319.

Lombardino AJ, Li XC, Hertel M, Nottebohm F. 2005. Replaceable neurons and neurodegenerative disease share depressed UCHL1 levels. Proc Natl Acad Sci USA 102:8036-8041.

Lorincz MT, Detloff PJ, Albin RL, O'Shea KS. 2004. Embryonic stem cells expressing expanded CAG repeats undergo aberrant neuronal differentiation and have persistent Oct-4 and REST/NRSF expression. Mol Cell Neurosci 26:135-143.

Lowe J, McDermott H, Landon M, Mayer RJ, Wilkinson KD. 1990. Ubiquitin carboxyl-terminal hydrolase (PGP 9.5) is selectively present in ubiquitinated inclusion bodies characteristic of human neurodegenerative diseases. J Pathol 161:153-160.

Lowry WE, Richter L, Yachechko R, Pyle AD, Tchieu J, Sridharan R, Clark AT, Plath K. 2008. Generation of human induced pluripotent stem cells from dermal fibroblasts. Proc Natl Acad Sci USA 105:2883-2888.

Luo Y, Fan Y, Zhou B, Xu Z, Chen Y, Sun X. 2012. Generation of induced pluripotent stem cells from skin fibroblasts of a patient with olivopontocerebellar atrophy. Tohoku J Exp Med 226:151-159.

Luthi-Carter R, Strand A, Peters NL, Solano SM, Hollingsworth ZR, Menon AS, Frey AS, Spektor BS, Penney EB, Schilling G. 2000. Decreased expression of striatal signaling genes in a mouse model of Huntington's disease. Hum Mol Genet 9:1259-1271.

Luthi-Carter R, Strand AD, Hanson SA, Kooperberg C, Schilling G, La Spada AR, Merry DE, Young AB, Ross CA, Borchelt DR. 2002. Polyglutamine and transcription: Gene expression changes shared by DRPLA and Huntington's disease mouse models reveal context-independent effects. Hum Mol Genet 11:1927-1937.

Ma Y, Lin H, Qiu C. 2012. High-efficiency transfection and siRNA-mediated gene knockdown in human pluripotent stem cells. Curr Protoc Stem Cell Biol Chapter 2:5C. 2.1-5C. 2.9.

Mah N, Wang Y, Liao MC, Prigione A, Jozefczuk J, Lichtner B, Wolfrum K, Haltmeier M, Flöttmann M, Schaefer M. 2011. Molecular insights into reprogramming-initiation events mediated by the OSKM gene regulatory network. PloS One 6:e24351.

Maherali N, Hochedlinger K. 2008. Guidelines and techniques for the generation of induced pluripotent stem cells. Cell Stem Cell 3:595-605.

Maherali N, Sridharan R, Xie W, Utikal J, Eminli S, Arnold K, Stadtfeld M, Yachechko R, Tchieu J, Jaenisch R. 2007. Directly reprogrammed fibroblasts show global epigenetic remodeling and widespread tissue contribution. Cell Stem Cell 1:55-70.

Mandel JL. 1994. Trinucleotide diseases on the rise. Nat Genet 7:453-455.

Manto M, Marmolino D. 2009. Animal models of human cerebellar ataxias: A cornerstone for the therapies of the twenty-first century. Cerebellum 8:137-154.

Marchetto MCN, Carromeu C, Acab A, Yu D, Yeo GW, Mu Y, Chen G, Gage FH, Muotri AR. 2010. A model for neural development and treatment of Rett syndrome using human induced pluripotent stem cells. Cell 143:527-539.

Marchetto MCN, Yeo GW, Kainohana O, Marsala M, Gage FH, Muotri AR. 2009. Transcriptional signature and memory retention of human-induced pluripotent stem cells. PLoS One 4:e7076.

Marion RM, Strati K, Li H, Tejera A, Schoeftner S, Ortega S, Serrano M, Blasco MA. 2009. Telomeres acquire embryonic stem cell characteristics in induced pluripotent stem cells. Cell Stem Cell 4:141-154.

Marsh JL, Lukacsovich T, Thompson LM. 2009. Animal models of polyglutamine diseases and therapeutic approaches. J Biol Chem 284:7431-7435.

Marsh JL, Thompson LM. 2006. *Drosophila* in the study of neurodegenerative disease. Neuron 52:169-178.

Martinez E, Palhan VB, Tjernberg A, Lymar ES, Gamper AM, Kundu TK, Chait BT, Roeder RG. 2001. Human STAGA complex is a chromatin-acetylating transcription coactivator that interacts with pre-mRNA splicing and DNA damage-binding factors in vivo. Mol Cell Biol 21:6782-6795.

Martínez-Cerdeño V, Lemen JM, Chan V, Wey A, Lin W, Dent SR, Knoepfler PS. 2012. N-myc and GCN5 regulate significantly overlapping transcriptional programs in neural stem cells. PloS One 7:e39456.

Matilla A, Gorbea C, Einum DD, Townsend J, Michalik A, van Broeckhoven C, Jensen CC, Murphy KJ, Ptacek LJ, Fu YH. 2001. Association of ataxin-7 with the proteasome subunit S4 of the 19S regulatory complex. Hum Mol Genet 10:2821-2831.

Mattout A, Biran A, Meshorer E. 2011. Global epigenetic changes during somatic cell reprogramming to iPS cells. J Mol Cell Biol 3:341-350.

Mauger C, Del-Favero J, Ceuterick C, Lübke U, van Broeckhoven C, Martin JJ. 1999. Identification and localization of ataxin-7 in brain and retina of a patient with cerebellar ataxia type II using anti-peptide antibody. Mol Brain Res 74:35-43.

Mayshar Y, Ben-David U, Lavon N, Biancotti JC, Yakir B, Clark AT, Plath K, Lowry WE, Benvenisty N. 2010. Identification and classification of chromosomal aberrations in human induced pluripotent stem cells. Cell Stem Cell 7:521-531.

Mazzola JL, Sirover MA. 2001. Reduction of glyceraldehyde-3-phosphate dehydrogenase activity in Alzheimer's disease and in Huntington's disease fibroblasts. J Neurochem 76:442-449.

Mazzola JL, Sirover MA. 2002. Alteration of nuclear glyceraldehyde-3-phosphate dehydrogenase structure in Huntington's disease fibroblasts. Mol Brain Res 100:95-101.

Mazzola JL, Sirover MA. 2003. Subcellular alteration of glyceraldehyde-3-phosphate dehydrogenase in Alzheimer's disease fibroblasts. J Neurosci Res 71:279-285.

McBride JL, Boudreau RL, Harper SQ, Staber PD, Monteys AM, Martins I, Gilmore BL, Burstein H, Peluso RW, Polisky B. 2008. Artificial miRNAs mitigate shRNA-mediated toxicity in the brain: Implications for the therapeutic development of RNAi. Proc Natl Acad Sci USA 105:5868-5873.

McCampbell A, Taylor JP, Taye AA, Robitschek J, Li M, Walcott J, Merry D, Chai Y, Paulson H, Sobue G. 2000. CREB-binding protein sequestration by expanded polyglutamine. Hum Mol Genet 9:2197-2202.

McMahon SJ, Pray-Grant MG, Schieltz D, Yates JR, Grant PA. 2005. Polyglutamine-expanded spinocerebellar ataxia-7 protein disrupts normal SAGA and SLIK histone acetyltransferase activity. Proc Natl Acad Sci USA 102:8478-8482.

Menzies FM, Rubinsztein DC. 2010. Broadening the therapeutic scope for rapamycin treatment. Autophagy 6:286-287.

Metzger S, Bauer P, Tomiuk J, Laccone F, Didonato S, Gellera C, Soliveri P, Lange HW, Weirich-Schwaiger H, Wenning GK. 2006. The S18Y polymorphism in the UCHL1 gene is a genetic modifier in Huntington's disease. Neurogenetics 7:27-30.

Michalik A, Del-Favero J, Mauger C, Löfgren A, Van Broeckhoven C. 1999. Genomic organisation of the spinocerebellar ataxia type 7 (SCA7) gene responsible for autosomal dominant cerebellar ataxia with retinal degeneration. Hum Genet 105:410-417.

Michalik A, Martin JJ, Van Broeckhoven C. 2003. Spinocerebellar ataxia type 7 associated with pigmentary retinal dystrophy. Eur J Hum Genet 12:2-15.

Michalik A, Van Broeckhoven C. 2004. Proteasome degrades soluble expanded polyglutamine completely and efficiently. Neurobiol Dis 16:202-211.

Michalik A, Van Broeckhoven C. 2003. Pathogenesis of polyglutamine disorders: Aggregation revisited. Hum Mol Genet 12:173-186.

Miller J, Arrasate M, Shaby BA, Mitra S, Masliah E, Finkbeiner S. 2010. Quantitative relationships between huntingtin levels, polyglutamine length, inclusion body formation, and neuronal death provide novel insight into Huntington's disease molecular pathogenesis. J Neurosci 30:10541-10550.

Miller VM, Xia H, Marrs GL, Gouvion CM, Lee G, Davidson BL, Paulson HL. 2003. Allele-specific silencing of dominant disease genes. Proc Natl Acad Sci USA 100:7195-7200.

Mitra S, Tsvetkov AS, Finkbeiner S. 2009. Single neuron ubiquitin-proteasome dynamics accompanying inclusion body formation in Huntington disease. J Biol Chem 284:4398-4403.

Miura K, Okada Y, Aoi T, Okada A, Takahashi K, Okita K, Nakagawa M, Koyanagi M, Tanabe K, Ohnuki M. 2009. Variation in the safety of induced pluripotent stem cell lines. Nat Biotechnol 27:743-745.

Monckton DG, Cayuela ML, Gould FK, Brock GJR, de Silva R, Ashizawa T. 1999. Very large (CAG)n DNA repeat expansions in the sperm of two spinocerebellar ataxia type 7 males. Hum Mol Genet 8:2473-2478.

Montie HL, Cho MS, Holder L, Liu Y, Tsvetkov AS, Finkbeiner S, Merry DE. 2009. Cytoplasmic retention of polyglutamine-expanded androgen receptor ameliorates disease via autophagy in a mouse model of spinal and bulbar muscular atrophy. Hum Mol Genet 18:1937-1950.

Mookerjee S, Papanikolaou T, Guyenet SJ, Sampath V, Lin A, Vitelli C, DeGiacomo F, Sopher BL, Chen SF, La Spada AR. 2009. Posttranslational modification of ataxin-7 at lysine 257 prevents autophagy-mediated turnover of an N-terminal caspase-7 cleavage fragment. J Neurosci 29:15134-15144.

Mushegian AR, Vishnivetskiy SA, Gurevich VV. 2000. Conserved phosphoprotein interaction motif is functionally interchangeable between ataxin-7 and arrestins. Biochemistry 39:6809-6813.

Nagata E, Sawa A, Ross CA, Snyder SH. 2004. Autophagosome-like vacuole formation in Huntington's disease lymphoblasts. Neuroreport 15:1325-1328.

Nakagawa M, Takizawa N, Narita M, Ichisaka T, Yamanaka S. 2010. Promotion of direct reprogramming by transformation-deficient myc. Proc Natl Acad Sci USA 107:14152-14157.

Nakamura Y, Tagawa K, Oka T, Sasabe T, Ito H, Shiwaku H, La Spada AR, Okazawa H. 2012. Ataxin-7 associates with microtubules and stabilizes the cytoskeletal network. Hum Mol Genet 21:1099-1110.

Nakatsuji N, Nakajima F, Tokunaga K. 2008. HLA-haplotype banking and iPS cells. Nat Biotechnol 26:739-740.

Nardacchione A, Orsi L, Brusco A, Franco A, Grosso E, Dragone E, Mortara P, Schiffer D, De Marchi M. 1999. Definition of the smallest pathological CAG expansion in SCA7. Clin Genet 56:232-234.

Narlikar GJ, Fan HY, Kingston RE. 2002. Cooperation between complexes that regulate chromatin structure and transcription. Cell 108:475-487.

Nasir J, Floresco SB, O'Kusky JR, Diewert VM, Richman JM, Zeisler J, Borowski A, Marth JD, Phillips AG, Hayden MR. 1995. Targeted disruption of the Huntington's disease gene results in embryonic lethality and behavioral and morphological changes in heterozygotes. Cell 81:811-823.

Niclis J, Trounson A, Dottori M, Ellisdon A, Bottomley S, Verlinsky Y, Cram D. 2009. Human embryonic stem cell models of Huntington disease. Reprod Biomed Online 19:106-113.

Nishikawa K, Li H, Kawamura R, Osaka H, Wang YL, Hara Y, Hirokawa T, Manago Y, Amano T, Noda M. 2003. Alterations of structure and hydrolase activity of Parkinsonism-associated human ubiquitin carboxyl-terminal hydrolase L1 variants. Biochem Biophys Res Commun 304:176-183.

Ohi Y, Qin H, Hong C, Blouin L, Polo JM, Guo T, Qi Z, Downey SL, Manos PD, Rossi DJ. 2011. Incomplete DNA methylation underlies a transcriptional memory of somatic cells in human iPS cells. Nat Cell Biol 13:541-549.

Ohnishi Y, Tamura Y, Yoshida M, Tokunaga K, Hohjoh H. 2008. Enhancement of allele discrimination by introduction of nucleotide mismatches into siRNA in allele-specific gene silencing by RNAi. PloS One 3:e2248.

Okada M, Oka M, Yoneda Y. 2010. Effective culture conditions for the induction of pluripotent stem cells. Biochim Biophys Acta 1800:956-963.

Oki K, Tatarishvili J, Wood J, Koch P, Wattananit S, Mine Y, Monni E, Tornero D, Ahlenius H, Ladewig J. 2012. Human-Induced pluripotent stem cells form functional neurons and improve recovery after grafting in Stroke-Damaged brain. Stem Cells 30:1120-1133.

Okita K, Ichisaka T, Yamanaka S. 2007. Generation of germline-competent induced pluripotent stem cells. Nature 448:313-317.

Okita K, Yamanaka S. 2011. Induced pluripotent stem cells: Opportunities and challenges. Philos Trans R Soc Lond B Biol Sci 366:2198-2207.

Orr HT, Zoghbi HY. 2007. Trinucleotide repeat disorders. Annu Rev Neurosci 30:575-621

Osaka H, Wang YL, Takada K, Takizawa S, Setsuie R, Li H, Sato Y, Nishikawa K, Sun YJ, Sakurai M. 2003. Ubiquitin carboxy-terminal hydrolase L1 binds to and stabilizes monoubiquitin in neuron. Hum Mol Genet 12:1945-1958.

Palhan VB, Chen S, Peng GH, Tjernberg A, Gamper AM, Fan Y, Chait BT, La Spada AR, Roeder RG. 2005. Polyglutamine-expanded ataxin-7 inhibits STAGA histone acetyltransferase activity to produce retinal degeneration. Proc Natl Acad Sci USA 102:8472-8477.

Pandey UB, Batlevi Y, Baehrecke EH, Taylor JP. 2007. HDAC6 at the intersection of autophagy, the ubiquitin-proteasome system and neurodegeneration. Autophagy 3:643-645.

Pang ZP, Yang N, Vierbuchen T, Ostermeier A, Fuentes DR, Yang TQ, Citri A, Sebastiano V, Marro S, Südhof TC. 2011. Induction of human neuronal cells by defined transcription factors. Nature 476:220-223.

Papapetrou EP, Tomishima MJ, Chambers SM, Mica Y, Reed E, Menon J, Tabar V, Mo Q, Studer L, Sadelain M. 2009. Stoichiometric and temporal requirements of Oct4, Sox2, Klf4, and c-myc expression for efficient human iPSC induction and differentiation. Proc Natl Acad Sci USA 106:12759-12764.

Park IH, Arora N, Huo H, Maherali N, Ahfeldt T, Shimamura A, Lensch MW, Cowan C, Hochedlinger K. 2008. Disease-specific induced pluripotent stem cells. Cell 134:877-886.

Park IH, Zhao R, West JA, Yabuuchi A, Huo H, Ince TA, Lerou PH, Lensch MW, Daley GQ. 2007. Reprogramming of human somatic cells to pluripotency with defined factors. Nature 451:141-146.

Pasi C, Dereli-Öz A, Negrini S, Friedli M, Fragola G, Lombardo A, Van Houwe G, Naldini L, Casola S, Testa G. 2011. Genomic instability in induced stem cells. Cell Death Differ 18:745-753.

Pera MF, Andrade J, Houssami S, Reubinoff B, Trounson A, Stanley EG, Ward-van Oostwaard D, Mummery C. 2004. Regulation of human embryonic stem cell differentiation by BMP-2 and its antagonist noggin. J Cell Sci 117:1269-1280.

Perrier AL, Tabar V, Barberi T, Rubio ME, Bruses J, Topf N, Harrison NL, Studer L. 2004. Derivation of midbrain dopamine neurons from human embryonic stem cells. Proc Natl Acad Sci USA 101:12543-12548.

Perrin V, Régulier E, Abbas-Terki T, Hassig R, Brouillet E, Aebischer P, Luthi-Carter R, Déglon N. 2007. Neuroprotection by Hsp104 and Hsp27 in lentiviral-based rat models of Huntington's disease. Mol Ther 15:903-911.

Persichetti F, Carlee L, Faber PW, McNeil SM, Ambrose CM, Srinidhi J, Anderson MA, Barnes GT, Gusella JF, MacDonald ME. 1996. Differential expression of normal and mutant Huntington's disease gene alleles. Neurobiol Dis 3:183-190.

Petersén Å, Larsen KE, Behr GG, Romero N, Przedborski S, Brundin P, Sulzer D. 2001. Expanded CAG repeats in exon 1 of the Huntington's disease gene stimulate dopamine-mediated striatal neuron autophagy and degeneration. Hum Mol Genet 10:1243-1254.

Pfister EL, Kennington L, Straubhaar J, Wagh S, Liu W, DiFiglia M, Landwehrmeyer B, Vonsattel JP, Zamore PD, Aronin N. 2009. Five siRNAs targeting three SNPs may provide therapy for three-quarters of Huntington's disease patients. Curr Biol 19:774-778.

Pomp O, Brokhman I, Ziegler L, Almog M, Korngreen A, Tavian M, Goldstein RS. 2008. PA6-induced human embryonic stem cell-derived neurospheres: A new source of human peripheral sensory neurons and neural crest cells. Brain Res 1230:50-60.

Prigione A, Fauler B, Lurz R, Lehrach H, Adjaye J. 2010. The senescence-related mitochondrial/oxidative stress pathway is repressed in human induced pluripotent stem cells. Stem Cells 28:721-733.

Prigione A, Hossini AM, Lichtner B, Serin A, Fauler B, Megges M, Lurz R, Lehrach H, Makrantonaki E, Zouboulis CC. 2011b. Mitochondrial-associated cell death mechanisms are reset to an embryonic-like state in aged donor-derived iPS cells harboring chromosomal aberrations. PloS One 6:e27352.

Prigione A, Lichtner B, Kuhl H, Struys EA, Wamelink M, Lehrach H, Ralser M, Timmermann B, Adjaye J. 2011a. Human induced pluripotent stem cells harbor homoplasmic and heteroplasmic mitochondrial DNA mutations while maintaining human embryonic stem cell–like metabolic reprogramming. Stem Cells 29:1338-1348.

Pulst SM, Santos N, Wang D, Yang H, Huynh D, Velazquez L, Figueroa KP. 2005. Spinocerebellar ataxia type 2: PolyQ repeat variation in the CACNA1A calcium channel modifies age of onset. Brain 128:2297-2303.

Rajamohan D, Matsa E, Kalra S, Crutchley J, Patel A, George V, Denning C. 2012. Current status of drug screening and disease modelling in human pluripotent stem cells. Bioessays (Epub ahead of print).

Ramesar RS, Bardien S, Beighton P, Bryer A. 1997. Expanded CAG repeats in spinocerebellar ataxia (SCA1) segregate with distinct haplotypes in South African families. Hum Genet 100:131-137.

Ramos-Mejia V, Muñoz-Lopez M, Garcia-Perez JL, Menendez P. 2010. iPSC lines that do not silence the expression of the ectopic reprogramming factors may display enhanced propensity to genomic instability. Cell Res 20:1092-1095.

Ravikumar B, Vacher C, Berger Z, Davies JE, Luo S, Oroz LG, Scaravilli F, Easton DF, Duden R, O'Kane CJ. 2004. Inhibition of mTOR induces autophagy and reduces toxicity of polyglutamine expansions in fly and mouse models of Huntington disease. Nat Genet 36:585-595.

Renna M, Jimenez-Sanchez M, Sarkar S, Rubinsztein DC. 2010. Chemical inducers of autophagy that enhance the clearance of mutant proteins in neurodegenerative diseases. J Biol Chem 285:11061-11067.

Rizzino A. 2010. Stimulating progress in regenerative medicine: Improving the cloning and recovery of cryopreserved human pluripotent stem cells with ROCK inhibitors. Regen Med 5:799-807.

Rodriguez-Lebron E, Denovan-Wright EM, Nash K, Lewin AS, Mandel RJ. 2005. Intrastriatal rAAV-mediated delivery of anti-huntingtin shRNAs induces partial reversal of disease progression in R6/1 Huntington's disease transgenic mice. Mol Ther 12:618-633.

Rodriguez-Lebron E, Paulson HL. 2005. Allele-specific RNA interference for neurological disease. Gene Ther 13:576-581.

Rosenblatt A, Brinkman R, Liang K, Almqvist E, Margolis R, Huang C, Sherr M, Franz M, Abbott M, Hayden M. 2001. Familial influence on age of onset among siblings with Huntington disease. Am J Med Genet 105:399-403.

Ross CA, Tabrizi SJ. 2011. Huntington's disease: From molecular pathogenesis to clinical treatment. Lancet Neurol 10:83-98.

Sadri-Vakili G, Menon A, Farrell L, Keller-McGandy C, Cantuti-Castelvetri I, Standaert D, Augood S, Yohrling G, Cha JHJ. 2006. Huntingtin inclusions do not down-regulate specific genes in the R6/2 Huntington's disease mouse. Eur J Neurosci 23:3171-3175.

Saegusa H, Wakamori M, Matsuda Y, Wang J, Mori Y, Zong S, Tanabe T. 2007. Properties of human Cav2. 1 channel with a spinocerebellar ataxia type 6 mutation expressed in Purkinje cells. Mol and Cell Neurosci 34:261-270.

Saigoh K, Wang YL, Suh JG, Yamanishi T, Sakai Y, Kiyosawa H, Harada T, Ichihara N, Wakana S, Kikuchi T. 1999. Intragenic deletion in the gene encoding ubiquitin carboxy-terminal hydrolase in gad mice. Nat Genet 23:47-51.

Sánchez-Danés A, Richaud-Patin Y, Carballo-Carbajal I, Jiménez-Delgado S, Caig C, Mora S, Di Guglielmo C, Ezquerra M, Patel B, Giralt A. 2012. Disease-specific phenotypes in dopamine neurons from human iPS-based models of genetic and sporadic Parkinson's disease. EMBO Mol Med 4:380-95.

Sapp E, Schwarz C, Chase K, Bhide P, Young A, Penney J, Vonsattel J, Aronin N, DiFiglia M. 1997. Huntingtin localization in brains of normal and Huntington's disease patients. Ann Neurol 42:604-612.

Sarkar S, Davies JE, Huang Z, Tunnacliffe A, Rubinsztein DC. 2007. Trehalose, a novel mTOR-independent autophagy enhancer, accelerates the clearance of mutant huntingtin and α-synuclein. J Biol Chem 282:5641-5652.

Sarkar S, Krishna G, Imarisio S, Saiki S, O'Kane CJ, Rubinsztein DC. 2008. A rational mechanism for combination treatment of Huntington's disease using lithium and rapamycin. Hum Mol Genet 17:170-178.

Sathasivam K, Hobbs C, Turmaine M, Mangiarini L, Mahal A, Bertaux F, Wanker EE, Doherty P, Davies SW, Bates GP. 1999. Formation of polyglutamine inclusions in non-CNS tissue. Hum Mol Genet 8:813-822.

Schaffar G, Breuer P, Boteva R, Behrends C, Tzvetkov N, Strippel N, Sakahira H, Siegers K, Hayer-Hartl M, Hartl FU. 2004. Cellular toxicity of polyglutamine expansion proteins: Mechanism of transcription factor deactivation. Mol Cell 15:95-105.

Scheel H, Tomiuk S, Hofmann K. 2003. Elucidation of ataxin-3 and ataxin-7 function by integrative bioinformatics. Hum Mol Genet 12:2845-2852.

Scholefield J, Greenberg LJ, Weinberg MS, Arbuthnot PB, Abdelgany A, Wood MJA. 2009. Design of RNAi hairpins for mutation-specific silencing of ataxin-7 and correction of a SCA7 phenotype. PLoS One 4:e7232.

Scholefield J, Wood MJA. 2010. Therapeutic gene silencing strategies for polyglutamine disorders. Trends Genet 26:29-38.

Schwartz SD, Hubschman JP, Heilwell G, Franco-Cardenas V, Pan CK, Ostrick RM, Mickunas E, Gay R, Klimanskaya I, Lanza R. 2012. Embryonic stem cell trials for macular degeneration: A preliminary report. Lancet 379:713-720.

Schwarz DS, Ding H, Kennington L, Moore JT, Schelter J, Burchard J, Linsley PS, Aronin N, Xu Z, Zamore PD. 2006. Designing siRNA that distinguish between genes that differ by a single nucleotide. PLoS Genet 2:e140.

Seo H, Sonntag KC, Isacson O. 2004. Generalized brain and skin proteasome inhibition in Huntington's disease. Ann Neurol 56:319-328.

Sequeiros J, Martindale J, Seneca S. 2010. EMQN best practice guidelines for molecular genetic testing of SCAs. Eur J Hum Genet 18:1173-1176.

Seriola A, Spits C, Simard JP, Hilven P, Haentjens P, Pearson CE, Sermon K. 2011. Huntington's and myotonic dystrophy hESCs: Down-regulated trinucleotide repeat instability and mismatch repair machinery expression upon differentiation. Hum Mol Genet 20:176-185.

Setsuie R, Wada K. 2007. The functions of UCH-L1 and its relation to neurodegenerative diseases. Neurochem Int 51:105-111.

Shibata M, Lu T, Furuya T, Degterev A, Mizushima N, Yoshimori T, MacDonald M, Yankner B, Yuan J. 2006. Regulation of intracellular accumulation of mutant huntingtin by Beclin 1. J Biol Chem 281:14474-14485.

Shimohata T, Nakajima T, Yamada M, Uchida C, Onodera O, Naruse S, Kimura T, Koide R, Nozaki K, Sano Y. 2000. Expanded polyglutamine stretches interact with TAFII130, interfering with CREB-dependent transcription. Nat Genet 26:29-36.

Shirendeb U, Reddy AP, Manczak M, Calkins MJ, Mao P, Tagle DA, Hemachandra Reddy P. 2011. Abnormal mitochondrial dynamics, mitochondrial loss and mutant huntingtin oligomers in Huntington's disease: Implications for selective neuronal damage. Hum Mol Genet 20:1438-1455.

Sibley CR, Wood MJA. 2011. Identification of allele-specific RNAi effectors targeting genetic forms of Parkinson's disease. PloS One 6:e26194.

Smith, DC. Development of a SCA7 patient-derived lymphoblast cell model for testing RNAi knock-down of the disease-causing gene. MSc dissertation, University of Cape Town, 2011.

Smith D, Bryer A, Watson L, Greenberg L. 2012. Inherited polyglutamine spinocerebellar ataxias in South Africa. S Afr Med J 102:683-686.

Smith RA, Miller TM, Yamanaka K, Monia BP, Condon TP, Hung G, Lobsiger CS, Ward CM, McAlonis-Downes M, Wei H. 2006. J Clin Invest 116:2290-2296.

Smith WC, Harland RM. 1992. Expression cloning of noggin, a new dorsalizing factor localized to the Spemann organizer in Xenopus embryos. Cell 70:829-840.

Sohocki MM, Sullivan LS, Mintz-Hittner HA, Birch D, Heckenlively JR, Freund CL, McInnes RR, Daiger SP. 1998. A range of clinical phenotypes associated with mutations in *CRX*, a photoreceptor transcription-factor gene. Am J Hum Genet 63:1307-1315.

Soldner F, Hockemeyer D, Beard C, Gao Q, Bell GW, Cook EG, Hargus G, Blak A, Cooper O, Mitalipova M. 2009. Parkinson's disease patient-derived induced pluripotent stem cells free of viral reprogramming factors. Cell 136:964-977.

Sopher BL, Ladd PD, Pineda VV, Libby RT, Sunkin SM, Hurley JB, Thienes CP, Gaasterland T, Filippova GN, La Spada AR. 2011. CTCF regulates ataxin-7 expression through promotion of a convergently transcribed, antisense noncoding RNA. Neuron 70:1071-1084.

Squitieri F, Falleni A, Cannella M, Orobello S, Fulceri F, Lenzi P, Fornai F. 2010. Abnormal morphology of peripheral cell tissues from patients with Huntington disease. J Neural Transm 117:77-83.

Stadtfeld M, Nagaya M, Utikal J, Weir G, Hochedlinger K. 2008. Induced pluripotent stem cells generated without viral integration. Science 322:945-949.

Steffan JS, Kazantsev A, Spasic-Boskovic O, Greenwald M, Zhu YZ, Gohler H, Wanker EE, Bates GP, Housman DE, Thompson LM. 2000. The Huntington's disease protein interacts with p53 and CREB-binding protein and represses transcription. Proc Natl Acad Sci USA 97:6763-6768.

Stenoien DL, Cummings CJ, Adams HP, Mancini MG, Patel K, DeMartino GN, Marcelli M, Weigel NL, Mancini MA. 1999. Polyglutamine-expanded androgen receptors form aggregates that sequester heat shock proteins, proteasome components and SRC-1, and are suppressed by the HDJ-2 chaperone. Hum Mol Genet 8:731-741.

Stevanin G, Giunti P, David G, Belal S, Dürr A, Ruberg M, Wood N, Brice A. 1998. De novo expansion of intermediate alleles in spinocerebellar ataxia 7. Hum Mol Genet 7:1809-1813.

Stewart CL, Stuhlmann H, Jähner D, Jaenisch R. 1982. De novo methylation, expression, and infectivity of retroviral genomes introduced into embryonal carcinoma cells. Proc Natl Acad Sci USA 79:4098-4102.

Stewart SA, Dykxhoorn DM, Palliser D, Mizuno H, Yu EY, An DS, Sabatini DM, Chen ISY, Hahn WC, Sharp PA. 2003. Lentivirus-delivered stable gene silencing by RNAi in primary cells. RNA 9:493-501.

Storey E, du Sart D, Shaw JH, Lorentzos P, Kelly L, McKinley Gardner R, Forrest SM, Biros I, Nicholson GA. 2000. Frequency of spinocerebellar ataxia types 1, 2, 3, 6, and 7 in Australian patients with spinocerebellar ataxia. Am J Med Genet 95:351-358.

Ström AL, Forsgren L, Holmberg M. 2005. A role for both wild-type and expanded ataxin-7 in transcriptional regulation. Neurobiol Dis 20:646-655.

Ström AL, Jonasson J, Hart P, Brännström T, Forsgren L, Holmberg M. 2002. Cloning and expression analysis of the murine homolog of the *spinocerebellar ataxia type 7* (*SCA7*) gene. Gene 285:91-99.

Swami M, Hendricks AE, Gillis T, Massood T, Mysore J, Myers RH, Wheeler VC. 2009. Somatic expansion of the Huntington's disease CAG repeat in the brain is associated with an earlier age of disease onset. Hum Mol Genet 18:3039-3047.

Taatjes DJ, Marr MT, Tjian R. 2004. Regulatory diversity among metazoan co-activator complexes. Nat Rev Mol Cell Biol 5:403-410.

Takahashi K, Narita M, Yokura M, Ichisaka T, Yamanaka S. 2009. Human induced pluripotent stem cells on autologous feeders. PLoS One 4:e8067.

Takahashi K, Tanabe K, Ohnuki M, Narita M, Ichisaka T, Tomoda K, Yamanaka S. 2007. Induction of pluripotent stem cells from adult human fibroblasts by defined factors. Cell 131:861-872.

Takahashi K, Yamanaka S. 2006. Induction of pluripotent stem cells from mouse embryonic and adult fibroblast cultures by defined factors. Cell 126:663-676.

Tanaka M, Machida Y, Niu S, Ikeda T, Jana NR, Doi H, Kurosawa M, Nekooki M, Nukina N. 2004. Trehalose alleviates polyglutamine-mediated pathology in a mouse model of Huntington disease. Nat Med 10:148-154.

Tao O, Shimazaki T, Okada Y, Naka H, Kohda K, Yuzaki M, Mizusawa H, Okano H. 2010. Efficient generation of mature cerebellar Purkinje cells from mouse embryonic stem cells. J Neurosci Res 88:234-247.

Taylor J, Grote SK, Xia J, Vandelft M, Graczyk J, Ellerby LM, La Spada AR, Truant R. 2006. Ataxin-7 can export from the nucleus via a conserved exportin-dependent signal. J Biol Chem 281:2730-2739.

Taylor S, Wakem M, Dijkman G, Alsarraj M, Nguyen M. 2010. A practical approach to RT-qPCR – publishing data that conform to the MIQE guidelines. Methods 50:S1-S5.

Thomson JA, Itskovitz-Eldor J, Shapiro SS, Waknitz MA, Swiergiel JJ, Marshall VS, Jones JM. 1998. Embryonic stem cell lines derived from human blastocysts. Science 282:1145-1147.

To K, Adamian M, Jakobiec F, Berson E. 1993. Olivopontocerebellar atrophy with retinal degeneration: An electroretinographic and histopathologic investigation. Ophthalmology 100:15-23.

Trond Aasen AR, Maria JB, Elena Garreta AC, Federico Gonzalez RV. 2008. Efficient and rapid generation of induced pluripotent stem cells from human keratinocytes. Nat Biotechnol 26:1276-1284.

Trottier Y, Biancalana V, Mandel JL. 1994. Instability of CAG repeats in Huntington's disease: Relation to parental transmission and age of onset. J Med Genet 31:377-382.

Tsai HF, Lin SJ, Li C, Hsieh M. 2005. Decreased expression of Hsp27 and Hsp70 in transformed lymphoblastoid cells from patients with spinocerebellar ataxia type 7. Biochem Biophys Res Commun 334:1279-1286.

Utikal J, Maherali N, Kulalert W, Hochedlinger K. 2009. Sox2 is dispensable for the reprogramming of melanocytes and melanoma cells into induced pluripotent stem cells. J Cell Sci 122:3502-3510.

Valenzuela DM, Economides AN, Rojas E, Lamb TM, Nunez L, Jones P, Lp N, Espinosa R, Brannan CI, Gilbert DJ. 1995. Identification of mammalian noggin and its expression in the adult nervous system. J Neurosci 15:6077-6084.

Van Bilsen PHJ, Jaspers L, Lombardi MS, Odekerken JCE, Burright EN, Kaemmerer WF. 2008. Identification and allele-specific silencing of the mutant huntingtin allele in Huntington's disease patient-derived fibroblasts. Hum Gene Ther 19:710-718.

Van de Warrenburg B, Frenken C, Ausems M, Kleefstra T, Sinke R, Knoers N, Kremer H. 2001. Striking anticipation in spinocerebellar ataxia type 7: The infantile phenotype. J Neurol 248:911-914.

Van Raamsdonk JM, Pearson J, Rogers DA, Bissada N, Vogl AW, Hayden MR, Leavitt BR. 2005. Loss of wild-type huntingtin influences motor dysfunction and survival in the YAC128 mouse model of Huntington disease. Hum Mol Genet 14:1379-1392.

Varas F, Stadtfeld M, de Andres-Aguayo L, Maherali N, Di Tullio A, Pantano L, Notredame C, Hochedlinger K, Graf T. 2009. Fibroblast-derived induced pluripotent stem cells show no common retroviral vector insertions. Stem Cells 27:300-306.

Varum S, Rodrigues AS, Moura MB, Momcilovic O, Easley CA, Ramalho-Santos J, Van Houten B, Schatten G. 2011. Energy metabolism in human pluripotent stem cells and their differentiated counterparts. PLoS One 6:e20914.

Veitch NJ, Ennis M, McAbney JP, Shelbourne PF, Monckton DG. 2007. Inherited CAG·CTG allele length is a major modifier of somatic mutation length variability in Huntington disease. DNA Repair 6:789-796.

Velier J, Kim M, Schwarz C, Kim TW, Sapp E, Chase K, Aronin N, DiFiglia M. 1998. Wild-type and mutant huntingtins function in vesicle trafficking in the secretory and endocytic pathways. Exp Neurol 152:34-40.

Venkatraman P, Wetzel R, Tanaka M, Nukina N, Goldberg AL. 2004. Eukaryotic proteasomes cannot digest polyglutamine sequences and release them during degradation of polyglutamine-containing proteins. Mol Cell 14:95-104.

Vierbuchen T, Ostermeier A, Pang ZP, Kokubu Y, Südhof TC, Wernig M. 2010. Direct conversion of fibroblasts to functional neurons by defined factors. Nature 463:1035-1041.

Vig PJS, Shao Q, Subramony S, Lopez ME, Safaya E. 2009. Bergmann glial S100B activates myo-inositol monophosphatase 1 and co-localizes to Purkinje cell vacuoles in SCA1 transgenic mice. Cerebellum 8:231-244.

Vilar M, Murillo-Carretero M, Mira H, Magnusson K, Besset V, Ibáñez CF. 2006. Bex1, a novel interactor of the p75 neurotrophin receptor, links neurotrophin signaling to the cell cycle. EMBO J 25:1219-1230.

Wang H, Ghosh A, Baigude H, Yang C, Qiu L, Xia X, Zhou H, Rana TM, Xu Z. 2008. Therapeutic gene silencing delivered by a chemically modified small interfering RNA against mutant SOD1 slows amyotrophic lateral sclerosis progression. J Biol Chem 283:15845-15852.

Wang HL, Chou AH, Lin AC, Chen SY, Weng YH, Yeh TH. 2010. Polyglutamine-expanded ataxin-7 upregulates Bax expression by activating p53 in cerebellar and inferior olivary neurons. Exp Neurol 224:486-494.

Wang Y, Adjaye J. 2011. A cyclic AMP analog, 8-br-cAMP, enhances the induction of pluripotency in human fibroblast cells. Stem Cell Rev 7:331-341.

Warburg O. 1956. On the origin of cancer cells. Science 123:309-314.

Watase K, Weeber EJ, Xu B, Antalffy B, Yuva-Paylor L, Hashimoto K, Kano M, Atkinson R, Sun Y, Armstrong DL. 2002. A long CAG repeat in the mouse Sca1 locus replicates SCA1 features and reveals the impact of protein solubility on selective neurodegeneration. Neuron 34:905-919.

Watson LM, Scholefield J, Greenberg LJ, Wood MJA. 2012. Polyglutamine disease: From pathogenesis to therapy. S Afr Med J 102:481-484.

Watson LM, Wood MJA. 2012. RNA therapy for polyglutamine neurodegenerative diseases. Expert Rev Mol Med 14:e3.

Weinberg MS, Wood MJA. 2009. Short non-coding RNA biology and neurodegenerative disorders: Novel disease targets and therapeutics. Hum Mol Genet 18:R27-39.

Wernig M, Meissner A, Foreman R, Brambrink T, Ku M, Hochedlinger K, Bernstein BE, Jaenisch R. 2007. In vitro reprogramming of fibroblasts into a pluripotent ES-cell-like state. Nature 448:318-324.

Wernig M, Zhao JP, Pruszak J, Hedlund E, Fu D, Soldner F, Broccoli V, Constantine-Paton M, Isacson O, Jaenisch R. 2008. Neurons derived from reprogrammed fibroblasts functionally integrate into the fetal brain and improve symptoms of rats with Parkinson's disease. Proc Natl Acad Sci USA 105:5856-5861.

Whitney A, Lim M, Kanabar D, Lin JP. 2007. Massive SCA7 expansion detected in a 7-month-old male with hypotonia, cardiomegaly, and renal compromise. Dev Med Child Neurol 49:140-143.

Wichterle H, Przedborski S. 2010. What can pluripotent stem cells teach us about neurodegenerative diseases? Nat Neurosci 13:800-804.

Wilkinson KD, Lee K, Deshpande S, Duerksen-Hughes P, Boss JM, Pohl J. 1989. The neuron-specific protein PGP 9.5 is a ubiquitin carboxyl-terminal hydrolase. Science 246:670-673.

Wilmut I, Schnieke A, McWhir J, Kind A, Campbell K. 1997. Viable offspring derived from fetal and adult mammalian cells. Nature 385:810-813.

Wilson P, Barber P, Hamid Q, Power B, Dhillon A, Rode J, Day I, Thompson R, Polak J, Wilson P. 1988. The immunolocalization of protein gene product 9.5 using rabbit polyclonal and mouse monoclonal antibodies. Br J Exp Pathol 69:91-104.

Wong RCB, Pébay A, Nguyen LTV, Koh KLL, Pera MF. 2004. Presence of functional gap junctions in human embryonic stem cells. Stem Cells 22:883-889.

Wyttenbach A, Carmichael J, Swartz J, Furlong RA, Narain Y, Rankin J, Rubinsztein DC. 2000. Effects of heat shock, heat shock protein 40 (HDJ-2), and proteasome inhibition on protein aggregation in cellular models of Huntington's disease. Proc Natl Acad Sci USA 97:2898-2903.

Xia H, Mao Q, Eliason SL, Harper SQ, Martins IH, Orr HT, Paulson HL, Yang L, Kotin RM, Davidson BL. 2004. RNAi suppresses polyglutamine-induced neurodegeneration in a model of spinocerebellar ataxia. Nat Med 10:816-820.

Xia H, Mao Q, Paulson HL, Davidson BL. 2002. siRNA-mediated gene silencing in vitro and in vivo. Nat Biotechnol 20:1006-1010.

Xia X, Zhou H, Huang Y, Xu Z. 2006. Allele-specific RNAi selectively silences mutant SOD1 and achieves significant therapeutic benefit in vivo. Neurobiol Dis 23:578-586.

Xin M, Yue T, Ma Z, Wu F, Gow A, Lu QR. 2005. Myelinogenesis and axonal recognition by oligodendrocytes in brain are uncoupled in Olig1-null mice. J Neurosci 25:1354-1365.

Xu W, Edmondson DG, Evrard YA, Wakamiya M, Behringer RR, Roth SY. 2000. Loss of Gcn5l2 leads to increased apoptosis and mesodermal defects during mouse development. Nat Genet 26:229-232.

Yamamoto A, Lucas JJ, Hen R. 2000. Reversal of neuropathology and motor dysfunction in a conditional model of Huntington's disease. Cell 101:57-66.

Yang N, Ng YH, Pang ZP, Südhof TC, Wernig M. 2011. Induced neuronal cells: How to make and define a neuron. Cell Stem Cell 9:517-525.

Yang SH, Cheng PH, Banta H, Piotrowska-Nitsche K, Yang JJ, Cheng ECH, Snyder B, Larkin K, Liu J, Orkin J. 2008. Towards a transgenic model of Huntington's disease in a non-human primate. Nature 453:921-924.

Yao S, Sukonnik T, Kean T, Bharadwaj RR, Pasceri P, Ellis J. 2004. Retrovirus silencing, variegation, extinction, and memory are controlled by a dynamic interplay of multiple epigenetic modifications. Mol Ther 10:27-36.

Yoo SY, Pennesi ME, Weeber EJ, Xu B, Atkinson R, Chen S, Armstrong DL, Wu SM, Sweatt JD, Zoghbi HY. 2003. SCA7 knockin mice model human SCA7 and reveal gradual accumulation of mutant ataxin-7 in neurons and abnormalities in short-term plasticity. Neuron 37:383-401.

Yoon SR, Dubeau L, De Young M, Wexler NS, Arnheim N. 2003. Huntington disease expansion mutations in humans can occur before meiosis is completed. Proc Natl Acad Sci USA 100:8834-8838.

Yoshida Y, Takahashi K, Okita K, Ichisaka T, Yamanaka S. 2010. Hypoxia enhances the generation of induced pluripotent stem cells. Cell Stem Cell 5:237-241.

Young JE, Gouw L, Propp S, Sopher BL, Taylor J, Lin A, Hermel E, Logvinova A, Chen SF, Chen S. 2007. Proteolytic cleavage of ataxin-7 by caspase-7 modulates cellular toxicity and transcriptional dysregulation. J Biol Chem 282:30150-30160.

Yu X, Ajayi A, Boga NR, Ström AL. 2012. Differential degradation of full-length and cleaved ataxin-7 fragments in a novel stable inducible SCA7 model. J Mol Neurosci 47:219-233.

Yu J, Vodyanik MA, Smuga-Otto K, Antosiewicz-Bourget J, Frane JL, Tian S, Nie J, Jonsdottir GA, Ruotti V, Stewart R. 2007. Induced pluripotent stem cell lines derived from human somatic cells. Science 318:1917-1920.

Yue Z, Horton A, Bravin M, DeJager PL, Selimi F, Heintz N. 2002. A novel protein complex linking the δ2 glutamate receptor and autophagy: Implications for neurodegeneration in lurcher mice. Neuron 35:921-933.

Yu ZX, Li SH, Nguyen HP, Li XJ. 2002. Huntingtin inclusions do not deplete polyglutamine-containing transcription factors in HD mice. Hum Mol Genet 11:905-914.

Yvert G, Lindenberg KS, Devys D, Helmlinger D, Landwehrmeyer GB, Mandel JL. 2001. SCA7 mouse models show selective stabilization of mutant ataxin-7 and similar cellular responses in different neuronal cell types. Hum Mol Genet 10:1679-1692.

Yvert G, Lindenberg KS, Picaud S, Landwehrmeyer GB, Sahel JA, Mandel JL. 2000. Expanded polyglutamines induce neurodegeneration and trans-neuronal alterations in cerebellum and retina of SCA7 transgenic mice. Hum Mol Genet 9:2491-2506.

Zamore PD, Tuschl T, Sharp PA, Bartel DP. 2000. RNAi: Double-stranded RNA directs the ATP-dependent cleavage of mRNA at 21 to 23 nucleotide intervals. Cell 101:25-33.

Zander C, Takahashi J, El Hachimi KH, Fujigasaki H, Albanese V, Lebre AS, Stevanin G, Duyckaerts C, Brice A. 2001. Similarities between spinocerebellar ataxia type 7 (SCA7) cell models and human brain: Proteins recruited in inclusions and activation of caspase-3. Hum Mol Genet 10:2569-2579.

Zhang J, Khvorostov I, Hong JS, Oktay Y, Vergnes L, Nuebel E, Wahjudi PN, Setoguchi K, Wang G, Do A. 2011. UCP2 regulates energy metabolism and differentiation potential of human pluripotent stem cells. EMBO J 30:4860-4873.

Zhang N, An MC, Montoro D, Ellerby LM. 2010. Characterization of human Huntington's disease cell model from induced pluripotent stem cells. PLoS Curr 2:RRN1193.

Zhang Y, Engelman J, Friedlander RM. 2009. Allele-specific silencing of mutant Huntington's disease gene. J Neurochem 108:82-90.

Zhang SC, Wernig M, Duncan ID, Brustle O, Thomson JA. 2001. In vitro differentiation of transplantable neural precursors from human embryonic stem cells. Nat Biotechnol 19:1129-1133.

Zhao X, Braun A, Braun JEA. 2008a. Biological roles of neural J proteins. Cell Mol Life Sci 65:2385-2396.

Zhao Y, Lang G, Ito S, Bonnet J, Metzger E, Sawatsubashi S, Suzuki E, Le Guezennec X, Stunnenberg HG, Krasnov A. 2008b. A TFTC/STAGA module mediates histone H2A and H2B deubiquitination, coactivates nuclear receptors, and counteracts heterochromatin silencing. Mol Cell 29:92-101.

Zhong J, Deng J, Phan J, Dlouhy S, Wu H, Yao W, Ye P, D'Ercole AJ, Lee WH. 2005. Insulin-like growth factor-I protects granule neurons from apoptosis and improves ataxia in weaver mice. J Neurosci Res 80:481-490.

Zhou Q, Anderson DJ. 2002. The bHLH transcription factors OLIG2 and OLIG1 couple neuronal and glial subtype specification. Cell 109:61-73.

Zhu S, Li W, Zhou H, Wei W, Ambasudhan R, Lin T, Kim J, Zhang K, Ding S. 2010. Reprogramming of human primary somatic cells by OCT4 and chemical compounds. Cell Stem Cell 7:651-655.

Zijlstra M, Rujano M, Van Waarde M, Vis E, Brunt E, Kampinga H. 2010. Levels of DNAJB family members (HSP40) correlate with disease onset in patients with spinocerebellar ataxia type 3. Eur J Neurosci 32:760-770.

Zu T, Duvick LA, Kaytor MD, Berlinger MS, Zoghbi HY, Clark HB, Orr HT. 2004. Recovery from polyglutamine-induced neurodegeneration in conditional SCA1 transgenic mice. J Neurosci 24:8853.

Appendices

Appendix 1 Ethics approval and patient consent forms

A1.1 Confirmation of ethics approval

UNIVERSITY OF CAPE TOWN

Health Sciences Faculty
Research Ethics Committee
Room E52-24 Groote Schuur Hospital Old Main Building
Observatory 7925
Telephone [021] 406 6338 • **Facsimile** [021] 406 6411
e-mail: shuretta.thomas@uct.ac.za

17 September 2009

REC REF: 380/2009

Prof J Greenberg
Human Genetics

Dear Prof Greenberg

PROJECT TITLE: ELUCIDATION OF THE ROLE OF MICRO-RNAs IN SPINOCEREBELLAR ATAXIA 7.

Thank you for addressing the issues raised by the Research Ethics Committee.

The Ethics Committee has **noted and approved** the Amended Patient Information Sheet for the above-mentioned study:

Please note that the ongoing ethical conduct of the study remains the responsibility of the principal investigator.

Please quote the REC. REF in all your correspondence.

Yours sincerely

Lesley Henley

PROFESSOR M BLOCKMAN
CHAIRPERSON, HSF HUMAN ETHICS

pp

A1.2 Example of an information sheet and consent form

Information Sheet

What is this study about?

There have been several methods developed to study neurodegenerative diseases, however, none of these include looking at the full complement of human genes in cells that are directly affected by the disease, such as nerve cells, which are ultimately destroyed during the course of these inherited conditions. The research approach for this project revolves around the acquisition and culturing of cells from patients and their unaffected family members that have a neurodegenerative condition so we can both gain a better understanding in the laboratory of what goes wrong in the disease at a cellular level, and also to develop effective therapies in the laboratory.

Requirements of the participant:

You have been asked to participate in this study, because a member (or members) of your family have been diagnosed with Spinocerebellar Ataxia type 7 (SCA7). The study will require the use of your DNA and RNA, which contain the genetic material required for your cells to work normally. Both DNA and RNA may be isolated from the white blood cells in your blood, and/or from skin cells (called fibroblasts). There are no more risks involved in this process than there would be for a standard blood-taking procedure and a skin punch biopsy.

Ideally, we would like to obtain both a blood and a skin sample from you. However, since the skin punch biopsy is a more invasive procedure, and may cause discomfort, you may choose to participate in this study by donation of a blood sample only. You will need to indicate your preference on the Consent Form on the reverse of this information sheet.

Anonymity

Any information given by you will remain strictly confidential. Your samples will be assigned an anonymous code, known only to the investigators working on the project.

Voluntary participation

Please be aware that your participation in the study is entirely voluntary and that you are free to refuse to participate or to withdraw from the study at any time. This study is being conducted according to the principles of the Declaration of Helsinki (2008), which looks after the interest of the participants. In addition, you will not be paid for taking part in this study, nor will there be any cost on your part.

Benefits of the Study

This study is purely for research purposes, and offers no direct benefit to you or your family, at this stage. However, in the long term, your participation in this study may allow us to find out more about the cause of SCA7, particularly due to the familial aspect of the disease. This may help us to develop a way to treat SCA7 and other similar diseases in the future.

Consent form

I, _____, have read and understand the patient information sheet attached.

I hereby agree to participate in this study, and I give my voluntary and informed consent to donate my blood/skin cells/hair (for keratinocytes isolated from plucked hair) (DELETE WHERE NOT APPLICABLE) to be cultured/immortalised, in order to provide a constant source of biological material for research into the disease-causing mechanism of Spinocerebellar Ataxia type 7 (SCA7) in my family. I understand that my samples will be allocated an anonymous code, and that my information will be treated with strict confidentiality. I also understand that I may refuse to participate or to withdraw from this study at any time.

The details of this study have been explained to me in a language that I understand and my questions have been answered by _____ DATE:_____

Patient Signature: _____

Witnessed Consent: _____

Date: _____

This protocol has been approved by the Department of Clinical Laboratory Sciences Research Committee as well as the UCT Research Ethics Committee of the Faculty of Health Sciences at UCT.

You are welcome to contact us should you have any questions.

Contact details:

Principal Investigator: Professor Jacquie Greenberg **+27 21 406 6299**

UCT Research Ethics Committee: Professor Mark Blockman (Chairman) **+27 21 406 6626**

Appendix 2 General cell culture protocols

A2.1 Reagents for general cell culture

General cell culture medium

500ml	DMEM
50ml	FCS (Life Technologies)
5ml	100X Antibiotic/antimycotic (Life Technologies)

Freezing medium

20% (v/v)	FCS (Life Technologies)
10% (v/v)	Dimethyl Sulphoxide (DMSO) (Sigma-Aldrich)
70% (v/v)	DMEM (Life Technologies)

A2.2 Thawing cells

- Thaw cryopreserved cells rapidly at 37°C
- Add cells to 4ml prewarmed DMEM + 10% FCS + 1X antibiotic/antimycotic
- Centrifuge at 1000-1500rpm for 4-5min in a standard benchtop centrifuge
- Remove supernatant and reconstitute in prewarmed DMEM+10%FCS+1X antibiotic/antimycotic, and add to T25-T75 flask (use approximately $1x10^6$ cells for T75 and 300 000 cells for T25)

A2.3 Passaging cells

- Aspirate medium and rinse with 10ml PBS
- Aspirate PBS and add 2-3ml TrypLE (Life Technologies)
- Incubate at 37°C for 3-5min

- Wash flask with DMEM + 10% FCS + 1X antibiotic/antimycotic and decant into a sterile centrifuge tube
- Centrifuge at 1000-1500rpm for 4-5min in a standard benchtop centrifuge
- Aspirate supernatant and resuspend cell pellet in an appropriate amount of fresh DMEM+10% FCS + 1X antibiotic/antimycotic to give the desired ratio for passaging into a new flask (usually 1:4).

A2.4 Cryopreservation of cell stocks

- Cell stocks were cryopreserved in Cell Freezing Medium (A2.1), at an approximate concentration of $>5x10^6$ cells/vial.

Appendix 3 General laboratory reagents and protocols

A3.1 Primers for CAG repeat length determination and SNP genotyping

Feature	Forward Primer (5'-3')	Reverse Primer (5'-3')
Atxn7 $(CAG)_n$ (Dorschner et al., 2002)	*ATTGTAGGAGCGGAAAGAATG	CCAGCATCACTTCAGGAC
rs3774729	AATGAACTGCCTGTCAACTC	GCTCACAGTCCATTTCCTAC

Key: HEX fluorescent labelling is indicated by an asterisk (*)

A3.2 Gene Ruler 100bp DNA Ladder Plus *Improved* (Fermentas)

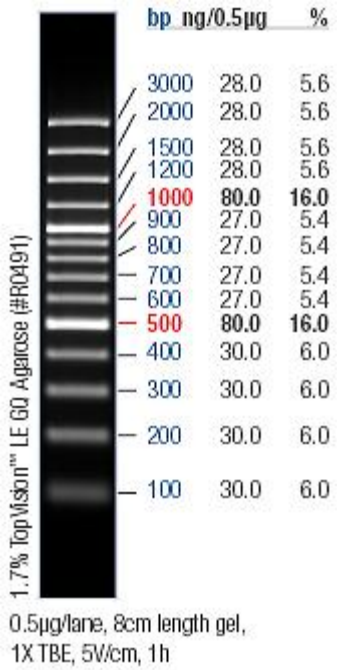

A3.3 Standard PCR reaction mix

Reagent	Final Concentration/Amount
GoTaq Buffer (Promega)	1x
dNTPs (Bioline, Michigan, USA)	200µM
Forward Primer	0.4 µM
Reverse Primer	0.4 µM
GoTaq DNA Polymerase (Promega)	0.5U
Template DNA	100ng

Made up to a final volume of 25µl with sterile distilled water.

A3.4 Standard PCR cycling conditions

1. 95°C for 5min
2. 95°C for 30 seconds

   T_a for 30 seconds

   72°C for 30 seconds
3. 72°C for 7min

Perform 30 cycles of Step 2.

A3.5 siRNA sequences

siRNA	Sense Sequence (5'-3')
siR-atxn-7	GCG TTA CTG TGG ATC TTT C tt
siR-p16	GCC ATG AAC AAT GTT CAT A tt
siR-NS (Sibley and Wood, 2011)	GAA GCA CCA GGA AAG AUA A tt

A3.6 Primers for qPCR

Gene Name	Forward Primer (5'-3')	Reverse Primer (5'-3')
ataxin-7	GCCAGCCGTGAACAATGTC	TTCCTCCCCGTGCTATTTTCA
ataxin-7 A allele	CAAAGTGCCAGCCAT	TAGCAAGCAGTTCAGACC
ataxin-7 G allele	CAAAGTGCCAGCCG	TAGCAAGCAGTTCAGACC
BAX	AAAGATGGTCACGGTCTGC	GCTGGACATTGGACTTCCTC
BEX1	GGAGGAGACTACAAGGATAGG	TCCTTTTCTTCATTTTCTTGGTT
DNAJA1	AAAGGAGGAGAACAGGCAATTAA	TAGGGTTACTGAGAGCTGATGT
GRIA2	CTATGGCATCGCAACACCTAA	GTCCTTGGCTCCACATTCAC
HSP27	ACGAGCTGACGGTCAAGAC	GGGGGCAGCGTGTATTTCC
HSP70	ATGGAATCTATAAGCAGGATCT	CACATACAGAAACTTGATAAGC
HSP105	CCCGTCAGTCATATCATTTGGA	AATCTTTTGAAGTTAGACACCGTATT
IGFBP5	CTTCATCCCGTACTTGTCCAC	TGTACCTGCCCAATTGTGAC
KAT2A	CTTCAGGTGGTTCATCAGGT	CATCTGCTTCCGCATGTTTC
OLIG1	GTTTGGAGAGCTGTATTTAAGACT	TTCTAAGAAACCCCCAGGATTTA
RBM3	CCTGGAGGGTATGGATATGGATA	TGTCTCATTTCAGTTGTCATAATTGT
SLC17A6	TCAACTACGACAGTGAGAAAGAT	GAATAGCCAACGACCAGGAG
SNRK	GCCCACACACCAACATGA	CTTGCATATTCCGCTCCAGA
UCHL1	TGAAGCAGACCATTGGGAAT	TGTTTCAGAACTGATCCATCCT

A3.7 Buffers for immunostaining

FACS buffer

0.01% (w/v)	Sodium azide NaN_3
1% (v/v)	FCS (Life Technologies)
10µg/ml	Human IgG1

Dissolved in PBS

4% FACS Fix (protect from light)

4ml	36% formaldehyde
36ml	FACS buffer

A3.8 Antibodies for immunofluorescence

Primary Antibodies

Epitope	Species	Source	Dilution/ Concentration	Application
Oct3/4	Rat	R&D Systems	0.1mg/ml	Viral titre/transduction of fibroblasts
Oct4	Rabbit	Abcam	1:200	Pluripotency marker
Nanog	Rabbit	Abcam	1:200	Pluripotency marker
Tra-1-60*		Millipore	1:200	Pluripotency marker
Alpha 1 Fetoprotein	Mouse	Abcam	1:50	In vitro differentiation
Alpha smooth muscle actin	Mouse	Abcam	1:100	In vitro differentiation
Forkhead box protein A2 (FOXA2)	Rabbit	Abcam	1:1000	In vitro differentiation
Alpha Sarcomeric actin	Rabbit	Abcam	1:100	In vitro differentiation
βIII-tubulin	Mouse	Covance	1:500	Neuronal Differentiation
Gamma-Aminobutyric acid (GABA)	Rabbit	Sigma-Aldrich	1:500	Neuronal Differentiation
Glial Fibrillary Acidic Protein (GFAP)	Rabbit	Dako	1:500	Neuronal Differentiation
Ataxin-7	Rabbit	Gift of Ana-Lena Strom (Stockholm University)	1:100	Neuronal Differentiation

*AlexaFluor 488 conjugated

Secondary Antibodies

Antibody	Fluorescent Label	Source	Dilution
Goat anti-mouse	AlexaFluor 594	Invitrogen	1:100-1:500
Goat anti-rabbit	AlexaFluor 488	Invitrogen	1:100-1:500
Goat anti-rat	AlexaFluor 488	Invitrogen	1:200

Appendix 4 iPSC culture reagents and protocols

A4.1 Media and reagents for iPSC culture

Plat-GP culture medium

450ml	DMEM (Life Technologies)
50ml	FCS (Life Technologies)
5ml	Antibiotic/antimycotic (Life Technologies)
500µl	Blasticidin (Sigma-Aldrich)

Filter (0.22µm) before use.

MEF medium

500ml	Advanced DMEM (Life Technologies)
50ml	FCS (Life Technologies)
5ml	GlutaMAX (Life Technologies)
500µl	β-mercaptoethanol (Sigma-Aldrich)

iMEF Freezing medium

10% (v/v)	DMSO (Sigma-Aldrich)
10% (v/v)	Advanced DMEM (Life Technologies)
80% (v/v)	FCS (Life Technologies)

mTeSR Medium

400ml	mTeSR 1 Basal Medium (Stem Cell Technologies)
100ml	mTeSR 1 5X Supplement (Stem Cell Technologies)

huESC Culture Medium

400ml	Knockout (KO) DMEM (Life Technologies)
100ml	KO Serum Replacement (Life Technologies)
5ml	Non-essential Amino Acids (Life Technologies)
3.5µl	β-mercaptoethanol (Sigma-Aldrich)
2.5ml	GlutaMAX (Life Technologies)
5ml	Antibiotic/antimycotic (Life Technologies)
500µl	bFGF (Stock 10µg/ml) (R&D Systems)

Filter (0.22µm) before use

EB Medium (Barcelona Stem Cell Bank)

500ml	KO DMEM (Life Technologies)
5ml	GlutaMAX (Life Technologies)
5ml	Non-essential amino acids (Life Technologies)
500µl	β-mercaptoethanol (Sigma-Aldrich)
50ml	FCS (Life Technologies)
5ml	Antibiotic/antimycotic (Life Technologies)

A4.2 Inactivation of mouse embryonic fibroblasts

Mouse embryonic fibroblasts (MEFs) are cryopreserved at passage 0-1 after harvesting from Pathology Oxford outbred (PO) mice embryos at 12.5 days.

Day 1:

- Thaw MEFs and resuspend in 10ml PBS
- Centrifuge at 1500rpm in a standard benchtop centrifuge
- Discard supernatant, resuspend in 30ml MEF medium and seed into a T175 flask.

Day 4:

- Split MEFs when they are ~80% confluent into 3 T175 flasks (=p2).

  (Remove medium, rinse with 10ml PBS, add 2ml TrypLE, incubate at 37^{o}C for about 5min or until cells have detached, add MEF medium and divide into 3 new flasks.)

Day 6:

- Split again when 80% confluent as described above, into 12 T175 flasks (=p3)

Day 7 or 8:

- Resuspend 2mg of Mitomycin C (Sigma-Aldrich) in sterile distilled water to give a 1mg/ml stock, and allow to dissolve overnight at 4°C.

Day 9:

- Dilute Mitomycin C to a final concentration of 10µg/ml in MEF medium.
- Remove MEF medium from cells, add 20ml of Mitomycin C solution per flask and incubate for 2.5 – 3 hours at 37^{o}C.

- Harvest cells by removing medium, washing with 10ml PBS, adding 3ml TrypLE and incubating for 5min at 37^{o}C.
- Remove cells into PBS (12ml per flask), pool, count and centrifuge at 1500rpm in a standard benchtop centrifuge.
- Resuspend pellet in iMEF freezing medium, and aliquot into precooled cryovials for cryopreservation.

The expected yield is 10-20 x 10^6 cells per flask.

A4.3 Preparation of iMEF feeder layer for iPSC culture

Gelatin-coated plates

- Add approximately 4ml EmbryoMax ES Cell Qualified 0.1% Gelatin Solution (Millipore) to 10cm plate (1ml per well of 6-well plate/10ml to T175 flask)
- Incubate at 37°C for 30min
- Remove gelatin, allow plates to dry (Drying is not essential – plates can be used immediately after gelatin has been aspirated if necessary)

Preparation of iMEF feeder layer

- Thaw the appropriate volume of cryopreserved iMEFs (approximately 5x10^5 cells/well of a 6-well plate) as described in A2.2, resuspending the cell pellet in DMEM + 10% FCS + 1% antibiotic/antimycotic
- Seed iMEFs onto gelatin-coated plates and incubate overnight at 37°C, 5% CO_2
- Approximately 5 hours before passaging/seeding iPSCs, aspirate plating medium from iMEFs, rinse three times with PBS to remove all traces of serum, and add an equal volume of huESC medium (A3.1) to the culture vessel

A4.4 Preparation of iMEF-conditioned huESC medium

Day 1:

- Seed iMEFs at $10x10^6$ cells per T175 flask, in 25ml DMEM+10% FCS+1X antibiotic/antimycotic.

Day 2:

- Aspirate culture medium from iMEFs.
- Wash iMEFs three times with PBS.
- Replace medium with 20ml huESC medium (without bFGF).

Day 3:

- Remove huESC medium from iMEFs and add bFGF to a final concentration of 10ng/ml
- Filter using 0.22µm filter (Millipore).
- Add 20ml huESC medium (without bFGF) to iMEFs to repeat procedure the following day.

Conditioned medium may be harvested for up to 10 days, and can be stored at -20°C for later use.

A4.5 Transition of iPSCs from iMEF feeders to feeder-free culture conditions

It takes 3 passages to eliminate all iMEFs and for the iPSCs to be fully adapted to mTeSR medium.

- Begin with one well of a 6-well plate of iPSCs that have been cultured for 6 days on iMEFs.
- Passage the cells, as described in A4.6, and transfer all the cells to one matrigel-coated well
- Feed as per A4.6.
- The cells should become confluent in a few days, and can then be split 1:2
- The next (third) passage, a few days later, is 1:4
- The cells are now considered adapted, and can be passaged routinely as per A4.6.

A4.6 Maintenance of iPSCs on Matrigel (BD Biosciences)

- Warm TrypLE (Life Technologies) to 37^{o}C in a water bath.
- Discard supernatant from confluent iPSCs and wash with 1ml of PBS.
- Add 1ml TrypLE to each well.
- Incubate for 5min at 37^{o}C until the cells have just begun to lift off plate
- Harvest cells from each well into a conical tube with 9ml of sterile PBS, and mix.
- Remove 10µl for cell count and centrifuge remaining cell suspension for 5min at 1500rpm using a standard benchtop centrifuge.
- Discard supernatant and resuspend cells to concentration of 2.5 x 10^5/ml in mTeSR medium (Stem Cell Technologies). Antibiotic/antimycotic may be added to the medium if desired.
- Add Rho-kinase inhibitor (Y-27632) (Sigma-Aldrich) to give a final concentration of 10µM.
- Add 2ml of cells in mTeSR medium to each matrigel-coated well (5 x 10^5 cells/well).
- Incubate at 37^{o}C, 5% CO_2.
- Change medium completely every day.
- Cells may be passaged again once they became confluent (approximately every 5 – 7 days).

A4.7 Primers to test expression of endogenous pluripotency genes

Gene	Forward Primer (5'-3')	Reverse Primer (5'-3')
OCT3/4	GACAGGGGGAGGGGAGGAGCTAGG	CTTCCCTCCAACCAGTTGCCCCAAAC
SOX2	GGGAAATGGGAGGGGTGCAAAAGAGG	TTGCGTGAGTGTGGATGGGATTGGTG
NODAL	GGGCAAGAGGCACCGTCGACATCA	GGGACTCGGTGGGGCTGGTAACGTTTC
c-MYC	GCGTCCTGGGAAGGGAGATCCGGAGC	TTGAGGGGCATCGTCGCGGGAGGCTG

A4.8 Primers to test expression of viral transgenes

Transgene	Forward Primer (5'-3')	Reverse Primer (5'-3')
pMXs-hc-MYC	CAACAACCGAAAATGCACCAGCCCCAG	TTATCGTCGACCACTGTGCTGCTG
pMXs-hKLF4	ACGATCGTGGCCCCGGAAAAGGACC	TTATCGTCGACCACTGTGCTGCTG
pMXs-hOCT3/4	CCCCAGGGCCCCATTTTGGTACC	TTATCGTCGACCACTGTGCTGCTG
pMXs-hSOX2	GGCACCCCTGGCATGGCTCTTGGCTC	TTATCGTCGACCACTGTGCTGCTG

A4.9 Primers to test *in vitro* differentiation from EBs

Gene	Forward Primer (5'-3')	Reverse Primer (5'-3')
FOXA2	TGGGAGCGGTGAAGATGGAAGGGCAC	TCATGCCAGCGCCCACGTACGACGAC
AFP	GAATGCTGCAAACTGACCACGCTGGAAC	TGGCATTCAAGAGGGTTTTCAGTCTGA
MSX1	CGAGAGGACCCCGTGGATGCAGAG	GGCGGCCATCTTCAGCTTCTCCAG
PAX6	ACCCATTATCCAGATGTGTTTGCCCGAG	ATGGTGAAGCTGGGCATAGGCGGCAG
MAP2	CAGGTGGCGGACGTGTGAAAATTGAGAGTG	CACGCTGGATCTGCCTGGGGACTGTG

Appendix 5 Reagents and protocols for neuronal differentiation

A5.1 Media for neuronal differentiation

Supplemented Neurobasal medium A (NBM)

500ml	Neurobasal-A Medium (Life Technologies)
2% (v/v)	B-27 Supplement (Life Technologies)
1% (v/v)	Insulin-Transferrin-Selenium-A (Life Technologies)
1% (v/v)	N2 Supplement (Life Technologies)
2mM	GlutaMAX (Life Technologies)
0.5% (v/v)	Antibiotic/antimycotic (Life Technologies)

For neurosphere formation add:

10ng/ml	EGF (Millipore)
10ng/ml	bFGF (R&D Systems)

A5.2 Preparation of non-adherent cell culture plates

- Prepare 120mg/ml poly 2-hydroxyethyl methacrylate (poly-HEMA) (Sigma-Aldrich) solution in 95% ethanol, stirring overnight to dissolve
- Filter using 0.22µm syringe-driven filter (Millipore)
- Coat wells with poly-HEMA solution (50µl per well of a 96-well plate)
- Allow poly-HEMA to evaporate at room temperature for approximately 3hrs
- Rehydrate surface with supplemented neurobasal medium without EGF and bFGF for at least 15min at 37°C
- Aspirate and add supplemented neurobasal medium with EGF and bFGF, and return to 37°C incubator until ready to use

A5.3 Preparation of poly-D-lysine and laminin-coated plates

- Prepare 10µg/ml poly-D-lysine (Sigma-Aldrich) in PBS
- Coat wells with poly-D-lysine solution (0.5ml per well of a 24-well plate) and incubate at room temperature for at least 30min, under UV light
- Aspirate solution and wash three times with PBS. Air dry.
- Coat plates with 5µg/ml natural mouse laminin (Sigma-Aldrich) in PBS (0.5ml per well of a 24-well plate) and incubate at 37°C for 60min
- Remove laminin solution and wash three times with PBS
- Add supplemented neurobasal medium without EGF or bFGF and return to the 37°C incubator until ready to use

Appendix 6 Genomic integrity of iPSCs

A6.1 Karyograms of 1519 fibroblasts (a), and the derived iPSC lines 1519A (b) and 1519C (c)

a

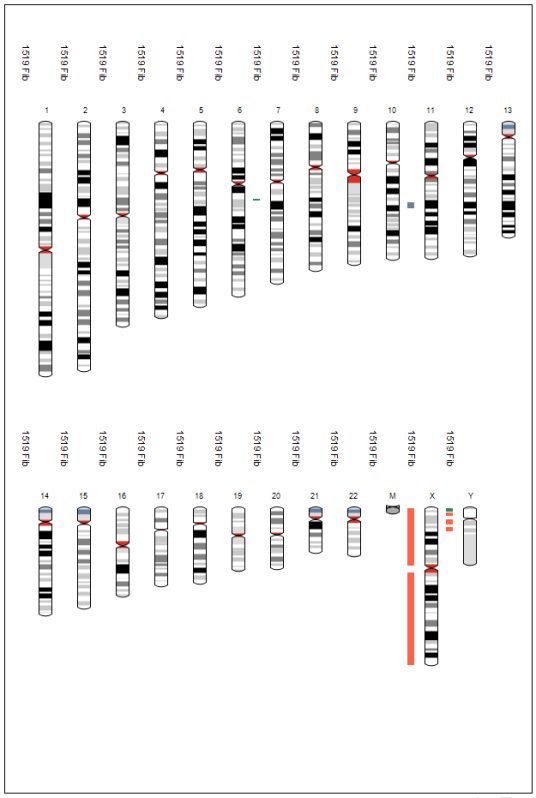

b

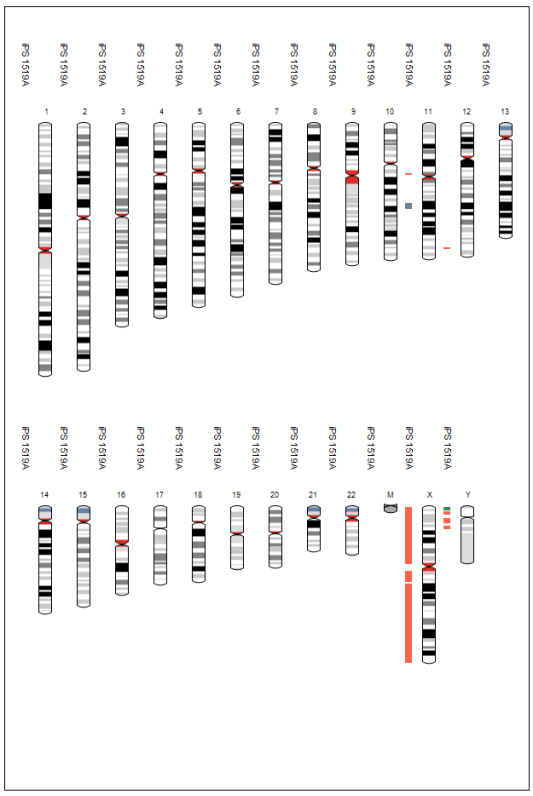

c

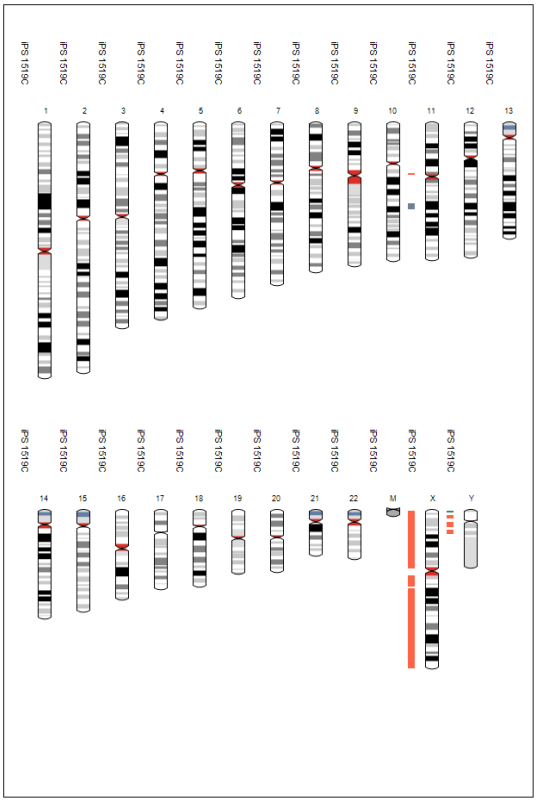

A6.2 Karyograms of SC Con fibroblasts (a), and the derived iPSC line iPS SC NHDF (b)

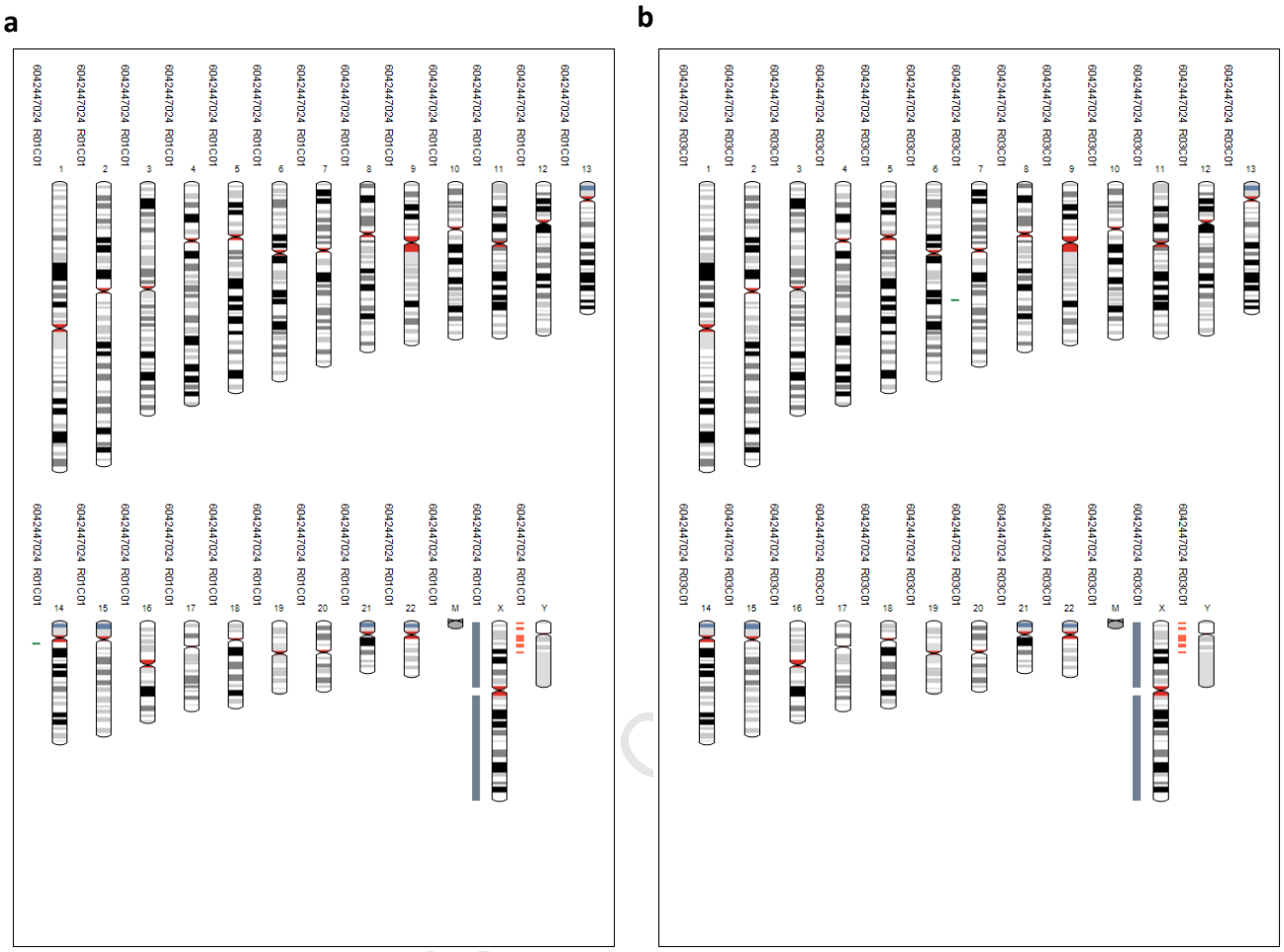

Data provided by Dr Sally Cowley and Ms Jane Vowles.

A6.3 Karyograms of JS Con fibroblasts (a), and the derived iPSC line iPS George (b)

a

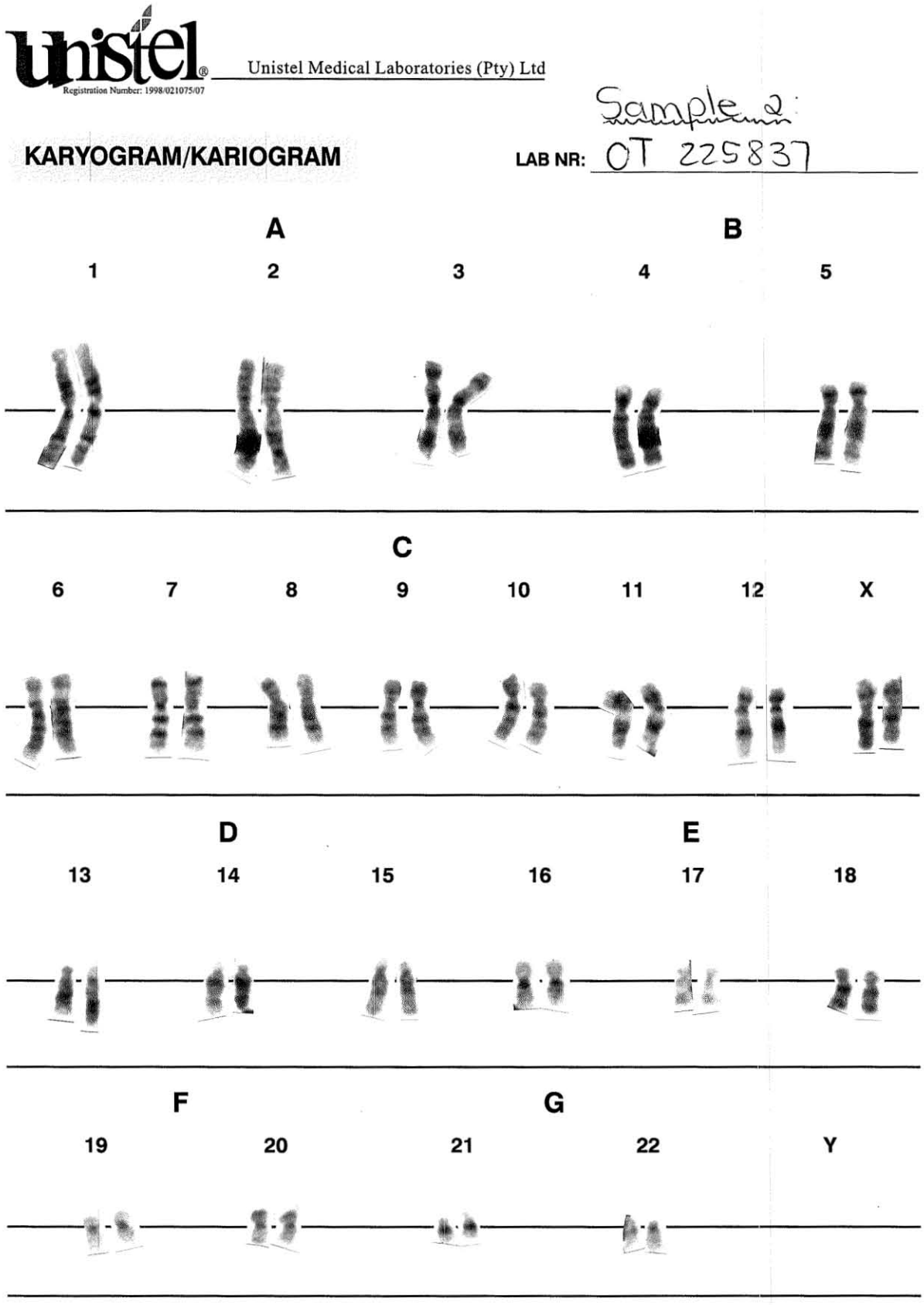

b

Unistel Medical Laboratories (Pty) Ltd
Registration Number: 1998/021075/07

KARYOGRAM/KARIOGRAM LAB NR: _____